THEORETICAL AND EXPERIMENTAL INVESTIGATION OF ACOUSTIC SILENCING SYSTEMS WITH AND WITHOUT AN AIR FLOW.

by

TAI CHEUNG LAI

Department of Mechanical Engineering,
The City University,
St John Street, London EC1V 4PB.

A thesis submitted for the Degree of Doctor of Philosophy at the City University, London.

July, 1976.

SUMMARY.

Acoustic silencing systems with reactive elements are investigated using an analogy with electrical transmission line theory. Plane wave mode of propagation is assumed and convective effects of the flow on the acoustic transmission in the system are investigated. The one-dimensional wave equation is solved and leads to the representation of a silencing element by a symmetrical fourpole. Attenuation-frequency characteristics of entire systems are calculated through matrix multiplication from computer programmes. Two test rigs were constructed for obtaining experimental results, one for systems without flow and the other for systems with an internal air flow up to a Mach number of 0.2 . Resonators, expansion chambers with and without internal tubes and combinations of these elements have been investigated within the frequency range of 50 Hz to 3000 Hz with reflection-free inlet and outlet pipe terminations. Both the sound source and the pick-up are connected to the test rigs from the side. Theoretical results have been compared with those obtained by the test rigs, and, in some cases for inlet and outlet pipes without reflection-free termination, to the results obtained by other workers. The Fast Fourier Transform has been used briefly as a technique for obtaining experimental results. A survey of definitions for attenuation has been undertaken and a comparison between the method of matrix multiplication and the alternative method of continuity has also been made. Computer programmes used for calculating the theoretical curves are presented.

NOTATION

a radius of circular connecting neck of a resonator.

A complex amplitude of incident wave in an acoustic element.

B complex amplitude of reflected wave in an acoustic element.

c velocity of sound.

c_o conductivity of a resonator neck.

f frequency of an acoustic signal.

j $\sqrt{-1}$

k wave number = $\frac{2\pi}{\lambda}$

ℓ length of an acoustic element.

M mean mach number of flow.

$\bar{P}$ instantaneous pressure at any point.

P complex amplitude of acoustic pressure at any point.

S cross-sectional area of an acoustic element.

S_o cross-sectional area of the inlet and outlet pipes.

s condensation at any point.

$\bar{U}$ mean flow velocity.

V complex amplitude of volume velocity at any point.

Z impedance at any point = $\frac{P}{V}$.

Z_o characteristic impedance of an acoustic conduit without flow = $\frac{\rho c}{S}$.

λ wave length.

ξ displacement of fluid particle.

ρ density of fluid medium.

ω angular frequency of an acoustic signal.

Subscripts

b branch

in input

n neck (of resonator)

open open-end

out output

t outlet pipe

Superscript

' for quantities related to straight pipe configurations.

TABLE OF CONTENTS.

INTRODUCTION

Sound propagation in ducts is of relevance in the study of mechano-acoustic systems such as internal combustion engines intakes and exhausts, reciprocating compressor intake and delivery systems, refrigeration and ventilating systems, intakes of turbo-jet engines, nuclear reactors, pneumatic drills and air motors etc. Although certain aspects of these systems are different, the general principles involved are similar. One way of attenuating the sound in ducts is by inserting an acoustic filter or 'silencer'. These filters can be classified as absorptive or reactive. Reactive filters comprise elements such as resonators and expansion chambers which reflect the sound back towards the source. Attenuation of sound is achieved by the formation of standing waves in the system. In this way no energy is destroyed during the silencing process and such a technique is generally described as reactive silencing, as opposed to absorptive silencing in which sound energy is destroyed and dissipated as heat.

The transmission of sound through ducts and simple reactive filters or silencers has been investigated on many occasions, although most of the early work was, due to experimental and theoretical difficulties, limited to the element alone rather than to the entire system. The theory previously developed was found to be inadequate for complicated systems, and silencer design and installation is still very much an empirical process based on experimental trial and error. This is particularly true in the case of the design of silencers for internal combustion engines.

In many instances where sound waves occur in ducts there is superimposed upon the acoustic wave a mean gas flow, which in various ways affects the performance of the system. Although quite a few papers have appeared dealing with sound propagation in ducts with internal flow, most have been orientated towards specific applications, and in general have been concerned with ducts with internal linings of resonator arrays or linings of absorptive materials. The need to reduce the sound from the intake of turbojet engines has given an impetus to the work on resonator arrays. There is a need for a general theory capable of handling the entire silencing system, including the filter elements, interconnecting pipes, source and outlet terminations.

SURVEY OF PREVIOUS WORK

2.1 Definition of Attenuation

Transmission Loss

The theory of sound propagation in ducts has been dealt with in standard texts on acoustics (1,2). However, the original theory of acoustic filtration or silencing was due to Stewart and Lindsay (3). Since then the subject has received considerable attention and numerous publications have appeared dealing with various aspects of reactive acoustic silencing in ducts, both with and without an internal gas flow. In these papers different definitions were given to the term 'attenuation' to suit the author's intention and convenience of experimental measurements, and this survey starts with a discussion of these definitions.

The most common definition is the 'transmission loss' which is defined as the ratio in dB of the energy in the incident wave in the inlet to the energy in the transmitted wave in the outlet pipe. The transmission loss can also be written in terms of the ratio of the amplitudes of the incident and transmitted wave. (Note here that the outlet pipe is the pipe downstream of the silencer while the inlet pipe is that connecting the silencer to the sound source). This definition of transmission loss was used by D. D. Davis and his co-workers (4) and the Motor Industry Research Association (5).

Igarashi and his colleagues (6,7) used a mathematically identical but physically different definition. Instead of using the ratio of waves in the inlet and outlet pipes, they compared the ratio of the wave amplitude in the outlet pipe with the wave in an equivalent straight pipe. Since the straight pipe possessed a non-reflective termination, the incident wave in the inlet pipe of the silencer and that in the straight pipe are the same.

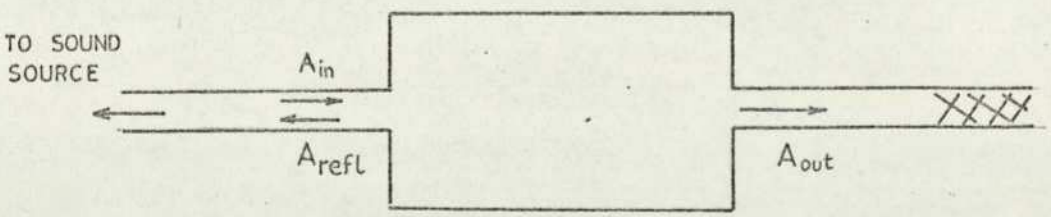

FIG 1a

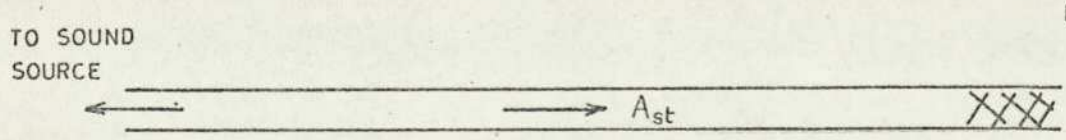

FIG 1b

Fig. 1a shows an acoustic filter in a pipe. The wave in the inlet pipe comprises an incident wave of amplitude A_{in} and a reflected wave of amplitude A_{refl}. In the outlet pipe, due to the non-reflective termination, only the incident wave A_{out} exists. When the filter is replaced by a straight pipe there will only be the incident wave of amplitude A_{st} as shown in Fig. 1b. When the impedance of the sound source is high enough, $A_{st} = A_{in}$.

Transmission Loss is defined as $20 \log_{10} \frac{A_{in}}{A_{out}}$ by D. D. Davis, MIRA etc. Igarashi and co-workers instead defined it as $20 \log_{10} \frac{A_{st}}{A_{out}}$ which is mathematically identical to the former, if the source is of high impedance.

Stewart and Lindsay in a series of papers employed a term 'transmission' which is the ratio of the transmitted sound power to the incident sound power. When referring to fig. 1a, this term 'transmission' is equal to $\frac{|A_{out}|^2}{|A_{in}|^2}$ (3,8,9,10,11,12). Lambert in two of his papers (13, 14) obtained experimentally and theoretically transmission losses for a side branch resonator with the presence of a mean gas flow, although he called these values insertion losses.

All the work mentioned above defined the transmission loss with a reflection free termination. This definition is by no means practical, but appears to be the only rational representation of the performance of a silencer on its own. Experimental results obtained usually agreed well with theoretical predictions.

Insertion Loss

A more practical quantity is the 'insertion loss' which is defined as the ratio in dB of the sound pressure levels measured at some external point to the system, with and without the silencer in the system, i.e. ratio of readings taken at the measuring points in Fig.1a and Fig.1b. Because an exact calculation of the insertion loss is complicated, most workers have only attempted to correlate their measurements with some simplified expression for attenuation. Although logical explanations were usually given, none were really convincing, and the only justification would appear to be good agreement between theoretical and experimental results.

D. D. Davis and his co-workers (4) took measurements of insertion losses with their test rig and compared them to some values of calculated transmission loss with an open finite outlet pipe. Total reflection of the pressure wave with a phase shift of 180° at the open end was assumed. The Motor Industry

Research Association in their reports used D. D. Davis' theory and performed laboratory tests to determine insertion loss for silencers. Experimental results were compared with theoretical predictions. Engine tests were performed to obtain insertion loss for the silencers in the presence of a gas flow. M. Fukuda in his paper (15) performed cold tests and engine tests to obtain values of insertion loss for the expansion chamber type of muffler. He also developed a theoretical expression for attenuation as the ratio of sound pressure levels at inlet and outlet of the silencer. Calling this theoretical expression transmission loss he compared it to the experimental insertion loss obtained from both cold tests and engine tests. A. V. Sreenath and M. L. Munjal (16) derived, by means of an electrical analogy, an expression for insertion loss as the ratio of power transferred to atmosphere from the system, with and without a silencer. Their expression, when simplified, is identical to that of Fukuda. However, no experimental results were given to prove the validity of this expression.

Insertion loss, as defined at the beginning of this section, is not satisfactory since it depends on source impedance, outlet pipe length, inlet pipe length and distance from end of outlet pipe to the measuring point. All these are not fixed quantities of the silencing system and thus will vary considerably in practice. With the exception of those of D. D. Davis and co-workers, all the results obtained experimentally for insertion loss by the above mentioned workers do not compare well with the theoretical calculations. However, insertion loss is still an important definition for practical purposes.

Other Definitions

Apart from the transmission loss and insertion loss there are other definitions for attenuation used by workers in the field of acoustic silencing. A. H. Davis and N. Fleming (17) defined attenuation as the ratio of sound pressure levels measured at the inlet and outlet of the silencer. Using an electrical analogy they derived a theoretical expression for this attenuation and then built a test rig to obtain experimental results, with and without air flow. Engine tests were also performed but no correlation of experiment with theory was attempted in this case. D. D. Davis and R. R. Czarnecki in their work (18) defined attenuation in a similar way as the ratio of sound pressure levels at the input and output of the silencer. The silencer used consisted of a series of identical resonators, and the theory for this set-up was developed by Stewart and Lindsay (3). By assuming an infinite number of identical resonators they obtained the attenuation of each resonator and the attenuation of m such resonators will be m times attenuation of one resonator.

So far all the work mentioned was performed on silencing systems without gas flow. There are papers dealing with systems with flow, but none have tackled the problem of sound propagation in an entire system, as has been attempted in the no flow case. Due to theoretical difficulties, changes in cross section of any kind were avoided, and a variety of definitions have been given in various papers for silencing with internal duct flow.

Mechel, Mertens and Schilz (19), Meyer, Mechel and Kurtze (20), Tack and Lambert (21), Doak and Vaidya (22) all presented their results in terms of attenuation per unit duct length, while S. H. Ko (23) gave attenuation over a definite length of duct, and Mungur and Plumblee (24) used attenuation per unit duct width.

E. J. Rice (25) employed the term sound power attenuation which he defined as the ratio of acoustic energies at the exit and entrance of the duct. This definition is basically the same as that of S. H. Ko.

R. J. Alfredson and P. O. A. L. Davies (26) defined attenuation as the ratio of maximum sound pressure level in the inlet pipe to that in the outlet pipe. They also measured the radiated sound pressure level from the outlet pipe at an external point and compared this quantity to the maximum inlet pipe sound pressure level. This is very similar to, but not exactly the same as, the insertion loss of the system. All the tests reported were carried out on an actual engine.

2.2 Effect of Finite Lengths of Outlet and Inlet Pipes

As has already been mentioned, to avoid mathematical difficulties, the attenuation characteristics of acoustic silencers are often calculated with the assumption of non-reflecting terminations (4, 6). This means both the inlet and outlet pipes are infinitely long. In order to calculate the insertion loss of a silencer, a finite outlet pipe must be assumed. Lindsay was among the first to investigate the effect of a finite termination (11), purely on a theoretical basis.

D. D. Davis in his paper also dealt with the effect of a finite outlet pipe. Following Lindsay, by assuming total reflection of pressure wave witha phase shift of 180° at the open end of the outlet pipe-which is equivalent to zero radiation impedance and is justified at low frequencies - they defined the attenuation as the difference between the sound pressure levels of the incident wave entering the muffler in the inlet pipe and the incident wave leaving the muffler in the outlet pipe, i.e. transmission loss for an open-ended termination. Arguing that the sound pressure in the open air

due to an open inlet pipe without muffler or a muffler with a finite outlet pipe is, at a given frequency, directly proportional to the pressure of the incident wave in the respective pipes, they went on to measure at a distance of 20 inches noise levels emitted from a muffler and from an open inlet pipe; the same loudspeaker acted as the noise source in both cases. Attenuation, which was in fact the insertion loss for the muffler, was found from these data. A comparison of the experimental and theoretical data showed good agreement both in magnitudes and frequencies. The effect of the finite outlet pipe as shown in Davis' paper was to decrease the attenuation drastically around the region of the resonant frequencies of the outlet pipe.

M. Fukuda in his paper (15) investigated extensively the various effects of outlet pipe on silencer attenuation. As far as the outlet pipe length is concerned Fukuda's theoretical results, obtained with the assumption of the outlet pipe being terminated with an open end, agree well with his experimental results, and his findings were similar to those of D. D. Davis. Fukuda also concluded experimentally that the attenuation of a muffler decreases when the outlet pipe diameter becomes large, thus, for a definite total outlet pipe area, a large number of outlet pipe is generally more advantageous than a small number.

The MIRA 1st report (5) also presented very satisfactory results for a simple expansion chamber silencer with a finite outlet pipe; both theoretical and experimental results were obtained using D. D. Davis' methods.

With the measurement of insertion loss the problem arises of radiation of sound from the pipe outlet. Although, as mentioned before, this problem was never adequately dealt with, A. H. Davis and N. Fleming as early as 1935 (17) calculated with the aid of network theory the expected sound level at an external point four inches from the outlet of the silencing system. Radiation from the outlet into a complete sphere was assumed. The experiments were conducted in an anechoic chamber and theoretical and experimental results for attenuation agreed reasonably well. A. V. Sreenath and M. L. Munjal in their paper (16) used a more exact value of radiation impedance for the outlet pipe. They used the expression for the acoustic impedance of an unflanged pipe, namely:-

$$Z = \frac{\pi f_o^2}{c_o} + j\omega \frac{0.6\,a}{S}$$

where f_o = frequency of sound wave,
C_o = velocity of sound at pipe outlet,
a = radius of pipe outlet,
s = area of pipe outlet,
and ω = circular frequency of sound wave.

This was expected to give a better representation of the outlet pipe opening than the condition of Z=0 which was used

by most workers. R. J. Alfredson (26) used a quantity 'Reflection Coefficient' which was defined as the ratio of incident to reflected waves in the outlet pipe. Measurement of this quantity showed that it is frequency dependent and can exceed unity in some cases. With the value of the 'Reflection Coefficient' known from measurement, the net energy flux in the outlet pipe can be calculated, and with it the level of the radiated sound, if spherical radiation is assumed. Measurement of the radiated sound pressure levels at a distance 3 ft. from the outlet pipe exit compared very favourably with the calculated values. Measurements showed that directional distortion at different frequencies was absent. It can also be seen from Alfredson's results that at a wave length corresponding to twice the length of the outlet pipe attenuation of the silencer drops to a low value, as had been shown earlier by D. D. Davis and M. Fukuda. (4,15)

As with outlet pipes, the effect of the inlet pipe on silencer performance was usually conveniently dealt with by assuming an infinitely long inlet pipe. M. Fukuda (15) was the first to include a finite inlet pipe in his mathematical model, using a four element matrix representation of the acoustic elements. His predictions of pass frequencies due to the finite inlet pipe were successfully verified by actual engine test measurements.

Earlier H. Martin (27) had already discussed the effect of finite inlet pipe in relation to the ideal location of a silencer along the exhaust pipe. His conclusion was that the effect of the inlet pipe would always be balanced by that of an outlet pipe of equal length in a single silencer system or in the case of two silencers, by that of an equal length connecting pipe.

Associated with the finite inlet pipe is the problem of source impedance. The source impedance has generally been assumed to be very high, so that the volume velocity emerging from the source remains constant whatever the change downstream. Sreenath and Munjal (16) accounted for the source impedance by assuming that the source consisted of a compliance, and hence the source impedance was inversely proportional to frequency, rather than independent of it. However, since the sound source must be different in each application in practice consideration of source impedance in a general silencer analysis is not justified.

2.3 Mounting of Transducer and Sound Source

The most widely used pressure transducer for measuring sound in ducts is the condenser microphone. Two ways of mounting the microphone have been used in non-flow cases. The first way is to mount the microphone with its axis parallel with that of the duct so that plane sound waves impinge normally on the diaphragm (4). The microphone size

has to be kept small to avoid disturbing the sound pattern in the duct. This method has the advantage that the microphone position is infinitely variable and results proved this method to be satisfactory in cases without flow.

The alternative is to insert the microphone from the side of the duct in a perpendicular position (5,6,7,14,28) In low frequency tests the microphone tip can be kept flush with the inner face of the duct wall and hence will cause no disturbance to the sound pattern at all, although this kind of disturbance was found later to be unimportant in cases without flow.

In flow cases most workers used transducers of their own design (19, 20, 26, 29). These transducers are usually of aerodynamic shape to minimise turbulence caused by their presence, so that only pressure fluctuations due to the sound waves are recorded. The opening which leads to the measuring diaphragm is so placed that the gas is flowing parallel to the diaphragm. When a conventional condenser microphone is used it should be inserted into the duct from the side to avoid the gas impinging on the diaphragm. Nose cones often cannot be used because of the small dimensions of the pipe. Due to the presence of the boundary layer, which results in a trapezoidal pressure gradient across the stream, the tip of the microphone should be placed on centre line of the duct. This will induce turbulence in the wake of the microphone thus giving rise to results which will not be comparable to those obtained by specially designed transducers.

The most common type of sound source is the electromagnetic loudspeaker and is often connected to the duct axially (4,5). Igarashi, Lambert and Mechel (6,14,19,) connected the loudspeaker to the duct via the side at a right angle to the duct axis while Dean, Davis and Fleming, Mason (17, 28, 29) made the connection at an acute angle. Sound source connection appears to be not as critical as transducer connection. The side connection method was adopted in this project because an air flow could then be easily supplied through the ducts.

2.4 Methods of Analysis

Method of Continuity

In their book Stewart and Lindsay (3) formulated and developed theories for acoustic silencers with reactive elements by means of the one-dimensional theory of sound propagation in ducts. Assuming continuity for both pressure and volume velocity at discontinuities, they calculated attenuation characteristics for silencers of various configurations and verified them with experimental results.

The diagram below shows the sound pressures and volume

velocities at an abrupt change in cross-section. The sound pressure at the junction is $\bar{P}$ where:-

$$\bar{P} = \bar{P}_1 = \bar{P}_2$$

The volume velocities V_1 and V_2 are related to the particle displacements ξ_1 and ξ_2 by the following expressions:-

$$V_1 = S_1 \frac{\partial \xi_1}{\partial t} \qquad \text{and} \qquad V_2 = S_2 \frac{\partial \xi_2}{\partial t}$$

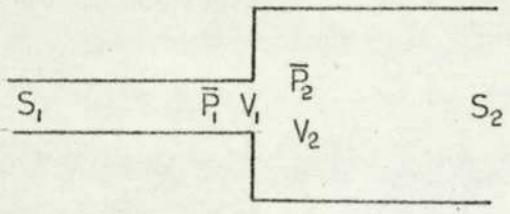

Continuity of flow gives,

$$S_1 \frac{\partial \xi_1}{\partial t} = S_2 \frac{\partial \xi_2}{\partial t}$$

i.e. $V_1 = V_2$

Employing the same method, D. D. Davis and his co-workers (4) made an extensive survey of the acoustic performance of exhaust mufflers for internal combustion engines at low frequencies. They calculated and measured the transmission loss for about eighty mufflers, including expansion chambers with and without internal connecting tubes, large and small side branch resonators and various combinations of the above. Agreement between experimental and theoretical results obtained was very good and their paper remains, in terms of results, the most comprehensive reference on the subject.

R. J. Alfredson (26) in his thesis published in 1970 applied the conditions of continuity of pressure and mass; the latter condition can be converted into continuity of volume velocity through a simple division by the density of the fluid medium. Expansion chambers with and without internal connecting tubes, and with a continuous mean gas flow were considered. The ratios of the magnitudes and the relative phase angles between sound waves in various regions of the tested silencers were calculated and obtained experimentally. Agreement between theoretical and experimental results was extremely good. A typical example is shown below (26).

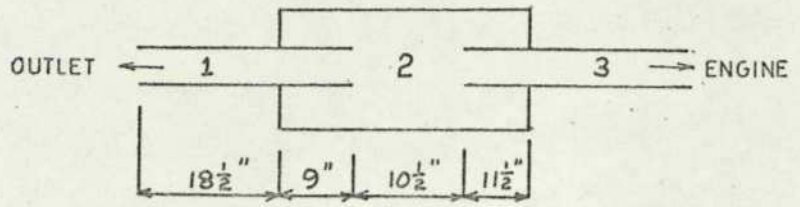

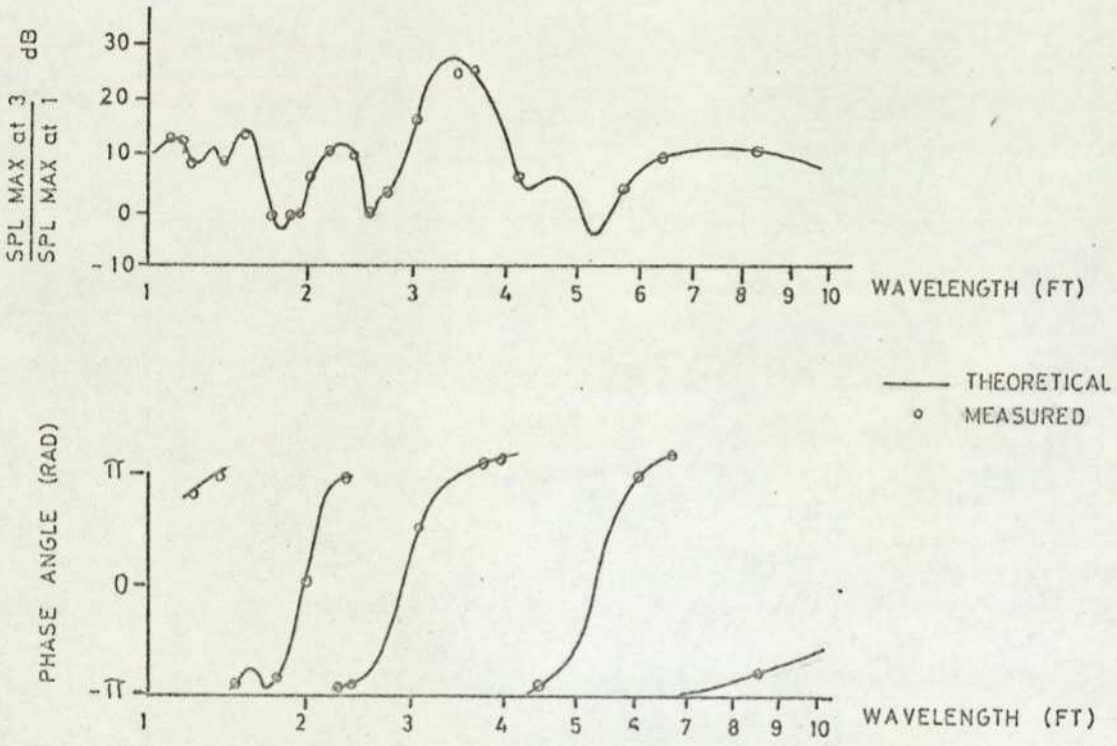

M. Fukuda in his paper (15) used continuity of impedance rather than continuity of pressure and volume velocity; the impedance was defined as the ratio of force to particle velocity at the point concerned. This is again basically the same as continuity of pressure and volume velocity, since force=pressure X area of pipe while volume velocity =particle velocity X area of pipe for plane sound waves. By concentrating mainly on the expansion chamber type of silencers, Fukuda investigated various important factors and the conclusions of note are as follows: partitions deteriorate the attenuation effect in the low frequency region and improve attenuation at high frequencies; the attenuation effect of a muffler decreases when an outlet pipe has a larger diameter and when the number of outlet pipes increases. In this paper different sonic speeds were calculated at different sections of the system in order to account for the effect of variations in temperature. General agreement between theoretical and experimental results was satisfactory.

A. V. Sreenath and M. L. Munjal (16) also calculated attenuation values for various reactive silencers by using continuity of an impedance which they defined as the ratio of sound wave pressure to mass velocity of the wave. Mass velocity was used instead of volume velocity because it was assumed that gas densities were different in various sections of the system due to differences in temperature. No direct experimental verification of the theory was given in this paper.

Method of Matrix Multiplication

The analogy between acoustic and electric filters had been obvious for a long time and, because the method of continuity becomes laborious when the number of elements is large, acoustic filter problems have often been treated in the same way as electric filters. (8,9,10,11,12,13,14,16, 17,18,27). At low frequencies the distributed mass and elasticity of the acoustic system can be represented by an electrical network with constant (or lumped) values of resistance, capacitance or inductance, and properties such as cut-off frequency and attenuation band can be predicted easily and quite accurately. At higher frequencies this simple analogy breaks down and the acoustic system has to be modelled on an electrical transmission line with distributed capacitance and inductance.

Igarashi and his co-workers (6,7) represented the acoustic elements by appropriate four-element matrices. In this way complicated combinations of filters could be analysed by simple matrix multiplication. This is known here as the Method of Matrix Multiplication and has been used to obtain the theoretical results presented in this thesis. With the use of digital computers this method is extremely powerful, in that numerical values can be substituted in the matrices at an early stage and the attenuation calculated. Igarashi and Toyama obtained some experimental results within the range of 50Hz to 3 kHz, and their results were in good agreement with theory.

R. Lambert in his paper (13) derived a four-element matrix to represent a side branch resonator in a system with uniform fluid flow. This matrix was very similar to that used by Igarashi and Fukuda (the difference between the matrices used by Lambert and Igarashi will be discussed in detail later in this chapter). In a separate paper (14) Lambert provided a satisfactory experimental verification of his theoretical prediction. It was thus shown that this method can be easily extended to deal with systems with a uniform internal flow.

2.5 Systems With Internal Flow

Uniform Laminar Flow

The problem of acoustic silencing had been dealt with for systems without a gas flow. In many cases there will be an

internal gas flow in the system, and in order to obtain a more realistic view the effect of flow has to be included.

The simplest way to include this effect is to assume a uniform laminar internal flow in the ducts. The simple wave equation will then be modified to the 'Convective Wave Equation' and its solution will give the convective effect of flow on the performance of the system. J. D. Trimmer in 1937 (30) analysed an acoustic duct with internal uniform laminar flow. His mathematical analysis revealed that the open pipe characteristic impedance was modified by a factor of $(1-M^2)$ where M is the local mach number of the internal flow. It was also shown that this flow acted as a resistive element so that various infinite values that occurred in the no flow case appeared as finite values.

D. S. Whitehead (31) in his work relating to the vibration of air in ducts with internal flow also came to the same conclusion but in a slightly different form, in that he concluded that the effect of flow is to reduce the resonant frequencies of the ducts by a factor of $(1-M^2)$. Both Trimmer and Whitehead's results imply that the length of the pipe is effectively increased.

R. F. Lambert in his paper (13) solved the convective wave equation and obtained a two by two matrix representation of a side branch resonator in a duct system. However, he did not prove the identity [eq. 8] in his paper from the definitions given [eqs. 9a & 9b] and attempts by the author were unsuccessful. The diagram shows the system Lambert was dealing with:-

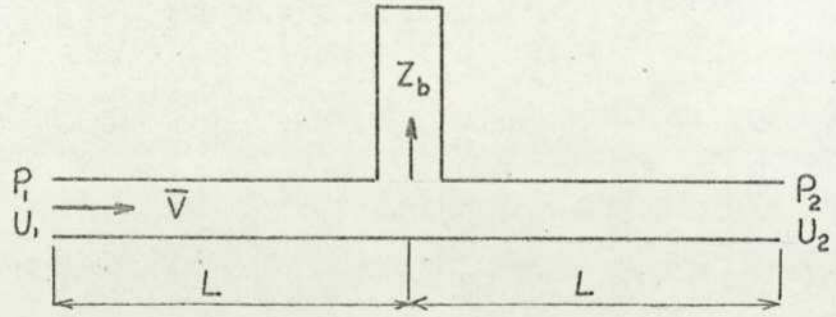

Without flow this system is represented by,

$$\begin{bmatrix} P_1 \\ U_1 \end{bmatrix} = \begin{bmatrix} \cos 2kL + j\frac{Z_o}{2Z_b}\sin 2kL & Z_o\left(j - \frac{Z_o}{2Z_b}\tan kL\right)\sin 2kL \\ \frac{1}{Z_o}\left(j + \frac{Z_o}{2Z_b}\cot kL\right)\sin 2kL & \cos 2kL + j\frac{Z_o}{2Z_b}\sin 2kL \end{bmatrix} \begin{bmatrix} P_2 \\ U_2 \end{bmatrix}$$

$$= \begin{bmatrix} A & B \\ C & D \end{bmatrix} \begin{bmatrix} P_2 \\ U_2 \end{bmatrix}$$

(can be derived by method used in (6), but see chapter 3.)

where Z_o=characteristic impedance of main duct.
Z_b=impedance of side branch.
k=wave number

Since A = D and AD - BC = 1 this four element matrix is a reversible four pole and this agrees with the physical significance of the system

The four element matrix given by Lambert, when without flow, simplifies to,

$$\begin{bmatrix} \cos 2kL + j\frac{Z_o}{2Z_b}\sin 2kL & -Z_o\left(1 + j\frac{Z_o}{2Z_b}\tan kL\right)\sin 2kL \\ -\frac{1}{Z_o}\left(1 - j\frac{Z_o}{2Z_b}\cot kL\right)\sin 2kL & \cos 2kL + j\frac{Z_o}{2Z_b}\sin 2kL \end{bmatrix}$$

This matrix differs from that derived earlier and is not a reversible four pole which means the silencing system is not reversible. Even when $Z_b = \infty$ when the matrix represents only an open pipe without flow, the condition of AD - CB = 1 is still not satisfied.

In a companion paper (14) Lambert presented experimental results for the silencer which he investigated. A graph of attenuation against frequency was given at regions around the resonance frequency of the silencer. The results showed that the flow acted as a damping element and attenuation at this resonant frequency was decreased as the flow velocity increased. An important point was that the frequency at which this peak attenuation occurred did not shift with variation in flow.

R. J. Alfredson (26) also assumed uniform mean flow. He produced experimental results to support his claim that neglecting the mean flow will lead to large errors in the estimation of the attenuation of the silencing system, especially when reflection at the outlet pipe opening is strong.

Turbulent Shear Flow

Due to the presence of the shear boundary layer, more realistic flow profiles have to be considered, particularly in the high frequency ranges, to account for the refractive effect of flow upon the sound wave. So far most of the work involving a realistic velocity profile has been related to ducts with internal linings of absorptive material. There has not been any published work on a complete reactive silencing system with internal shear flow. The greatest difficulty in such a project would be to establish the continuity conditions at the junctions of the system.

Findings from work concerning absorptive silencing with various flow profiles are not directly relevant to reactive silencing but nevertheless a brief survey is thought to be justified.

D. C. Pridmore - Brown (32) was the first to produce a satisfactory mathematical model for sound propagation in a duct with a shear flow. He considered both the constant gradient velocity profile and the one-seventh power law profile for the flow, and solves the wave equation analytically with a series method which involved tedious calculations and approximations.

D. Mungur in his papers with G. M. L. Gladwell and H. E. Plumblee (24, 33) used a fourth order Runge-Kutta method to solve the wave equation and calculate the pressure profile across the duct. With this method any velocity profile can be assumed and the method was proved to be more accurate and versatile than Pridmore-Brown's method.

Tack & Lambert (21) considered a general power law velocity profile for the flow. They also obtained a series solution for the pressure profile across the duct. And the conclusion drawn was that for engineering purposes a uniform-flow profile assumption, which is most accurate at low frequencies, should be adequate.

V. Mason (28) dealt with modal cut-off frequencies for sound propagation in a cylindrical duct with internal air flow, and used experimentally obtained velocity profiles for the determination of various acoustic modes. These velocity profiles took the form of a two-region profile in which a constant gradient profile exists in the boundary layer and a uniform profile at the centre of the stream. The fairly low flow speed used in Mason's work only altered the modal cut-off frequencies very slightly.

S. H. Ko (23) and S. D. Savkar (34) both employed a two-region velocity profile. Results obtained by Savkar were very much the same as those obtained by Mungur and Gladwell using a one-seventh power law profile.

2.6 Shift of Resonance Frequency of a Resonator With the Presence of Flow

With the presence of the air flow the definition and measurement of the resonance frequency of a Helmholtz resonator becomes more important.

Mechel, Mertens and Schilz (19), and Meyer, Mechel and Kurtze (20) in their papers measured the attenuation per unit length of a line of damped and undamped Helmholtz resonators with an internal flow in the system . Measurements

were made with a travelling microphone. The measurements in the duct for attenuation per unit length against frequeny showed that the attenuation magnitude decreases and the maximum attenuation point shifts to a higher frequency with increasing flow velocity. Their results agreed with what was predicted theoretically by S. M. Ko for lined ducts (23). The first phenomenon had been explained by Tack and Lambert (21) as due to reduction in time for any action responsible for attenuation to occur. The second point was attributed by Mechel and his colleagues to a flow-induced reduction of the oscillating mass in the resonator neck caused by irreversible turbulent movements there. This can be seen from the equation $f_o = \frac{c}{2\pi}\sqrt{\frac{A}{l_{eff} V}}$. Where A is the cross sectional area of the neck, l_{eff} is the effective neck length and V is the volume of the resonator. A decrease in the effective neck length l_{eff} will result in an increase of the resonance frequency. Lambert measured the transmission loss of a single resonator and observed the change in resonance frequency with change in flow speed. He found that the resonance frequency did not change with flow speed, but the transmission loss magnitude did.

Meyer, Mechel and Kurtze (20) also measured the resonance frequency of a resonator by putting the microphone inside the resonator with the sound source immediately outside the resonator neck. They found that the resonance frequency of the resonator shifted to a higher value with increase in flow velocity. This is to a certain extent also verified in Chapter 7.

Phillips (41) used two microphones, one outside and the other inside the resonator for measuring the resonance of a single resonator mounted at the side of a wind tunnel. Both microphones were placed as close as possible to the resonator neck and the resonator was treated as a spring-mass system with one degree of freedom. A shift of the resonance frequency was observed up to a permissible mean flow velocity of 75 m/sec. and no saturation of this shift was observed. McAuliffe (47) determined the resonance of a resonator with two orifices using a similar method but with a much smaller test rig. He started to obtain a shift in resonance frequency at 1.5 m/sec but a limiting value was reached at 4 m/sec. Anderson (48) with a flow mach number approximately equal to 0.2 also obtained this frequency shift with a simple resonator. He also discovered that the end correction for the resonator neck depends not only on flow velocity but also on the cavity volume. This to a certain extent explains the discrepancies among results obtained in references (41), (47), (48) and those presented in Chapter 7 of this thesis.

GENERAL THEORY OF ACOUSTIC TRANSMISSION IN DUCTS.

3.1 Matrix Representation of an Acoustic Element.

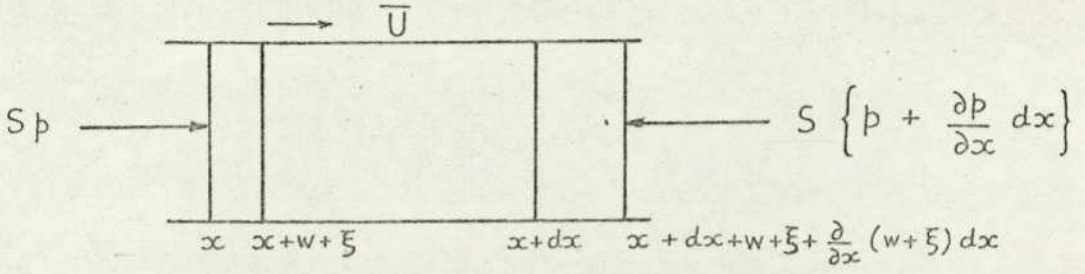

Fig III-1

Consider an element of frictionless fluid shown in Figure III-1 .

x = co-ordinate along the duct.

S = cross-sectional area of the duct.

$\overline{U}$ = mean flow velocity along the duct.

w = displacement of fluid particle due to mean flow in time dt.

ξ = displacement of fluid particle due to acoustic wave motion in time dt.

p = variation in pressure due to the sound wave.

From a one-dimensional analysis the new length of the element is :-

$$dx + \frac{\partial}{\partial x}(w + \xi)\, dx = dx\left(1 + \frac{\partial \xi}{\partial x}\right)$$

and $\frac{\partial w}{\partial x} = 0$ w being independent of x .

For conservation of mass :-

$$\rho_0 S\, dx = \rho S\, dx \left(1 + \frac{\partial \xi}{\partial x}\right)$$

where ρ_0 is the density of the undisturbed fluid, and ρ is the density of the fluid with the wave passing through.

Now since $\rho = \rho_0 (1 + s)$,

where $s = \frac{\rho - \rho_0}{\rho_0}$ and is the condensation of the fluid medium at the point considered.

$$\therefore \quad 1 = (1 + s)\left(1 + \frac{\partial \xi}{\partial x}\right)$$

$$s = -\frac{\partial \xi}{\partial x} \qquad \text{III-1}$$

neglecting second order terms.

Now , $\overline{p} = \overline{p}(\rho)$

Thus , $d\overline{p} = \left(\frac{d\overline{p}}{d\rho}\right) d\rho = p$

By definition , $(\rho - \rho_0)/\rho_0 = d\rho/\rho_0 = s$

And , $$\left(\frac{d\overline{p}}{d\rho}\right) = c^2 \qquad \text{III 2}$$

where c is the velocity of sound in the medium considered.

$$\therefore \quad p = \rho_0 c^2 s = -\rho_0 c^2 \frac{\partial \xi}{\partial x} \qquad \text{IV 3}$$

The net force on the element $= -S \frac{\partial p}{\partial x} dx$

$$= S\rho_0 c^2 \frac{\partial^2 \xi}{\partial x^2} dx$$

Product of mass of element and acceleration is

$$\rho_0 dx\, S \frac{D^2}{Dt^2}(w+\xi) = \rho_0 dx\, S \left\{ \frac{\partial}{\partial t} + (\bar{U} + \frac{\partial \xi}{\partial t}) \frac{\partial}{\partial x} \right\}^2 (w+\xi)$$

$$\doteq \rho_0 dx\, S \left\{ \frac{\partial^2}{\partial t^2} + 2\bar{U} \frac{\partial^2}{\partial t \partial x} + \bar{U}^2 \frac{\partial^2}{\partial x^2} \right\} (w+\xi) \quad , \text{since } \bar{U} \gg \frac{\partial \xi}{\partial t}$$

$$= \rho_0 dx\, S \left\{ \frac{\partial^2 \xi}{\partial t^2} + 2\bar{U} \frac{\partial^2 \xi}{\partial t \partial x} + \bar{U}^2 \frac{\partial^2 \xi}{\partial x^2} \right\}$$

Hence equation of motion is :-

$$S\rho_0 c^2 dx \frac{\partial^2 \xi}{\partial x^2} = S\rho_0 dx \left\{ \frac{\partial^2 \xi}{\partial t^2} + 2\bar{U} \frac{\partial^2 \xi}{\partial t \partial x} + \bar{U}^2 \frac{\partial^2 \xi}{\partial x^2} \right\}$$

$$\frac{\partial^2 \xi}{\partial x^2} = \frac{1}{c^2} \left\{ \frac{\partial^2 \xi}{\partial t^2} + 2\bar{U} \frac{\partial^2 \xi}{\partial x \partial t} + \bar{U}^2 \frac{\partial^2 \xi}{\partial x^2} \right\}$$

$$(1-M^2) \frac{\partial^2 \xi}{\partial x^2} = \frac{1}{c^2} \frac{\partial^2 \xi}{\partial t^2} + 2 \frac{M}{c} \frac{\partial^2 \xi}{\partial x \partial t} \quad , \text{where } M = \bar{U}/c \, .$$

This is the wave equation for particle displacement with mean gas flow velocity $\bar{U}$. D'Alembert's method can be used to solve this partial differential equation. By writing Dx for $\partial/\partial x$ the wave equation becomes

$$\frac{1}{c^2} \frac{d^2 \xi}{dt^2} + 2 \frac{M}{c} Dx \frac{d\xi}{dt} - (1-M^2) Dx^2 \xi = 0$$

$$\left\{ m^2 + 2Mc\, Dx\, m - (1-M^2) c^2 Dx^2 \right\} \xi = 0 \, , \text{ where } m = \frac{d}{dt}$$

$$m = (-2Mc\, Dx \pm \sqrt{4M^2 c^2 Dx^2 + 4(1-M^2) c^2 Dx^2}\,)/2$$

$$= -c\, Dx\, (M \pm 1)$$

$$\therefore \quad \xi = F_1(x)\, e^{-cDx(M+1)t} + F_2(x)\, e^{-cDx(M-1)t}$$

$$= F_1[x - c(M+1)t] + F_2[x - c(M-1)t]$$

Using the identity

$$F(x)\, e^{-Dx\, At} = F(x - At)$$

$$\xi(x,t) = f[x - (1+M)ct] + g[x + (1-M)ct]$$

Write $$\xi(x,t) = f\left\{-\frac{K}{1+M}[x-(1+M)ct]\right\} + g\left\{\frac{K}{1-M}[x+(1-M)ct]\right\} \quad *$$

$$= f\left(\omega t - \frac{K}{1+M}x\right) + g\left(\omega t + \frac{K}{1-M}x\right)$$

$$= f\left\{\omega\left(t - \frac{1}{(1+M)c}x\right)\right\} + g\left\{\omega\left(t + \frac{1}{(1-M)c}x\right)\right\}$$

This can be proved to be the most general and complete solution to the wave equation. (See Appendix 1). If $\xi(x,t)$ is a simple harmonic wave, then the solution to the wave equation is

$$\xi(x,t) = Ae^{j(\omega t - \frac{K}{1+M}x)} + Be^{j(\omega t + \frac{K}{1-M}x)} \quad \text{— III-4}$$

where A and B are complex amplitudes of particle displacement for incident and reflected waves respectively.

This solution represents one downstream wave with velocity $c(1+M)$ and an upstream wave with velocity $c(1-M)$ in the duct. Both waves have frequency ω.

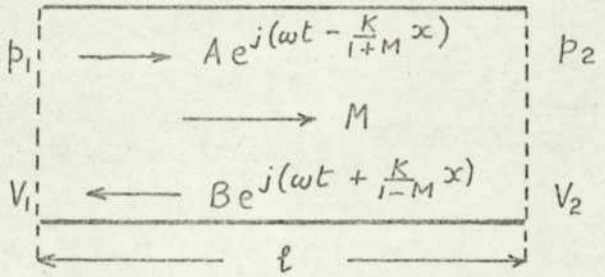

Fig. III-2

Figure III-2 shows a duct element of length ℓ with downstream and upstream waves.

As derived above,

$$p = -\rho c^2 \frac{\partial \xi}{\partial x} \quad , \quad V = S\frac{\partial \xi}{\partial t}$$

$$\therefore \quad p = \rho c^2 j\frac{K}{1+M} Ae^{j(\omega t - \frac{K}{1+M}x)} - \rho c^2 j\frac{K}{1-M} Be^{j(\omega t + \frac{K}{1-M}x)}$$

* It is possible to add the two constants $-k/(1+M)$ and $k/(1-M)$ to the functions of $\xi(x,t)$ since in this case the wave frequency is invariant to a stationary transducer and equals ω.

$$V = j S\omega A e^{j(\omega t - \{k/(1+M)\}x)} + j S\omega B e^{j(\omega t + \{k/(1-M)\}x)}$$

Put $A' = j\rho c^2 \frac{k}{1+M} A$, $B' = -j\rho c^2 \frac{k}{1-M} B$

Then. $P = A' e^{j(\omega t - \{k/(1+M)\}x)} + B' e^{j(\omega t + \{k/(1-M)\}x)}$.

$$V = \frac{1}{Z_0} A'(1+M) e^{j(\omega t - \{k/(1+M)\}x)} - \frac{1}{Z_0} B'(1-M) e^{j(\omega t + \{k/(1-M)\}x)}$$

Considering amplitudes only,

at $x = 0$, $P_1 = A' + B'$ ——— (1)

$$V_1 = \frac{1}{Z_0}\{A'(1+M) - B'(1-M)\} \quad \text{——— (2)}$$

at $x = 1$, $P_2 = A' e^{-j\{k/(1+M)\}\ell} + B' e^{j\{k/(1-M)\}\ell}$ —— (3)

$$V_2 = \frac{1}{Z_0}\{A'(1+M) e^{-j\{k/(1+M)\}\ell} - B'(1-M) e^{j\{k/(1-M)\}\ell}\} \quad (4)$$

From (3) $(1+M)P_2 = A'(1+M) e^{-j\frac{K}{1+M}\ell} + B'(1+M) e^{j\frac{K}{1-M}\ell}$ (5)

Subtract (4) from (5), $(1+M)P_2 - V_2 Z_0 = 2B' e^{j\frac{K}{1-M}\ell}$

Multiply (3) by (1-M)

$$(1-M)P_2 = A'(1-M) e^{-j\frac{K}{1+M}\ell} + B'(1-M) e^{j\frac{K}{1-M}\ell} \quad (6)$$

Add (4) to (6),

$$(1-M)P_2 + Z_0 V_2 = 2A' e^{-j\frac{K}{1+M}\ell}$$

$$A' = \frac{1}{2} e^{j\frac{K}{1+M}\ell}\{(1-M)P_2 + V_2 Z_0\}$$

$$B' = \frac{1}{2} e^{-j\frac{K}{1-M}\ell}\{(1+M)P_2 - V_2 Z_0\}$$

Now, $P_1 = \frac{1}{2}\{e^{j\frac{K}{1+M}\ell} + e^{-j\frac{K}{1-M}\ell}\} P_2$

$$+ (V_2 Z_0 - M P_2)\frac{1}{2}\{e^{j\frac{K}{1+M}\ell} - e^{-j\frac{K}{1-M}\ell}\}$$

$$= \frac{1}{2}\{e^{j\frac{(1-M)}{1-M^2}k\ell} + e^{-j\frac{1+M}{1-M^2}k\ell}\} P_2$$

$$+ \frac{1}{2}(V_2 Z_0 - M P_2)\{e^{j\frac{1-M}{1-M^2}k\ell} - e^{-j\frac{1+M}{1-M^2}k\ell}\}.$$

$$= \{\cos(\tfrac{k\ell}{1-M^2})\}\{e^{-j\frac{M}{1-M^2}k\ell}\} P_2 + \{j\sin(\tfrac{k\ell}{1-M^2})\}\{e^{-j\frac{M}{1-M^2}k\ell}\}(V_2 Z_0 - M P_2)$$

$$= e^{-j\frac{M}{1-M^2}k\ell}\{(\cos\tfrac{k\ell}{1-M^2} - jM\sin\tfrac{k\ell}{1-M^2}) P_2$$

$$+ (jZ_0 \sin\tfrac{k\ell}{1-M^2}) V_2\}$$

$$V_1 = \frac{1}{Z_o}\left\{(1+M)\tfrac{1}{2}\, e^{j\frac{k\ell}{1+M}}\left[(1-M)P_2 + V_2 Z_o\right] - (1-M)\tfrac{1}{2}\, e^{-j\frac{k\ell}{1-M}}\left[(1+M)P_2 - V_2 Z_o\right]\right\}$$

$$V_1 = \frac{1}{Z_o}\left\{(1-M^2)P_2\left[\tfrac{1}{2}\, e^{j\frac{1-M}{1-M^2}k\ell} - \tfrac{1}{2}\, e^{-j\frac{1+M}{1-M^2}k\ell}\right] + (1+M)V_2 Z_o \tfrac{1}{2}\, e^{j\frac{1-M}{1-M^2}k\ell} + (1-M)V_2 Z_o \tfrac{1}{2}\, e^{-j\frac{1+M}{1-M^2}k\ell}\right\}$$

$$= \frac{1}{Z_o}\left\{(1-M^2)P_2\, e^{-j\frac{M}{1-M^2}k\ell}\, j\sin\frac{k\ell}{1-M^2} + V_2 Z_o\, e^{-j\frac{M}{1-M^2}k\ell}\cos\frac{k\ell}{1-M^2} + MV_2 Z_o\, e^{-j\frac{M}{1-M^2}k\ell}\, j\sin\frac{k\ell}{1-M^2}\right\}$$

$$= e^{-j\frac{M}{1-M^2}k\ell}\left\{\left(j\frac{1-M^2}{Z_o}\sin\frac{k\ell}{1-M^2}\right)P_2 + \left(\cos\frac{k\ell}{1-M^2} + jM\sin\frac{k\ell}{1-M^2}\right)V_2\right\}$$

$$\begin{bmatrix} P_1 \\ V_1 \end{bmatrix} = e^{-j\frac{M}{1-M^2}k\ell}\begin{bmatrix} \cos\frac{k\ell}{1-M^2} - jM\sin\frac{k\ell}{1-M^2} & j\frac{\rho c}{S}\sin\frac{k\ell}{1-M^2} \\ j\frac{S}{\rho c}(1-M^2)\sin\frac{k\ell}{1-M^2} & \cos\frac{k\ell}{1-M^2} + jM\sin\frac{k\ell}{1-M^2} \end{bmatrix}\begin{bmatrix} P_2 \\ V_2 \end{bmatrix} \qquad \text{III-5}$$

This matrix represents the relation between pressures and volume velocities at two general points a distance l apart in an acoustic duct with mean flow. The matrix forms the basis of the method of matrix multiplication. The exponential term can be disregarded as it does not affect the amplitude. For M=0, the no flow case, the relation reduces to the form,

$$\begin{bmatrix} P_1 \\ V_1 \end{bmatrix} = \begin{bmatrix} \cos k\ell & j\frac{\rho c}{S}\sin k\ell \\ j\frac{S}{\rho c}\sin k\ell & \cos k\ell \end{bmatrix}\begin{bmatrix} P_2 \\ V_2 \end{bmatrix} \qquad \text{III-6}$$

3.2 Characteristic Impedance of a Duct with Flow.

The characteristic impedance of a wave in a duct is defined as the impedance anywhere along a duct with an infinite length.

From III-5,

$$P_1 = \left[\cos \frac{k\ell}{1-M^2} - jM \sin \frac{k\ell}{1-M^2}\right] P_2 + j\left[\frac{\rho c}{S} \sin \frac{k\ell}{1-M^2}\right] V_2$$

$$V_1 = j\left[\frac{S}{\rho c}(1-M^2) \sin \frac{k\ell}{1-M^2}\right] P_2 + \left[\cos \frac{k\ell}{1-M^2} + jM \sin \frac{k\ell}{1-M^2}\right] V_2$$

Thus

$$Z_1 = \frac{P_1}{V_1} = \frac{\left[\cos \frac{k\ell}{1-M^2} - jM \sin \frac{k\ell}{1-M^2}\right] P_2 + j\left[\frac{\rho c}{S} \sin \frac{k\ell}{1-M^2}\right] V_2}{j\left[\frac{S}{\rho c}(1-M^2) \sin \frac{k\ell}{1-M^2}\right] P_2 + \left[\cos \frac{k\ell}{1-M^2} + jM \sin \frac{k\ell}{1-M^2}\right] V_2}$$

$$= \frac{\left[\cos \frac{k\ell}{1-M^2} - jM \sin \frac{k\ell}{1-M^2}\right] Z_2 + j\left[\frac{\rho c}{S} \sin \frac{k\ell}{1-M^2}\right]}{j\left[\frac{S}{\rho c}(1-M^2) \sin \frac{k\ell}{1-M^2}\right] Z_2 + \left[\cos \frac{k\ell}{1-M^2} + jM \sin \frac{k\ell}{1-M^2}\right]} \quad \text{— III-7}$$

Where $Z_2 = P_2 / V_2$

For an infinite duct, impedances along the duct are constant, so $Z_1 = Z_2$

$$Z_2 \cos \frac{k\ell}{1-M^2} - jZ_2 M \sin \frac{k\ell}{1-M^2} + j\frac{\rho c}{S} \sin \frac{k\ell}{1-M^2}$$

$$= Z_2 \cos \frac{k\ell}{1-M^2} + jZ_2 M \sin \frac{k\ell}{1-M^2} + j\frac{S}{\rho c} Z_2^2 (1-M^2) \sin \frac{k\ell}{1-M^2}$$

$$\frac{S}{\rho c}(1-M^2) Z_2^2 + 2MZ_2 - \frac{\rho c}{S} = 0$$

$$\therefore \quad Z_2 = \frac{-2M \pm \sqrt{4M^2 + 4(1-M^2)}}{2\frac{S}{\rho c}(1-M^2)}$$

$$Z_2 = -\frac{\rho c}{S} \frac{1}{1-M} \quad \text{——————— III — 8}$$

$$\text{or} \quad Z_2 = \frac{\rho c}{S} \frac{1}{1+M} \quad \text{——————— III — 9}$$

III-8 is the characteristic impedance for upstream wave propagation. The negative sign indicates that the wave travels in the opposite direction to that of positive values of l.
III-9 is the characteristic impedance for downstream wave propagation. Thus for a duct with flow there exist two values for characteristic impedance, depending on the direction of flow. Both these values simplify to $\rho c/S$ for $M = 0$.

3.3 Resonance in Ducts.

For a duct with an open end, Z_2 in equation III-7 would be zero. Therefore,

$$Z_1 = \frac{j \frac{\rho c}{S} \sin \frac{k\ell}{1-M^2}}{\cos \frac{k\ell}{1-M^2} + jM \sin \frac{k\ell}{1-M^2}}$$

$$|Z_1|^2 = \frac{\left(\frac{\rho c}{S}\right)^2 \sin^2 \frac{k\ell}{1-M^2}}{\cos^2 \frac{k\ell}{1-M^2} + M^2 \sin^2 \frac{k\ell}{1-M^2}}$$

For Z_1 to be a maximum or minimum, $d|Z_1|^2/d(k\ell) = 0$

This leads to, $\sin \frac{2k\ell}{1-M^2} = 0$

i.e. $\frac{2k\ell}{1-M^2} = 0, \pi, 2\pi, 3\pi, \ldots$

$\frac{k\ell}{1-M^2} = 0, \pi/2, \pi, 3\pi/2 \ldots$

$\frac{2\pi f}{c} \frac{\ell}{1-M^2} = 0, \pi/2, \pi, 3\pi/2 \ldots$

$\frac{\ell}{1-M^2} = 0, \frac{\lambda}{4}, \frac{\lambda}{2}, \frac{3\lambda}{4} \ldots$

For $\ell/(1-M^2) = 0, \lambda/2, \lambda \ldots$ $Z_1 = 0$.
This is the condition for resonance of an open duct.

For $\ell/(1-M^2) = \lambda/4, 3\lambda/4 \ldots$ $Z_1 = \frac{\rho c/S}{M}$

Thus for $M \neq 0$, Z_1 varies between a minimum of zero and a maximum of $(\rho c/S)/M$. For $M = 0$, Z_1 varies between zero and infinity.

For a duct with a closed end, Z_2 in equation III-7 would be infinity. Hence,

$$Z_1 = -j \frac{\rho c}{S} \frac{1}{1-M^2} \cot \frac{k\ell}{1-M^2} - \frac{\rho c}{S} \frac{M}{1-M^2}$$

For $\frac{\ell}{1-M^2} = 0, \lambda/2, \lambda \ldots$

$\frac{k\ell}{1-M^2} = 0, \pi, 2\pi, \ldots$ and $Z_1 = \infty$

For $\frac{\ell}{1-M^2} = \frac{\lambda}{4}, \frac{3\lambda}{4} \ldots$

$k\ell/(1-M^2) = \pi/2, 3\pi/2, \ldots$ and $Z_1 = -(\rho c/S)(M/(1-M^2))$

This is the condition of resonance of a closed duct, and is the condition of operation for the "$\frac{1}{4}$ wave tubes".

It will be seen that for both the open and closed duct,

when $\ell/(1-M^2) = n\frac{\lambda}{2}$ where $n = 1, 2, 3, \ldots\ldots$ Z_2 is transferred to Z_1, i.e. for a closed duct, $Z_1 = Z_2 = \infty$ and for an open duct, $Z_1 = Z_2 = 0$.

3.4 Matrix Element for Sound Source Connection.

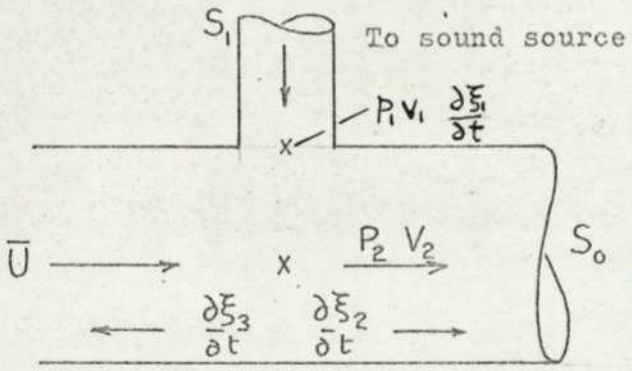

Fig. III-3

Fig. III-3 shows the side branch connection to the sound source. This type of arrangement is studied here because it is the kind that is used in the experimental set-up described in this thesis. V_2 is the volume velocity in the pipe travelling to the right. The pipe to the left of the connection is terminated by non-reflective material, thus giving an upstream characteristic impedance $\rho c/S_o(1-M)$. ξ is the particle displacement due to the sound wave alone and $\bar{U}$ is the mean gas flow velocity along the duct.

Since pipe dimensions are small compared with the wavelengths $P_1 = P_2$.

Assuming no gas flow down the side branch, continuity of flow gives,

$$S_1\left\{\frac{\partial \xi_1}{\partial t}\right\} = S_o\left\{\frac{\partial \xi_2}{\partial t} + \bar{U}\right\} + S_o\left\{\frac{\partial \xi_3}{\partial t} - \bar{U}\right\}$$

$$S_1\frac{\partial \xi_1}{\partial t} = S_o\frac{\partial \xi_2}{\partial t} + S_o\frac{\partial \xi_3}{\partial t}$$

i.e. $$V_1 = V_2 + \frac{P_2}{\rho c/S_o(1-M)}$$

The connection to the source is therefore represented by the following matrix,

$$\begin{bmatrix} P_1 \\ V_1 \end{bmatrix} = \begin{bmatrix} 1 & 0 \\ \frac{S_o}{\rho c}(1-M) & 1 \end{bmatrix} \begin{bmatrix} P_2 \\ V_2 \end{bmatrix}$$

$$= \begin{bmatrix} 1 & 0 \\ S_o/\rho c & 1 \end{bmatrix} \begin{bmatrix} P_2 \\ V_2 \end{bmatrix} \quad \text{for } M = 0.$$

3.5 Matrix Element for Transducer Connection.

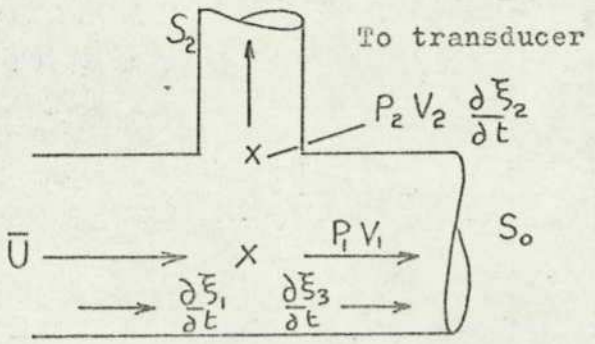

Fig. III-4

Fig. III-4 shows the transducer connection. The pipe to the right is terminated by the downstream characteristic impedance $\rho c / S_o(1+M)$.

Again $P_1 = P_2$ and assuming no flow down the side branch,

$$S_o \left\{ \frac{\partial \xi_1}{\partial t} + \bar{U} \right\} = S_2 \left\{ \frac{\partial \xi_2}{\partial t} \right\} + S_o \left\{ \frac{\partial \xi_3}{\partial t} + \bar{U} \right\}$$

$$S_o \frac{\partial \xi_1}{\partial t} = S_2 \frac{\partial \xi_2}{\partial t} + S_o \frac{\partial \xi_3}{\partial t}$$

i.e. $$V_1 = V_2 + \frac{P_2}{\rho c / S_o(1+M)}$$

Thus

$$\begin{bmatrix} P_1 \\ V_1 \end{bmatrix} = \begin{bmatrix} 1 & 0 \\ \frac{S_o}{\rho c}(1+M) & 1 \end{bmatrix} \begin{bmatrix} P_2 \\ V_2 \end{bmatrix}$$

$$= \begin{bmatrix} 1 & 0 \\ S_o/\rho c & 1 \end{bmatrix} \begin{bmatrix} P_2 \\ V_2 \end{bmatrix} \quad \text{for } M = 0.$$

4.a THEORY FOR ACOUSTIC SILENCERS WITHOUT FLOW

4.a.1 Simple Expansion Chamber

Consider the configuration as shown in Fig. IV-1.

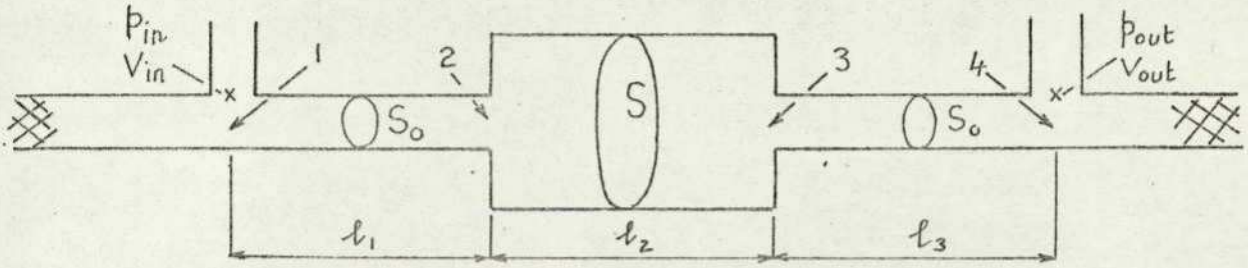

Fig. IV-1 Simple Expansion Chamber.

Both inlet and outlet pipes can be considered to be of equal cross-sectional area and of infinite length. With the assumption of continuity of pressure and volume velocity at discontinuities, the system is represented by,

$$\begin{bmatrix} p_{in} \\ V_{in} \end{bmatrix} = \begin{bmatrix} 1 & 0 \\ \frac{S_o}{\rho c} & 1 \end{bmatrix} \begin{bmatrix} \cos k\ell_1 & j\frac{\rho c}{S_o}\sin k\ell_1 \\ j\frac{S_o}{\rho c}\sin k\ell_1 & \cos k\ell_1 \end{bmatrix} \begin{bmatrix} \cos k\ell_2 & j\frac{\rho c}{S}\sin k\ell_2 \\ j\frac{S}{\rho c}\sin k\ell_2 & \cos k\ell_2 \end{bmatrix}$$

$$\begin{bmatrix} \cos k\ell_3 & j\frac{\rho c}{S_o}\sin k\ell_3 \\ j\frac{S_o}{\rho c}\sin k\ell_3 & \cos k\ell_3 \end{bmatrix} \begin{bmatrix} 1 & 0 \\ \frac{S_o}{\rho c} & 1 \end{bmatrix} \begin{bmatrix} p_{out} \\ V_{out} \end{bmatrix}$$

It is proved in Appendix 2 that values for ℓ_1 and ℓ_3 are immaterial. Thus the expression is simplified to :-

$$\begin{bmatrix} p_{in} \\ V_{in} \end{bmatrix} = \begin{bmatrix} 1 & 0 \\ \frac{S_o}{\rho c} & 1 \end{bmatrix} \begin{bmatrix} \cos k\ell_2 & j\frac{\rho c}{S}\sin k\ell_2 \\ j\frac{S}{\rho c}\sin k\ell_2 & \cos k\ell_2 \end{bmatrix} \begin{bmatrix} 1 & 0 \\ \frac{S_o}{\rho c} & 1 \end{bmatrix} \begin{bmatrix} p_{out} \\ V_{out} \end{bmatrix}$$

Since the microphone has a very high impedance, $V_{out} = 0$ and hence there is no reflected wave in the outlet pipe. p_{out} is the pressure of the incident wave in the outlet pipe.

$$V_{in} = \cos k\ell_2 \; \frac{S_o}{\rho c} \left[2 + j \tan k\ell_2 \left(\frac{S}{S_o} + \frac{S_o}{S} \right) \right] p_{out}$$

$$|V_{in}|^2 = \cos^2 k\ell_2 \; \frac{S_o^2}{(\rho c)^2} \left[4 + \tan^2 k\ell_2 \left(\frac{S}{S_o} + \frac{S_o}{S} \right)^2 \right] |p_{out}|^2$$

If the simple expansion chamber is replaced by a straight pipe as shown in Fig. IV-2, then $S = S_o$ in the matrix and there is no reflected wave in the pipe at all.

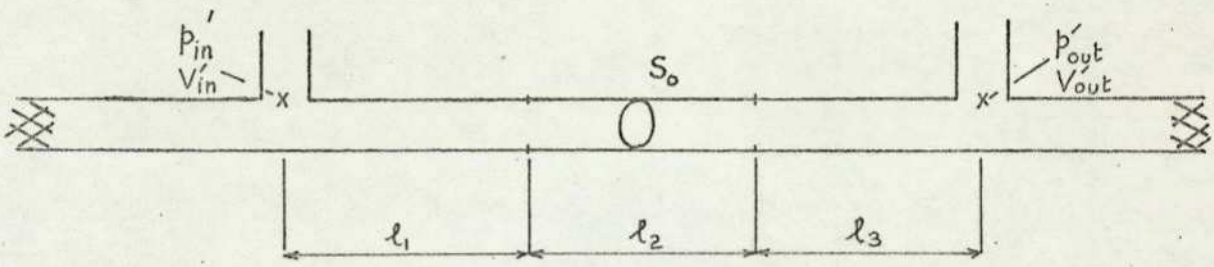

Fig. IV-2 Straight Pipe.

$$\begin{bmatrix} p'_{in} \\ V'_{in} \end{bmatrix} = \begin{bmatrix} 1 & 0 \\ \frac{S_o}{\rho c} & 1 \end{bmatrix} \begin{bmatrix} \cos k\ell_2 & j \frac{\rho c}{S_o} \sin k\ell_2 \\ j \frac{S_o}{\rho c} \sin k\ell_2 & \cos k\ell_2 \end{bmatrix} \begin{bmatrix} 1 & 0 \\ \frac{S_o}{\rho c} & 1 \end{bmatrix} \begin{bmatrix} p'_{out} \\ V'_{out} \end{bmatrix} \quad \text{— IV-2}$$

$$V_{in}' = \cos k\ell_2 \; \frac{S_o}{\rho c} \left(2 + j\, 2 \tan k\ell_2 \right) p'_{out}$$

$$|V_{in}'|^2 = 4 \; \frac{S_o^2}{(\rho c)^2} \; |p'_{out}|^2 \qquad \text{——— IV-3}$$

If the characteristic impedance of the branch pipe connected to the sound source is much greater than that of the inlet pipe, then $V_{in} \doteq V_{in}'$ and p'_{out} equals the pressure of incident wave in the inlet pipe with the muffer installed (Appendix 3).

Transmission loss or attenuation of the muffler is defined as :-

$$\text{Attenuation} = 10 \log_{10} \frac{|p'_{out}|^2}{|p_{out}|^2} \qquad \text{——— IV-4}$$

$$= 10 \log_{10} \frac{\dfrac{|V_{in}'|^2}{4 \dfrac{S_o^2}{(\rho c)^2}}}{\dfrac{|V_{in}|^2}{\cos^2 k\ell_2 \dfrac{S_o^2}{(\rho c)^2} \left[4 + \tan^2 k\ell_2 \left(\dfrac{S}{S_o} + \dfrac{S_o}{S} \right)^2 \right]}}$$

$$= 10 \log_{10} \left[1 + \frac{1}{4} \left(\frac{S}{S_o} - \frac{S_o}{S} \right)^2 \sin^2 k\ell_2 \right]$$

In general, any acoustic element in a no flow case can be represented by a four-element symmetrical matrix in the form $\begin{bmatrix} A & B \\ C & D \end{bmatrix}$ with A=D and AD-BC=1 and the expression for the system reads :-

$$\begin{bmatrix} P_{in} \\ V_{in} \end{bmatrix} = \begin{bmatrix} 1 & 0 \\ S_o/\rho c & 1 \end{bmatrix} \begin{bmatrix} A & B \\ C & D \end{bmatrix} \begin{bmatrix} 1 & 0 \\ S_o/\rho c & 1 \end{bmatrix} \begin{bmatrix} P_{out} \\ V_{out} \end{bmatrix}$$

The transmission loss or attenuation of the system would be found in a similar manner as shown above, i.e. by the process of replacing the acoustic element by a straight pipe. The method is used to obtain the attenuation for the other silencing configurations in this chapter unless stated otherwise.

4.a.2 Resonator With a Neck

The system is represented by Fig. IV-3 and the matrix equation for the system is given by equation IV - 5.

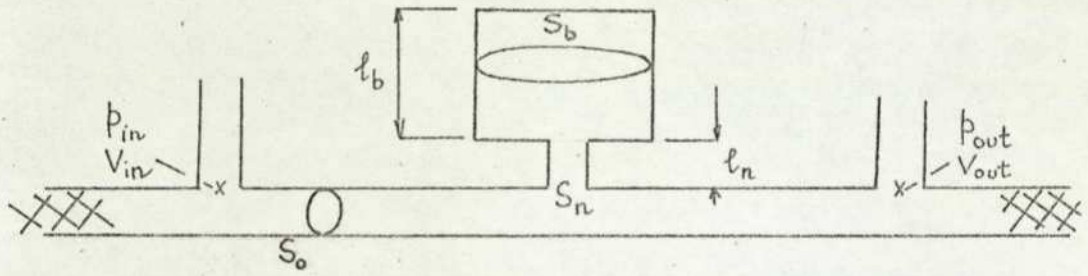

Fig. IV-3 Resonator.

$$\begin{bmatrix} P_{in} \\ V_{in} \end{bmatrix} = \begin{bmatrix} 1 & 0 \\ S_o/\rho c & 1 \end{bmatrix} \begin{bmatrix} 1 & 0 \\ \frac{1}{Z_R} & 1 \end{bmatrix} \begin{bmatrix} 1 & 0 \\ S_o/\rho c & 1 \end{bmatrix} \begin{bmatrix} P_{out} \\ V_{out} \end{bmatrix} \quad \text{— IV 5}$$

Z_R is the combined impedance of the resonator and its neck. This impedance value equals the resultant series value of the separate impedances of the resonator cavity and the neck with damping neglected and is given by (35) as $j\frac{\rho\omega}{c_o} + \frac{\rho c}{S_b} \frac{1}{j\tan k\ell_b}$

where S_b = cross-sectional area of the resonator.
c_o = conductivity of neck.

$$= \frac{S_n}{\ell''_n}$$

and where S_n = cross-sectional area of neck.
ℓ''_n = effective length of neck
= physical length of neck + constant x radius of neck.

For no flow cases, this constant has been found to lie somewhere between 1.5 and 1.7 (3,4,6,35), and in this work the value of 1.7 has been used.

For resonator necks consisting of multiple openings the determination of C_o is very much an empirical procedure. The same can be said for resonators with considerable viscous damping in the neck.

When the frequency under consideration is low, the 'Lumped Parameter Method' can be used, and $\tan k\ell_b \longrightarrow k\ell_b$.

$$Z_R = j\frac{\rho\omega}{C_o} + \frac{\rho c}{S_b}\frac{1}{jk\ell_b}$$

$$= j\frac{\rho\omega}{C_o} + \frac{\rho c^2}{j\omega V_b}$$

where $V_b = S_b\ell_b$ = volume of resonator cavity.

When $$j\frac{\rho\omega}{C_o} + \frac{\rho c^2}{j\omega V_b} = 0$$

$$\omega = c\sqrt{\frac{C_o}{V_b}} = c\sqrt{\frac{S_n}{S_b\ell_b\ell_n''}} \qquad \text{IV - 6}$$

This is defined as the resonant frequency of the resonator and at this frequency the attenuation is greatest.

The resonant frequency of a resonator depends critically on the value of C_o and the shape of the attenuation - frequency curve depends on the parameter $\frac{\sqrt{C_o V_b}}{2S_o}$ (4).

The larger this parameter becomes, the broader is the attenuation peak. Thus in silencer design the effect of a slight inaccuracy in the selection of the resonant frequency can be minimised by choosing a large value of $\frac{\sqrt{C_o V_b}}{2S_o}$.

Viscous friction in the resonator neck can be considerable if the neck diameter is small. This friction is usually assumed to be proportional to the particle velocity in the neck. For the resonator necks considered in this work the viscous friction term was neglected.

4.a.3 Expansion Chamber With Internal Pipes

This system is shown in Fig. IV-4. It can be

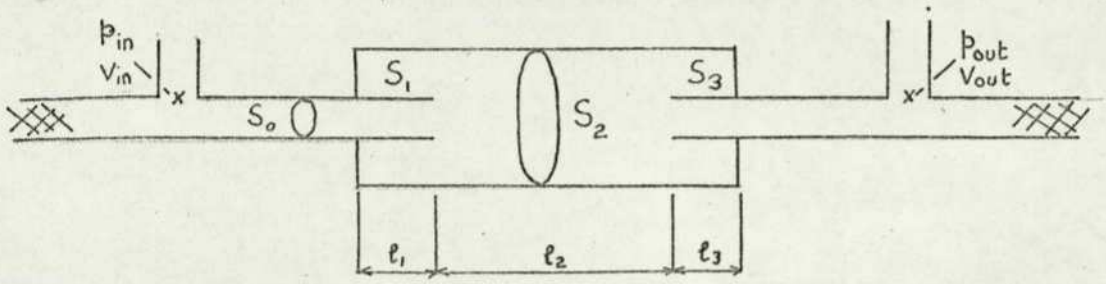

Fig. IV-4 Expansion Chamber with Internal Tubes.

treated as an expansion chamber of length ℓ_2 and area S_2, with two closed branch pipes of lengths ℓ_1 and ℓ_3, and areas S_1, and S_3 respectively connected to the ends. The matrix representation of this element reads :-

$$\begin{bmatrix} p_{in} \\ V_{in} \end{bmatrix} = \begin{bmatrix} 1 & 0 \\ \frac{S_0}{\rho c} & 1 \end{bmatrix} \begin{bmatrix} 1 & 0 \\ \frac{1}{Z_1} & 1 \end{bmatrix} \begin{bmatrix} \cos k\ell_2 & j\frac{\rho c}{S_2}\sin k\ell_2 \\ j\frac{S_2}{\rho c}\sin k\ell_2 & \cos k\ell_2 \end{bmatrix} \begin{bmatrix} 1 & 0 \\ \frac{1}{Z_3} & 1 \end{bmatrix} \begin{bmatrix} 1 & 0 \\ \frac{S_0}{\rho c} & 1 \end{bmatrix} \begin{bmatrix} p_{out} \\ V_{out} \end{bmatrix}$$

$$= \begin{bmatrix} 1 & 0 \\ \frac{S_0}{\rho c} & 1 \end{bmatrix} \begin{bmatrix} 1 & 0 \\ -j\frac{1}{\frac{\rho c}{S_1}\cot k\ell_1} & 1 \end{bmatrix} \begin{bmatrix} \cos k\ell_2 & j\frac{\rho c}{S_2}\sin k\ell_2 \\ j\frac{S_2}{\rho c}\sin k\ell_2 & \cos k\ell_2 \end{bmatrix} \begin{bmatrix} 1 & 0 \\ -j\frac{1}{\frac{\rho c}{S_3}\cot k\ell_3} & 1 \end{bmatrix} \begin{bmatrix} 1 & 0 \\ \frac{S_0}{\rho c} & 1 \end{bmatrix} \begin{bmatrix} p_{out} \\ V_{out} \end{bmatrix} \quad \text{— IV-7}$$

where $S_1 = S_3 = S_2 - S_0$

Z_1 is the impedance of the first branch pipe measured at the exit of the inlet pipe, and Z_3 is the impedance of the second branch pipe measured at the entrance of the outlet pipe. (See Appendix 4)

4.a.4 Expansion Chamber With Resonator

This system consists of a simple expansion chamber in series with a resonator as shown in Fig. IV-5 and can be represented by equation IV - 8.

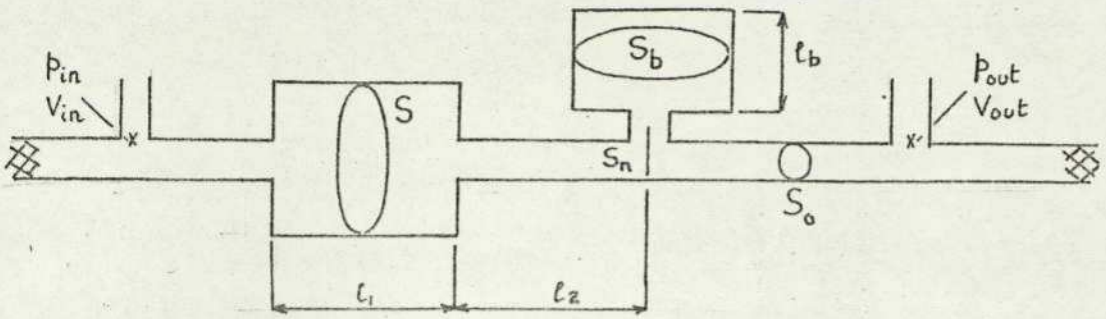

Fig. IV-5 Expansion Chamber in Series with Resonator.

$$\begin{bmatrix} p_{in} \\ V_{in} \end{bmatrix} = \begin{bmatrix} 1 & 0 \\ \frac{S_o}{\rho c} & 1 \end{bmatrix} \begin{bmatrix} \cos k\ell_1 & j\frac{\rho c}{S}\sin k\ell_1 \\ j\frac{S}{\rho c}\sin k\ell_1 & \cos k\ell_1 \end{bmatrix} \begin{bmatrix} \cos k\ell_2 & j\frac{\rho c}{S_o}\sin k\ell_2 \\ j\frac{S_o}{\rho c}\sin k\ell_2 & \cos k\ell_2 \end{bmatrix}$$

$$\begin{bmatrix} 1 & 0 \\ 1/\left\{ j\frac{\rho\omega\ell_n''}{S_n} + \frac{\rho c}{S_b}\frac{1}{j\tan k\ell_b} \right\} & 1 \end{bmatrix} \begin{bmatrix} 1 & 0 \\ \frac{S_o}{\rho c} & 1 \end{bmatrix} \begin{bmatrix} p_{out} \\ V_{out} \end{bmatrix} \qquad \text{IV-8}$$

4.a.5 Finite Outlet Pipe

A silencing system with a simple expansion chamber and a finite outlet pipe is shown in Fig. IV-6.

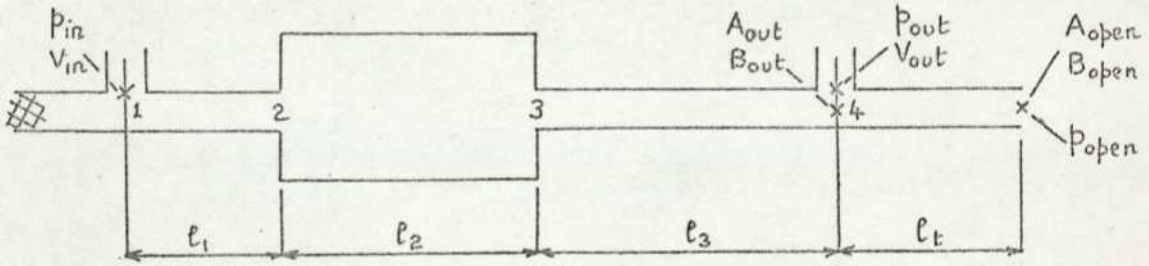

Fig. IV-6 Simple Expansion Chamber with Finite Outlet Pipe.

The finite outlet pipe length is ℓ_t and it has an open end. A_{out} and B_{out} are amplitudes of the incident and reflected pressure waves respectively at point 4 of the outlet pipe. A_{open} and B_{open} are amplitudes of the incident and reflected pressure waves respectively at open end of the outlet pipe. This system reads :-

$$\begin{bmatrix} p_{in} \\ V_{in} \end{bmatrix} = \begin{bmatrix} 1 & 0 \\ \frac{S_o}{\rho c} & 1 \end{bmatrix} \begin{bmatrix} \cos k\ell_2 & j\frac{\rho c}{S}\sin k\ell_2 \\ j\frac{S}{\rho c}\sin k\ell_2 & \cos k\ell_2 \end{bmatrix} \begin{bmatrix} \cos k\ell_3 & j\frac{\rho c}{S_o}\sin k\ell_3 \\ j\frac{S_o}{\rho c}\sin k\ell_3 & \cos k\ell_3 \end{bmatrix} \begin{bmatrix} 1 & 0 \\ \frac{1}{j\frac{\rho c}{S_o}\tan k\ell_t} & 1 \end{bmatrix} \begin{bmatrix} p_{out} \\ V_{out} \end{bmatrix} \qquad \text{IV-9}$$

$1/j\frac{\rho c}{S_o}\tan k\ell_t$ is the impedance of the part of the outlet pipe length ℓ_t, measured between point 4 and the open end. (See Appendix 5)

The relationship between P_{out} and A_{out} at point 4 is given by,

$$|p_{out}| = |A_{out}| \cdot 2 \sin k\ell_t \qquad \text{(See Appendix 6)}$$

Since the sound pressure in the open air due to an outlet pipe with open end is, at a given frequency, directly proportional to the pressure of the incident wave travelling in the pipe (4), the attenuation of this system is defined as :-

$$\text{Attenuation} = 10 \log_{10} |p_{out}'|^2 / |A_{out}|^2 \qquad \text{— IV 10}$$

Where P_{out}' is defined as under section 4.a.1 of this chapter. (See eq. IV - 3)

Another silencing system with a resonator and a finite outlet pipe is shown in Fig. IV-7.

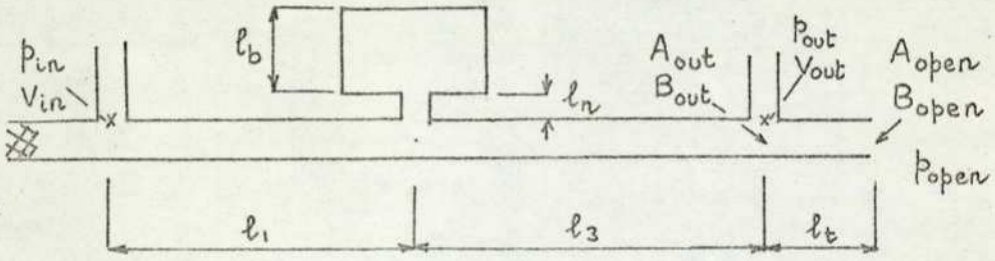

Fig.IV-7 Resonator with Finite Outlet Pipe.

This system is represented by :-

$$\begin{bmatrix} p_{in} \\ V_{in} \end{bmatrix} = \begin{bmatrix} 1 & 0 \\ S_o/\rho c & 1 \end{bmatrix} \begin{bmatrix} 1 & 0 \\ 1/\left\{ j\frac{\rho\omega\ell_n''}{S_n} + \frac{\rho c}{S_b} j\frac{1}{\tan k\ell_b} \right\} & 1 \end{bmatrix}$$

$$\begin{bmatrix} \cos k\ell_3 & j\frac{\rho c}{S_o}\sin k\ell_3 \\ j\frac{S_o}{\rho c}\sin k\ell_3 & \cos k\ell_3 \end{bmatrix} \begin{bmatrix} 1 & 0 \\ 1/j\frac{\rho c}{S_o}\tan k\ell_t & 1 \end{bmatrix} \begin{bmatrix} p_{out} \\ V_{out} \end{bmatrix} \qquad \text{— IV-11}$$

where again $|p_{out}| = |A_{out}| \cdot 2\sin k\ell_t$

Attenuation of this system is again defined as in eq. IV - 10

4.a.6 Finite Inlet Pipe.

Fig. IV-8 shows a system consisting of a simple expansion chamber with a finite inlet pipe.

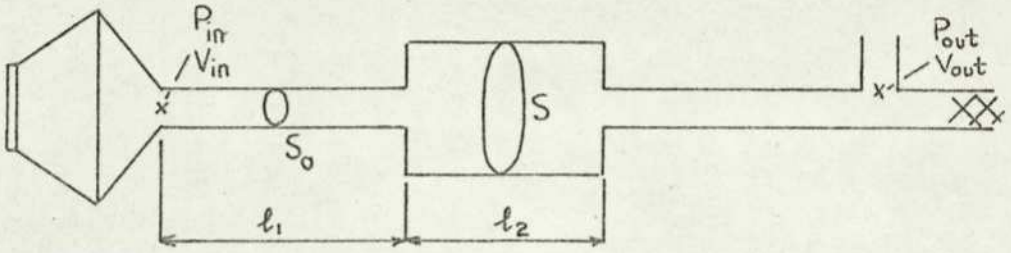

Fig. IV-8. Simple Expansion Chamber with finite inlet pipe.

This system reads :-

$$\begin{bmatrix} P_{in} \\ V_{in} \end{bmatrix} = \begin{bmatrix} \cos k\ell_1 & j\frac{\rho c}{S_0}\sin k\ell_1 \\ j\frac{S_0}{\rho c}\sin k\ell_1 & \cos k\ell_1 \end{bmatrix} \begin{bmatrix} \cos k\ell_2 & j\frac{\rho c}{S}\sin k\ell_2 \\ j\frac{S}{\rho c}\sin k\ell_2 & \cos k\ell_2 \end{bmatrix} \begin{bmatrix} 1 & 0 \\ \frac{S_0}{\rho c} & 1 \end{bmatrix} \begin{bmatrix} P_{out} \\ V_{out} \end{bmatrix} \qquad \text{IV - 12}$$

Fig. IV-9 shows a straight pipe with its inlet side connected to a loudspeaker while the outlet side is infinitely long.

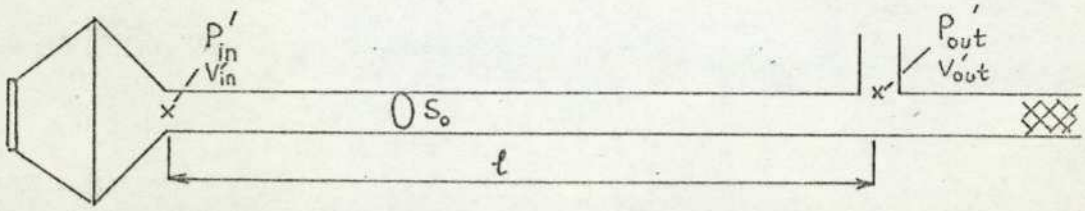

Fig. IV-9. Straight Pipe with finite inlet pipe.

This system is represented by the following matrix :-

$$\begin{bmatrix} P'_{in} \\ V'_{in} \end{bmatrix} = \begin{bmatrix} \cos k\ell & j\frac{\rho c}{S_0}\sin k\ell \\ j\frac{S_0}{\rho c}\sin k\ell & \cos k\ell \end{bmatrix} \begin{bmatrix} 1 & 0 \\ \frac{S_0}{\rho c} & 1 \end{bmatrix} \begin{bmatrix} P'_{out} \\ V'_{out} \end{bmatrix}$$

$$|V'_{in}|^2 = \frac{S_0^2}{(\rho c)^2}\,|P'_{out}|^2 \qquad \text{IV - 13}$$

Equation IV-13 can be compared with equation IV-3.

As the impedance of the loudspeaker is much greater than that of the system connected to it the inlet volume velocity remains constant.

Attenuation for a system with a finite inlet pipe is defined as

$$10 \log_{10} \frac{|P'_{out}|^2}{|P_{out}|^2} .$$

Another system with a resonator and a finite inlet pipe is shown in Fig. IV-10.

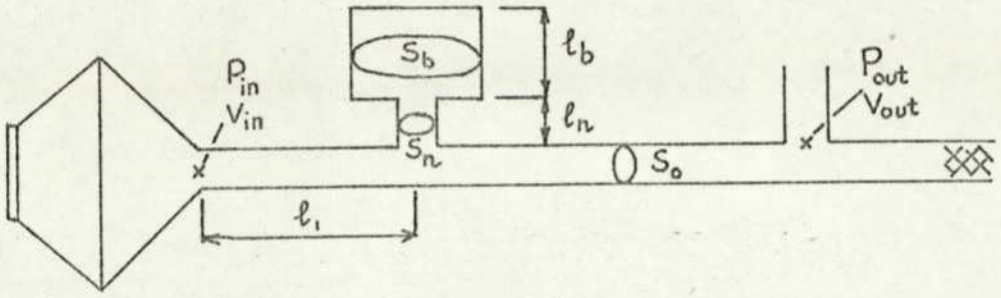

Fig. IV-10. Resonator with finite inlet pipe.

This system reads :-

$$\begin{bmatrix} P_{in} \\ V_{in} \end{bmatrix} = \begin{bmatrix} \cos k\ell_1 & j\frac{\rho c}{S_o} \sin k\ell_1 \\ j\frac{S_o}{\rho c} \sin k\ell_1 & \cos k\ell_1 \end{bmatrix} \begin{bmatrix} 1 & 0 \\ 1/\left\{ \frac{j\rho\omega\ell''_n}{S_n} + \frac{\rho c}{S_b} \frac{1}{j\tan k\ell_b} \right\} & 1 \end{bmatrix}$$

$$\begin{bmatrix} 1 & 0 \\ \frac{S_o}{\rho c} & 1 \end{bmatrix} \begin{bmatrix} P_{out} \\ V_{out} \end{bmatrix} \qquad \text{— IV — 14}$$

Attenuation is again defined, with reference to equation IV-13, as

$$10 \log_{10} \frac{|P'_{out}|^2}{|P_{out}|^2} .$$

4.b THEORY FOR ACOUSTIC SILENCERS WITH MEAN FLOW

4.b.1 Simple Expansion Chamber

Consider the system shown in Fig. IV-1 with a continuous airflow in the system, M_1 , M_2 are the mean mach numbers of the flow in the various sections of the system of length, ℓ_1 , ℓ_2 etc. A uniform flow profile is assumed in all sections of the system. With reference to Chapter III and Appendix 2, and with again the assunption of continuity of pressure and volume velocity at discontinuities, the expression representing the system can be written down as :-

$$\begin{bmatrix} p_{in} \\ V_{in} \end{bmatrix} = \begin{bmatrix} 1 & 0 \\ \frac{S_o}{\rho c}(1-M_1) & 1 \end{bmatrix} \begin{bmatrix} \cos \frac{k\ell_2}{1-M_2^2} - jM_2 \sin \frac{k\ell_2}{1-M_2^2} & j\frac{\rho c}{S} \sin \frac{k\ell_2}{1-M_2^2} \\ j\frac{S}{\rho c}(1-M_2^2) \sin \frac{k\ell_2}{1-M_2^2} & \cos \frac{k\ell_2}{1-M_2^2} + jM_2 \sin \frac{k\ell_2}{1-M_2^2} \end{bmatrix}$$

$$\begin{bmatrix} 1 & 0 \\ \frac{S_o}{\rho c}(1+M_1) & 1 \end{bmatrix} \begin{bmatrix} p_{out} \\ V_{out} \end{bmatrix} \qquad \text{—— IV – 15}$$

V_{in} can be obtained by applying a procedure similar to that used in the no flow case.

$$V_{in} = \frac{S_o}{\rho c}\left[2\cos \frac{k\ell_2}{1-M_2^2} + j\,2M_1M_2 \sin \frac{k\ell_2}{1-M_2^2} + j\left(\frac{S}{S_o} + \frac{S_o}{S}\right)\sin \frac{k\ell_2}{1-M_2^2} - j\left(\frac{S}{S_o}M_2^2 + \frac{S_o}{S}M_1^2\right)\sin \frac{k\ell_2}{1-M_2^2}\right] p_{out}$$

For steady flow $S_o M_1 = S M_2$

$$V_{in} = \frac{S_o}{\rho c}\left[2\cos \frac{k\ell_2}{1-M_2^2} + j\left(\frac{S}{S_o} + \frac{S_o}{S}\right)\sin \frac{k\ell_2}{1-M_2^2}\right] p_{out}$$

$$|V_{in}|^2 = \left(\cos^2 \frac{k\ell_2}{1-M_2^2}\right)\left(\frac{S_o}{\rho c}\right)^2 \left[4 + \left(\tan^2 \frac{k\ell_2}{1-M_2^2}\right)\left(\frac{S}{S_o} + \frac{S_o}{S}\right)^2\right] |p_{out}|^2$$

If the muffler is replaced by a straight pipe as shown in Fig. IV-2 then S=S. and as in the no-flow case,

$$|V_{in}'|^2 = 4\left(\frac{S_o}{\rho c}\right)^2 |p_{out}'|^2 \qquad \text{—— IV–16}$$

Transmission loss or attenuation of the silencing system is again defined as in a no-flow case :-

$$\text{Attenuation} = 10 \log_{10} \frac{|p_{out}'|^2}{|p_{out}|^2} \qquad \text{—— IV 17}$$

$$= 10 \log_{10}\left[1 + \frac{1}{4}\left(\frac{S}{S_o} - \frac{S_o}{S}\right)^2 \sin^2 \frac{k\ell_2}{1-M_2^2}\right]$$

Eq. IV-16 shows that for a straight pipe the air flow does not affect acoustic transmission in the pipe in anyway. Since both sound source and transducer were stationary with respect to a fixed reference frame, a Doppler shift in frequency does not occur. The final expression for the attenuation shows that the Attenuation Frequency Characteristic for a simple expansion chamber will have the same maximum attenuation with or without flow. The effect of the flow is to change the wave number from K to $K/(1-M_2^2)$ and thus the loops in the curve will be contracted. The effect of this change in wave number for a simple expansion chamber is equivalent to increasing the length of the chamber. Only the mach number inside the expansion chamber will affect the attenuation and this mach number is usually quite small.

4.b.2 Resonator With A Neck

The system is represented by Fig. IV-3 with mach no. M_o in the pipe area S_o. No flow is assumed in the resonator and hence its impedance remains the same as that in a no-flow case. The system reads :-

$$\begin{bmatrix} p_{in} \\ V_{in} \end{bmatrix} = \begin{bmatrix} 1 & 0 \\ \frac{S_o}{\rho c}(1-M_o) & 1 \end{bmatrix} \begin{bmatrix} 1 & 0 \\ \frac{1}{Z_R} & 1 \end{bmatrix} \begin{bmatrix} 1 & 0 \\ \frac{S_o}{\rho c}(1+M_o) & 1 \end{bmatrix} \begin{bmatrix} p_{out} \\ V_{out} \end{bmatrix} \quad \text{— IV-18}$$

where Z_R = impedance of the resonator

$$= j \frac{\rho \omega}{c_o} + \frac{\rho c}{S_b} \quad \frac{1}{j \tan k \ell_b}$$

$$V_{in} = \left(2 \frac{S_o}{\rho c} + \frac{1}{Z_R}\right) p_{out}$$

This expression is identical to that for a no-flow case, and thus according to the hypothesis of no flow in the resonator the gas flow in the system will not affect the above defined attenuation of the system at all. The analysis of this system is therefore similar to that of section 4.a.2

Attenuation has been calculated according to the definition given in eq. IV-17. Thus the entire Attenuation Frequency Characteristic for a resonator system with flow will be identical to that for a system without flow.

In practice gas will enter the resonator and a mathematical analysis for the flow in the resonator is difficult. Discrepancies between theoretical and experimental results are thus to be expected.

4.b.3 Expansion Chamber With Internal Tubes

This system is shown in Fig. IV-4. The mach number for the inlet and outlet pipes is M_o and the mach number for the central part of length ℓ_2 is M_2

In practice turbulence flow will exist in the equivalent branches ℓ_1 and ℓ_3. However, to facilitate a theoretical analysis, no air flow is assumed in these branches. Thus the impedance for these branches would be represented by the expression given in Appendix 4. The expression for this system reads :-

$$\begin{bmatrix} p_{in} \\ V_{in} \end{bmatrix} = \begin{bmatrix} 1 & 0 \\ \frac{S_o}{\rho c}(1-M_o) & 1 \end{bmatrix} \begin{bmatrix} 1 & 0 \\ -j\,\frac{1}{\frac{\rho c}{S_1}\cot k\ell_1} & 1 \end{bmatrix}$$

$$\begin{bmatrix} \cos k\ell_2/(1-M_2^2) - jM_2 \sin k\ell_2/(1-M_2^2) & j\frac{\rho c}{S_2}\sin k\ell_2/(1-M_2^2) \\ j\frac{S_o}{\rho c}(1-M_2^2)\sin k\ell_2/(1-M_2^2) & \cos k\ell_2/(1-M_2^2) + jM_2 \sin k\ell_2/(1-M_2^2) \end{bmatrix}$$

$$\begin{bmatrix} 1 & 0 \\ 1/(-j\,\frac{\rho c}{S_3}\cot k\ell_3) & 1 \end{bmatrix} \begin{bmatrix} 1 & 0 \\ \frac{S_o}{\rho c}(1+M_o) & 1 \end{bmatrix} \begin{bmatrix} p_{out} \\ V_{out} \end{bmatrix} \quad \text{IV-19}$$

This mathematical model is unlikely to be applicable in practice, especially in high frequency regions and regions where the two equivalent branches will be expected to have a prominent effect.

4.b.4 Simple Expansion Chamber In Series With Resonator

Fig. IV-5 represents this system. Flow is assumed only in the inlet, outlet, connecting pipes, and the expansion chamber but not in the resonator.

$$\begin{bmatrix} p_{in} \\ V_{in} \end{bmatrix} = \begin{bmatrix} 1 & 0 \\ \frac{S_o}{\rho c}(1-M_o) & 1 \end{bmatrix}$$

$$\begin{bmatrix} \cos k\ell_1/(1-M_1^2) - jM_1 \sin k\ell_1/(1-M_1^2) & j\frac{\rho c}{S}\sin k\ell_1/(1-M_1^2) \\ j\frac{S}{\rho c}(1-M_1^2)\sin k\ell_1/(1-M_1^2) & \cos k\ell_1/(1-M_1^2) + jM_1 \sin k\ell_1/(1-M_1^2) \end{bmatrix}$$

$$\begin{bmatrix} \cos k\ell_2/(1-M_2^2) - jM_2 \sin k\ell_2/(1-M_2^2) & j\frac{\rho c}{S_o}\sin k\ell_2/(1-M_2^2) \\ j\frac{S_o}{\rho c}(1-M_2^2)\sin k\ell_2/(1-M_2^2) & \cos k\ell_2/(1-M_2^2) + jM_2 \sin k\ell_2/(1-M_2^2) \end{bmatrix}$$

$$\begin{bmatrix} 1 & 0 \\ 1/Z_R & 1 \end{bmatrix} \begin{bmatrix} 1 & 0 \\ \frac{S_o}{\rho c}(1+M_o) & 1 \end{bmatrix} \begin{bmatrix} p_{out} \\ V_{out} \end{bmatrix} \quad \text{—— IV 20}$$

Where Z_R = impedance of the resonator

$$= j\,\frac{\rho\omega}{c_o} + \frac{\rho c}{S_b}\,\frac{1}{j\tan k\ell_b}$$

$M_2 = M_o$ = mean mach no. in pipes with area S_o

M_1 = mean mach no. in simple expansion chamber with area S.

4.b.5 Finite Outlet Pipe With Flow

The system shown in Fig. IV-6 with a mean flow is considered. This system is represented as :-

$$\begin{bmatrix} P_{in} \\ V_{in} \end{bmatrix} = \begin{bmatrix} 1 & 0 \\ \frac{S_o}{\rho c}(1-M_1) & 1 \end{bmatrix} \begin{bmatrix} \cos\frac{k\ell_2}{1-M_2^2} - jM_2 \sin\frac{k\ell_2}{1-M_2^2} & j\frac{\rho c}{S}\sin\frac{k\ell_2}{1-M_2^2} \\ j\frac{S}{\rho c}(1-M_2^2)\sin\frac{k\ell_2}{1-M_2^2} & \cos\frac{k\ell_2}{1-M_2^2} + jM_2\sin\frac{k\ell_2}{1-M_2^2} \end{bmatrix}$$

$$\begin{bmatrix} \cos\frac{k\ell_3}{1-M_3^2} - jM_3\sin\frac{k\ell_3}{1-M_3^2} & j\frac{\rho c}{S_o}\sin\frac{k\ell_3}{1-M_3^2} \\ j\frac{S_o}{\rho c}(1-M_3^2)\sin\frac{k\ell_3}{1-M_3^2} & \cos\frac{k\ell_3}{1-M_3^2} + jM_3\sin\frac{k\ell_3}{1-M_3^2} \end{bmatrix}$$

$$\begin{bmatrix} 1 & 0 \\ \frac{S_o}{\rho c}M_t - j\frac{S_o}{\rho c}\cot\frac{k\ell_t}{1-M_t^2} & 1 \end{bmatrix} \begin{bmatrix} P_{out} \\ V_{out} \end{bmatrix} \qquad \text{—— IV – 21}$$

(see Appendix 5)

$$|P_{out}| = |A_{out}| \cdot 2\sin\frac{k\ell_t}{1-M_t^2} \qquad \text{———— IV – 22}$$

(see Appendix 6)

$M_1 = M_3 = M_t$ = mean mach no. in pipes of area S_o

M_2 = mean mach no. in simple expansion chamber area S.

A_{out} is then compared to P'_{out} as defined in eq. IV-16 and :-

$$\text{Attenuation} = 10\log_{10}\frac{|P'_{out}|^2}{|A_{out}|^2} \qquad \text{—— IV – 23}$$

Alternatively, A_{out} can be compared to the incident wave in a finite straight pipe of the same length as that of the silencer system with a mean flow. The expression for this system can be obtained by substituting in eq. IV-21 $S = S_o$ and $M_2 = M_1 = M_3 = M_t$. The final outcome of the mathematical manipulation leads to,

$$|V'_{in}|^2 = 4\frac{S_o^2}{(\rho c)^2}|A'_{out}|^2 \qquad \text{—— IV – 24}$$

Where V'_{in} = Inlet volume velocity of the finite straight pipe.

A'_{out} = Incident pressure wave amplitude in the finite straight pipe.

In this case,

$$\text{Attenuation} = 10\log_{10}\frac{|A'_{out}|^2}{|A_{out}|^2} \qquad \text{—— IV – 25}$$

Comparison of eq. IV-16 and eq. IV-24 indicates that the flow is in no way affecting the acoustic transmission in a finite straight pipe and there is no physical difference in comparing A_{out} of the silencer system to the incident wave in a finite or infintie straight pipe. This is applicable also to a case without flow.

A system with a resonator and a finite outlet pipe, as shown in Fig. IV-7, with a mean flow is represented by equation IV-26

$$\begin{bmatrix} P_{in} \\ V_{in} \end{bmatrix} = \begin{bmatrix} 1 & 0 \\ \frac{S_o}{\rho c}(1-M_1) & 1 \end{bmatrix} \begin{bmatrix} 1 & 0 \\ 1 \Big/ \left\{ j \frac{\rho \omega l''_n}{S_n} + \frac{\rho c}{S_b} \frac{1}{j \tan k l_b} \right\} & 1 \end{bmatrix}$$

$$\begin{bmatrix} \cos \frac{k}{1-M_3^2} l_3 & -j M_3 \sin \frac{k}{1-M_3^2} l_3 & j \frac{\rho c}{S_o} \sin \frac{k}{1-M_3^2} l_3 \\ j \frac{S_o}{\rho c}(1-M_3^2) \sin \frac{k}{1-M_3^2} l_3 & \cos \frac{k}{1-M_3^2} l_3 + j M_3 \sin \frac{k}{1-M_3^2} l_3 & \end{bmatrix}$$

$$\begin{bmatrix} 1 & 0 \\ \frac{S_o}{\rho c} M_t - j \frac{S_o}{\rho c} \cot \frac{k l_t}{1-M_t^2} & 1 \end{bmatrix} \begin{bmatrix} P_{out} \\ V_{out} \end{bmatrix} \quad \text{— IV-26}$$

where again,

$$|P_{out}| = |A_{out}| \cdot 2 \sin \frac{k l_t}{1-M_t^2}$$

$M_1 = M_3 = M_t$ = mean Mach number in pipes of area S_o .

Attenuation is defined as before for a system with a simple expansion chamber.

Theoretical results for Fig. VII-2 to Fig. VII-44 were obtained by substituting numerical values in equations IV-1 to IV-26.

APPARATUS

5.a. TEST RIG FOR EXPERIMENTS WITHOUT FLOW

5.a.1 Preliminary Tests

Before the test rig was constructed various preliminary tests were carried out in order to gain information which could be used in the design of the test rig.

It was found that insulation between loudspeaker and microphone was essential in order to prevent transmission of vibration and noise from the loudspeaker. Rigid holding of the test rig was also necessary.

Foam and glass wool were tested as absorbent materials and no substantial differences in absorptive properties were found. Comparative tests were carried out using the layout shown in Fig. V-1. The outlet pipe was filled with foam, glass wool or left empty and the signals received by the microphone were compared when tested with the same input. Foam was finally preferred because of ease of handling. As much foam as possible was packed in. Satisfactory absorption at low frequencies, particularly at below 100 Hz, was found to be extremely difficult.

Small obstacles were found to cause only slight disturbance to the sound field within the range of test frequencies. The effect of small obstacles was investigated by recording signals with the microphone holder at two different positions, as shown in Fig. V-4a and V-4b. Fig. V-4a shows the microphone holder in the working position. Its end face was machined to fit the circular face of the test pipe. Fig. V-4b shows the microphone holder turned 90° along the vertical axis so that its curved end effectively provided a small obstacle to the sound field. Since readings taken in both cases were identical it was concluded that a $\frac{1}{8}$" microphone could be used to obtain experimental data accurately.

It has been shown theoretically that the longitudinal position of the microphone has no effect on the final result, and an experimental investigation confirmed this theoretical prediction.

5.a.2 Description of First Test Rig

The first test rig was set up as shown in Fig. V-1 for the straight pipe test. PVC pipes of 0.028 m internal diameter were used as the inlet and outlet pipes. A Rank Wharfedale 0.3 m diameter 20 W loudspeaker was used as the sound source. A sheet metal cone 0.6 m long, converging from 0.3 m to 0.013 m internal diameter, was made to join the loudspeaker to a 0.013 m diameter brass pipe, which in turn joined the inlet pipe at the side. The characteristic impedance of the air in the brass pipe would be about four times that of the inlet pipe.

A Bruel and Kjaer type 1024 sine wave generator was used to supply the signal through a Pye power amplifier to provide an input of about 10 W to the loudspeaker. The frequency of the signal was measured by an Advance Instruments digital frequency counter.

The loudspeaker-cone assembly was enclosed by a wooden box, which was then covered by sand in a concrete enclosure with 0.04 m wall thickness for noise insulation. At the receiving end a Bruel and Kjaer 1/8 in. condenser microphone was used as the signal pick-up. It was inserted into the outlet pipe at the side through a short perspex tube. A concentric layer of silicone rubber was inserted between the microphone and the perspex tube to avoid the transmission of any vibration and impact to the microphone. The pipe system and microphone were placed in sand to avoid interference from other sound sources and to prevent transmission of vibration. Both inlet and outlet pipes were terminated by foam strips, 1.3 m long, packed into 1 m of pipe length to simulate an infinite pipe. The noise level measured by the microphone was displayed on the meter of a Bruel and Kjaer type 2606 measuring amplifer.

5.b. TEST RIG FOR EXPERIMENTS WITH FLOW

5.b.1 Description of Second Test Rig

A second rig was constructed so that tests with an air flow could be carried out. See Fig. V-2. Brass pipes of 0.023 m internal diameter were used as the test section which would take various silencer configurations later in the experiment. This will be referred to as the main pipe. To each end of this main pipe a metal cone 1 m long, diverging from 0.023 m to 0.071 m internal diameter, was connected. The interiors of these two cones were lined with foam for sound absorption. To each of the cones was then connected approximately 4 m of 0.071 m internal diameter brass pipes with internal foam lining for further absorption. The foam lining for the brass pipe was in the form of circular rings 0.071 m diameter

with a 0.023 m diameter hole at the centre. A piece of fine wire mesh was rolled into the form of a cylinder 0.023 m in diameter and inserted through the hole in the foam rings. This was used to ensure a smooth flow of air through the pipes at both ends of the rig while the noise carried by the flow was absorbed. The air flow was supplied by a centrifugal fan giving a Mach number up to 0.2 . A piece of 60 gauge wire mesh was placed across the stream at a distance of 1 m from the fan at the entrance of the inlet pipe to reduce the turbulence of the flow. This arrangement managed to reduce the overall measured flow noise from 75 dB to 65 dB. Spectral analyses of the flow noise revealed that it had a substantially flat response between 50 Hz and 3 kHz. The effect of the fan was also reduced by connecting it to the inlet pipe through a flexible connector. Another piece of mesh was placed across the connecting pipe between the loudspeaker cone and the main test pipe to minimise the flow going down to the loudspeaker. A Fane 50 W loudspeaker was used instead of the 20 W Wharfedale loudspeaker in the first rig. The cone that was used in the first rig was used again for connecting the loudspeaker to the inlet pipe and was reinforced by fibre glass to minimise vibration. The power provided to the Fane loudspeaker during the test with flow was about 40 W. A Pitot-static tube connected to the manometer was fixed at 0.3 m from the measuring microphone to determin the overall Mach number of the flow in the ducts. The measuring equipment used was identical to that used for the first test rig. As the input signal level during these tests was as high as 120 dB, the interference from other sources was relatively small and the test rig was not surrounded by any form of insulation, although the loudspeaker was placed in an adjacent room.

5.b.2 Test on Doppler Frequency Shift.

The test was carried out to check the existence of a Doppler frequency shift. The straight pipe set-up of Fig. V- 2 was used with an air flow of Mach number 0.1, and power of 40 W was provided to the loudspeaker. The frequency of the signal received by the microphone was checked by another digital frequency counter (not shown in Fig. V-2). This signal was also displayed on an oscilloscope. The following table was obtained.

Nominal Freq. Hz	Signal Freq. Hz	Pick-up Freq. Hz
100	Severe	Vibration
200		
300	300	300
400	401	401
500	502	501
600	599	599
700	698	698
800	799	799
900	900	900
1000	999	999
1100	1102	1102
1200	1198	1198
1300	1301	1301
1400	1400	1400
1500	1500	1501
1600	1598	1598
1700	1698	1698
1800	1798	1798
1900	1901	1901
2000	2002	2001
2100	2101	2101
2200	2200	2200
2300	2298	2298
2400	2400	2400
2500	2500	2500
2600	2598	2597
2700	2700	2699
2800	2802	2802
2900	2899	2899
3000	3000	2999

This table proves clearly that the air flow did not cause a Doppler frequency shift on the signal received by the microphone, and thus the assumption of unchanged frequency made in deriving the theory in section 111-1 is correct.

The signal received was displayed on an oscilloscope and apart from the range between 100 Hz to 300 Hz and at 800 Hz when vibration of the loudspeaker cone assembly became very severe, the signal was a reasonably good sine wave. Between 100 Hz to 300 Hz no recording was made die to severe vibration of the test rig. This appears to be one of the reasons for poor results within this frequency range.

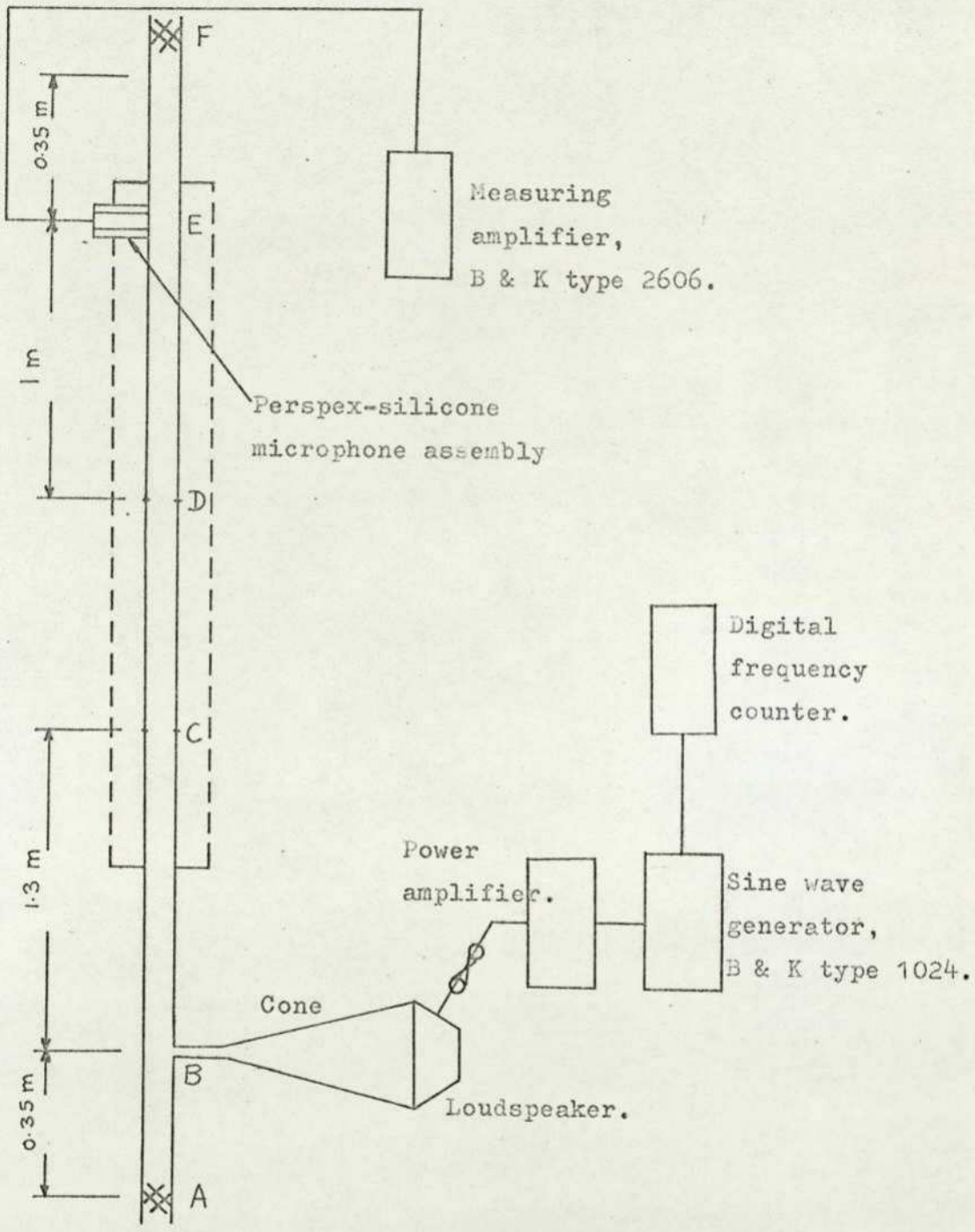

Fig. V-I.

Layout for Straight Pipe Test of First Test Rig.

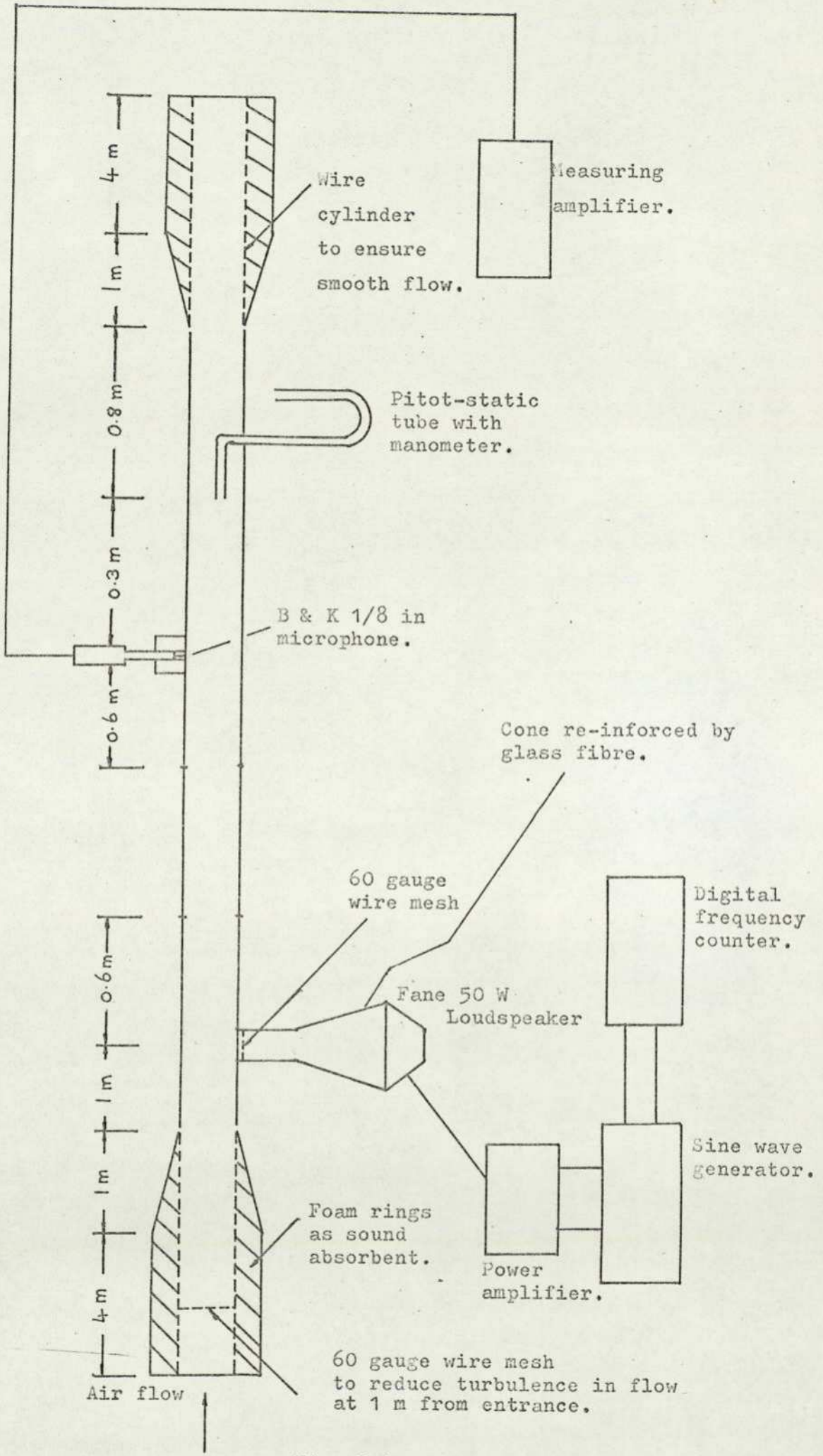

Fig. V-2.

Layout for Straight Pipe Test of Second Test Rig

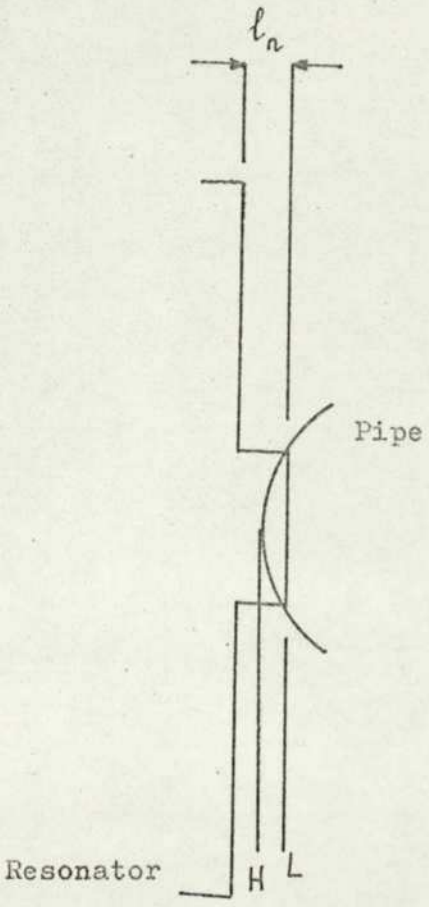

Fig. V-3.
Details of the Connecting Neck of the Resonator.

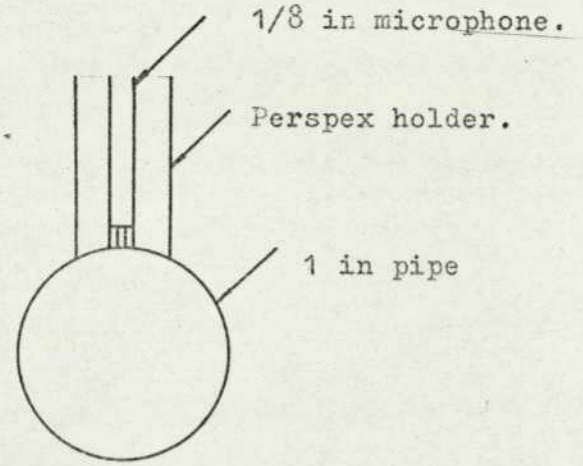

Fig. V-4a
Microphone Holder to Fit the Circular Shape of the Test Pipe.

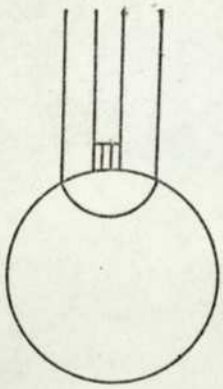

Fig. V-4b.
Microphone Holder turned 90° to provide an effective Obstacle.

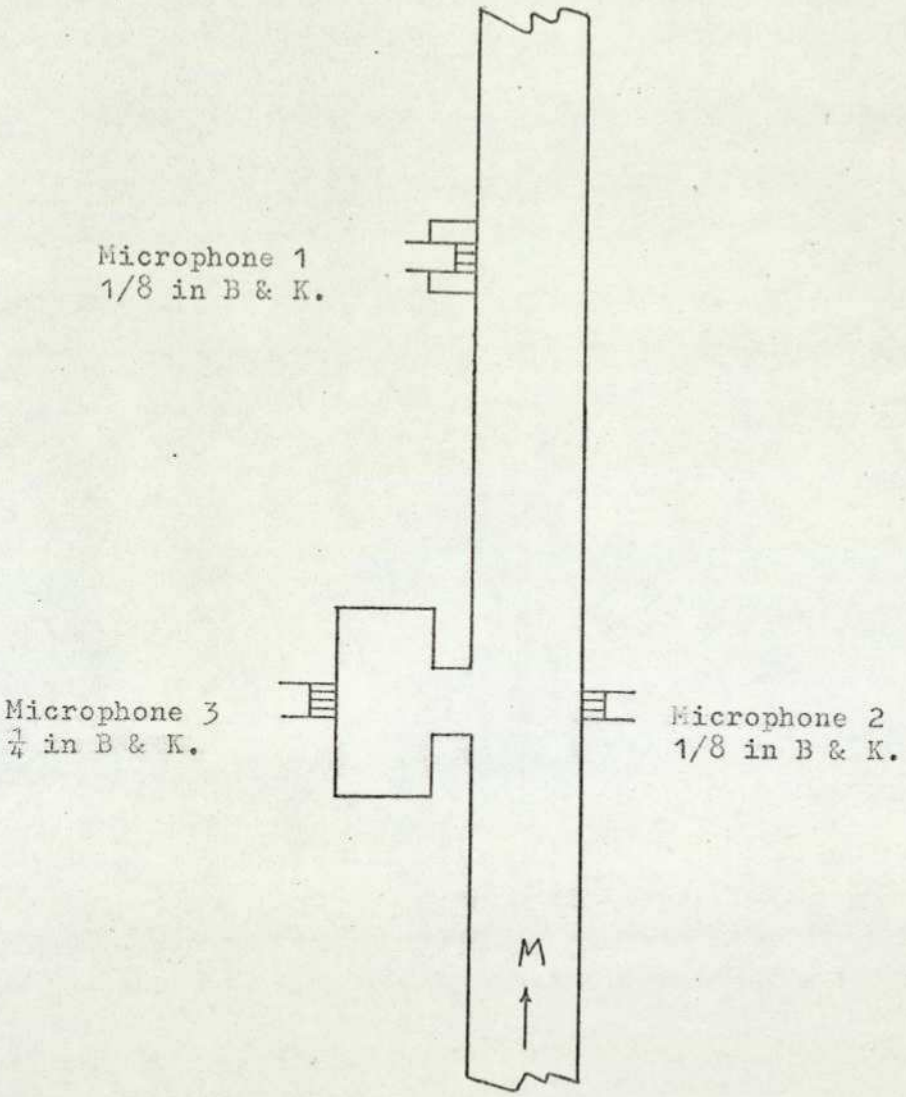

Fig. V-5.
Set-up for Determining Phase Difference between Signals picked up at Various Points.

TESTING AND ANALYSIS

6.a. Discrete Sine Wave Test

In this method the frequency response curves for the silencer and for the straight pipe were obtained separately, and the transmission loss determined from the difference. The frequency response curves can be obtained by recording both traces on frequency calibrated paper and the subtraction carried out manually at discrete frequency points. Due to inaccuracy in frequency determination on the traces, the results obtained by this method were unsatisfactory. A digital version of this method was used with signals fed into the loudspeaker at 50 Hz interval and output signals recorded by the microphone. A digital frequency counter was used for accurate recording of the input signal frequency. Recordings were made for both the straight pipe and the silencing systems. Subtraction was then made at each experimental points. This digital method has one slight disadvantage in that sharp changes in the response curves might be overlooked. The major advantage of the method of difference is that any undesirable inherent resonances in the system as a whole are eliminated and would not affect the final result. The discrete sine wave method was used in obtaining most of the results in this thesis.

6.b. Method of Broad Band Noise Input

Instead of using a single frequency signal as input to the loudspeaker a broad band (20-20 000 Hz) frequency random signal was used. The signal received by the microphone was recorded on magnetic tape. The recorded signal was replayed and filtered by a constant bandwidth (2 Hz) wave analyser. A level recorder was mechanically coupled to this wave analyser through a drive shaft so that the frequency response of the system could be directly traced on a chart. The difference method was again used for obtaining the attenuation frequency characteristics. With this method it was impossible to calibrate the chart in terms of frequency with sufficient accuracy due to the continuous nature of the filtering process, particularly as the frequency increased.

6.c. Fast Fourier Transform Method

The test method using discrete sine wave as the input is a lengthy test and in the presence of air flow the level of the input signal has to be very high in order to obtain a high signal to noise ratio for good results. As an alternative a test method was developed in which a broad band input was fed to the loudspeaker and the signal analysis performed digitally using fast Fourier Transform programmes.

The method consists of recording the signal on magnetic tape through the microphone amplifier and a low pass filter as shown in Fig. V-6.a. The low pass filter should have a cut-off frequency equal to the highest frequency under investigation so that unwanted high frequencies and consequently aliasing errors are eliminated. In practice the highest frequency that can be investigated is determined by the fastest available sampling rate.

In this case a Thermionic T 3000 FM tape recorder with a frequency response from D.C. to 5 KHz was used with a recording speed of 15 in./sec.; the measuring amplifier was a B&K 2606 and the low pass filter a Barr & Stroud variable filter with the cut-off adjusted to 800 Hz. The magnetic tape was then replayed into an analogue to digital converter capable of sampling at a rate of 2048 times per second and linked to a Ferranti FM 1600 B computer. The sampling frequency was more than twice that of the cut-off of the low pass filter, thus the Nyquist sampling criterion was satisfied and aliasing errors reduced. The Ferranti computer was used to produce a computer compatible paper tape with 4096 numbers. The paper tape then formed the input data for fast Fourier Transform programmes written for the ICL 1905 computer. Details of these programmes can be found in reference (49). Thus the digitising process and the power spectrum computations were performed in two separate stages. A schematic diagram of the digitising process is shown in Fig. V-6.b.

Some of the graphs presented in this thesis were plotted from results obtained by the fast Fourier Transform method.

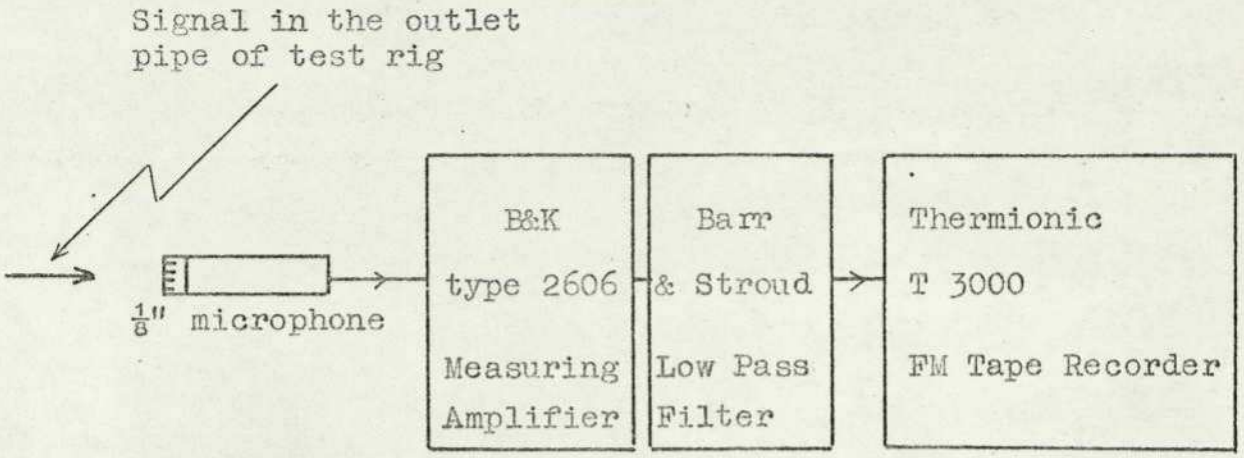

Fig. V-6.a. Recording of Signal for Fast Fourier Transform Method.

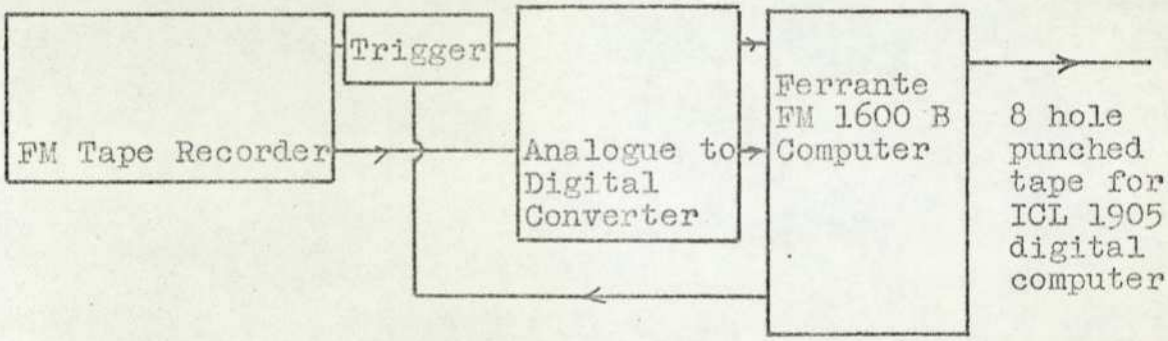

Fig. V-6.b. Schematic Diagram of the Digitising Process.

7.a. RESULTS OBTAINED BY FIRST RIG (NO FLOW)

Straight pipe

The layout for the straight pipe test is shown in Fig. V-1. Sine wave signals from 100 Hz to 3000 Hz were fed into the loudspeaker at 50 Hz intervals with ± 2 Hz accuracy. The output was measured by the microphone and the measuring amplifier. Tests were made with the microphone at distances of 2.35 m, 2.45 m and 2.65 m from the loudspeaker and the results shown in Fig. VII-1. The noise level in the pipe varied from 70 to 100 dB, with approximately 10 watt power input to the loudspeaker.

The curves are not independent of frequency as expected theoretically for 100% absorption but, however, differ little with different microphone positions. The only appreciable discrepancies among these curves occur between 100 Hz and 300 Hz. This is extremely important as it verifies that the frequency dependence was not, for the most part, due to standing waves inside the pipe, and justifies the use of the method of difference described above. The curve for the microphone at 2.65 m from the loudspeaker was used as the master curve for obtaining the attenuation frequency characteristic for this test rig. Care was taken to ensure that the end pipes were not disturbed throughout the test series.

Great effort was expended in attempting to obtain a flat response curve for the straight pipe by varying the tightness of the foam packing in the inlet and outlet pipes, but due to the inherent resonances of the loudspeaker and connecting cone, plus the complication due to their connection to the main duct from the side, a response curve with sound pressure level variation up to 30 dB had to be accepted.

7.a.1. Simple Expansion Chamber

An expansion chamber as shown in Fig. IV-1 was used to replace the straight pipe CD. The expansion chamber was made from a PVC pipe of 0.076 m internal diameter. Brass end pieces 0.025 m thick were made having a sliding fit with the inside of this 0.076 m pipe and the outside of the 0.028 m diameter pipe so that length ℓ_2 could be altered. Signals up to 5000 Hz were fed into the loudspeaker to check the validity of the assumption of plane waves with ℓ = 0.535 m (Fig. VII-2). The experimental method so described was found to be generally satisfactory. The assumption of plane wave started to fail at about 4300 Hz when the wavelength was approximately 0.08 m, the maximum diameter in the pipe system. At this frequency propagation of higher order modes would be expected in the expansion chamber.

Tests were then run up to 3 kHz for simple expansion chambers with ℓ = 0.305, 0.406 and 0.460 m (Fig. VII-3, VII-4, VII-5), with the signal input identical to that for the straight pipe test. Attenuation frequency characteristics

were obtained by eq. IV-4 and are in good agreement with the theoretical curves, particularly the zero attenuation points. These points can be obtained by using the formula

$$f = \frac{343}{2\ell} \cdot n \qquad \text{i.e. } \sin k\ell = 0,\ k\ell = n\pi$$

where ℓ = length of the simple expansion chamber.

n = 1, 2, 3 .....

343 is velocity of sound in m/s at typical laboratory conditions.

Karal's correction factor (39) for the expansion chamber length was not used due to the relatively small expansion ratio at discontinuities and this omission was proved justified.

Maximum attenuation obtained was about 13 dB and will increase with the term S/S_o.

Graph VII-6 shows the attenuation frequency characteristic of a simple expansion chamber with length 0.58 m. This graph was obtained from the second test rig by the Fast Fourier Transform Method with 4096 numbers split into 16 groups. Thus the number of samples per group was 256 and the resolution between points was 8 Hz. Comparing these results in graph VII-6 to those obtained theoretically it can be seen that the zero attenuation points agree very well with that predicted by calculations. Unfortunately due to the limited number of data points (4096) that could be handled by the Ferranti computer the analysis could only be carried out up to a frequency of 800 Hz with a resolution of 8 Hz, and this is the only apparent disadvantage of an otherwise satisfactory method.

7.a.2. Resonator with a Neck.

A resonator in the form of cylinder with a neck was tested as shown in Fig. IV-3. Length of the cylinder was varied to obtain different volumes for the resonator. Fig. V-3 shows the detail of the connecting neck under consideration and the physical significance of 'ℓ_n'.

Two sets of theoretical attenuation frequency characteristic were calculated with ℓ_b = 0.0508 m and 0.0254 m, S_b = 0.0022 m^2: one from a distributed parameter model and the other with lumped-parameter as described in section 4.a.2. The length of the neck was 0.0076 m while the diameter was 0.00953 m, i.e. a = 0.004765 m.

The effect of end corrections to the connecting neck was investigated (Fig. VII-7 & VII-8) and was found to be significant. The curves with end corrections applied to the neck agree with experimental curves considerably better

than the curve without, the value for the end correction being 1.7 times the radius of the circular cross-section of the neck as given in (35). This is the end correction applied to an open pipe having infinite flanges at both ends. As expected, this correction appeared to be slightly too large, since the neck did not have infinite-flanged terminations. The correct value for the correction should be between 1.7 times and 1.2 times the radius of the neck, the latter being the end correction applied to an open pipe with unflanged terminations.

Errors in this case might also be due to the fact that the neck was not curved to fit the pipe, that ℓ_n should be measured from level H instead of level L as shown in Fig. V-3, and that measurements of the neck dimensions were not accurate enough.

For the two resonators tested, the lumped-parameter method agree very well with the more exact distributed-parameter method in predicting attenuation. However, the lumped-parameter method would only give the first of a series of resonant frequencies as given by eq. IV-6 while the distributed-parameter method also gives the higher resonant frequencies as given by $Z_R = j\frac{\rho\omega}{c_o} + \frac{\rho c}{S_b}\frac{1}{j\tan k\ell_b} = 0$ although only the first was detected to fall within the frequency range investigated in this project.

Viscous friction affecting the air mass moving in the resonator neck was neglected, thus resulting in a very sharp attenuation peak. Experimental results agree fairly well with theoretical curve showing that, for the neck dimensions considered, viscous friction can be neglected. The Theoretical investigation of viscous friction effects is generally difficult owing to the involvement of the friction factor which usually has to be determined experimentally. For most practical purposes viscous friction of fluid inside the resonator neck can be ignored.

Another quantity which is of an empirical nature is the 'conductivity' of the resonator neck. In systems with more than one orifice forming the neck of the resonator, the neck area and neck length are not clearly defined and determination of end corrections to the neck becomes very arbitrary.

In necks with a large number of orifices the attenuation peak is very broad and exact location of the resonant frequency of the resonator is usually not too important, as was shown in Fig. 13-b of (4).

Computer programs were also used to investigate the nature of conductivity, and comparisons with D.D. Davis' experimental results for mufflers 78, 79, 80 were made. All three mufflers had more than one orifice. Different values for the term 'conductivity' were tried in the computer programs. It was found that good agreement can be obtained by using the empirical formula as follows:-

$$\text{Conductivity} = \frac{\text{combined area of all orifices}}{\text{thickness of sheet metal + correction factor X radius of one orifice.}}$$

The results were shown as Fig. VII-18, VII-19, VII-20, the correction factor for Fig. VII-19 and VII-20 being 1.7. Again, as shown in Fig. VII-7 and VII-8, this value is slightly too large. The correction factor for Fig. VII-18 is 1.5 and this gives very good prediction for the attenuation peak of the resonantor.

Graph 9 shows an attenuation frequency characteristic for a resonator with ℓ_b = 0.0508 m, ℓ_n = 0.0193 m and a = 0.004765 m. This graph was obtained from the second test rig by the Fast Fourier Transform method with an 8 Hz resolution, and the resonant frequency of the resonator can be seen clearly.

The attenuation level of around 15 dB attained by this method was comparable to that obtained by the Discrete Sine Wave Method. The location of the attenuation peak has been predicted accurately in this case with the 1.7 correction factor for the resonator neck.

7.a.3. Expansion Chamber With Internal Pipes

As shown in Fig. IV-4 the inlet and outlet pipes were pushed into the expansion chamber to form the equivalent branch pipes. Cross sectional area of the branch pipes would be the difference between the areas of the expansion chamber and the inlet pipe. Attenuation frequency characteristics were obtained with the procedure given in section 4.a.3 and the three different sets of values for l_1, l_2 and l_3 were as follows:-

ℓ_1 (m)	ℓ_2 (m)	ℓ_3 (m)
0.127	0.406	0.0254
0.127	0.356	0.0762
0.127	0.305	0.127

The attenuation frequency characteristics obtained (Fig. VII-10, VII-11, VII-12) were complicated but good agreement appeared between theoretical and experimental results. A few of the zero attenuation points were not registered because they were between steep slopes on the graph. Readings at high attenuation points (above 25 dB) were not satisfactory. The highest attenuation recorded in this set of experiments was around 45 dB.

The loops on all three attenuation frequency characteristics correspond to an expansion chamber length 0.558 m. This is the overall length of the expansion chamber tested. For all three curves two maxima occur at 675 Hz and 2025 Hz. These frequencies correspond to $kl_1 = \frac{\pi}{2}, \frac{3\pi}{2} \ldots\ldots$ i.e. $\cot kl_1 = 0$ and is given by

$f = \frac{343}{4\ell_1} n$ where $n = 1,3,5\ldots$. For Fig VII-10 the

maximum corresponds to $kl_3 = \pi/2 = 3375$ Hz and thus did not appear in the graph, while for Fig. VII-11 this frequency is 1125 Hz and the maximum can be seen quite clearly, For Fig. VII-12, with $l_3 = l_1$, maxima due to each length coincided resulting in extremely high attenuations at the corresponding frequencies, although experimentally these attenuation levels were not achieved.

In locations of maximum attenuation points slight discrepancies occur between theoretical and experimental results. The predicted frequencies for these maxima are slightly higher than the experimental and the difference becomes more apparent with increasing frequencies. This may be explained by the fact that the end corrections to the equivalent branch pipes have not been applied. As in the case for a resonator neck, the value for the end correction is determined empirically.

It can be seen that the introduction of internal tubes in expansion chambers is a simple and effective way of obtaining high attenuation at particular frequencies and this method has been used widely in silencer design.

7.a.4. Simple Expansion Chamber in Series with Resonator

The simple expansion chamber and the resonator were combined to give the system shown in Fig. IV-5. Tests were conducted with the dimensions of the expansion chamber and resonator as follows:-

l_1 (m)	l_b (m)
0.305	0.0254
0.305	0.0508
0.460	0.0508

The distance between the expansion chamber and resonator was kept constant at 0.38 m. Fig. VII-13, VII-14 and VII-15 show the theoretical and experimental curves and the agreement can be considered as satisfactory. In Fig. VII-13 and VII-14 at around 800 Hz the experimental curve shows slight fluctuations in attenuation level. This may be explained as due to the effect of the resonator on the attenuation characteristic of the expansion chamber. As frequency increases and the effect of the resonator diminishes the curve settles to that of a simple expansion chamber with zero attenuation points at 560 Hz, 1120 Hz, 1700 Hz, 2250 Hz and 2800 Hz corresponding to $\sin k l_1 = 0$. In Fig. VII-15 experimental results agree very well with calculated values although experimental peak attenuation due to the resonator was missed. End corrections of 1.7 times neck radius had been applied to the resonator neck in all cases in the theoretical calculations.

7.a.5. Finite Outlet Pipe

No test rig was constructed to carry out tests for the effect of a finite outlet pipe. Theoretical curves were plotted for a simple expansion chamber with a finite outlet pipe as shown in Fig. VII-16 and VII-17 using the arrangements described in section 4.a.5. The area ratio between the simple expansion chamber and the pipe was approximately 8 to 1, the terminating impedance of the outlet pipe was assumed zero. Fig. VII-16 shows the attenuation frequency characteristic for a simple expansion chamber length ℓ = 0.460 m with an outlet pipe length ℓ_t = 0.7 m and zero radiation impedance.

It can be seen from the attenuation frequency characteristic that at frequencies corresponding to $k\ell_t = n\pi$, i.e. at 245 Hz, 490 Hz, 735 Hz etc., the attenuation is always at a minimum. These minima reach a magnitude of around -17 dB and indicates that at these frequencies the sound level emitted by the system with a simple expansion chamber is higher than that by a straight pipe. Also at frequencies corresponding to $k\ell = n\pi$, the attenuation is always zero, a characteristic of a simple expansion chamber.

Fig. VII-17 shows attenuation frequency characteristic for a simple expansion chamber ℓ = 0.460 m with an outlet pipe of equal length. Due to the equality in length of the expansion chamber and outlet pipe, the minimum points due to the outlet pipe coincide with the zero attenuation points due to the simple expansion chamber at 375 Hz, 750 Hz, 1125 Hz, 1500 Hz etc. It is shown clearly on the graph that at this frequency zero attenuation was obtained at a point which would otherwise be a minimum point.

Expression IV-11 was used to evaluate the attenuation frequency characteristic for a system with a resonator and finite outlet pipe, shown in D.D. Davis' paper (4) as mufflers 78, 79, 80. These theoretical curves were compared to the experimental results given in the same paper and presented in Fig. VII-18, VII-19, VII-20. The conductivities of these mufflers were calculated as described on page 54. The calculated minimum attenuation point due to the outlet pipe did not quite coincide with the experimental minimum. This might be due to inaccuracies in determining the length of the outlet pipe or due to the omission of the 0.6R end correction in the calculation. In Fig. VII-18 two minima due to the finite outlet pipe can be seen. General agreement between D.D. Davis' experimental results and that calculated is satisfactory. In any case, it had been proved mathematically that attenuation obtained through expression IV-11 is identical to that from eq. D-10 in D.D. Davis' paper. A sonic velocity of 2000 ft/sec was used in the calculation, the same value used by Davis in his paper.

M. Fukuda in his paper (15) also looked into the effect of outlet pipe length on attenuation of a silencer with zero radiation impedance. The silencing system considered was a

simple expansion chamber with finite inlet and outlet pipes. Area ratio between the expansion chamber and the pipes was 25 to 1. The silencer was shown in Fig. 17 of his paper and the results in Fig. 19 of the same paper. The experimental results obtained by Fukuda were compared to the theoretically calculated attenuation frequency characteristics obtained by eq. IV-9 and IV-10 for this particular silencer and are shown in Fig. VII-21, VII-22 and VII-23. Locations of minimum attenuation points due to the finite outlet pipe were predicted despite the omission of the 0.6R end correction. The theoretical attenuation levels generally did not agree well with the experimental results obtained by an engine test. This is expected since the experimental results were obtained with the system having a finite inlet pipe whereas an infinite inlet pipe was assumed in the calculation. A uniform temperature, and hence one sonic velocity of 450 m/s was assumed in the silencing system, as compared to different sonic velocity values in different sections of Fukuda's set-up.

7.a.6. Finite Inlet Pipe

Again only theoretical results are given for systems with finite inlet pipe. Fig. IV-8 shows a simple expansion chamber connected directly to a loudspeaker with the outlet pipe having a non-reflecting termination. Area ratio between the expansion chamber and the main pipe was approximately 8 to 1. Attenuation is defined as in section 4.a.6.

Fig. VII-24 shows the attenuation frequency characteristic for a simple expansion chamber length equal to 0.46 m with a finite inlet pipe 0.35 m long. The first zero attenuation point at 373 Hz due to the expansion chamber is clearly seen. At around 245 Hz a minimum of -12 dB is present which is the first of a series and can be predicted by $f = \frac{c}{4\ell} n$

where ℓ = length of the finite inlet pipe

$n = 1, 3, 5, \ldots\ldots$

c is the velocity of sound in m/sec.

The second minimum due to the inlet pipe is around 735 Hz.

The same simple expansion chamber with an inlet pipe 0.23 m long was investigated and the attenuation frequency characteristic shown in Fig. VII-25. Since the length of the inlet pipe is half that of the expansion chamber the minima due to these two sections coincide at 373 Hz. The graph shows the negative attenuation due to the finite inlet pipe being brought to zero because the simple expansion chamber has zero attenuation at this frequency.

It can be seen that to avoid the presence of a prominent negative attenuation due to the finite inlet pipe the length of the inlet pipe can be chosen to be half that of the expansion chamber in the system.

As in the case of the finite outlet pipe, comparisons are made between experimental results given by Fukuda (15) for a simple expansion chamber with finite inlet and outlet pipes in Fig.19 of his paper and that obtained theoretically by eq. IV-12 and IV-13. Since the theoretical curve is calculated for a system with an infinite outlet pipe and Fukuda's systems have finite outlet pipes of lengths 0.145 m and 0.36 m respectively, comparison was made in the low frequency region where the effect of the outlet pipe is not predominant. From Fig. VII-26 it can be seen the minimum due to the 0.36 m long inlet pipe was accurately predicted in each case. The level of attenuation calculated for the system is considerably above that obtained by Fukuda with a 0.145 m long outlet pipe, but agrees well with Fukuda's experimental results for a 0.36 m long outlet pipe up to around 500 Hz.

A system consisting of a resonator and a finite inlet pipe as shown in Fig. IV-10 was also considered. The dimensions of the resonator and neck assembly used were identical to that used for mufflers No. 78, 79 and 80 in D.D. Davis' work (4) and the lengths of the inlet pipes were chosen to be half of the lengths of the outlet pipes used by D.D. Davis. The attenuation frequency characteristics drawn as shown in Fig. VII-27, VII-28 and VII-29 show much resemblance to Fig. VII-18, VII-19 and VII-20 respectively. It can thus be concluded that theeffect of a finite inlet pipe on the attenuation of a system is similar to that of a finite outlet pipe with twice the length.

7.b. RESULTS OBTAINED BY SECOND RIG (NO FLOW AND WITH AIR FLOW)

7.b.1. Simple Expansion Chamber

A simple expansion chamber similar to that shown in Fig. IV-1 but with a diameter 0.071 m was used in the test rig shown in Fig. V-2. This simple expansion chamber would replace the central test pipe of 0.023 m dia. The method of 'Discrete Sine Wave Testing' identical to that used in the no flow case was used for a frequency range between 50 Hz to 2.5 kHz. Three different lengths of the expansion chamber were tested. An air flow with a local Mach number of 0.1 in the inlet pipe was going through the rig.

Simple expansion chambers with ℓ = 0.305, 0.406 and 0.58 m were tested and the attenuation frequency characteristic obtained for M_o = 0.1. These curves are shown as Fig. VII-31, VII-32, VII-33. The experimental results agree reasonably well with theoretical curves although the degree of agreement was inferior to that in the no-flow case with the first rig. At below 300 Hz errors become more apparent. Generally the results are more erratic than those for the no-flow case. There appear to be a shift of zero attenuation points towards the higher frequencies with the presence of flow for all three graphs indicating the shift predicted by theory is inaccurate. However, tests conducted with and without flow for the same simple expansion chamber showed a flow of M_o = 0.1 gives no measurable shift of zero attenuation points and it was concluded that this shift shown in the graphs might in fact be due to inaccuracies in measuring the length of the expansion chamber. The agreement on level of attenuation between theoretical and experimental results was satisfactory. During the straight pipe test it was observed at various frequencies the reading obtained by the microphone was reduced by up to 5 dB due to the presence of air flow.

Theoretical attenuation frequency characteristics were given for ℓ = 0.305, 0.406 and 0.460 m for a simple expansion chamber with an expansion ratio of roughly 7.8 to 1. Curves were obtained for M_o = 0, 0.99 and shown in Fig. VII-30. M_o=1 gives $\frac{k}{1-M_o^2}\ell = \infty$ and this can give irrational conditions for some configurations and was thus not dealt with.

From these theoretical graphs it can be seen that with M_o=0.99, i.e. mach number of approximately 0.1 in the simple expansion chamber, the effect of flow was just barely noticeable and the zero attenuation points can be determined by $\sin\left(\frac{k}{1-M^2}\ell\right) = 0$, i.e. $f = n\frac{c}{2\ell}(1-M^2)$ where ℓ is the length of the expansion chamber and M the mach number in it; and n is an integer. This shows the internal flow has effectively increased the length of the expansion chamber from ℓ to $\frac{\ell}{1-M^2}$.

The Fast Fourier Transform Method was then used to obtain attenuation frequency characteristics for an expansion chamber with length equal to 0.58 m. Tests were performed on the same chamber with an air flow of M=0.1 with 4096 nos. split into 16 groups (Fig. VII-34). A comparison with Fig. VII-6 shows no detectable shift in zero attenuation frequencies. Attenuation frequency characteristics obtained for the same simple expansion chamber with and without flow look very similar.

7.b.2. Resonator with a Neck

A resonator similar to that used in the no-flow case was employed in the tests with air flow. Details of the resonator neck were esentially the same as those shown in Fig. V-3. The outside of the neck the actual length of which is 0.0193 m was threaded so that the resonator can be screwed on to the side of the main pipe inside which was an air flow. Radius of the neck is 0.00476 m and an end correction factor of 1.7was used. Tests were conducted with two volumes of the resonator (ℓ_b = 0.0254 m and 0.0508 m) as in the case without flow and attenuation frequency characteristic was obtained in each case.

Fig. VII-35 shows attenuation frequency characteristics for a resonator with length equals 0.0254 m. In cases for M_o = 0.105 and M_o = 0.123 the peak of attenuation obtained experimentally coincide with that predicted by theory for M_o = 0 at around 370 Hz. This is in agreement with results presented in (14), (20), (47) and indicates at low mach numbers the resonant frequency of a resonator is not duly affected. When M_o = 0.2 this peak shifts to around 400 Hz. For a resonator with length equals 0.0508 m the peaks of attenuation obtained by experiment for M_o = 0.105 and M_o = 0.123 were seen to occur around 275 Hz which is a slightly higher frequency than the 260 Hz obtained theoretically for M_o = 0.0 (Fig. VII-36). Thus flow effect at low mach number is more prominent on larger resonators. All the experimental curves are broader than the theoretical and this can be explained by the neglecting in theory the turbulence which penetrates into the resonator neck and increases the acoustic resistance there. The shift of the maximum attenuation points shows the effective mass oscillating in the neck was proportional to a shorter length than the corrected neck length but not to the extent of the uncorrected length as suggested by Phillips (41). The resonant frequencies calculated for the 0.0254 m and 0.0508 m resonators using the uncorrected neck length are 440 Hz and 310 Hz respectively.

Two microphones, one placed at the end of the resonator (mic. 3) and the other opposite the neck (mic. 2) in the main pipe were used for recording sound pressure levels as shown in Fig. V-5. Difference in these sound pressure level readings are shown in Fig. VII-37. Test data were obtained for a resonator length of 0.0254 m both with

internal air flow $M_o = 0.2$ and without flow in the main duct. The maximum of difference in the case without flow is seen to lie around 350 Hz and with the presence of flow this peak shifts to around 400 Hz. This shift is in agreement with that for maximum attenuation in Fig. VII-35 and suggests the maxima measured by the two different methods are similar in nature. Both can be calculated from the equation $f_o = \frac{c}{2\pi}\sqrt{\frac{A}{\ell_{eff} V}}$.

Where A is the cross sectional area of the neck, ℓ_{eff} is the effective neck length and V is the volume of the resonator. It has been shown by Phillips (41) and Anderson (48) the two microphone method of measurement registered a shift at a lower flow rate than the measurement for transmission loss. It is also found that the sound pressure level recorded by microphone 2 opposite the resonator neck is always at a minimum at the resonant frequency of the resonator as stated in (41). Treating the resonator as a single degree freedom system the phase difference between the signals recorded by the two microphones should be 90° at resonance. However, phase measurements were unsuccessful due to the lack of a phase meter.

Fig. VII-38 shows the attenuation frequency characteristic for a resonator 0.0508 m long obtained by the Fast Fourier Transform method. The air flow in the system was $M_o = 0.105$. 4096 numbers splitted into 16 groups with a resolution of 8 Hz were used for the analysis. A signal to noise ratio of 20 dB was provided for both the tests for the resonator and the straight pipe. Apart from a slightly lower attenuation level, the curve obtained is very similar to that obtained by the discrete frequency method shown in Fig. VII-36. Thus the Fast Fourier Transform can be a useful technique in obtaining attenuation frequency characteristics of various silencing systems, with or without flow.

7.b.3. Expansion Chamber with Internal Tubes

A system similar to that shown in Fig. IV-4 with a mean flow was considered. Lengths of 0.127 m, 0.305 m and 0.127 m for ℓ_1 , ℓ_2 and ℓ_3 respectively were used to obtain the theoretical attenuation frequency characteristic.

Experimental results were obtained for the silencer both for $M_o = 0$ and $M_o = 0.1$. As shown in Fig. VII-39, these results compare quite favourably to the theoretical curve predicted for $M_o = 0$. The two experimental curves are almost identical showing that the flow has little effect in this system. Input into the loudspeaker for these tests was reduced to around 10 W so that the lowest sound pressure level from the loudspeaker recorded by the microphone was comparable with the noise level produced by the air flow. The aim of this was to see the behaviour of attenuation when flow noise and signal have comparable levels. Apparently

no unexpected interaction between signal and flow noise was observed apart from inferior results for the flow case at regions of high attenuation due to the presence of flow noise. Locations of the high attenuation regions due to resonance of the equivalent branch pipes remain unchanged with presence of flow substantiating the assumption of no flow in the branch pipes. At regions of low attenuation the magnitude of attenuation has been predicted fairly well. At frequencies below 300 Hz discrepancies between theoretical and experimental result are quite obvious.

7.b.4. Simple Expansion Chamber in Series with Resonator

No experimental results are available for this configuration shown in Fig. IV-5. Theoretical results were obtained by computation for systems with the following dimensions:-

ℓ_1 (m)	ℓ_2 (m)	ℓ_b (m)
0.305	0.38	0.0254
0.305	0.20	0.0508

Area ratio between the simple expansion chamber and the straight pipe was about 8 to 1 as in the case without flow. No flow was assumed in the resonator and end correction of 1.7 times neck radius was applied to the resonator neck. Attenuation frequency characteristics were plotted for M_o=0 and M_o=0.8 and shown as Fig. VII-40 and VII-41. The curves reveal clearly the high attenuation due to the resonator and the attenuation loops are due to the simple expansion chamber. When M_o=0.8 ripples can be seen superimposed on top of the main attenuation loops. These ripples are due to the resonance effect in the connecting pipe and frequencies for the minima can be determined, to a fair degree of accuracy, by,

$$\text{Sin } k \frac{\ell_2}{1-M_2^2} = 0$$

where ℓ_2 = length of the connecting pipe.

M_2 = mach no. in connecting pipe.

or $f = n \frac{c}{2\ell_2} (1 - M_2^2)$, where n = 1, 2, 3.....

f calculated by the above formula does not give the exact locations of the minima since effect due to the other elements in the system has been neglected. It can be seen that larger the effective length of the connecting pipe, smaller is f and the ripples become prominent. In Fig. VII-40 for M_o=0.8, the width of each of these ripples is given by,

$$f = \frac{343}{2\text{x}0.38} (1-0.8^2) = 162 \text{ Hz.}$$

The corresponding value in Fig. VII-41 for M_o=0.8 is,

$$f = \frac{343}{2\text{x}0.2} (1-0.8^2) = 309 \text{ Hz.}$$

A minimum is clearly shown in Fig. VII-41 around this frequency. In the case without flow in Fig. VII-40 a minimum at 451 Hz was calculated by the above method and the graph shows the minimum at 400 Hz.

As in the case of no flow, while frequency increases the effect of the resonator diminishes and the connecting pipe becomes part of the infinite outlet pipe. The ripples can then be seen to subside. It would be obvious with $M_o < 0.5$ the effect of air flow on the attenuation frequency characteristic of this system is negligible.

7.b.5. Finite Outlet Pipe with Flow

Expressions IV-21, IV-22 and IV-23 were used to calculate the attenuation frequency characteristic for a simple expansion chamber with a finite outlet pipe and a mean flow described in section 7.a.5. No experimental results were obtained for this system and the theoretical curves are shown in Fig. VII-16 and VII-17 for M_o=0.2 and 0.4 respectively. Zero radiation impedance is assumed as in the case without flow. Shifts of minimum and zero attenuation points for the finite outlet pipe and the expansion chamber as a consequence of the air flow can be seen. The first minimum attenuation point due to the outlet pipe on Fig. VII-16 is at 245 Hz without flow and shifts to $245(1-0.2^2) \simeq 235$ Hz for M_o=0.2 in the outlet pipe. The other minimum attenuation points shift accordingly and the accumulative effect is obvious as frequency increases. The shift for the zero attenuation points are not so obvious due to the much reduced mach number in the expansion chamber. The magnitudes of maximum and minimum attenuation were not much affected by the presence of flow. A similar situation occurs in Fig. VII-17. In this set up since the flow has effectively increased the length of the outlet pipe the minimum attenuation points due to the outlet pipe no longer coincide with the zero attenuation points due to the expansion chamber. The first of a series of minimum attenuation points has been seen to shift from 375 Hz to $375\ (1-0.4^2) = 315$ Hz. The first zero attenuation point due to the expansion chamber almost remains unchanged at 375 Hz.

Fig. VII-42, VII-43 and VII-44 show the theoretical attenuation-frequency characteristics for systems consisting a resonator with a finite outlet pipe with flow. The dimensions for the systems are the same as those in Fig.VII-18, VII-19 and VII-20 , respectively.The results were calculated from equation IV-26 and indicate the minimum attenuation points due to the outlet pipe are, as in the case for a simple expansion chamber , given by the expression

$$f = f_o(1 - M_o^2)$$

where f is the frequency of minimum attenuation with flow, f_o is the frequency of minimum attenuation without flow, and M_o is the Mach number in the outlet pipe. Again it is shown that the attenuation level is not affected by the flow. From the above analysis it may be concluded that the internal flow will not have a substantial effect on the attenuation performance of the finite outlet pipe of a silencing system.

Designing a High Performance Silencer with the Method of Matrix Multiplication

For illustrative purpose a silencing system without flow is designed by computing its attenuation frequency characteristic with the Method of Matrix Multiplication, (Fig. VII-45). Overall length of the system is 0.6 m while the areas for the inlet and outlet pipes and the silencing section are 0.000616 m^2 and 0.00484m^2 respectively. Two expansion chambers, both 0.16 m long with internal tubing at one end, form the basic design of the silencer. The maximum resultant attenuation obtained with the two expansion chambers in series is more than 50 dB. Zero attenuation points due to these two expansion chambers occur at 1072 Hz, 2144 Hz, 3216 Hz etc. The finite outlet pipe considered is designed to be 0.16 m so that its zero attenuation points coincide with those due to the expansion chambers. In order to increase the attenuation level at 1072 Hz the internal tube in one of the expansion chambers is made 0.077 m long. This brings the attenuation at 1114 Hz to 60 dB. The internal tube in the other expansion chamber is 0.04 m long and this eliminates the zero attenuation point at 2144 Hz and lifts the attenuation level in that region to around 30 dB. Three resonators all with a volume of 0.000338 m^3 are used to increase the attenuation level at various specific points. One with a conductivity of 0.15 helps to broaden the high attenuation level around 1000 Hz. Two others with conductivities 0.01 and 0.0014 are used to increase attenuation at 300 Hz and 100 Hz respectively. The low frequency content below 300 Hz usually is very difficult to eliminate while high frequency content

above 3000 Hz can be reduced effectively by absorptive material. Attenuation band due to a resonator can of course be broadened by increasing the attenuation parameter $\frac{\sqrt{c_o V_b}}{2S_o}$ to satisfy specific requirements. Effect of inlet pipe is not considered since this part of the system varies for different cases. Overall attenuation of the presented silencer is above 30 dB which if achieved in practice, would be considered satisfactory. Different silencing elements can be incorporated in the system by simply adding matrices to the computer program without affecting the rest of the system.

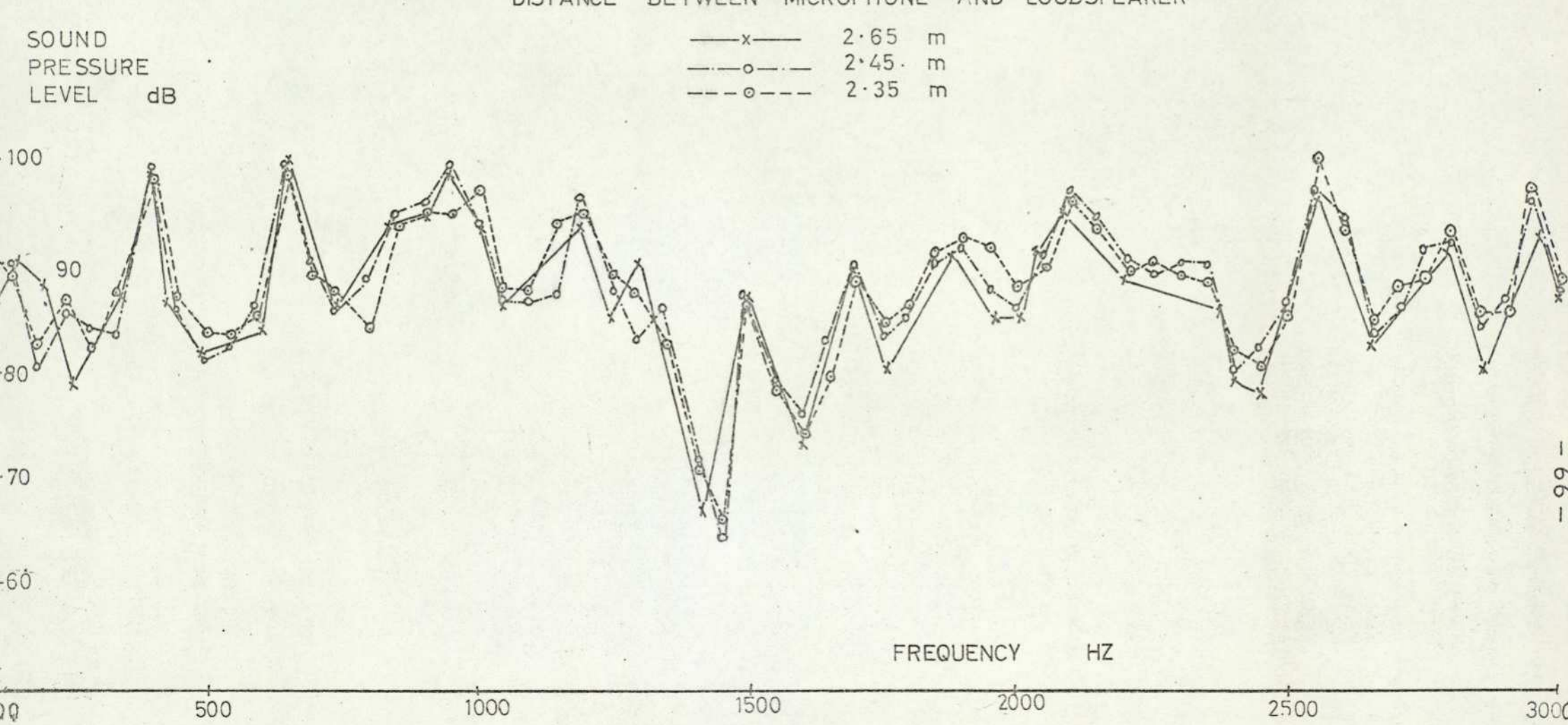

FIG. VII-1 FREQUENCY RESPONSE OF A STRAIGHT PIPE.

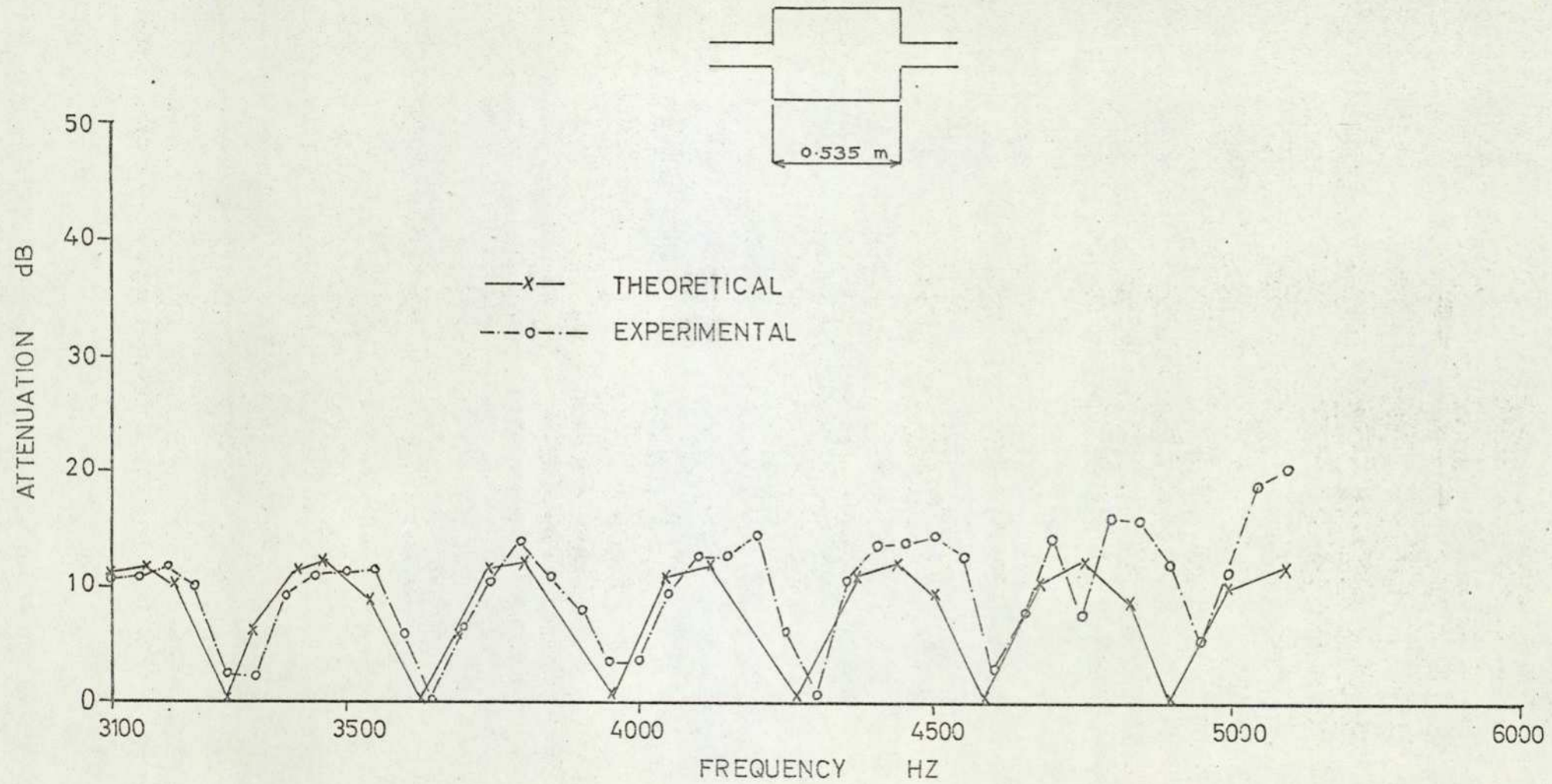

FIG. VII-2. ATTENUATION - FREQUENCY CHARACTERISTICS OF A SIMPLE EXPANSION CHAMBER.

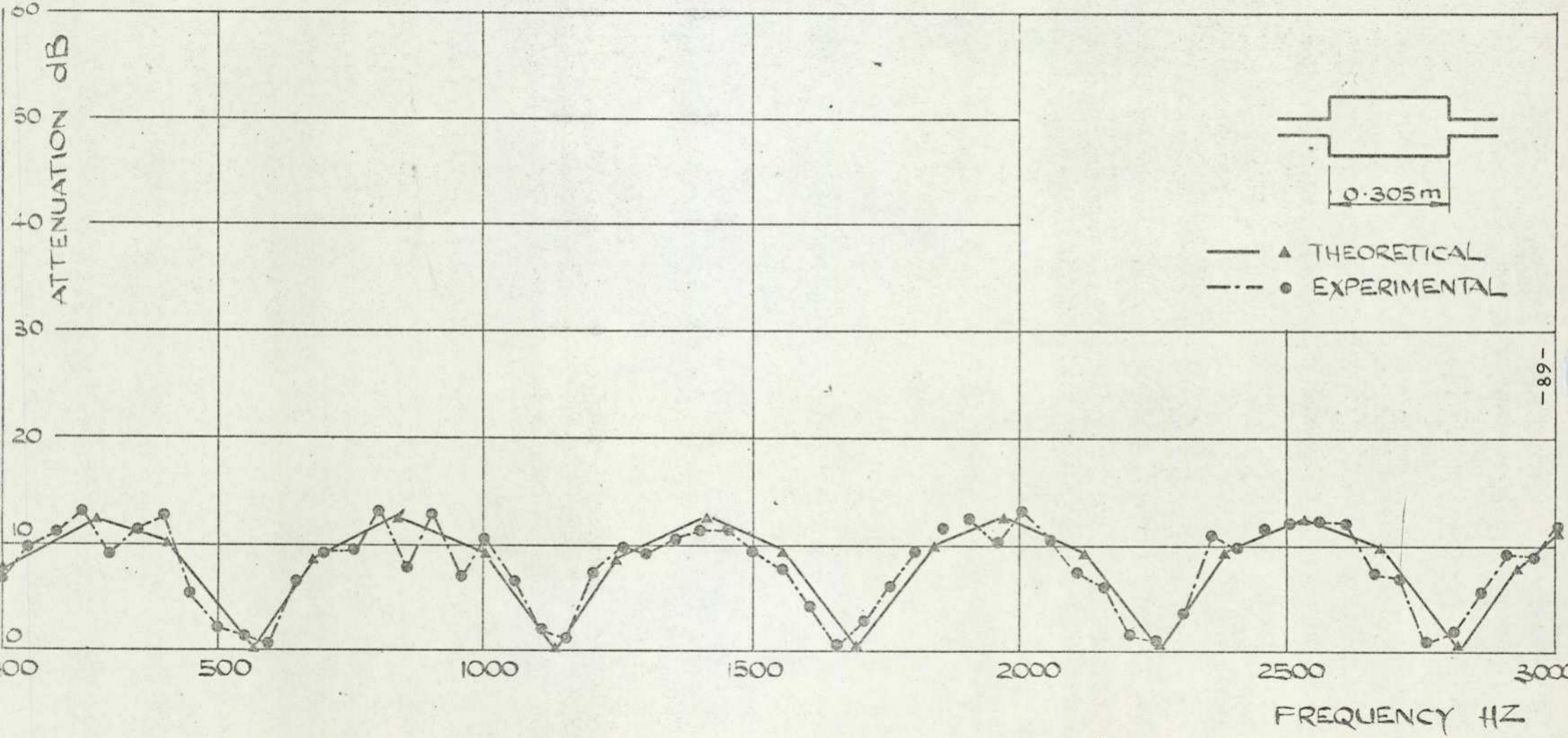

FIG. VII-3 ATTENUATION FREQUENCY CHARACTERISTICS for SIMPLE EXPANSION CHAMBER

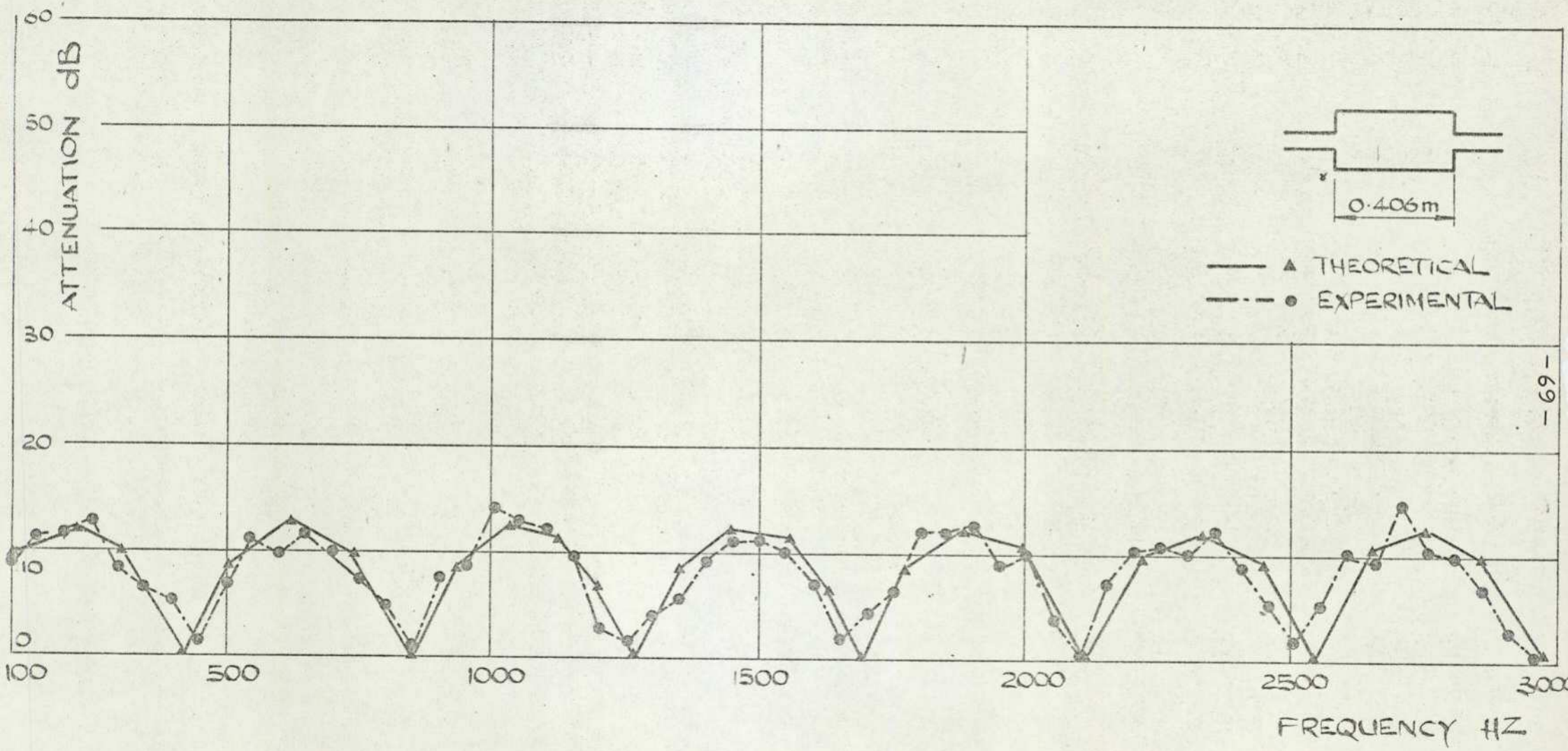

FIG. VII-4 ATTENUATION FREQUENCY CHARACTERISTICS for SIMPLE EXPANSION CHAMBER

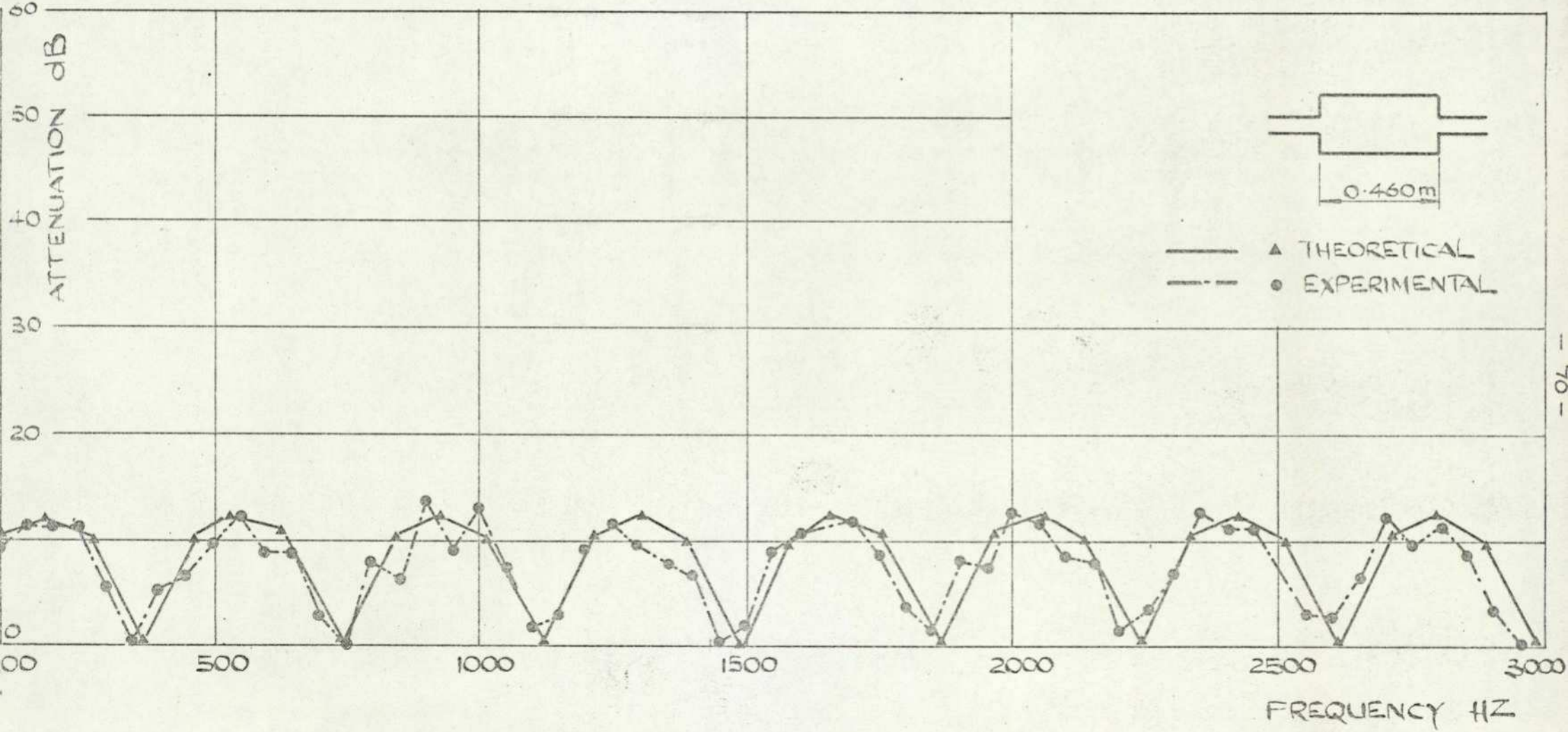

FIG. VII-5 ATTENUATION FREQUENCY CHARACTERISTICS for SIMPLE EXPANSION CHAMBER

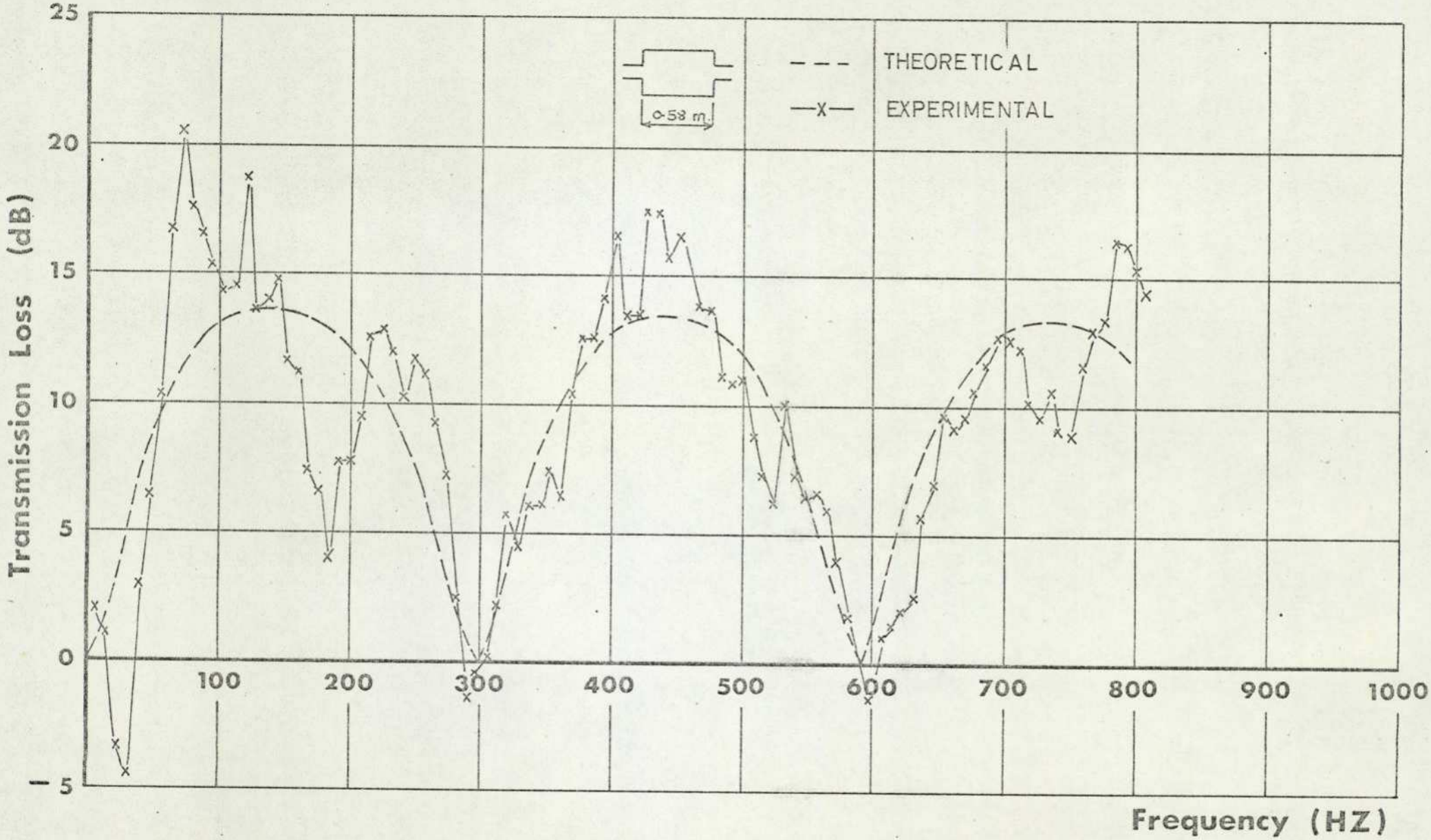

FIG. VII - 6. ATTENUATION – FREQUENCY CHARACTERISTICS FOR SIMPLE EXPANSION CHAMBER.

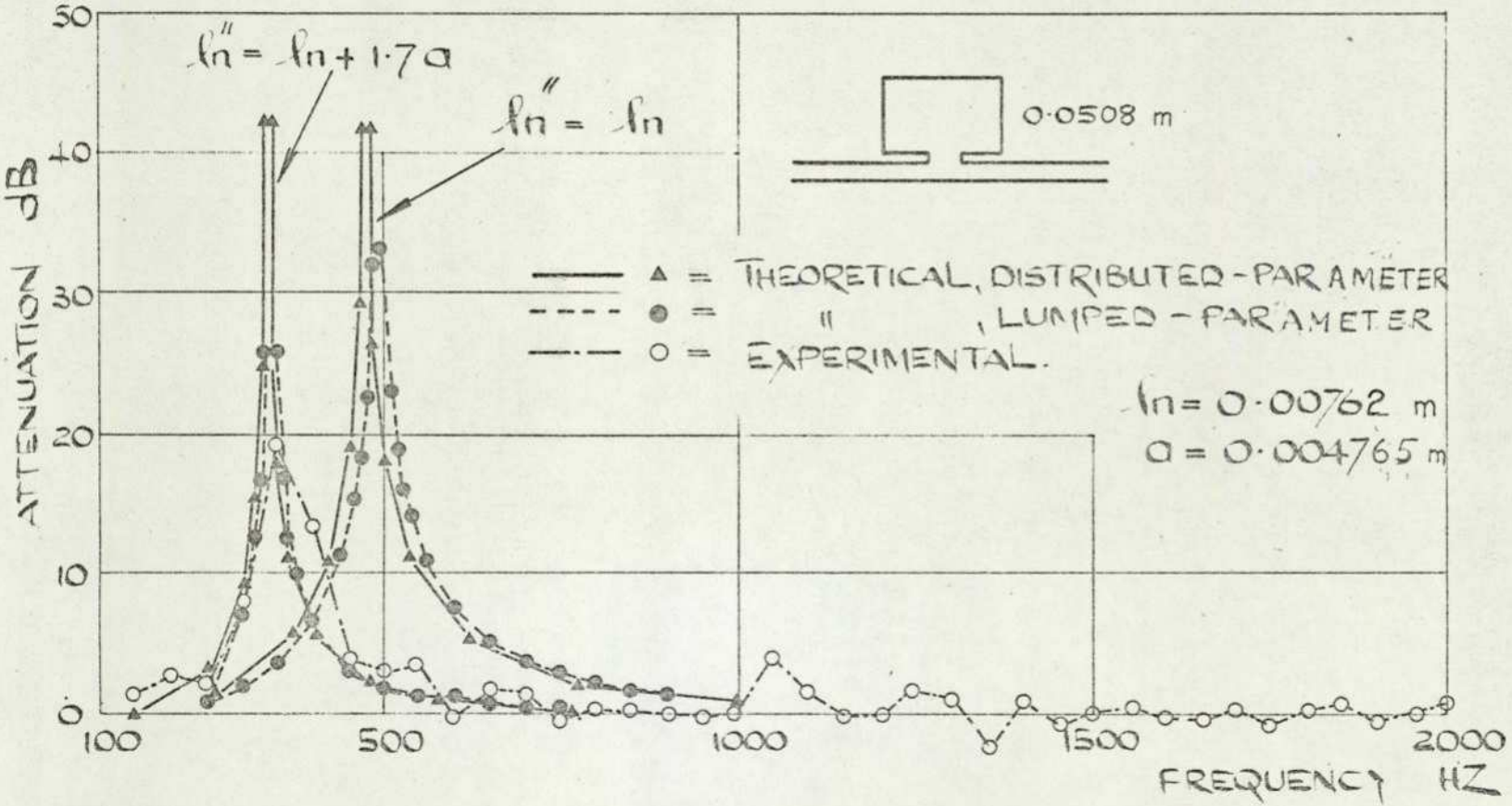

FIG. VII 7. ATTENUATION FREQUENCY CHARACTERISTICS for RESONATOR.

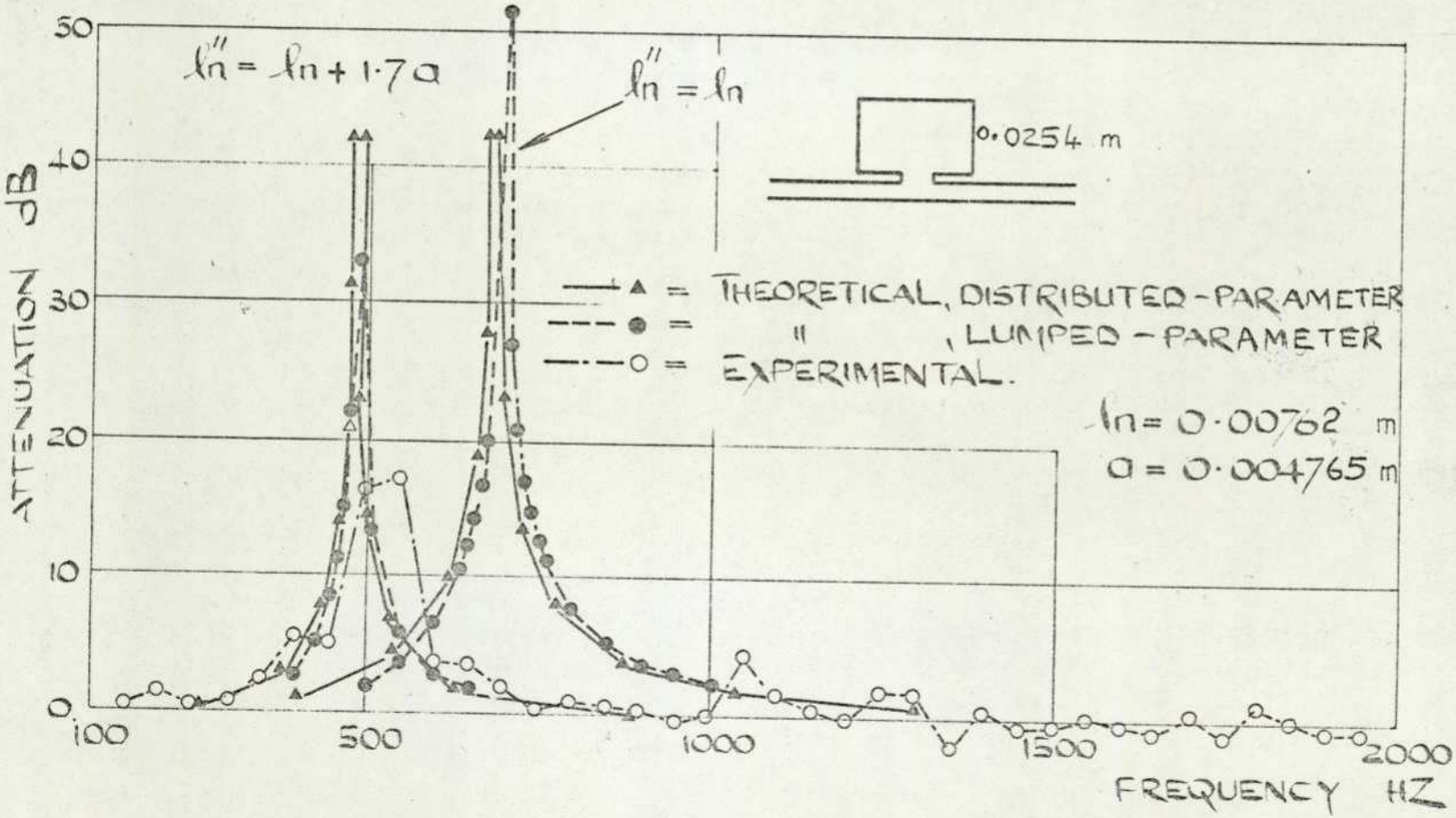

FIG. VII-8. ATTENUATION FREQUENCY CHARACTERISTICS for RESONATOR.

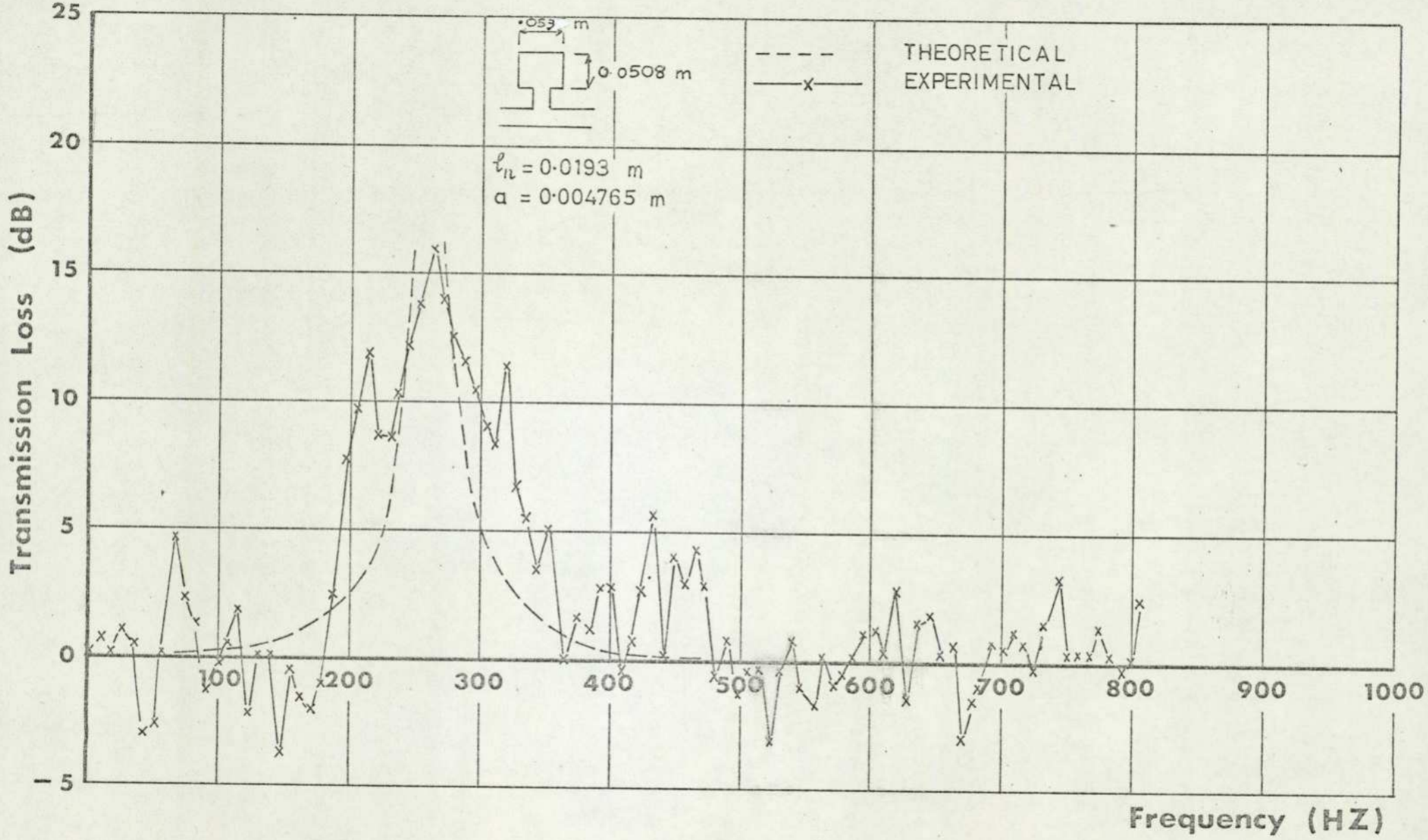

FIG. VII-9. ATTENUATION – FREQUENCY CHARACTERISTIC FOR RESONATOR.

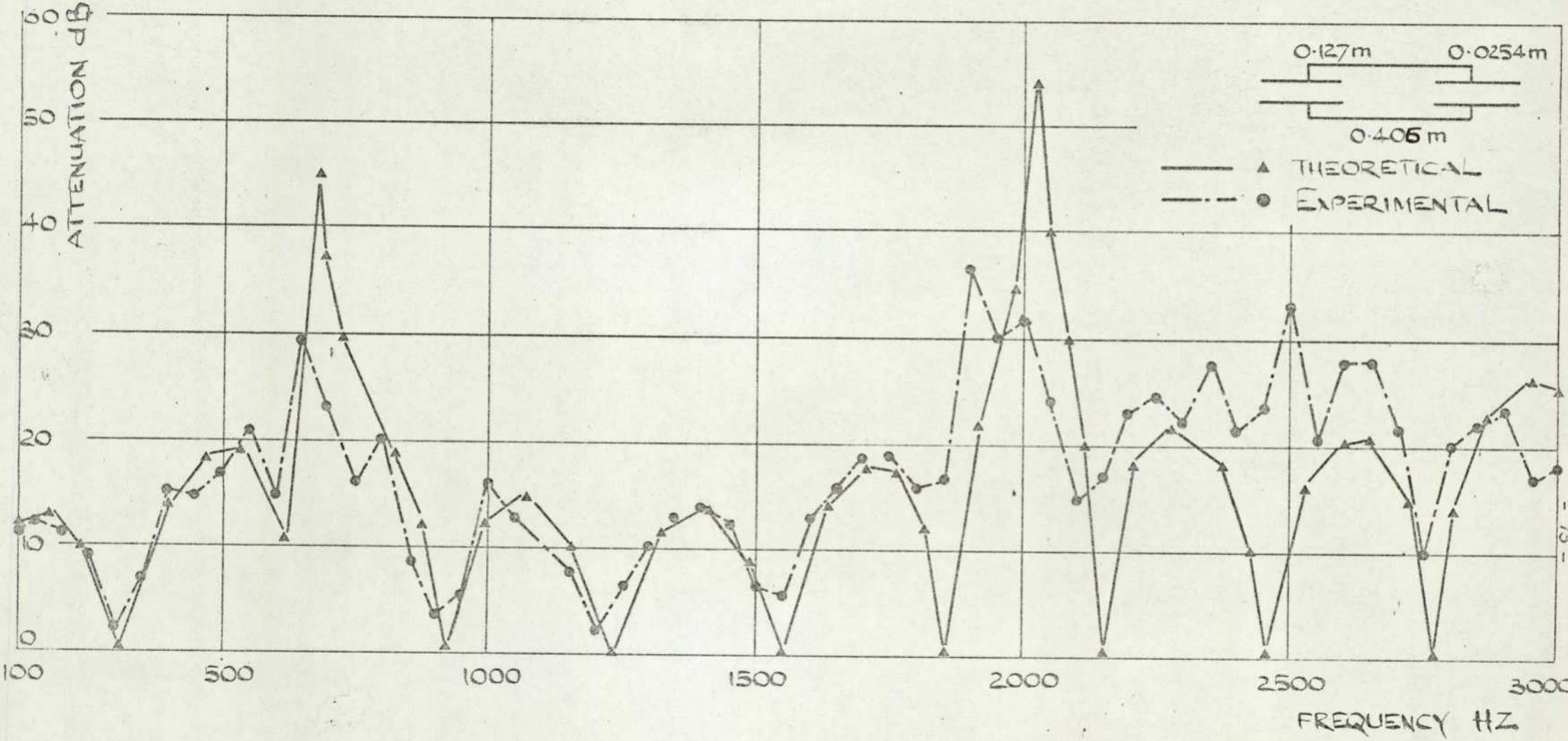

FIG. VII-10. ATTENUATION FREQUENCY CHARACTERISTICS for EXPANSION CHAMBER WITH INTERNAL PIPES.

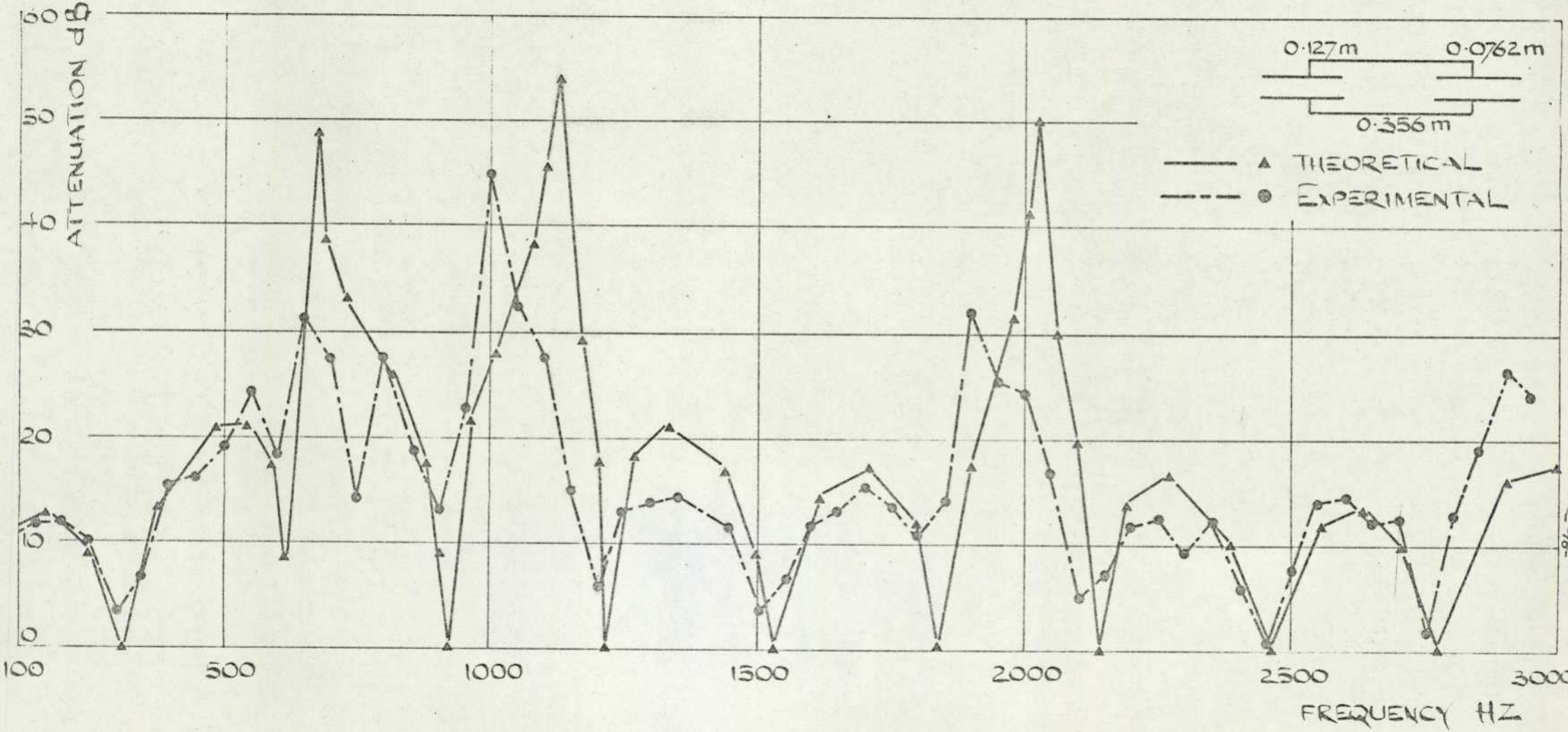

FIG. VII-11. ATTENUATION FREQUENCY CHARACTERISTICS FOR EXPANSION CHAMBER WITH INTERNAL PIPES.

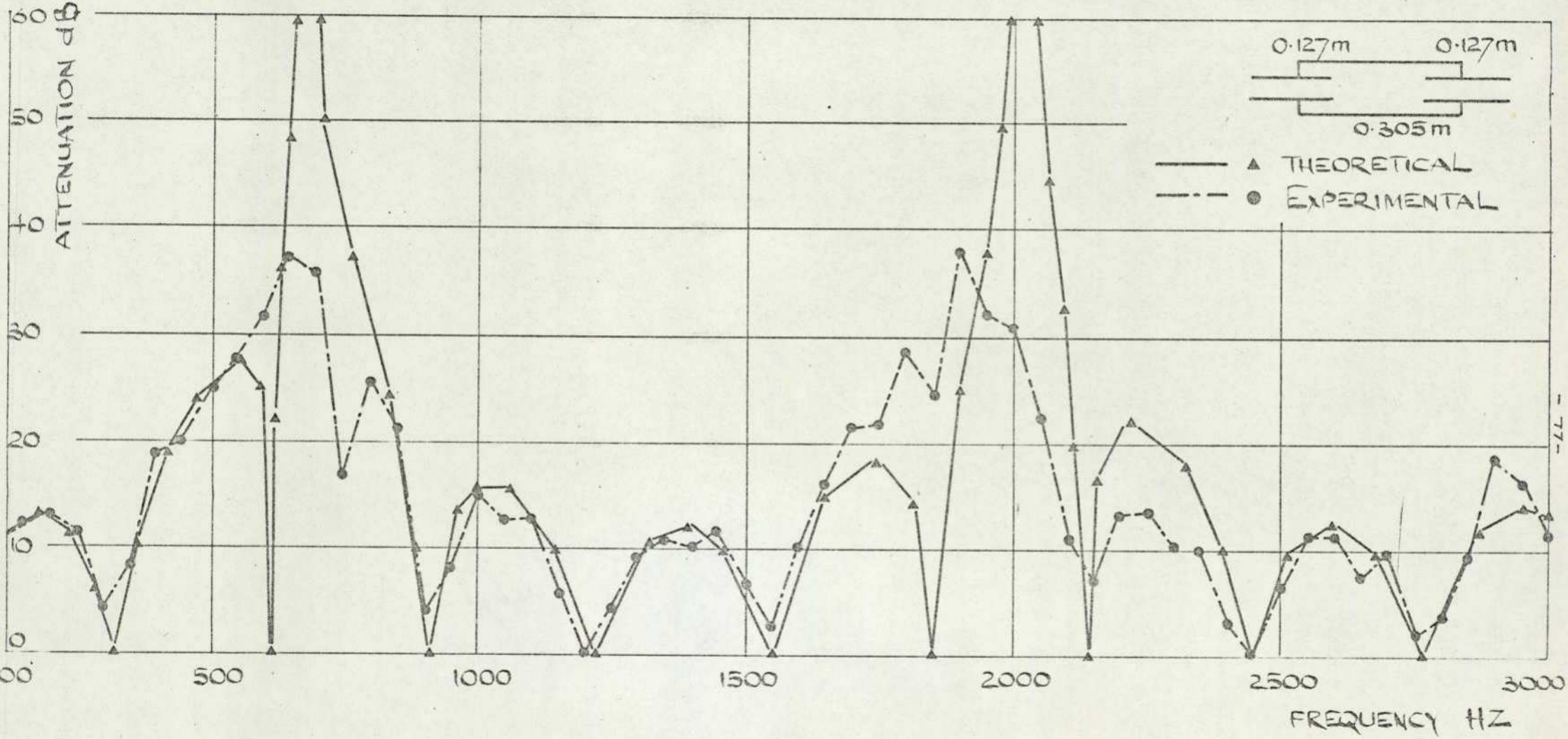

FIG. VII-12. ATTENUATION FREQUENCY CHARACTERISTICS for EXPANSION CHAMBER WITH INTERNAL PIPES.

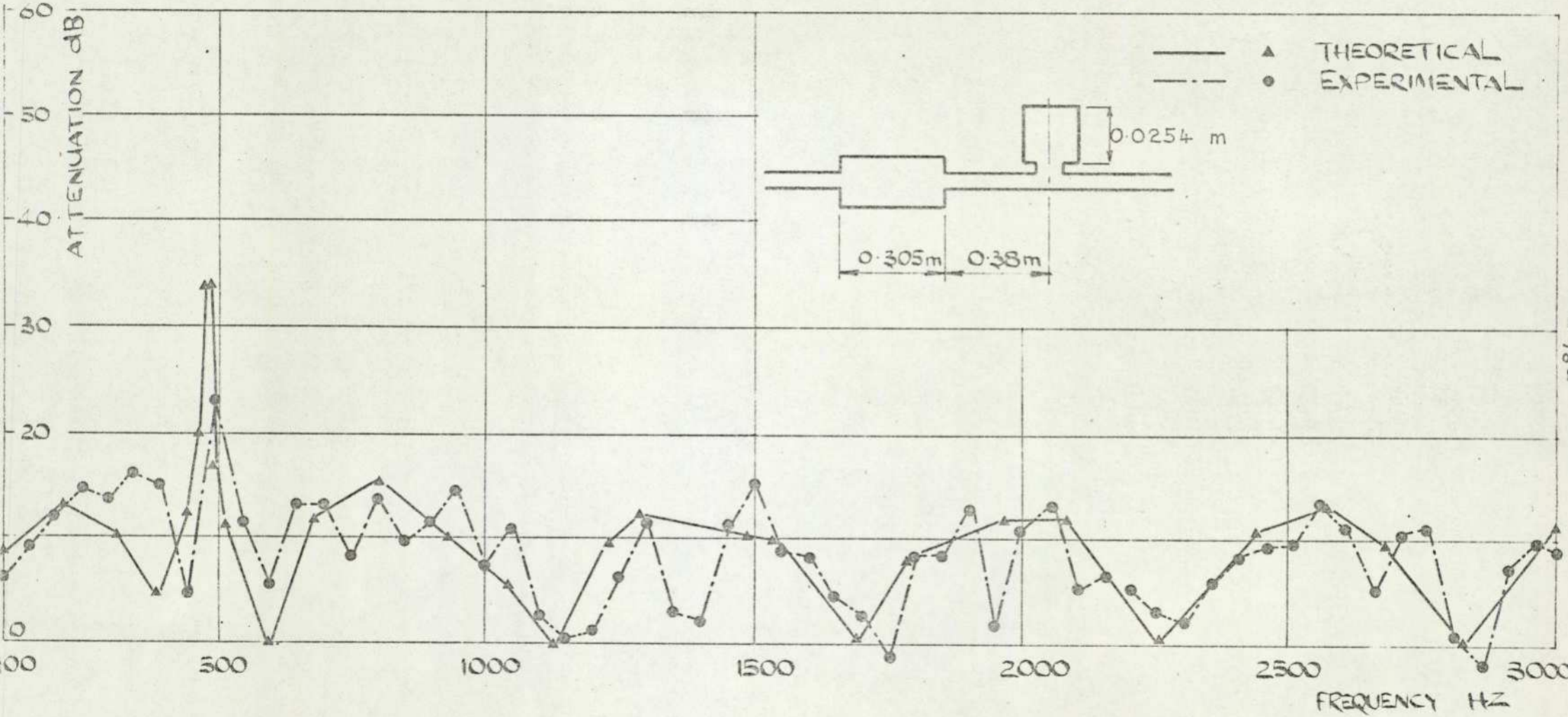

FIG. VII-13. ATTENUATION FREQUENCY CHARACTERISTICS for EXPANSION CHAMBER IN SERIES WITH RESONATOR

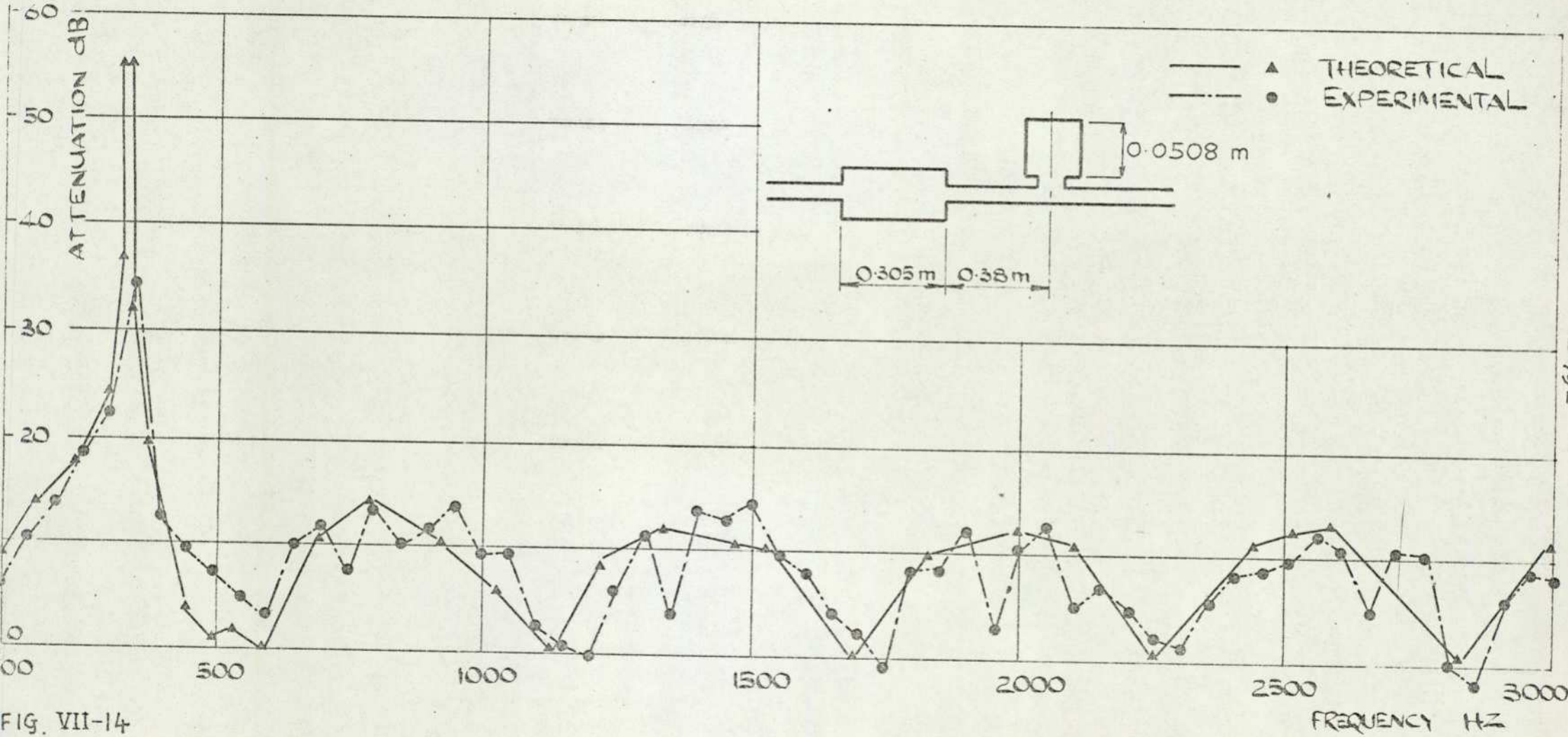

FIG. VII-14

ATTENUATION FREQUENCY CHARACTERISTICS for EXPANSION CHAMBER IN SERIES WITH RESONATOR

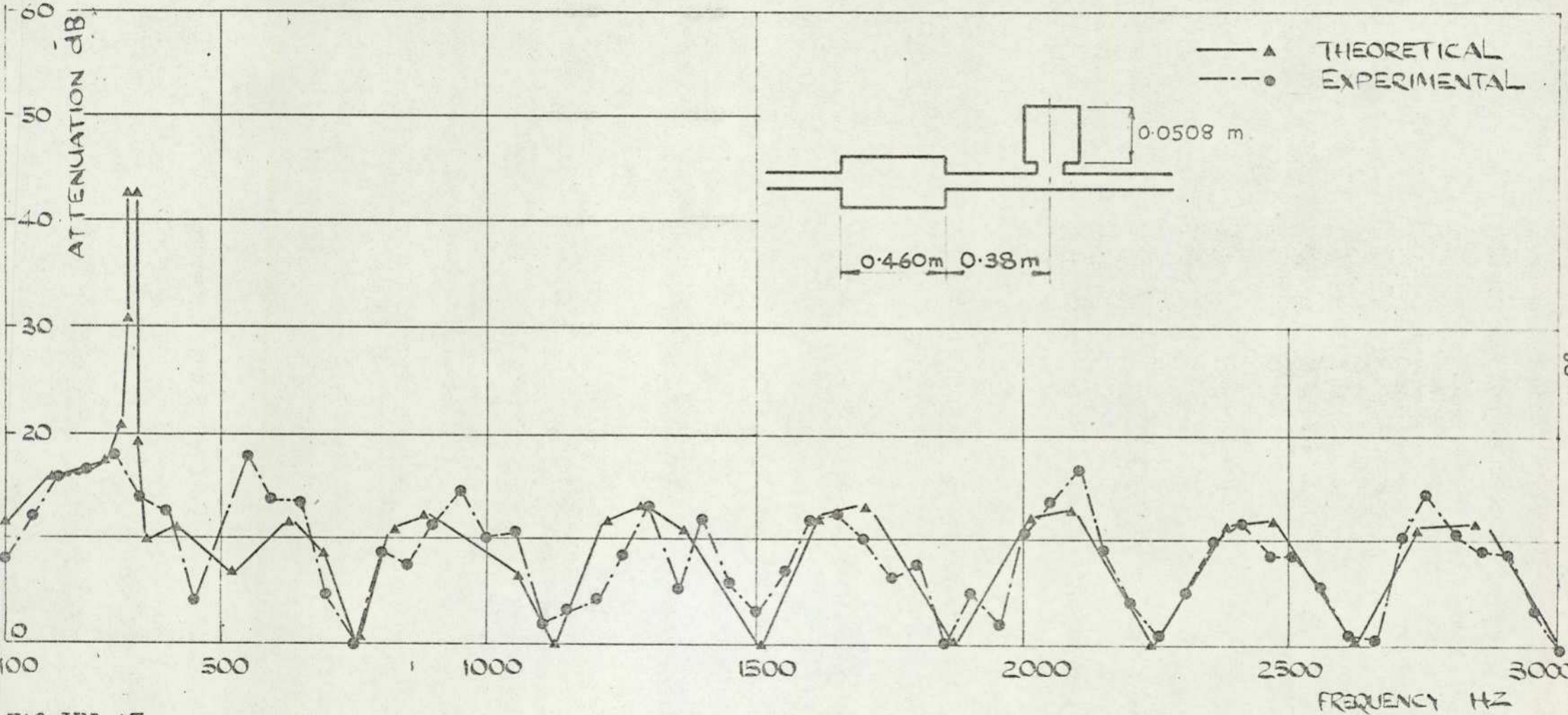

FIG VII-15

ATTENUATION FREQUENCY CHARACTERISTICS for EXPANSION CHAMBER IN SERIES WITH RESONATOR

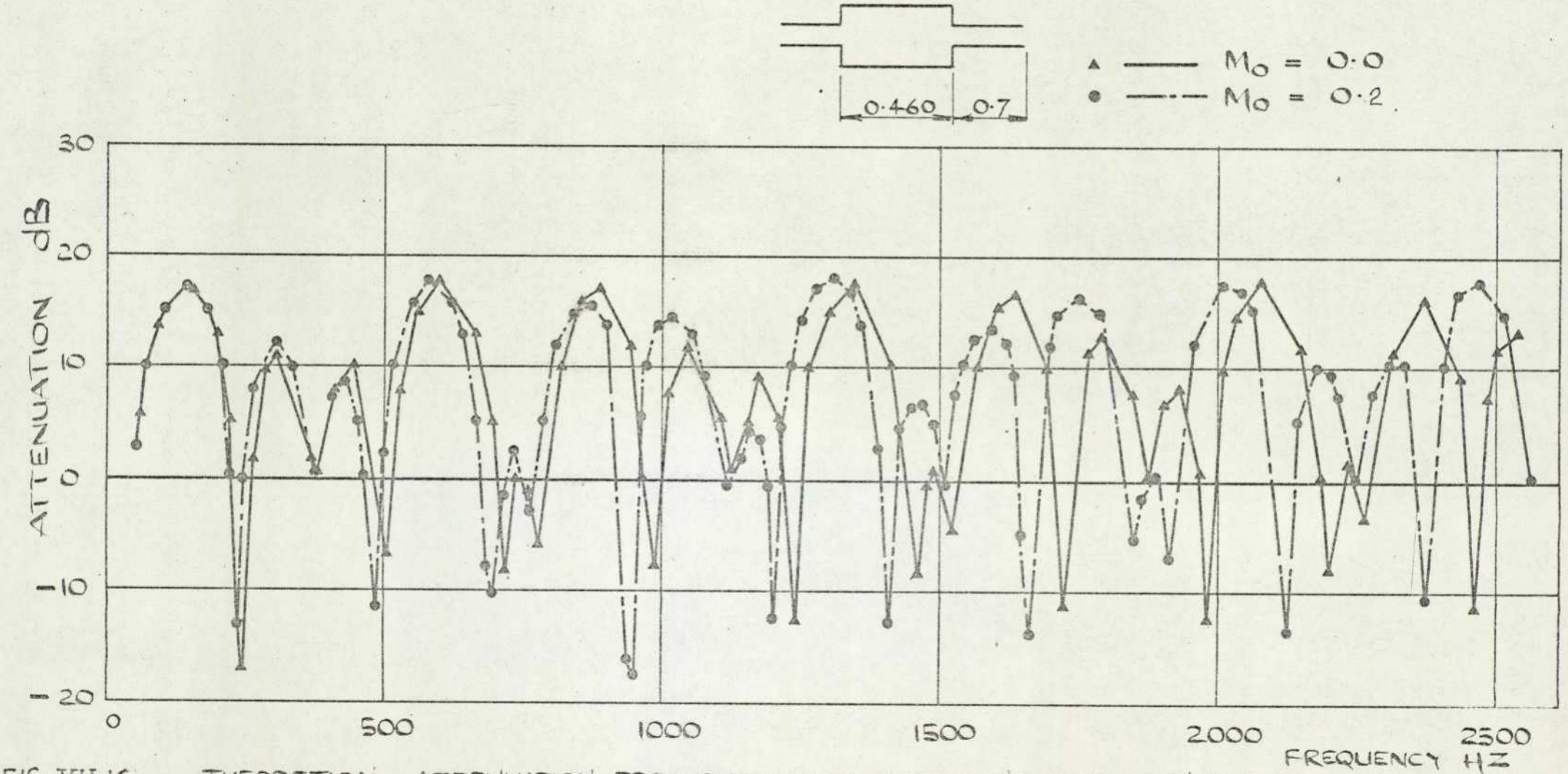

FIG VII-16 THEORETICAL ATTENUATION-FREQUENCY CHARACTERISTICS FOR SIMPLE EXPANSION CHAMBER WITH FINITE OUTLET PIPE.

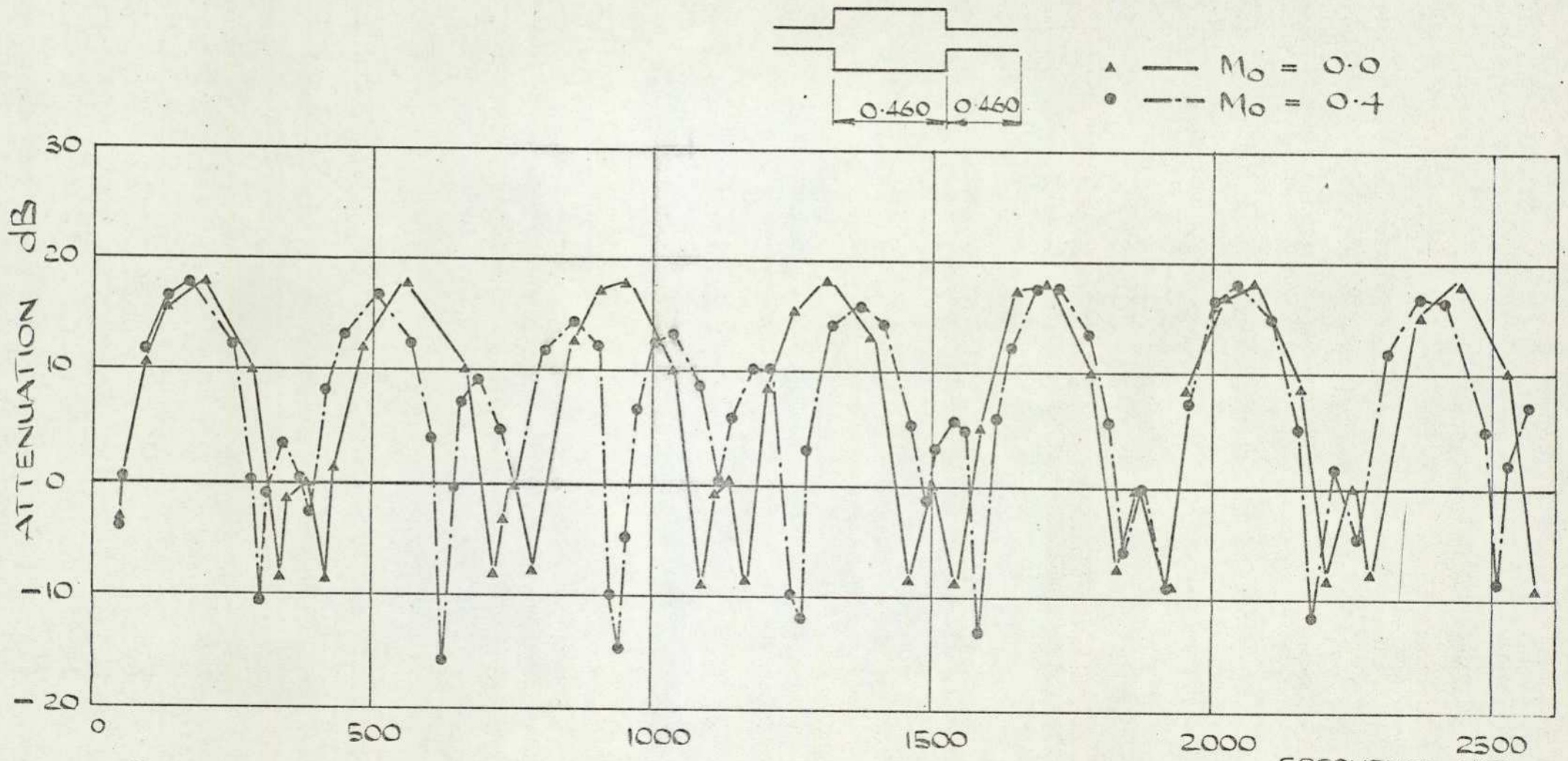

FIG VII-17 THEORETICAL ATTENUATION-FREQUENCY CHARACTERISTICS FOR SIMPLE EXPANSION CHAMBER WITH FINITE OUTLET PIPE.

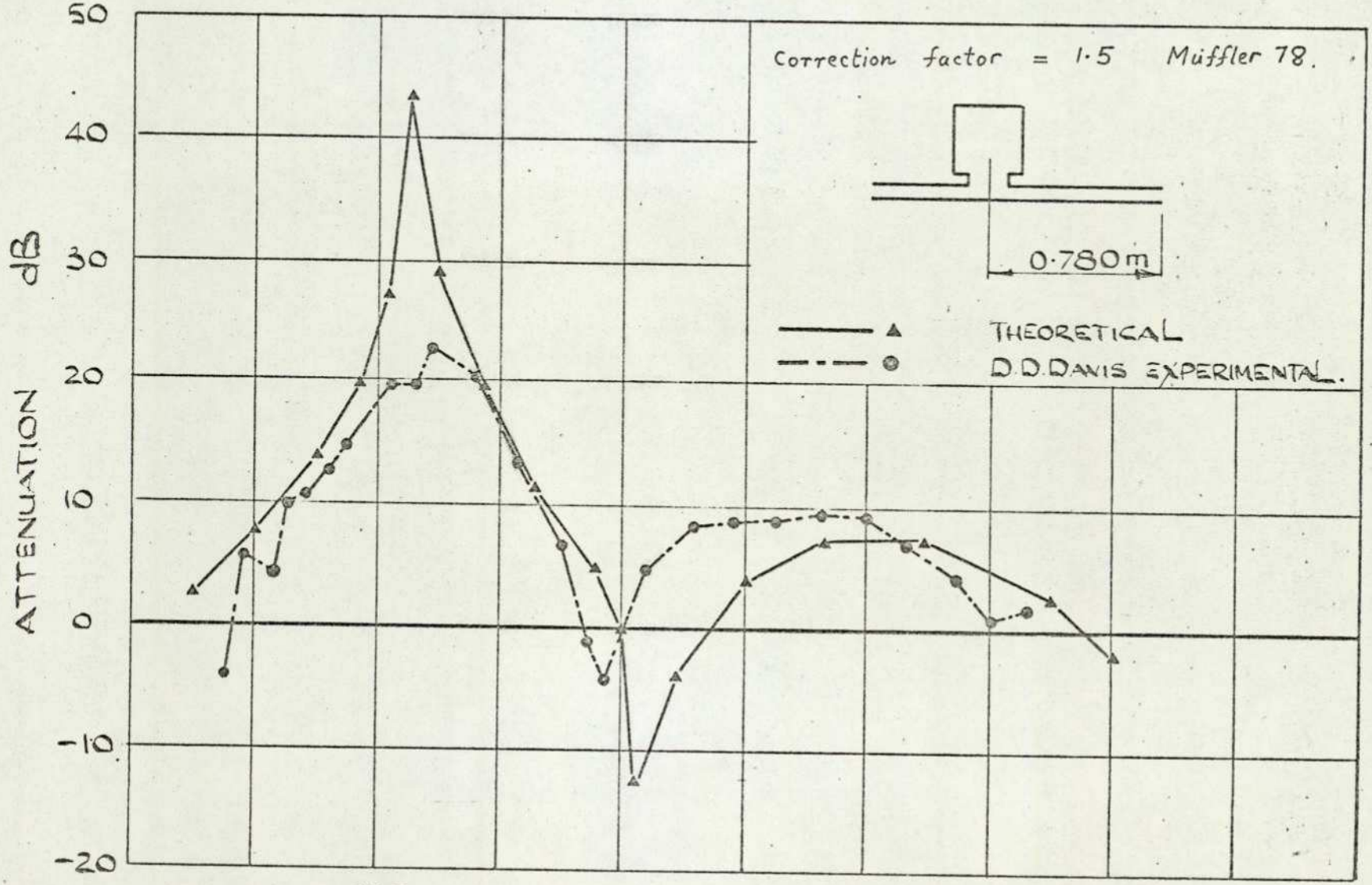

FIG. VII-18.

ATTENUATION -FREQUENCY CHARACTISTICS WITH FINITE OUTLET PIPE FOR RESONATOR

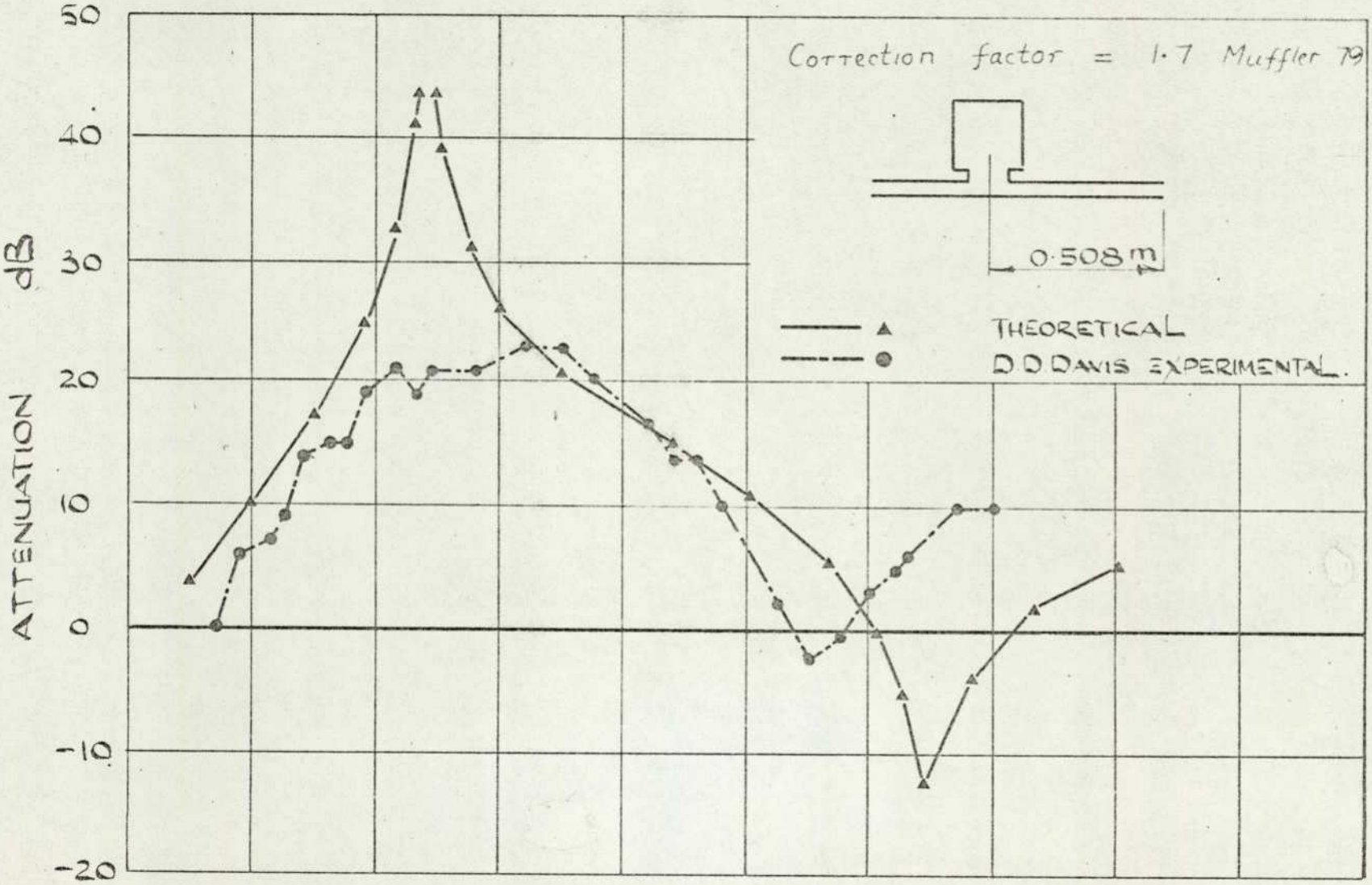

FIG VII-19

ATTENUATION -FREQUENCY CHARACTISTICS WITH FINITE OUTLET PIPE FOR RESONATOR

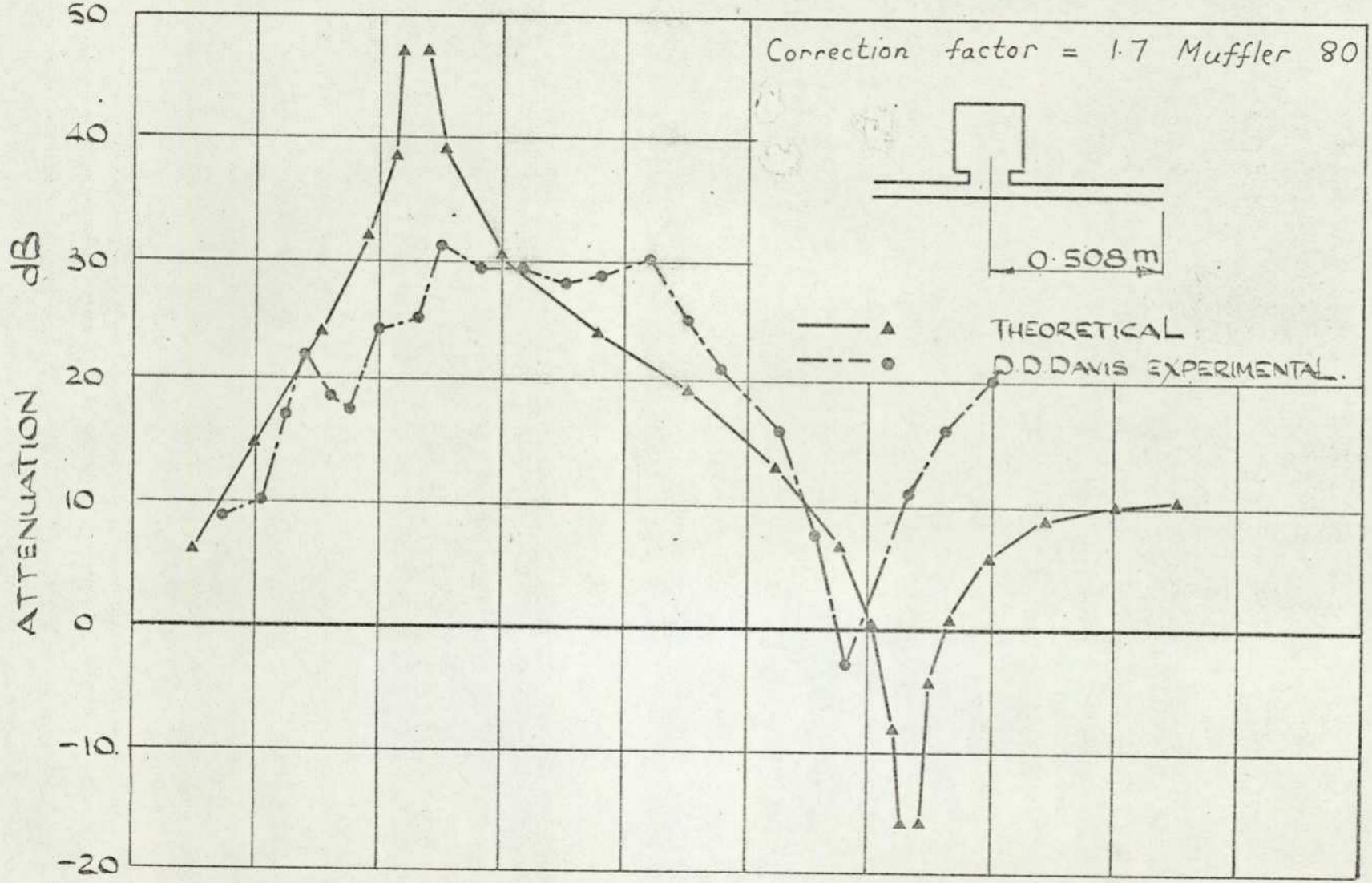

FIG VII-20.

ATTENUATION - FREQUENCY CHARACTISTICS WITH FINITE OUTLET PIPE FOR RESONATOR

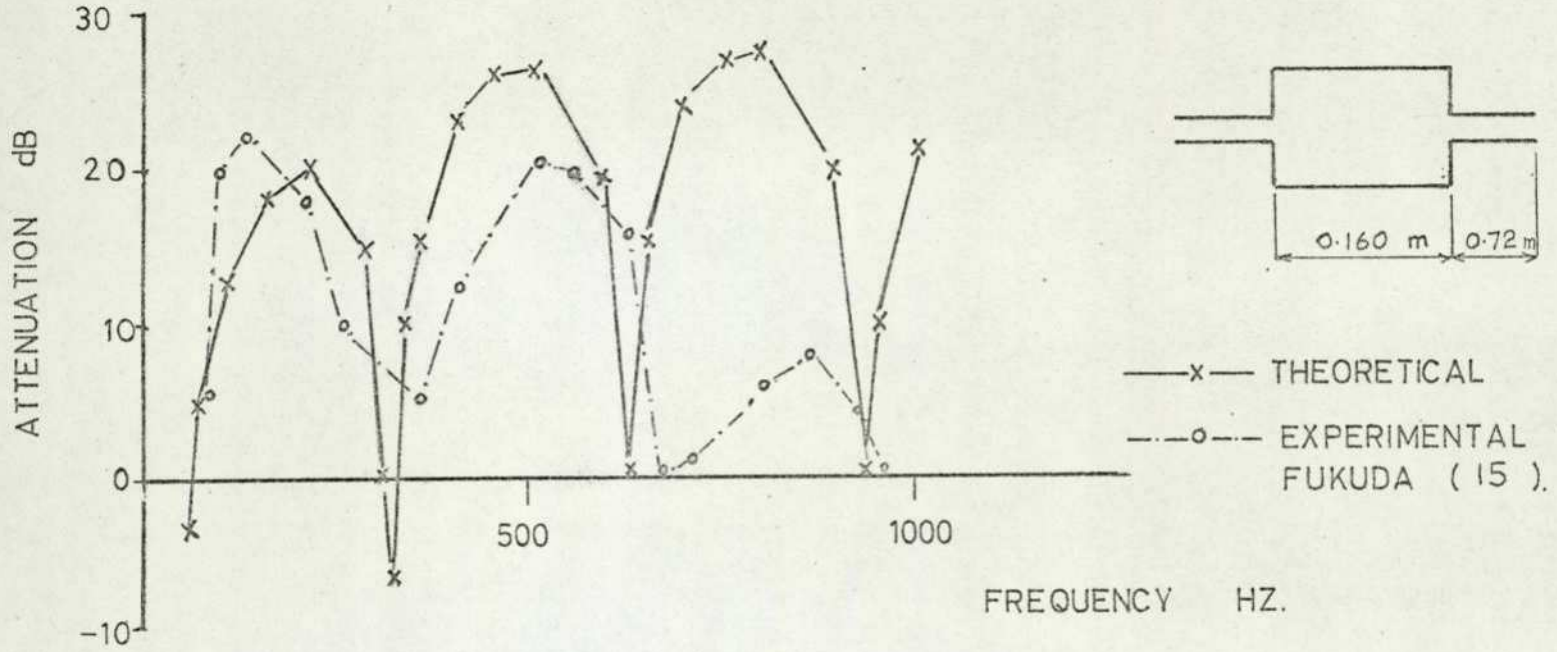

FIG. VII - 21
ATTENUATION FREQUENCY CHARACTERISTIC OF SIMPLE EXPANSION CHAMBER WITH FINITE OUTLET PIPE.

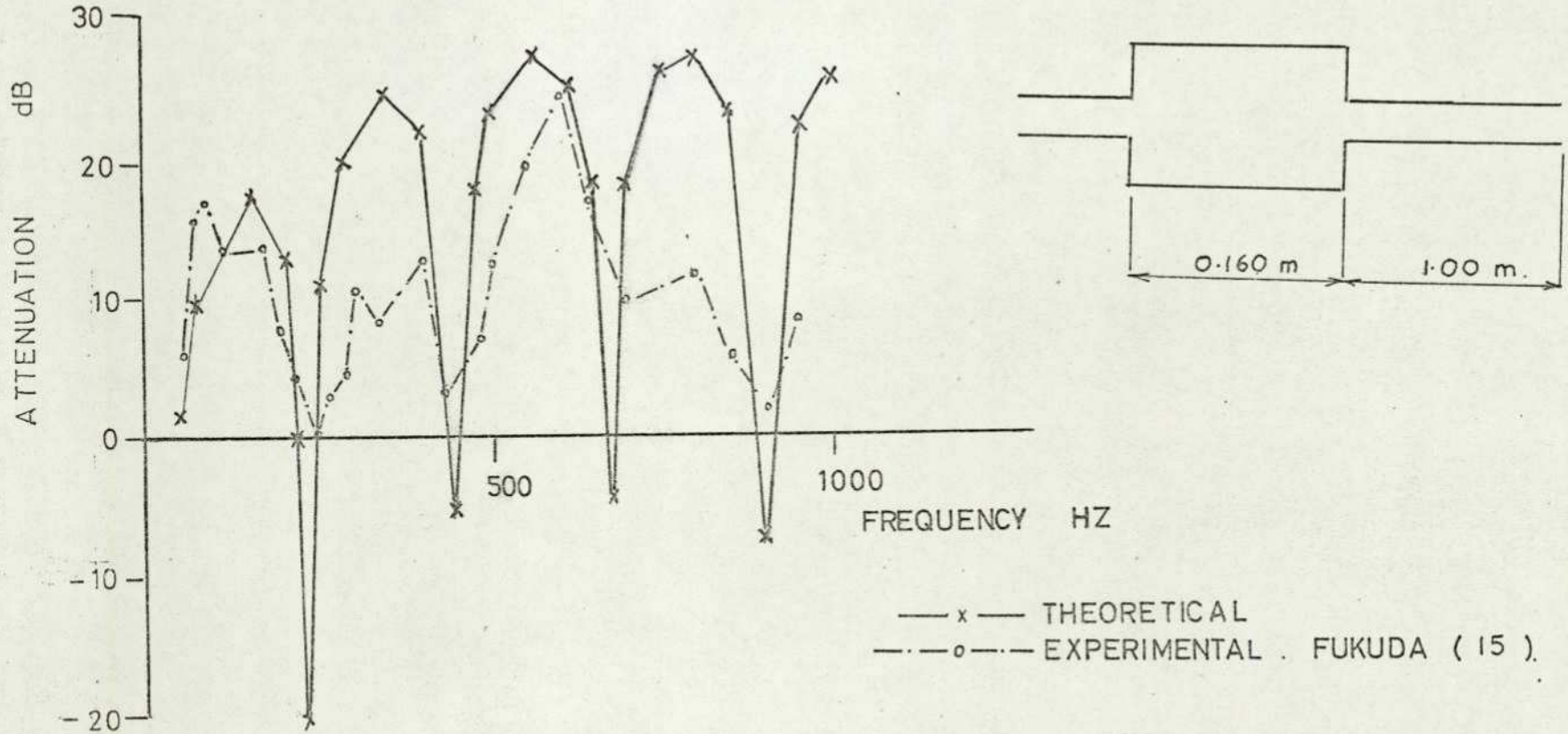

FIG. VII – 22 ATTENUATION – FREQUENCY CHARACTERISTIC OF SIMPLE EXPANSION CHAMBER WITH FINITE OUTLET PIPE.

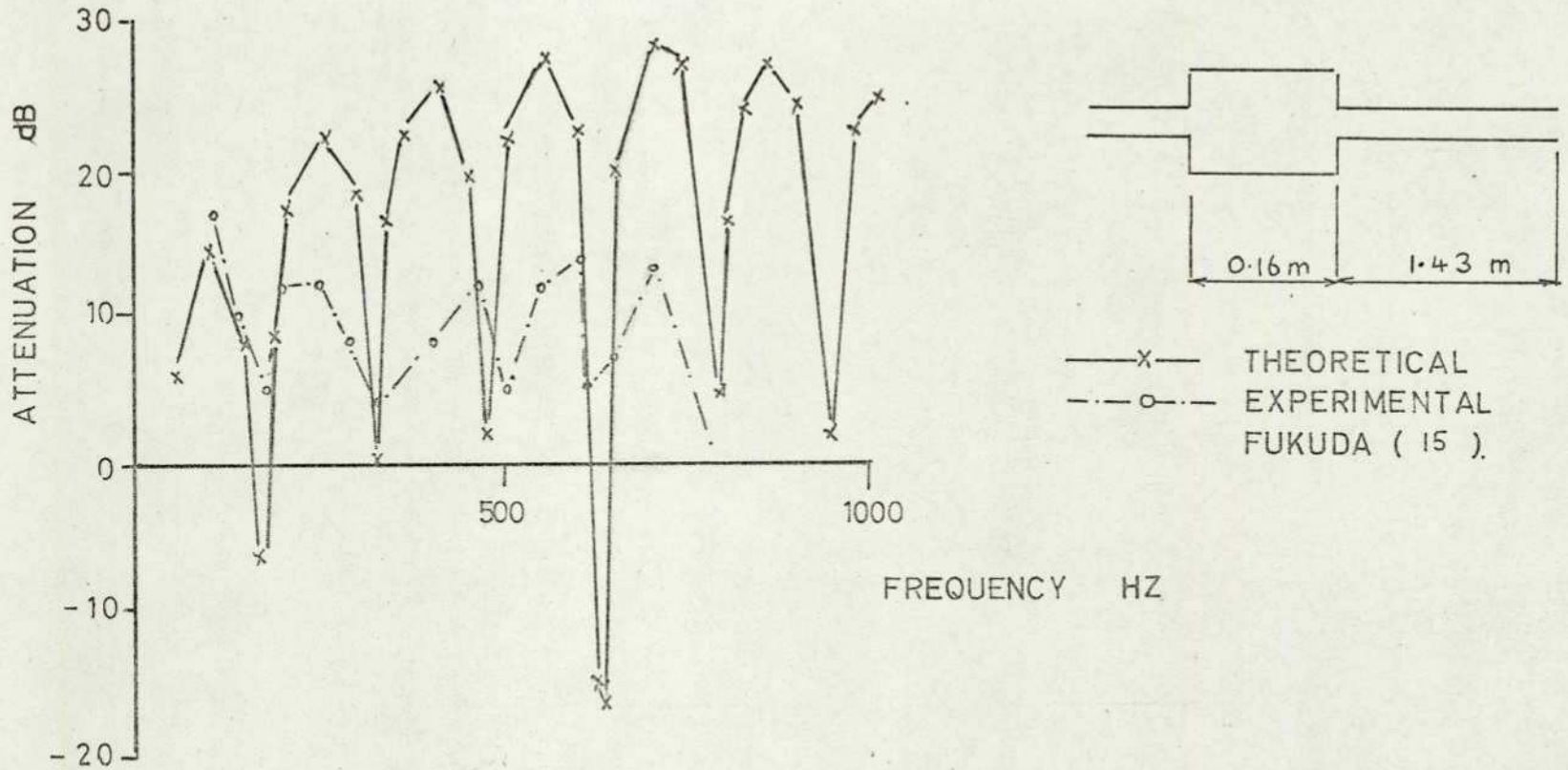

FIG. VII-23. ATTENUATION — FREQUENCY CHARACTERISTIC OF SIMPLE EXPANSION CHAMBER WITH FINITE OUTLET PIPE.

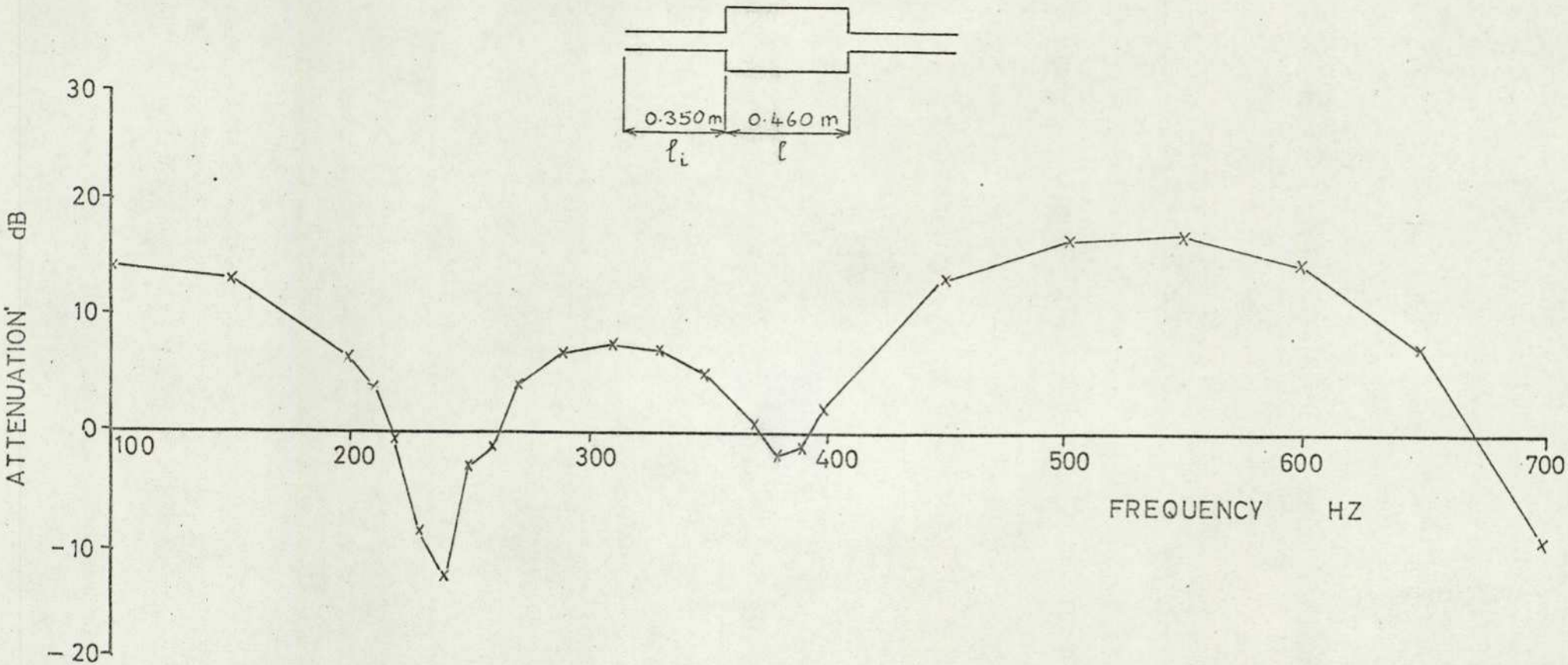

FIG. VII - 24
THEORETICAL ATTENUATION FREQUENCY CHARACTERISTIC OF SIMPLE EXPANSION CHAMBER WITH FINITE INLET PIPE.

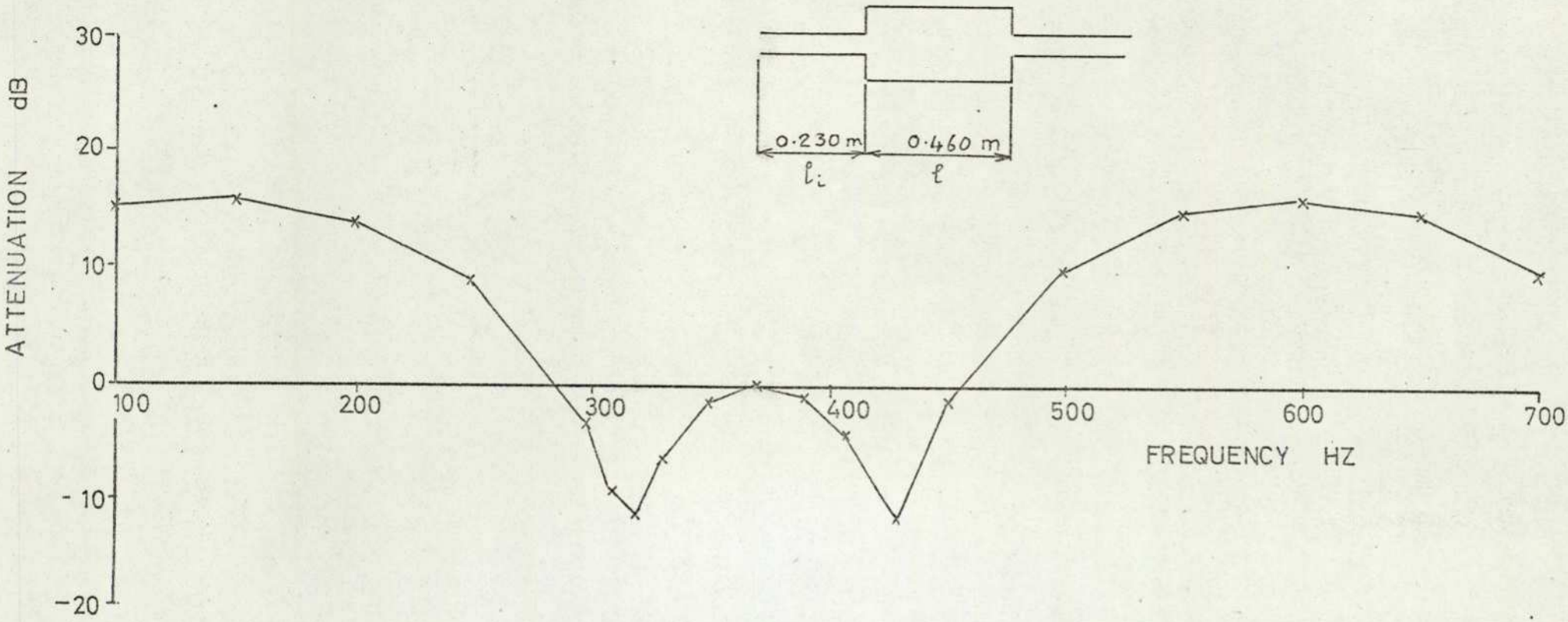

FIG. VII - 25

THEORETICAL ATTENUATION FREQUENCY CHARACTERISTIC OF SIMPLE EXPANSION CHAMBER WITH FINITE INLET PIPE.

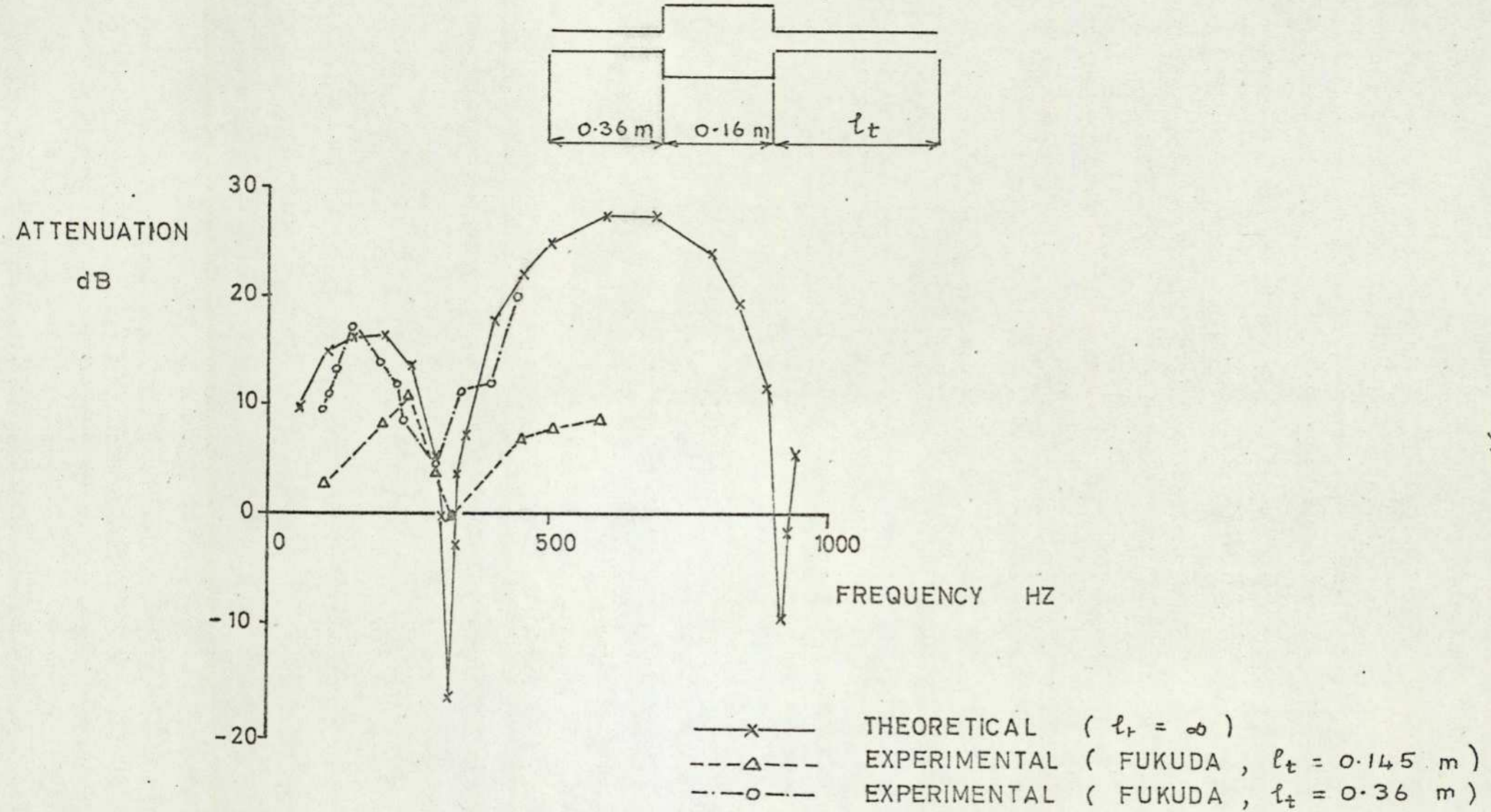

FIG. VII 26.
ATTENUATION FREQUENCY CHARACTERISTICS OF SIMPLE EXPANSION CHAMBER WITH FINITE INLET PIPE

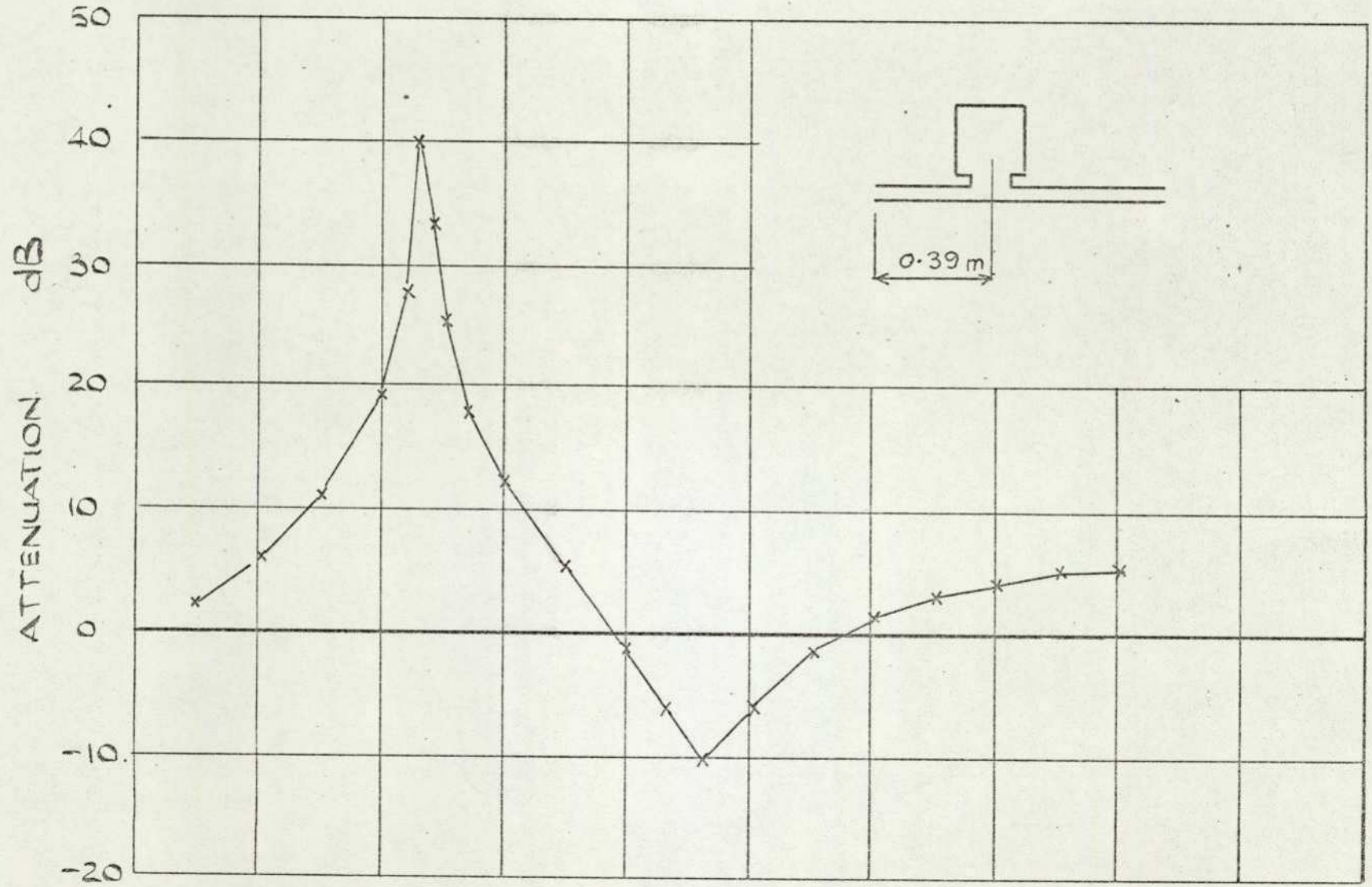

FIG. VII-27

ATTENUATION-FREQUENCY CHARACTISTICS WITH FINITE INLET PIPE FOR RESONATOR

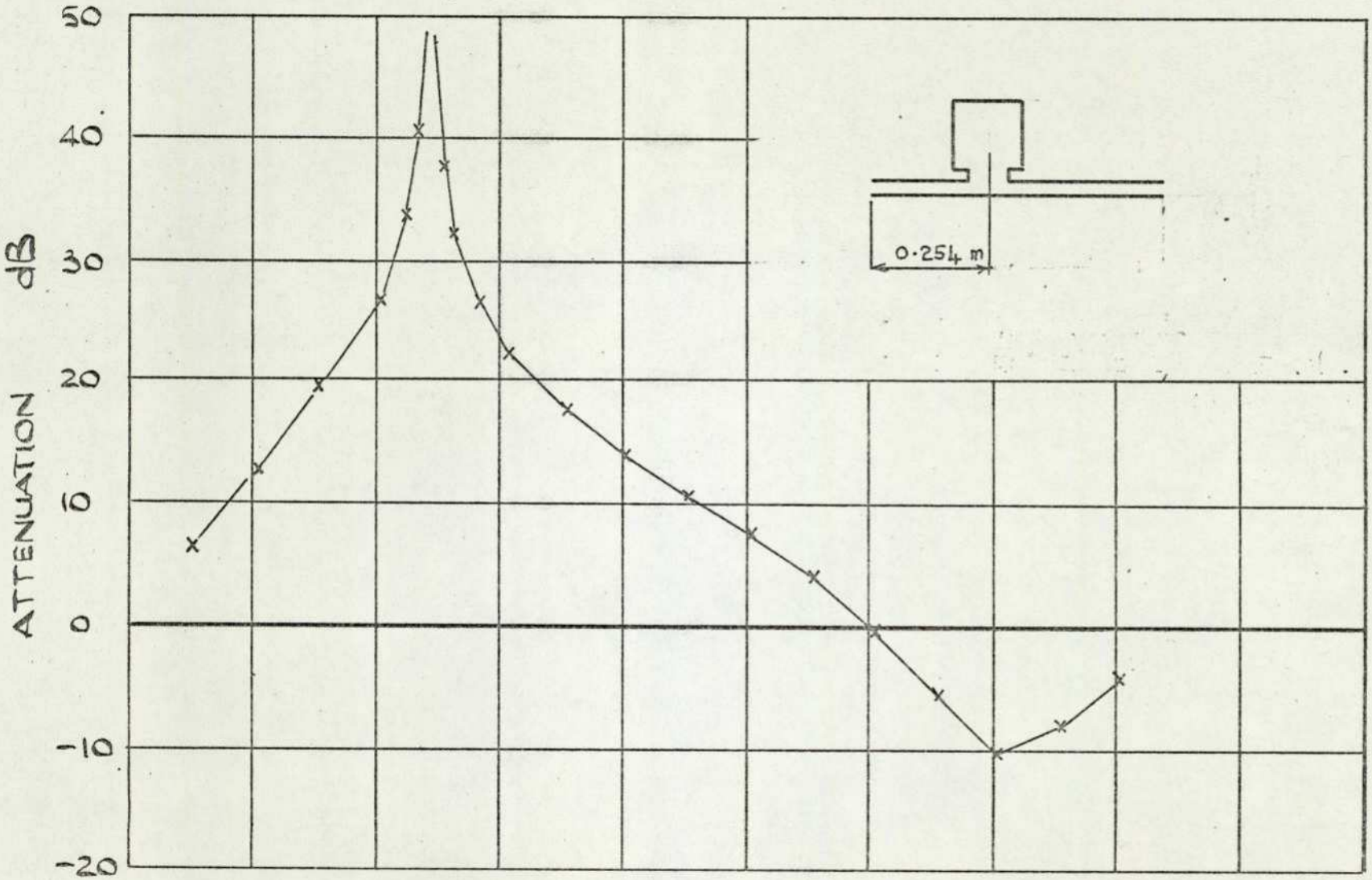

FIG. VII-28.
ATTENUATION -FREQUENCY CHARACTISTICS WITH FINITE INLET PIPE FOR RESONATOR

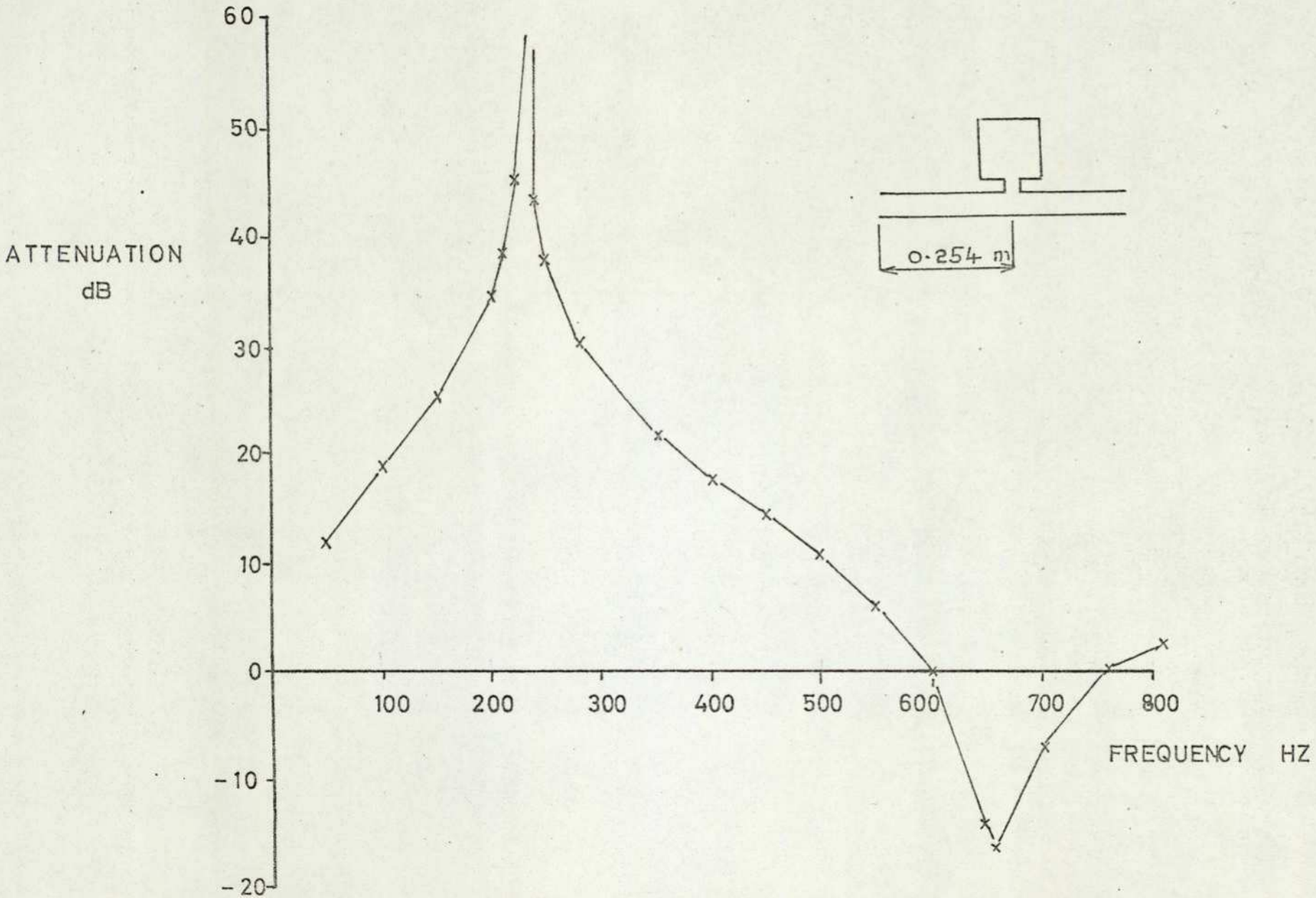

FIG. VII - 29
THEORETICAL ATTENUATION FREQUENCY CHARACTERISTIC FOR RESONATOR WITH FINITE INLET PIPE.

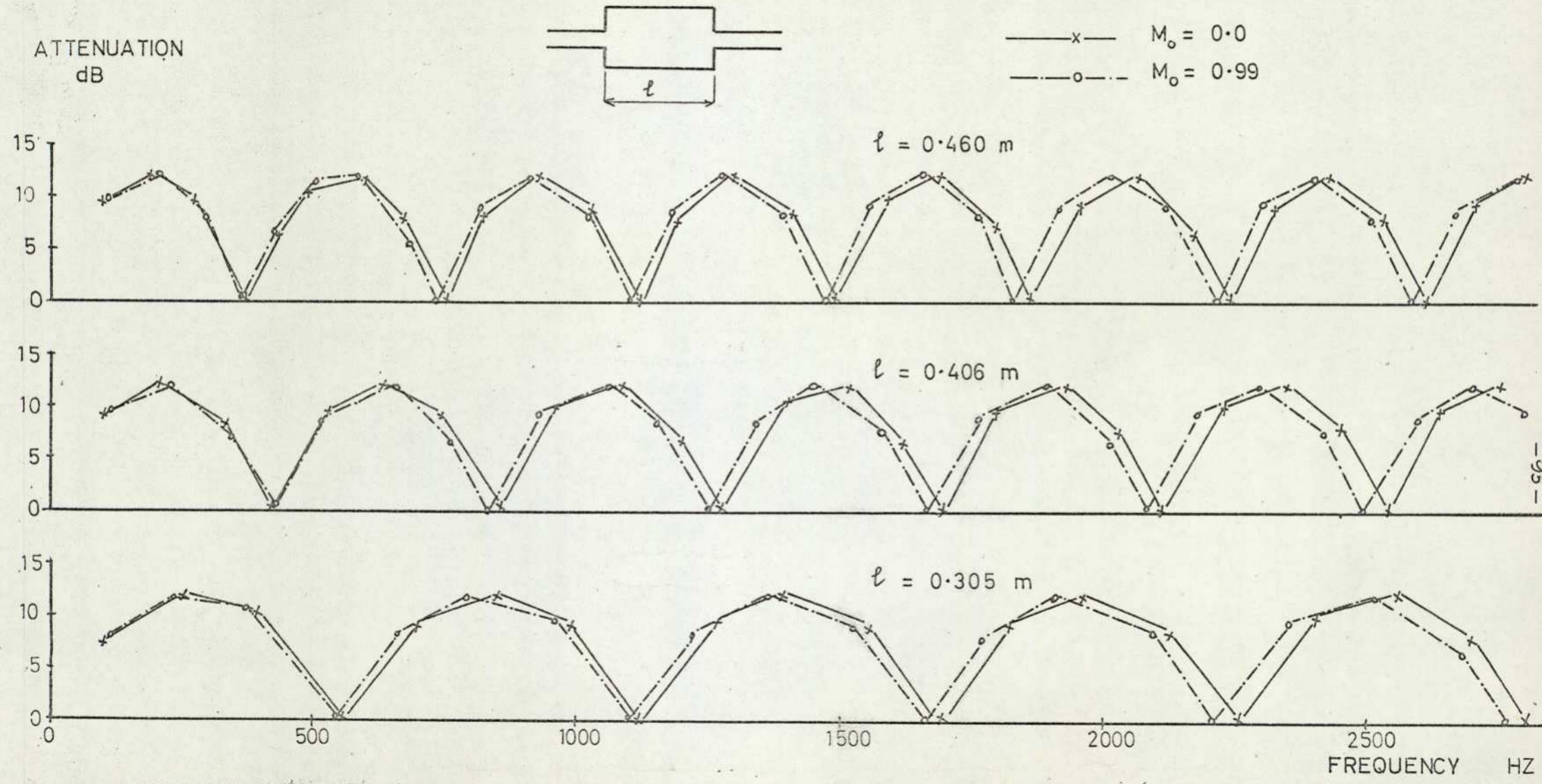

FIG. VII - 30 THEORETICAL ATTENUATION FREQUENCY CHARACTERISTICS OF SIMPLE-EXPANSION CHAMBER WITH FLOW

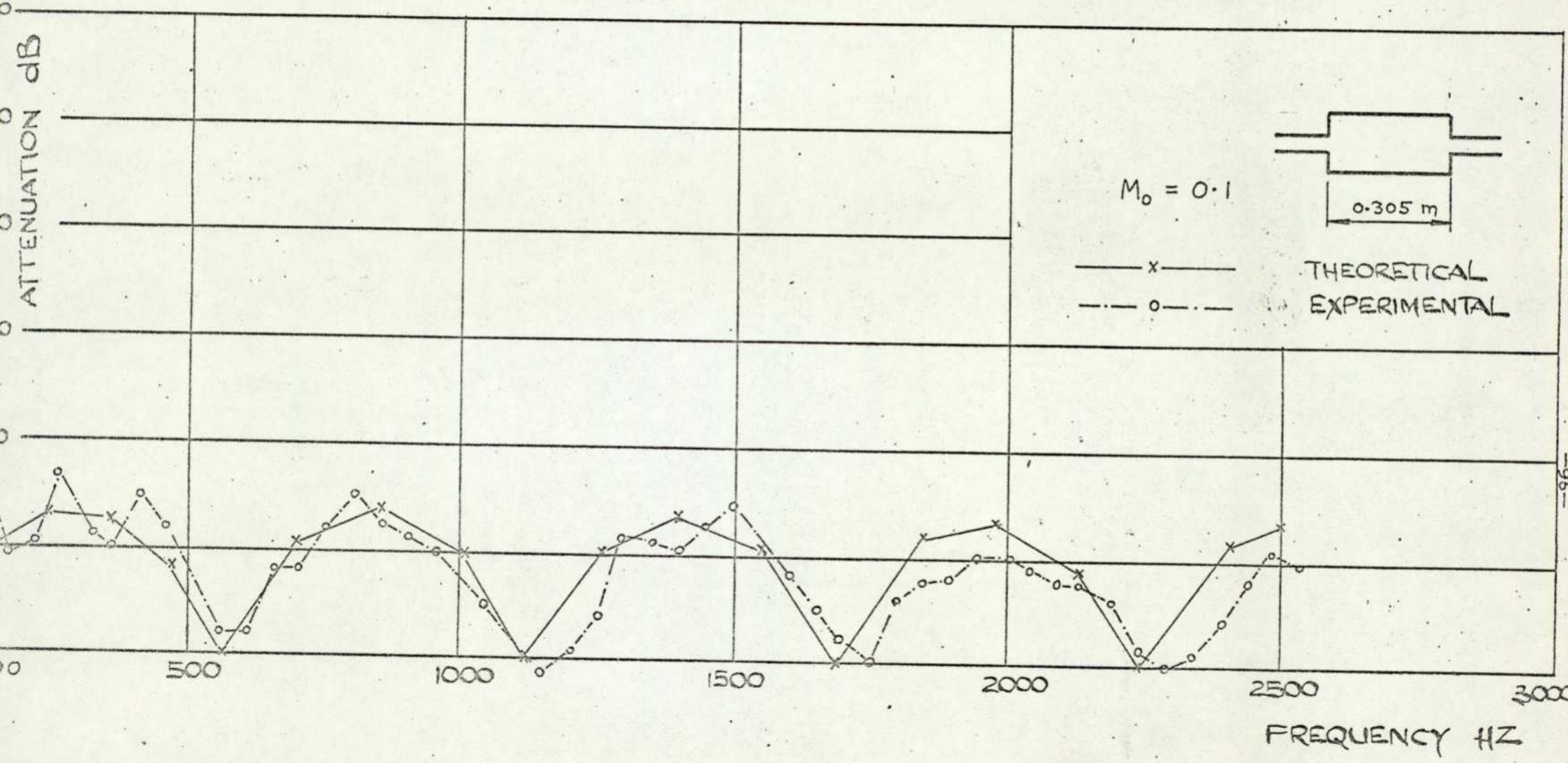

FIG. VII-31. ATTENUATION FREQUENCY CHARACTERISTICS for SIMPLE EXPANSION CHAMBER with INTERNAL AIR FLOW.

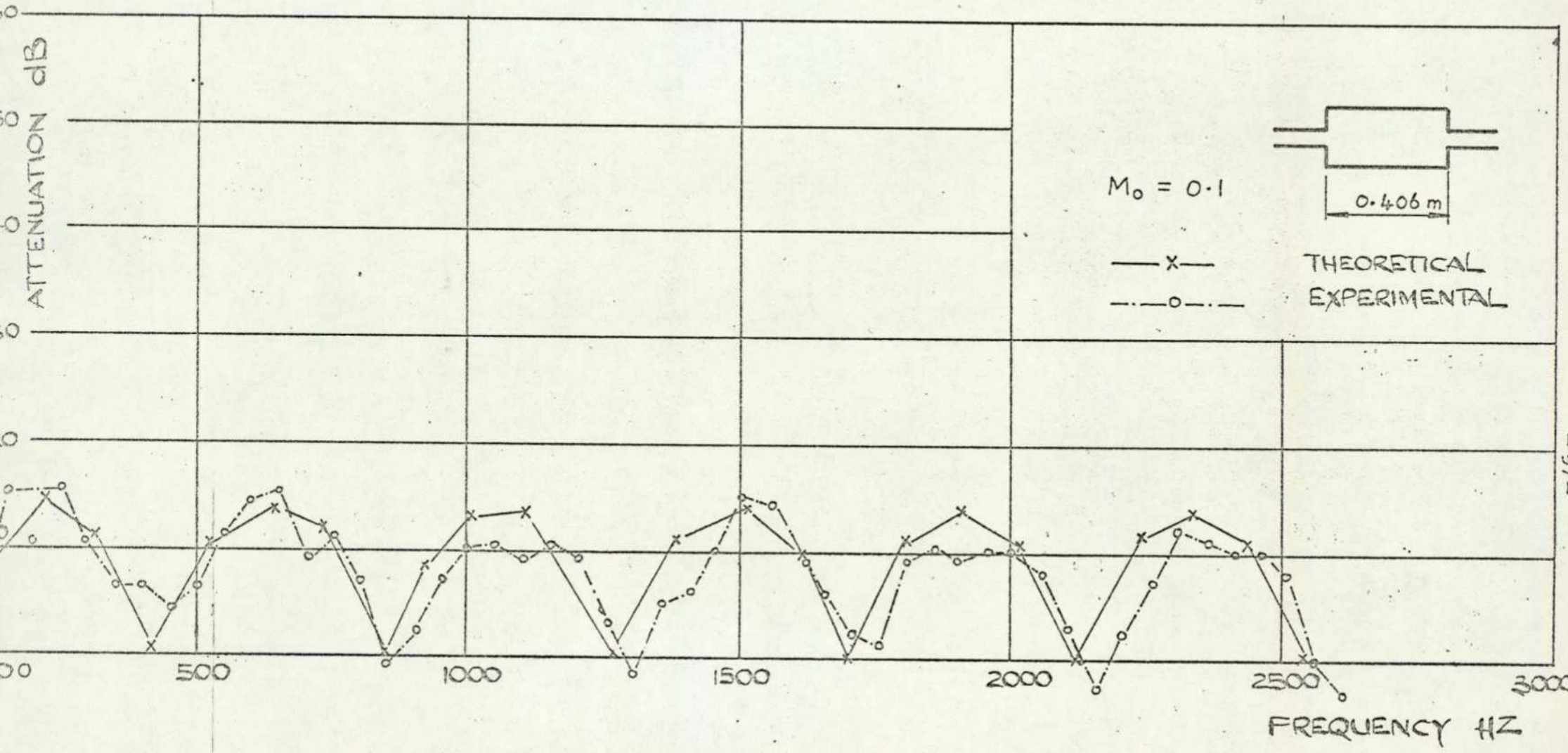

FIG. VII-32. ATTENUATION FREQUENCY CHARACTERISTICS for SIMPLE EXPANSION CHAMBER with INTERNAL AIR FLOW.

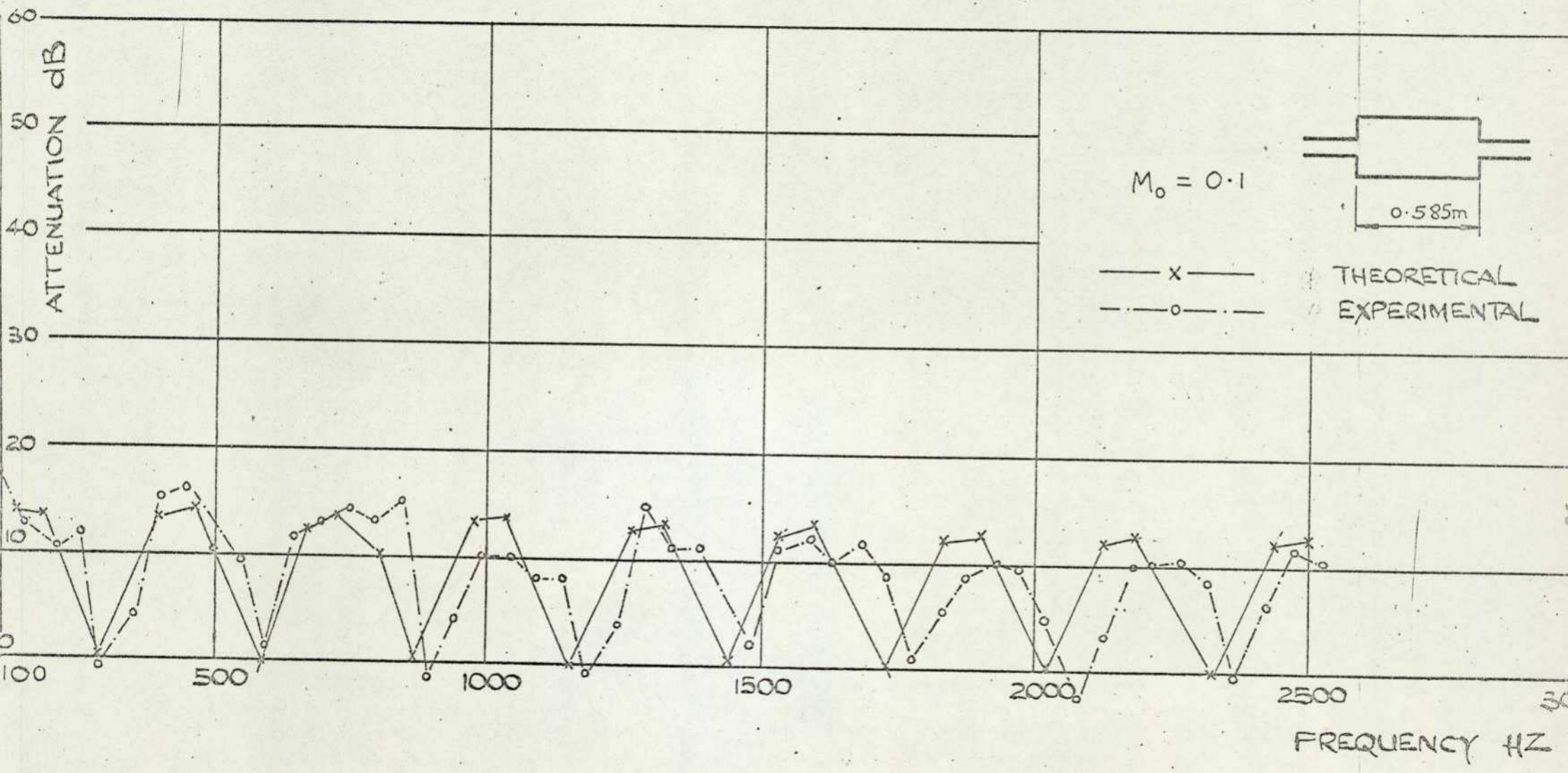

FIG. VII-33. ATTENUATION FREQUENCY CHARACTERISTICS for SIMPLE EXPANSION CHAMBER with INTERNAL AIR FLOW.

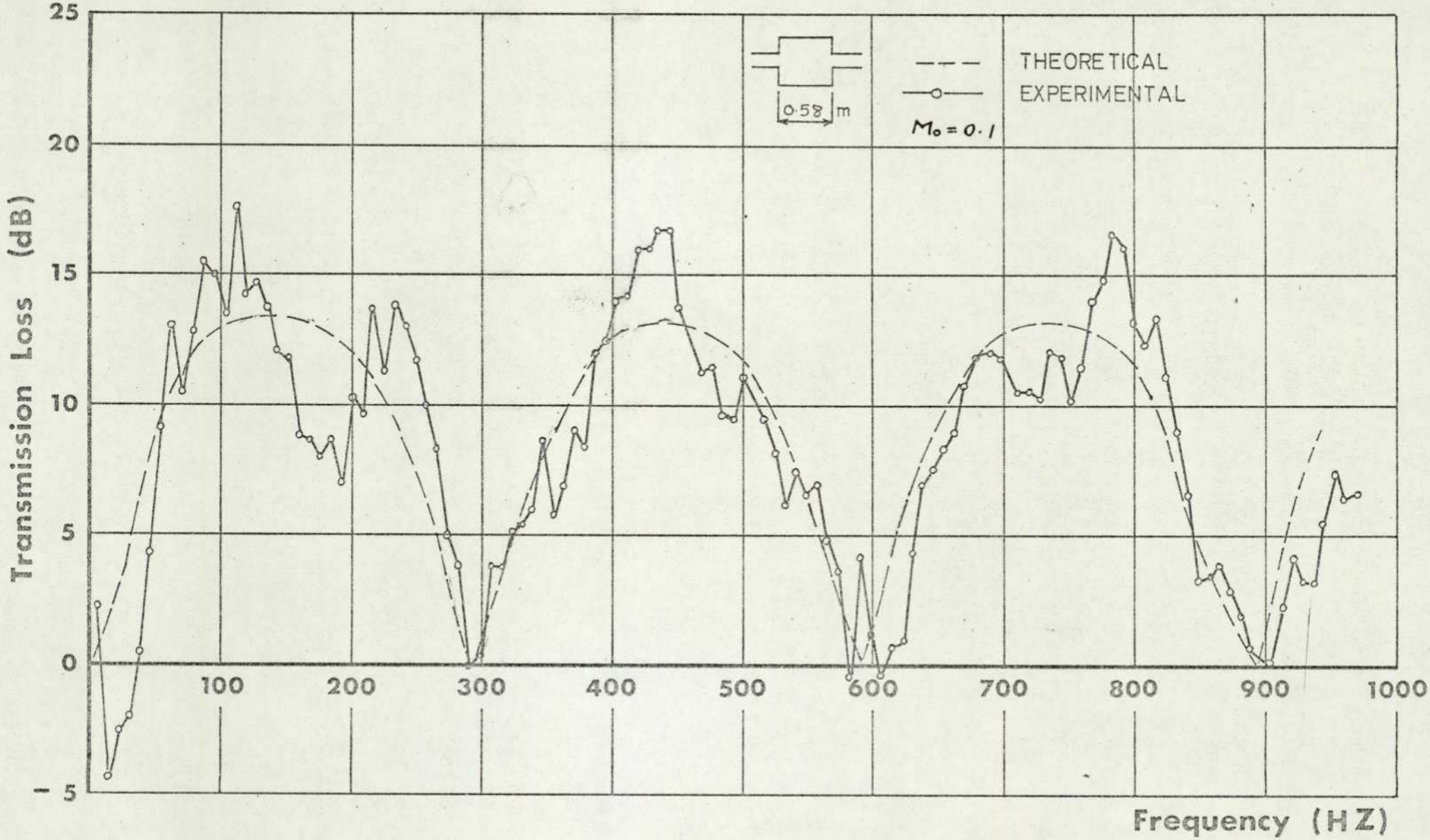

FIG VII—34.
ATTENUATION – FREQUENCY CHARACTERISTICS OF SIMPLE EXPANSION CHAMBER WITH INTERNAL AIR FLOW.

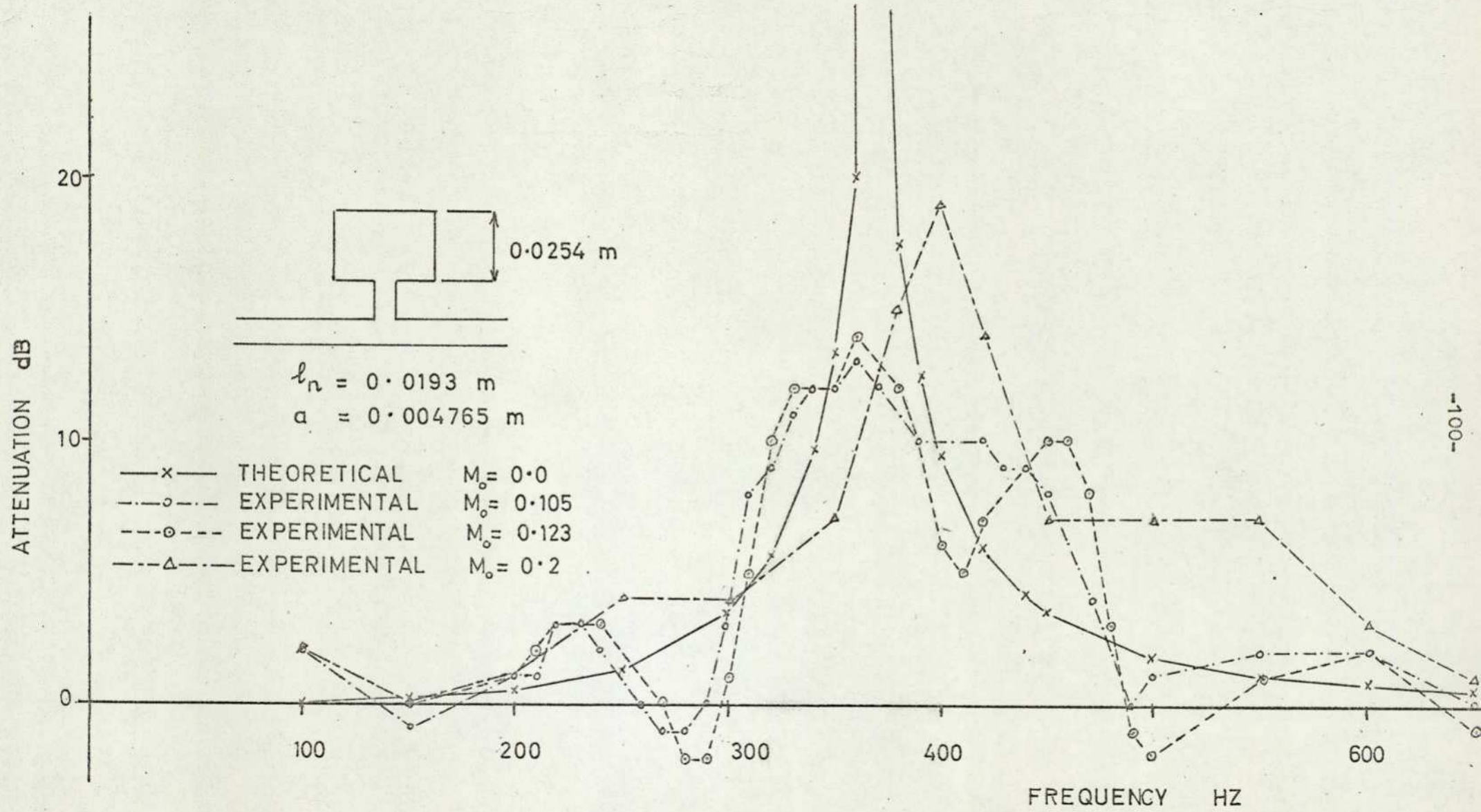

FIG. VII-35
ATTENUATION FREQUENCY CHARACTERISTICS OF RESONATOR WITH FLOW.

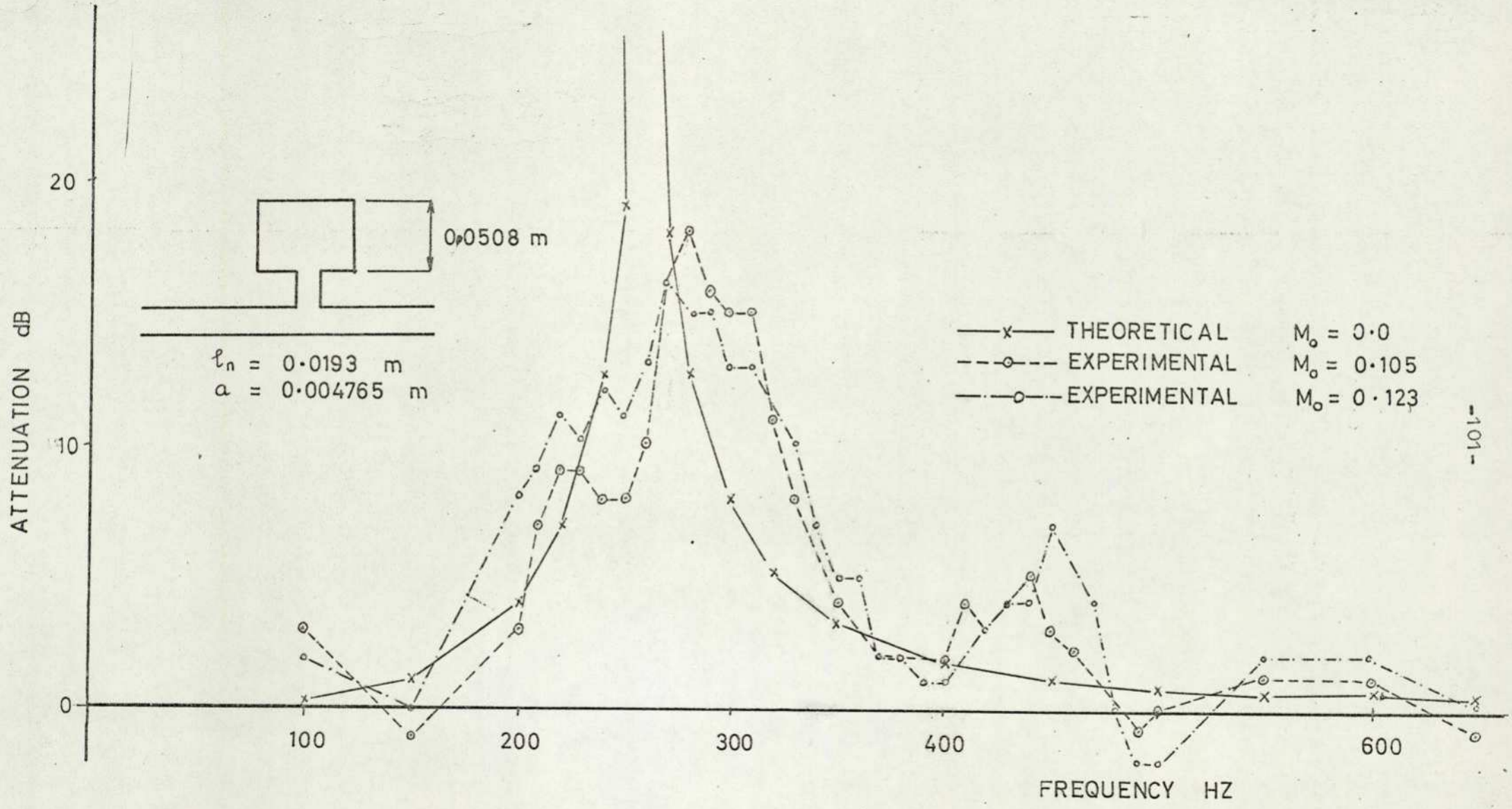

FIG. VII 36
ATTENUATION FREQUENCY CHARACTERISTICS OF RESONATOR WITH FLOW.

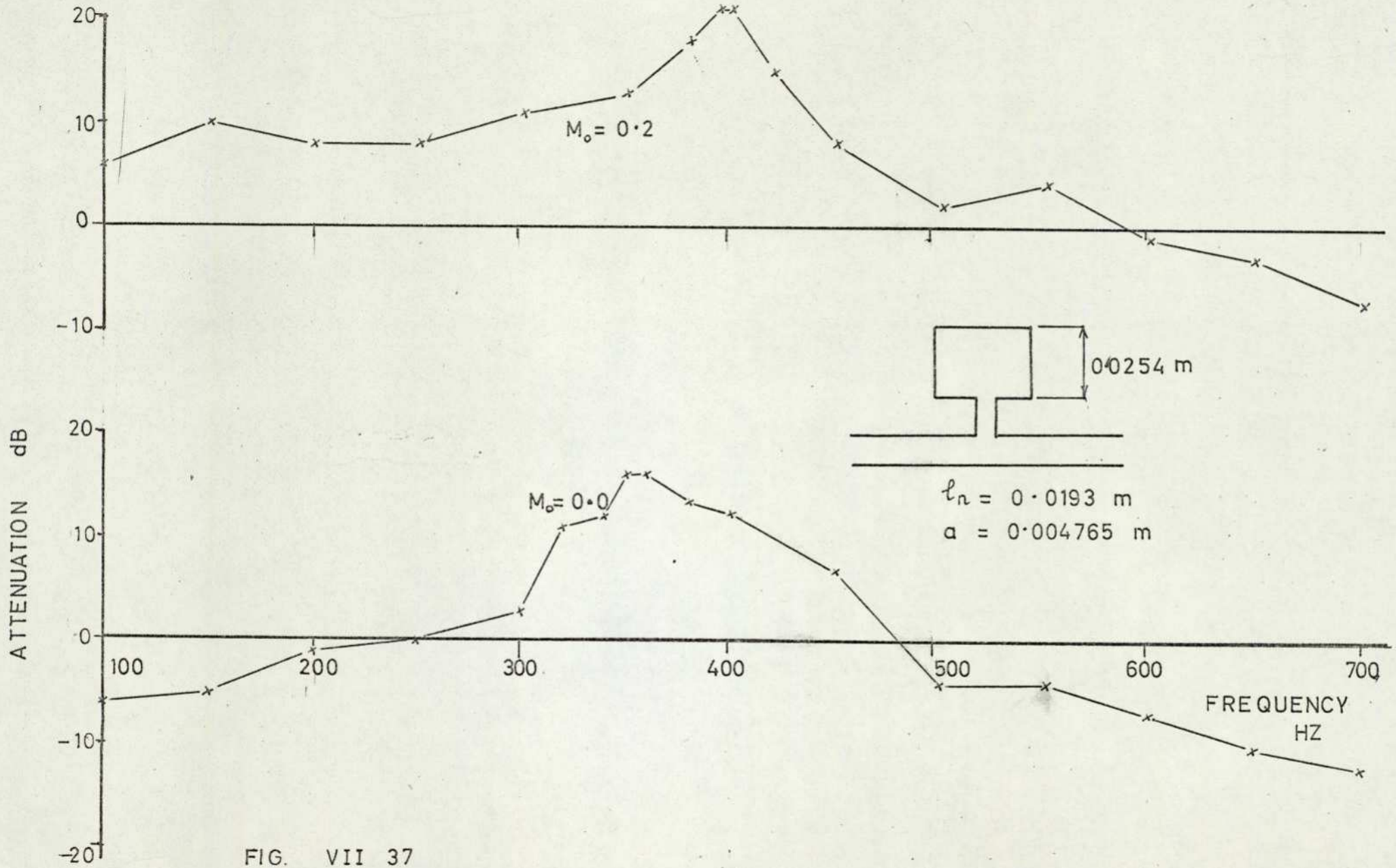

FIG. VII 37
DIFFERENCE IN READINGS OF MICROPHONES 2 AND 3.

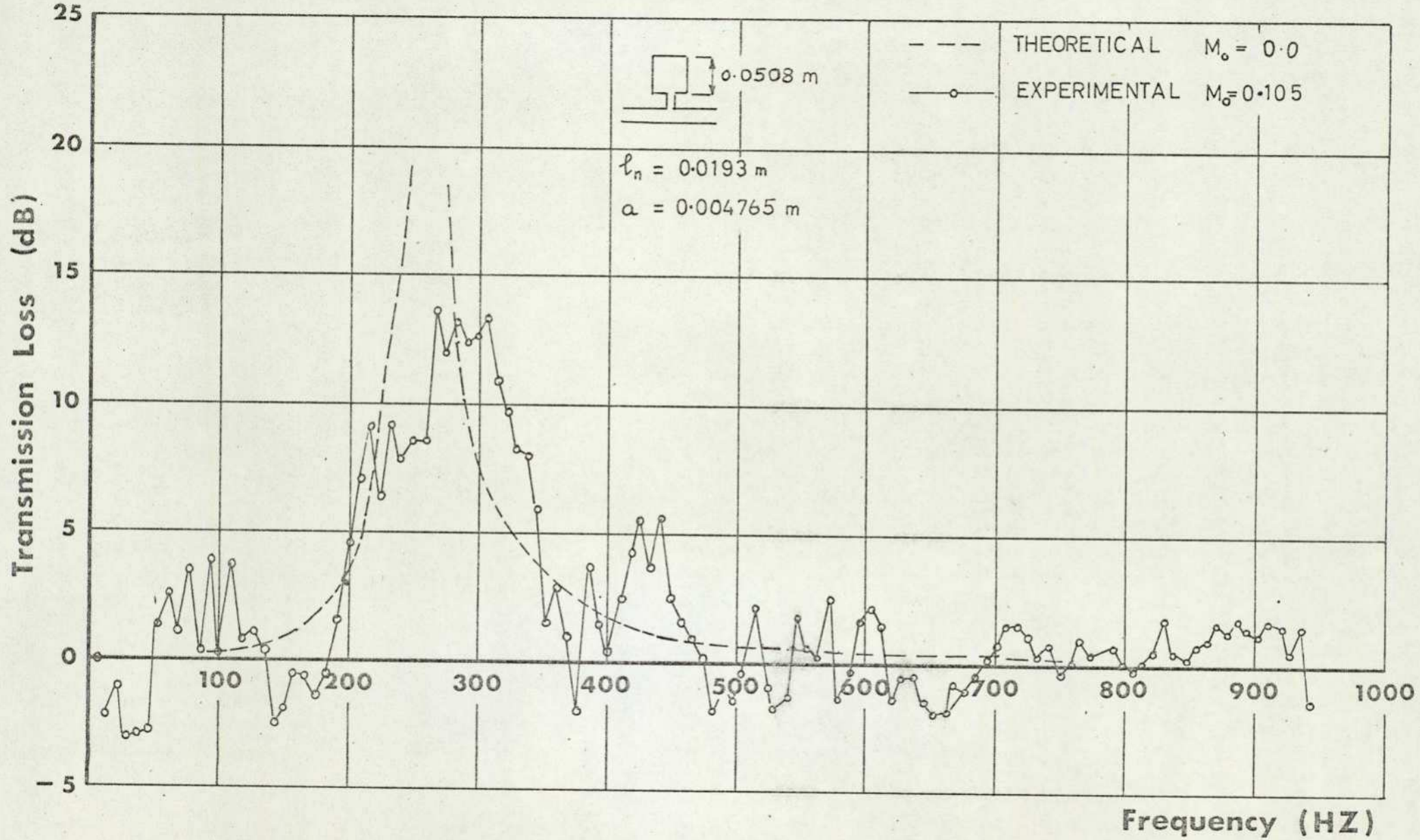

FIG. VII–38 ATTENUATION – FREQUENCY CHARACTERISTIC FOR RESONATOR WITH AIR FLOW.

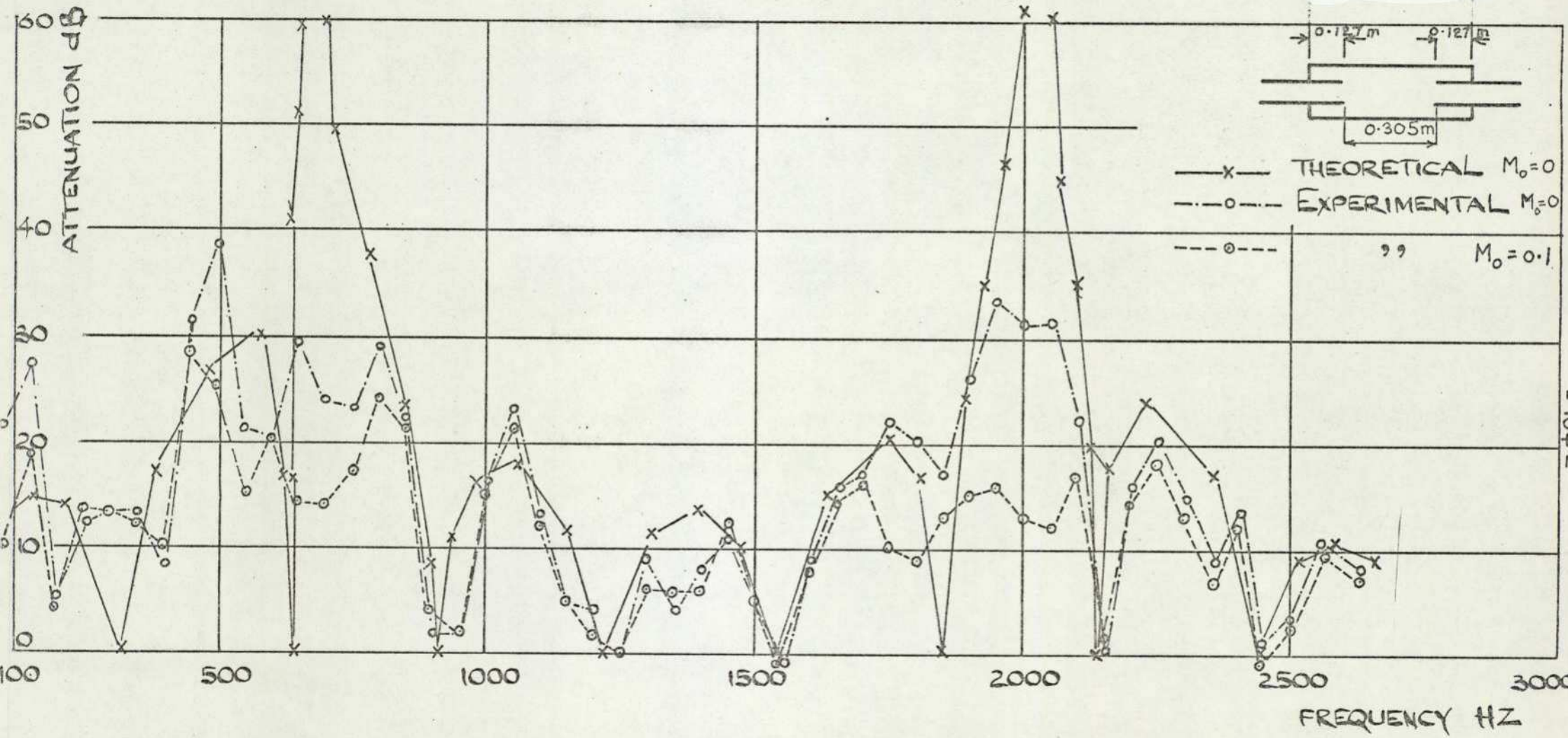

FIG. VII-39 ATTENUATION FREQUENCY CHARACTERISTICS for EXPANSION CHAMBER WITH INTERNAL PIPES.

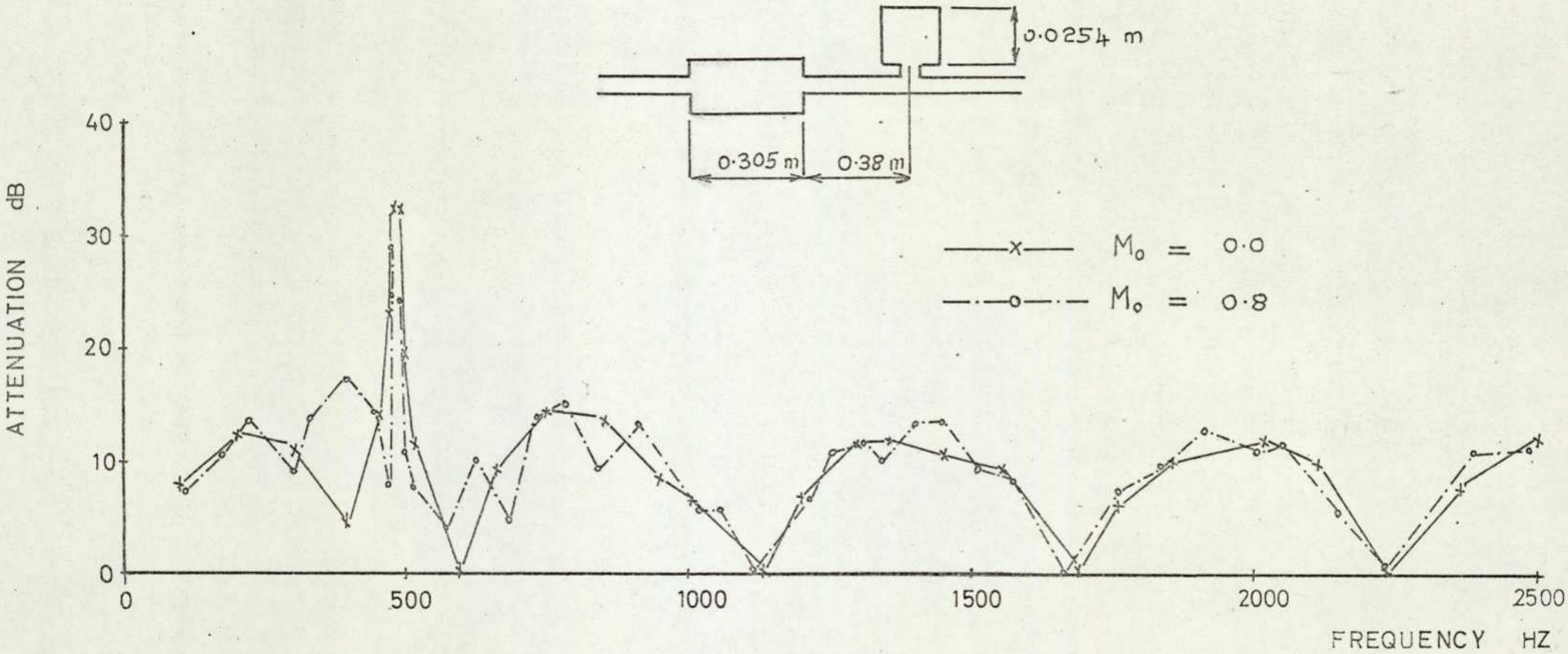

FIG. VII 40
THEORETICAL ATTENUATION FREQUENCY CHARACTERISTICS FOR EXPANSION CHAMBER IN SERIES WITH RESONATOR.

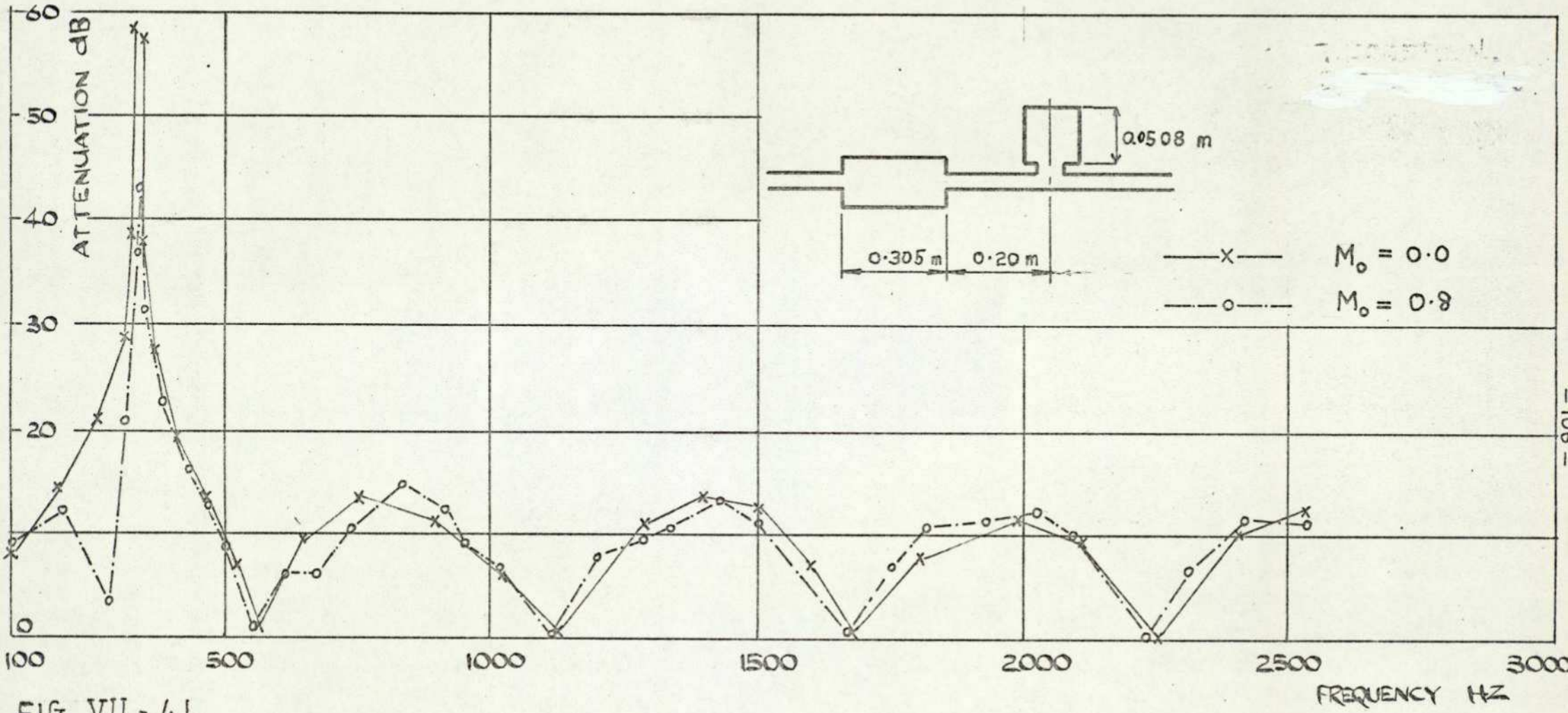

FIG. VII - 41

ATTENUATION FREQUENCY CHARACTERISTICS for EXPANSION CHAMBER IN SERIES WITH RESONATOR

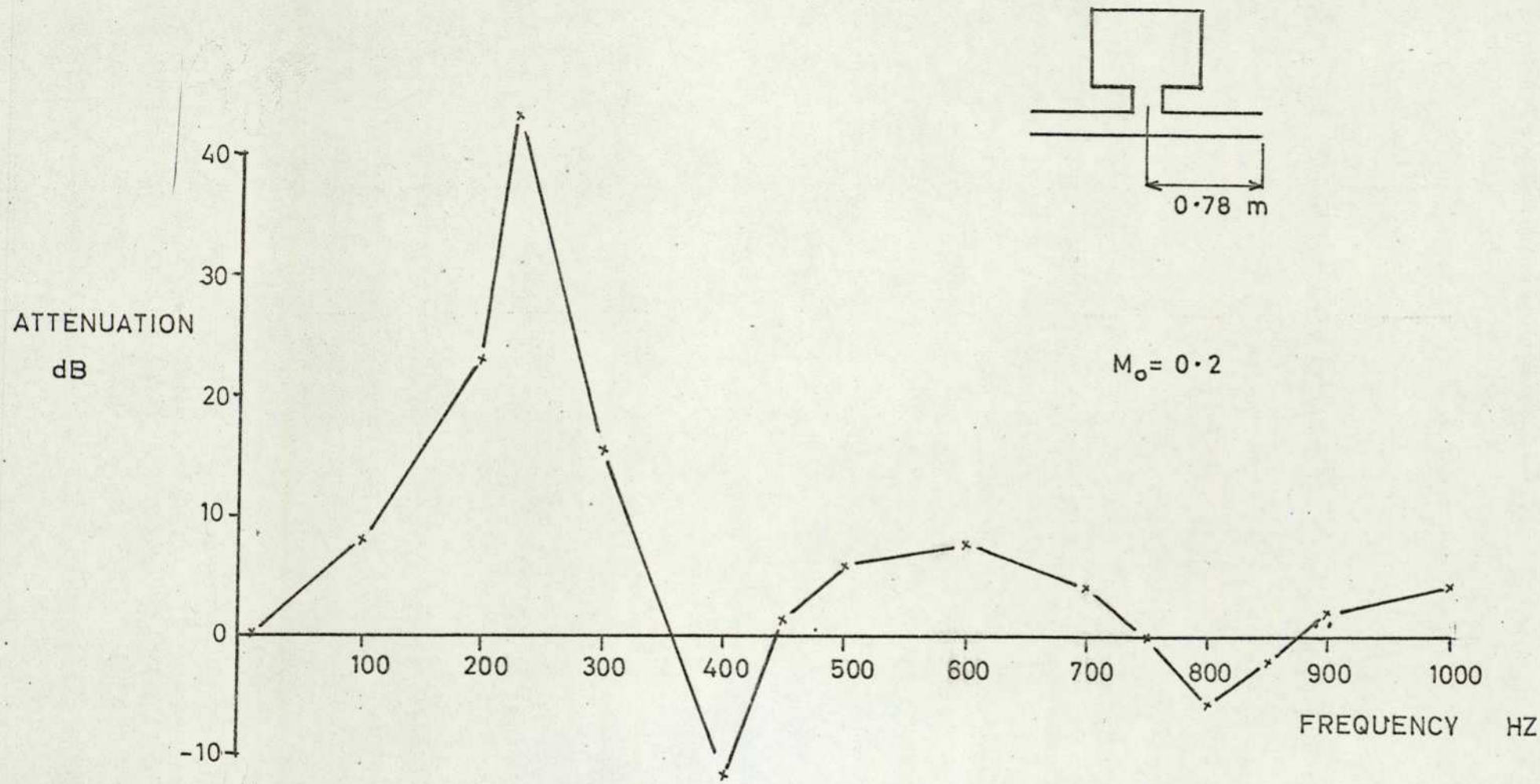

FIG. VII 42

THEORETICAL ATTENUATION FREQUENCY CHARACTERISTIC FOR RESONATOR WITH FINITE OUTLET PIPE.

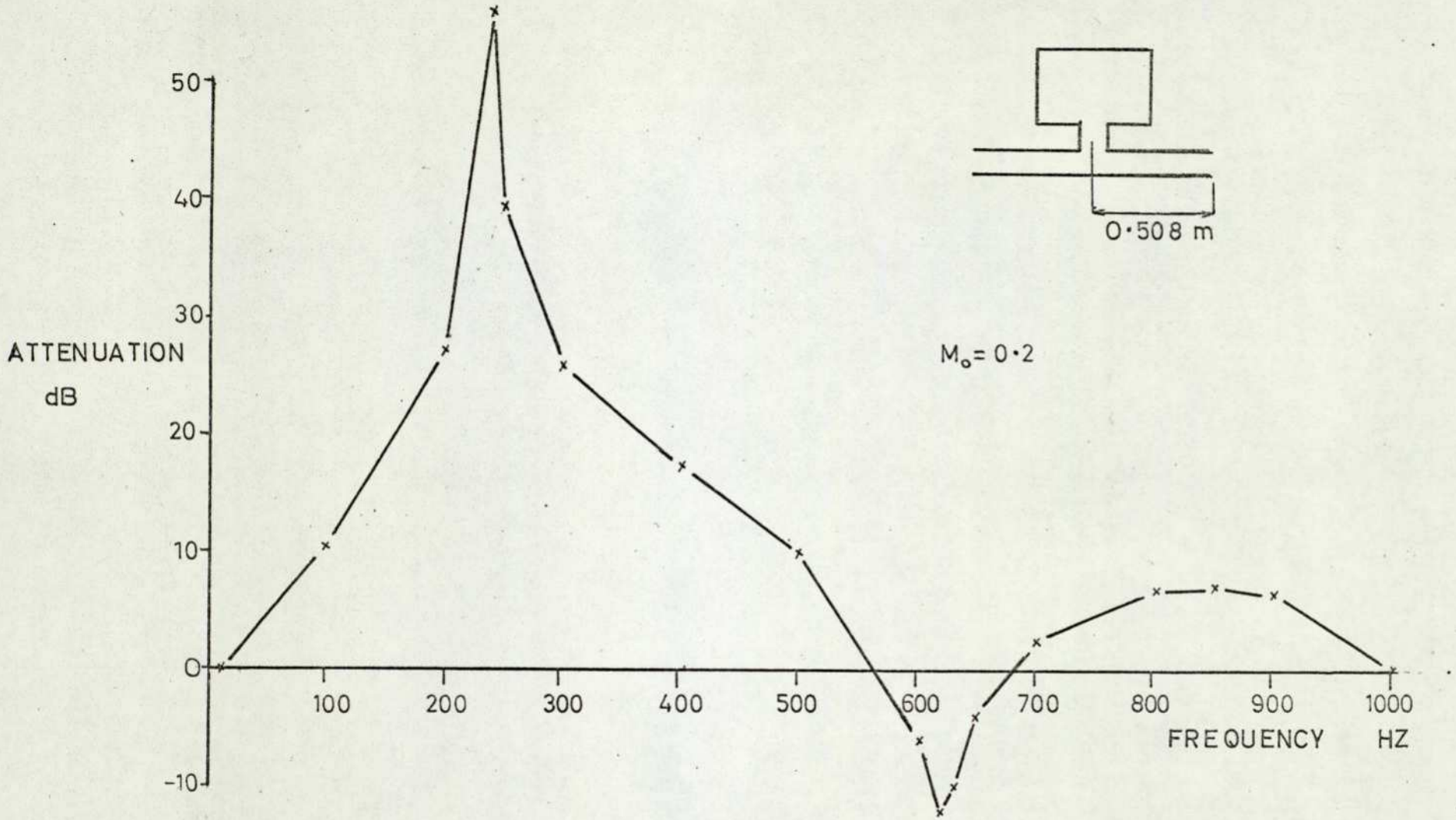

FIG. VII 43
THEORETICAL ATTENUATION FREQUENCY CHARACTERISTIC FOR RESONATOR WITH FINITE OUTLET PIPE.

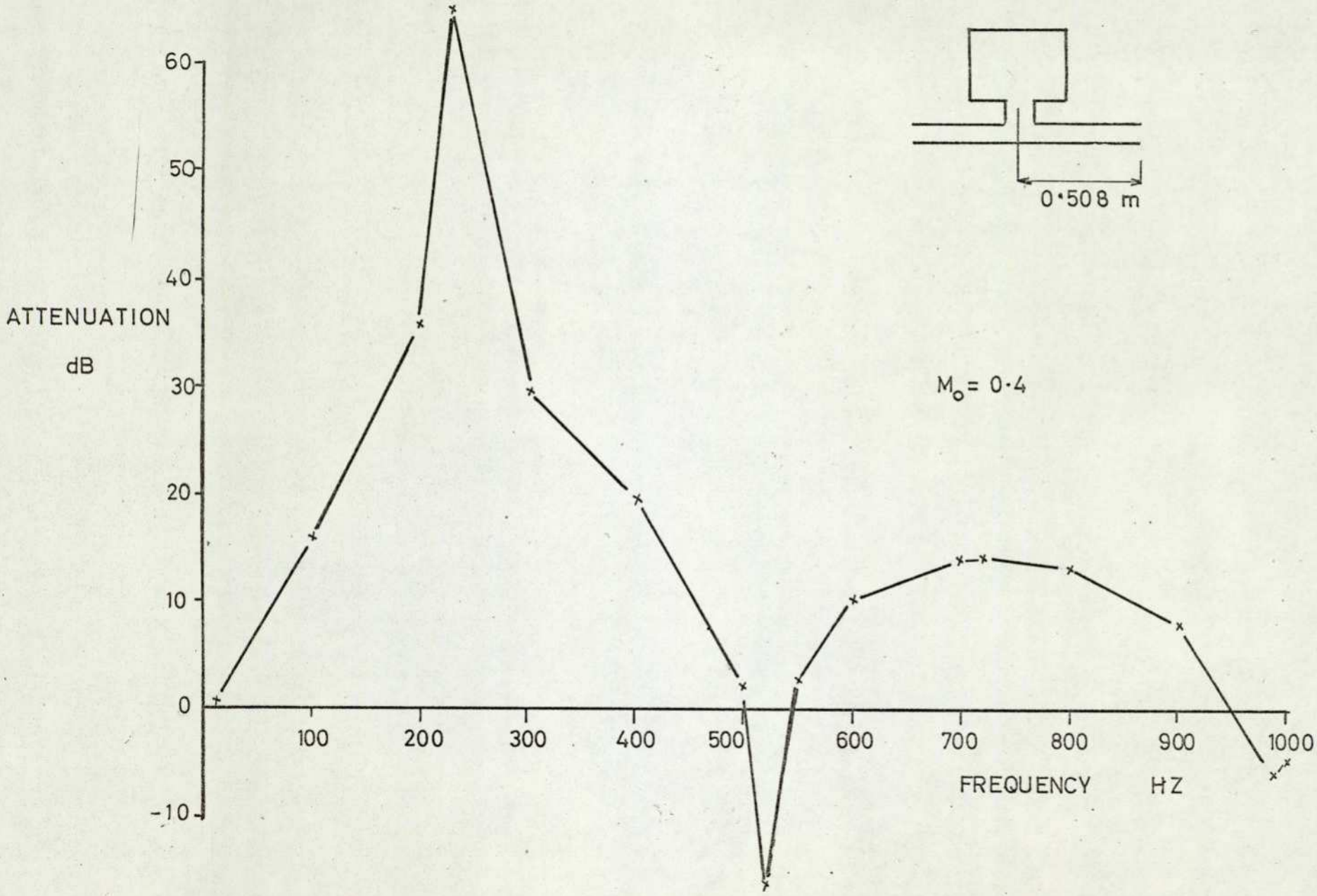

FIG. VII 44
THEORETICAL ATTENUATION FREQUENCY CHARACTERISTIC FOR RESONATOR WITH FINITE OUTLET PIPE.

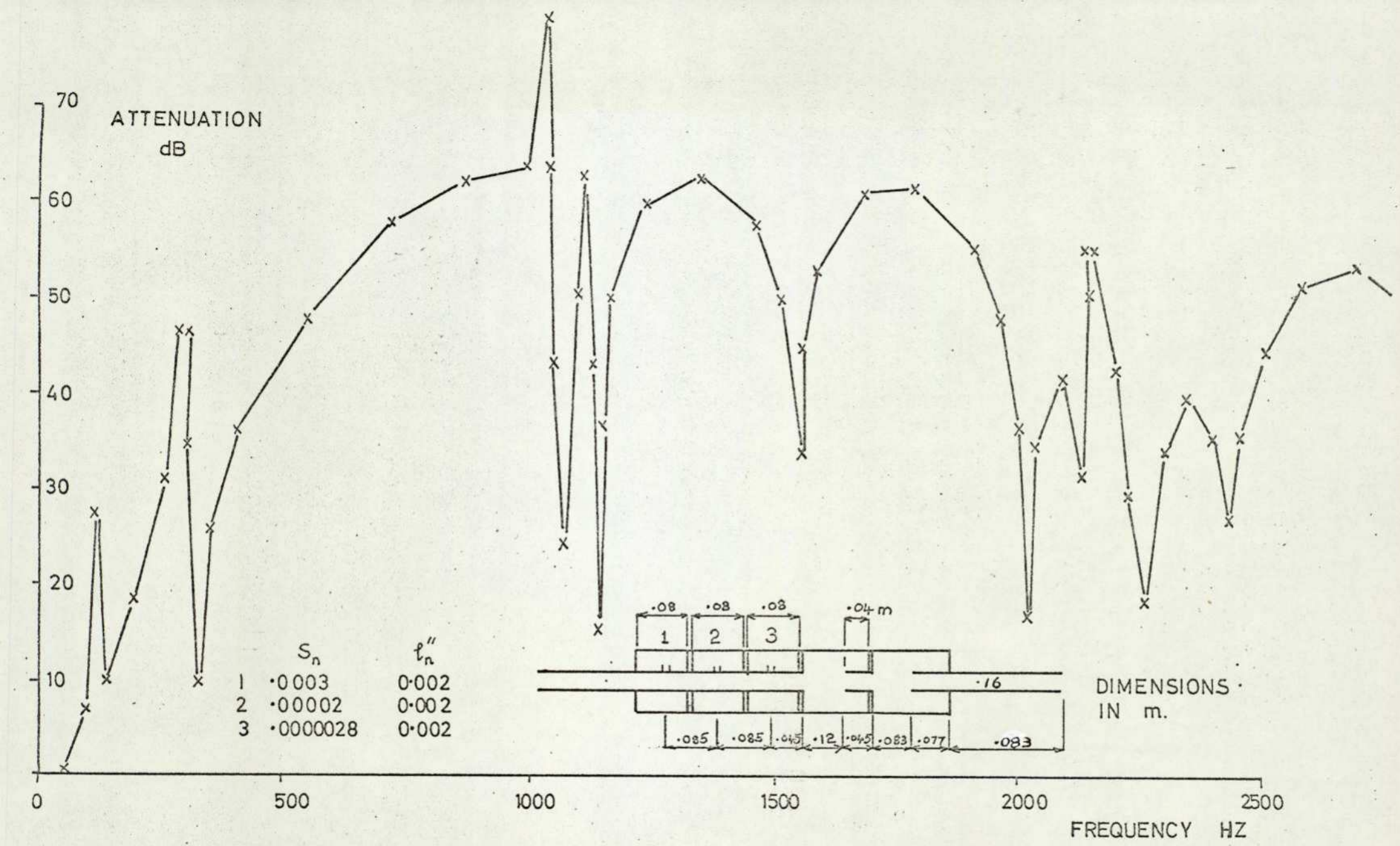

FIG. VII 45
ATTENUATION FREQUENCY CHARACTERISTIC FOR THE SILENCER DESIGNED TO GIVE HIGH PERFORMANCE

Conclusion.

The method of matrix multiplication has been proved to be a very convenient method for evaluating the attenuation-frequency characteristics of silencing systems consisting of reactive elements. Representation of an element by a four-pole enables any element to be included or excluded from a system by simply inserting or removing the appropriate matrix in the calculations. Theories developed for fairly complicated systems comprising resonators, expansion chambers with internal tubes, finite inlet and outlet pipes were found to be adequate and the systems can easily be investigated theoretically with the aid of an electronic computer. Thus the method of matrix multiplication is expected to supersede the conventional method of continuity. Connection of the sound source and the signal pick-up made from the side of the test rig was experimentally convenient and was also justified by theory and test results.

For simple expansion chambers, resonators and other systems with reflection-free terminations for both the inlet and outlet pipes, the calculated curves agree well with experimental data obtained under laboratory conditions. For systems with a finite outlet pipe results obtained by D.D.Davis and Fukuda were used to verify the theory. The system used by Davis was a resonator and his results were obtained with a loudspeaker as the sound source. These results have been predicted fairly accurately by the matrix method. Fukuda employed a simple expansion chamber and data were obtained from an engine test. Amplitudes of attenuation were not calculated accurately, but maxima and minima were predicted. This indicates that the present theory will give a correct estimate for the locations of the pass bands of a silencer when fitted to an engine.

Determination of the quantity 'conductivity' of a resonator neck remains an empirical process, especially when the number of orifices in the neck becomes large. Nevertheless, conductivity for a neck in the form of a small tube can be fairly accurately determined using an end correction factor of approximately 1.5 . When the neck was not too long the lumped-parameter method was found to be a suitable alternative to the more elaborate distributed-parameter method in calculating the fundamental resonant frequency of a resonator.

The effect of a uniform internal air flow of Mach number of 0.2 or less in the inlet and outlet pipes has been proved to be negligible for the expansion chambers because of the much reduced flow speed in these elements, and this was successfully predicted by theory. However, the behaviour of systems with resonators was different in that the resonant frequency of a resonator is increased in the presence of flow. This increase starts with a lower flow rate in the case of a larger resonator than that of a smaller resonator. The developed theory which ignored the flow entering the resonator through the neck was found to be inadequate in dealing with these systems.

Neglecting the viscous friction of the fluid medium has been proved justified except for the case of a resonator with flow when the viscous effect of flow in the resonator neck becomes predominant near resonance. Neglecting Karal's correction for the expansion chamber length was found to be acceptable for the expansion ratios considered, but the omission of the 0.6R end correction to the internal and outlet pipes might have caused slight discrepancies between theory and experimental results, particularly at high frequencies. The assumption that only the plane wave mode exists in the system is seen to be true when the wavelength of the signal investigated is less than the maximum diameter in the system.

The fast Fourier transform has been shown to be very successful as an alternative to the discrete frequency method in obtaining attenuation-frequency characteristics for simple expansion chambers and resonators. The only limitation experienced was that of the equipment available.

Expansion chambers with internal tubes were shown to be capable of producing fairly high attenuation levels in both flow and non-flow cases. Thus this configuration was used as the core for a theoretical design of a silencing system by the method of matrix multiplication.

APPENDIX 1.

To prove $\xi(x,t) = f\left[x-(1+M)ct\right] + g\left[x+(1-M)ct\right]$ is the most general and complete solution to the convective wave equation.

Put $U = x-(1+M)ct \quad , \quad V = x+(1-M)ct$

thus $\xi(x,t) = \epsilon\left[U, V\right]$

$$\frac{\partial \xi}{\partial x} = \frac{\partial \epsilon}{\partial U}\frac{\partial U}{\partial x} + \frac{\partial \epsilon}{\partial V}\frac{\partial V}{\partial x} = \frac{\partial \epsilon}{\partial U} + \frac{\partial \epsilon}{\partial V}$$

$$\left(\frac{\partial U}{\partial x} = 1 \quad , \quad \frac{\partial V}{\partial x} = 1\right)$$

$$\frac{\partial^2 \xi}{\partial x^2} = \frac{\partial}{\partial x}\left(\frac{\partial \xi}{\partial x}\right) = \frac{\partial}{\partial U}\left(\frac{\partial \epsilon}{\partial U}+\frac{\partial \epsilon}{\partial V}\right)\frac{\partial U}{\partial x} + \frac{\partial}{\partial V}\left(\frac{\partial \epsilon}{\partial U}+\frac{\partial \epsilon}{\partial V}\right)\frac{\partial V}{\partial x}$$

$$= \frac{\partial^2 \epsilon}{\partial U^2} + 2\frac{\partial^2 \epsilon}{\partial U \partial V} + \frac{\partial^2 \epsilon}{\partial V^2}$$

$$\frac{\partial^2 \xi}{\partial t \partial x} = \frac{\partial}{\partial t}\left(\frac{\partial \epsilon}{\partial U}+\frac{\partial \epsilon}{\partial V}\right) - \frac{\partial}{\partial U}\left(\frac{\partial \epsilon}{\partial U}+\frac{\partial \epsilon}{\partial V}\right)\frac{\partial U}{\partial t} + \frac{\partial}{\partial V}\left(\frac{\partial \epsilon}{\partial U}+\frac{\partial \epsilon}{\partial V}\right)\frac{\partial V}{\partial t}$$

$$= -(1+M)c\frac{\partial^2 \epsilon}{\partial U^2} - (1+M)c\frac{\partial^2 \epsilon}{\partial U \partial V} + (1-M)c\frac{\partial^2 \epsilon}{\partial V \partial U} + (1-M)c\frac{\partial^2 \epsilon}{\partial V^2}$$

$$= (1-M)c\frac{\partial^2 \epsilon}{\partial V^2} - 2Mc\frac{\partial^2 \epsilon}{\partial U \partial V} - (1+M)c\frac{\partial^2 \epsilon}{\partial U^2}$$

$$\frac{\partial \xi}{\partial t} = \frac{\partial \epsilon}{\partial U}\frac{\partial U}{\partial t} + \frac{\partial \epsilon}{\partial V}\frac{\partial V}{\partial t} = -(1+M)c\frac{\partial \epsilon}{\partial U} + (1-M)c\frac{\partial \epsilon}{\partial V}$$

$$\frac{\partial^2 \xi}{\partial t^2} = \frac{\partial}{\partial U}\left(-(1+M)c\frac{\partial \epsilon}{\partial U} + (1-M)c\frac{\partial \epsilon}{\partial V}\right)\frac{\partial U}{\partial t}$$

$$+ \frac{\partial}{\partial V}\left(-(1+M)c\frac{\partial \epsilon}{\partial U} + (1-M)c\frac{\partial \epsilon}{\partial V}\right)\frac{\partial V}{\partial t}$$

$$= (1+M)^2c^2\frac{\partial^2 \epsilon}{\partial U^2} - (1-M^2)c^2\frac{\partial^2 \epsilon}{\partial U \partial V} - (1-M^2)c^2\frac{\partial^2 \epsilon}{\partial V \partial U}$$

$$+ (1-M)^2c^2\frac{\partial^2 \epsilon}{\partial V^2}$$

$$= (1+M^2)c^2 \frac{\partial^2 \epsilon}{\partial U^2} - 2(1-M^2)c^2 \frac{\partial^2 \epsilon}{\partial U \partial V} + (1-M)^2 c^2 \frac{\partial^2 \epsilon}{\partial V^2}$$

Substituting these quantities into the differential equation

$$\frac{1}{c^2} \frac{\partial^2 \xi}{\partial t^2} + 2 \frac{M}{c} \frac{\partial^2 \xi}{\partial t \partial x} - (1-M^2) \frac{\partial^2 \xi}{\partial x^2} = 0$$

$$(1+M)^2 \frac{\partial^2 \epsilon}{\partial U^2} - 2(1-M^2) \frac{\partial^2 \epsilon}{\partial U \partial V} + (1-M)^2 \frac{\partial^2 \epsilon}{\partial V^2} + 2M(1-M) \frac{\partial^2 \epsilon}{\partial V^2}$$

$$-4M^2 \frac{\partial^2 \epsilon}{\partial U \partial V} - 2M(1+M) \frac{\partial^2 \epsilon}{\partial U^2} - (1-M^2) \frac{\partial^2 \epsilon}{\partial U^2} - 2(1-M^2) \frac{\partial^2 \epsilon}{\partial U \partial V}$$

$$-(1-M^2) \frac{\partial^2 \epsilon}{\partial V^2} = 0$$

This leads to $$-4 \frac{\partial^2 \epsilon}{\partial U \partial V} = 0$$

i.e. $$\frac{\partial^2 \epsilon}{\partial U \partial V} = 0$$

$$\frac{\partial}{\partial U} \left(\frac{\partial \epsilon}{\partial V} \right) = 0$$

Integrating $$\frac{\partial \epsilon}{\partial V} = F_2(V)$$

$$\epsilon = \int F_2(V) \, dV + F_1(U)$$

$$\therefore \quad \epsilon [U, V] = g(V) + f(U)$$

Thus $$\xi(x,t) = f[x-(1+M)ct] + g[x+(1-M)ct]$$

This solution is complete because it has two constants and is general because any solution must take the form of $\xi(x,t)$ as shown.

APPENDIX 2.

Effect of Sound Source and Transducer Position.

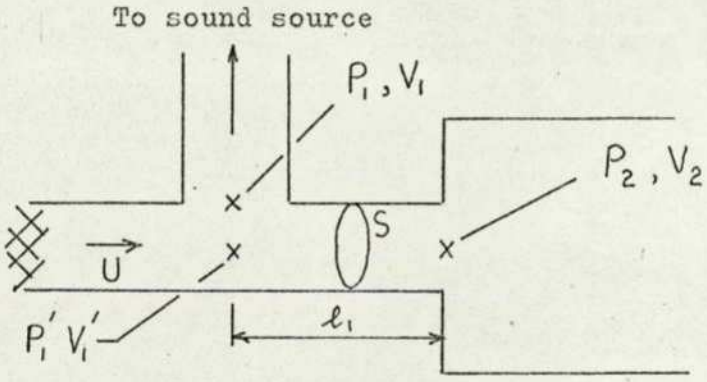

Figure a

We refer to figure a and assume that no gas flows down the sound source connection. The non-reflective termination at the left hand side of the pipe provides a characteristic impedance of $\frac{\rho c}{S}\frac{1}{1-M}$ and the relation between P_1, V_1 and P_2, V_2 is

$$\begin{bmatrix} P_1 \\ V_1 \end{bmatrix} = \begin{bmatrix} 1 & 0 \\ \frac{S}{\rho c}(1-M) & 1 \end{bmatrix}$$

$$e^{-j\frac{M}{1-M^2}k\ell_1}\begin{bmatrix} \cos\frac{k\ell_1}{1-M^2} - jM\sin\frac{k\ell_1}{1-M^2} & j\frac{\rho c}{S}\sin\frac{k\ell_1}{1-M^2} \\ j\frac{S}{\rho c}(1-M^2)\sin\frac{k\ell_1}{1-M^2} & \cos\frac{k\ell_1}{1-M^2} + jM\sin\frac{k\ell_1}{1-M^2} \end{bmatrix}\begin{bmatrix} P_2 \\ V_2 \end{bmatrix}$$

$$= e^{-j\frac{M}{1-M^2}k\ell_1}\begin{bmatrix} \cos\frac{k\ell_1}{1-M^2} - jM\sin\frac{k\ell_1}{1-M^2} & j\frac{\rho c}{S}\sin\frac{k\ell_1}{1-M^2} \\ \frac{S}{\rho c}(1-M)\, e^{j\frac{k\ell_1}{1-M^2}} & e^{j\frac{k\ell_1}{1-M^2}} \end{bmatrix}\begin{bmatrix} P_2 \\ V_2 \end{bmatrix}$$

$$V_1 = e^{-j\frac{M}{1-M^2}k\ell_1}\frac{S}{\rho c}(1-M)\, e^{j\frac{k\ell_1}{1-M^2}} P_2 + e^{-j\frac{M}{1-M^2}k\ell_1} e^{j\frac{k\ell_1}{1-M^2}} V_2$$

$$= e^{j\frac{k\ell_1}{1+M}}\left\{\frac{S}{\rho c}(1-M)\, P_2 + V_2\right\}$$

Thus $$|V_1| = \left|\frac{S}{\rho c}(1-M)\, P_2 + V_2\right|$$

Since ℓ_1 does not appear in this expression, it will not affect the attenuation and the matrix representing this portion of the duct can be neglected.

For the transducer location :-

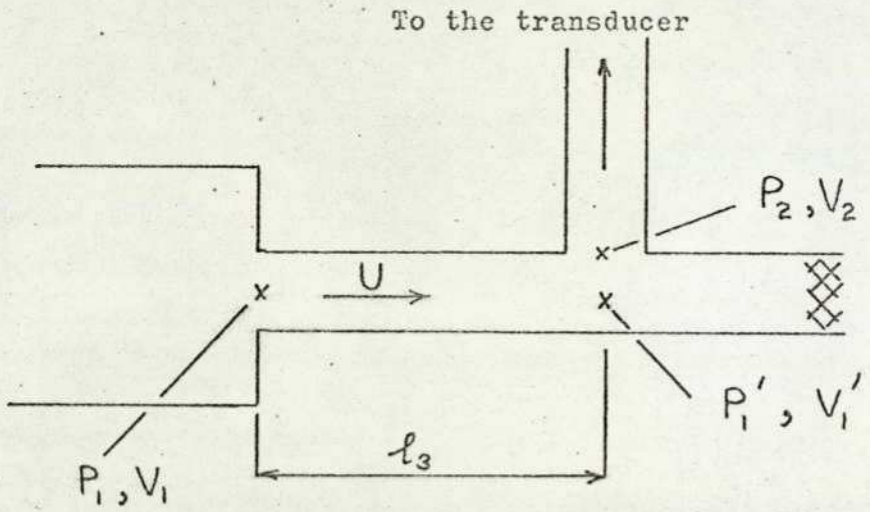

Figure b.

We refer to figure b and assume no gas flow down the transducer connection. The characteristic impedance at the right hand side of the pipe is $\frac{\rho c}{S}\frac{1}{1+M}$ and the relationship between P_1, V_1 and P_2, V_2 is

$$\begin{bmatrix} P_1 \\ V_1 \end{bmatrix} = e^{-j\frac{M}{1-M^2}k\ell_3} \begin{bmatrix} \cos\frac{k\ell_3}{1-M^2} - jM\sin\frac{k\ell_3}{1-M^2} & j\frac{\rho c}{S}\sin\frac{k\ell_3}{1-M^2} \\ j\frac{S}{\rho c}(1-M^2)\sin\frac{k\ell_3}{1-M^2} & \cos\frac{k\ell_3}{1-M^2} + jM\sin\frac{k\ell_3}{1-M^2} \end{bmatrix}$$

$$\begin{bmatrix} 1 & 0 \\ \frac{S}{\rho c}(1+M) & 1 \end{bmatrix} \begin{bmatrix} P_2 \\ V_2 \end{bmatrix}$$

$$\begin{bmatrix} P_1 \\ V_1 \end{bmatrix} = e^{-j\frac{M}{1-M^2}k\ell_3} \begin{bmatrix} \cos\frac{k\ell_3}{1-M^2} + j\sin\frac{k\ell_3}{1-M^2} & \cdot\, j\frac{\rho c}{S}\sin\frac{k\ell_3}{1-M^2} \\ \frac{S}{\rho c}(1+M)\, e^{j\frac{k\ell_3}{1-M^2}} & \cos\frac{k\ell_3}{1-M^2} + jM\sin\frac{k\ell_3}{1-M^2} \end{bmatrix} \begin{bmatrix} P_2 \\ V_2 \end{bmatrix}$$

$$V_2 = 0$$

$$V_1 = e^{j\frac{M}{1-M^2}k\ell_3}\ \frac{S}{\rho c}(1+M)\ e^{j\frac{k\ell_3}{1-M^2}}\ P_2$$

$$= \frac{S}{\rho c}(1+M)\ e^{j\frac{k\ell_3}{1+M}}\ P_2$$

$$|V_1| = \frac{S}{\rho c}(1+M)\ |P_2|$$

Thus ℓ_3 does not affect the attenuation and its representative matrix can be neglected. Physically this simply means that because of the non-reflecting nature of the outlet pipe only an incident wave is propagated down the outlet pipe and wherever the microphone is positioned it always measures the magnitude of this wave.

APPENDIX 3.

To prove that Volume Velocity in the inlet side branch remains constant for the Straight Pipe and the Silencer Configurations.

Consider a system with a change of impedance as shown in fig. c. Taking x=0 at the point of discontinuity (35) we have,

$$\frac{B}{A} = \frac{Z_{in} - Z_A}{Z_{in} + Z_A}$$

where Z_A = characteristic impedance of the small branch, and

Z_{in} = resultant impedance of branches to the right of the discontinuity.

The inlet junction of the system considered in this report is shown in figure d. With the mufflers replaced by a straight pipe the inlet junction is represented as in figure e.

With Z_{in} the parallel resultant impedances of the pipes going to the left and to the right in figure d,

$$P_{in}' = A' + B' = A'\left(1 + \frac{Z_{in} - Z_A}{Z_{in} + Z_A}\right) = A' \frac{2Z_{in}}{Z_{in} + Z_A}$$

$$V_{in}' = \frac{P_{in}'}{Z_{in}} = \frac{2A'}{Z_{in} + Z_A}$$

With the muffler in position the impedance changes to $Z_{in} + \delta Z_{in}$ as shown in figure f, while the pressure and volume velocity at the junction change to P_{in} and V_{in} respectively. A and B are the new incident and reflected wave amplitudes in the side branch.

$$\frac{B}{A} = \frac{Z_{in} + \delta Z_{in} - Z_A}{Z_{in} + \delta Z_{in} + Z_A}$$

$$P_{in} = A + B = A\left(1 + \frac{Z_{in} + \delta Z_{in} - Z_A}{Z_{in} + \delta Z_{in} + Z_A}\right) = 2A \frac{Z_{in} + \delta Z_{in}}{Z_{in} + \delta Z_{in} + Z_A}$$

$$V_{in} = \frac{P_{in}}{Z_{in} + \delta Z_{in}} = \frac{2A}{Z_{in} + \delta Z_{in} + Z_A}$$

Since the incident wave has not changed,

$$A' = A$$

If $Z_A \gg Z_{in} + \delta Z_{in}$, then $V_{in}' \doteq V_{in} = \frac{2A}{Z_A}$

(Note that $P_{in}' \neq P_{in}$)

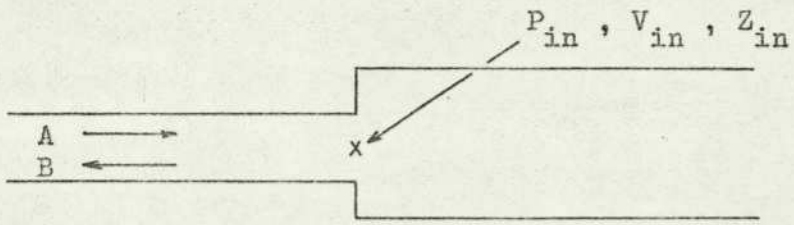

Figure c. Change of impedance at junction between two pipes.

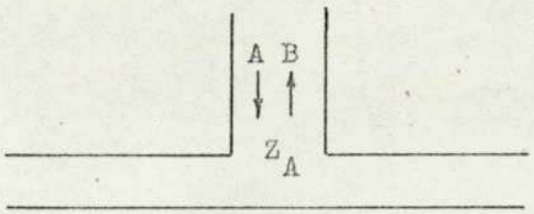

Figure d.

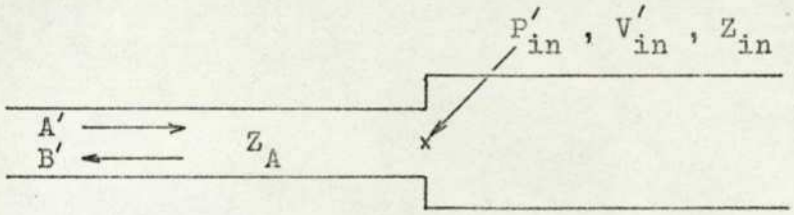

Figure e.

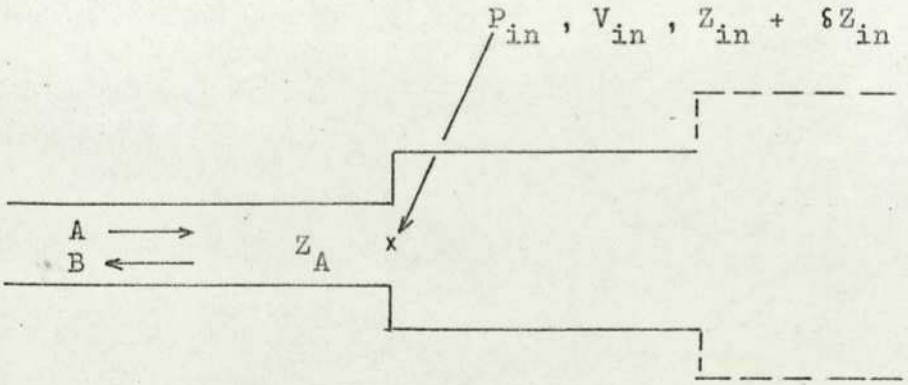

Figure f.

APPENDIX 4.

Expansion Chamber with Internal Tubes.

Quoting equation III-7 ,

$$Z_1 = \frac{\left[\cos \frac{k\ell}{1-M^2} - j M \sin \frac{k\ell}{1-M^2}\right] Z_2 + j\left[\frac{\rho c}{S} \sin \frac{k\ell}{1-M^2}\right]}{j\left[\frac{S}{\rho c}(1-M^2) \sin \frac{k\ell}{1-M^2}\right] Z_2 + \left[\cos \frac{k\ell}{1-M^2} + j M \sin \frac{k\ell}{1-M^2}\right]}$$

For M = 0 ,

$$Z_1 = \frac{(\cos k\ell) Z_2 + j \frac{\rho c}{S} \sin k\ell}{j \frac{S}{\rho c} (\sin k\ell) Z_2 + \cos k\ell}$$

$$= \frac{\rho c}{S} \frac{Z_2 + j \frac{\rho c}{S} \tan k\ell}{\frac{\rho c}{S} + j Z_2 \tan k\ell}$$

When $Z_2 = \infty$,

$$Z_1 - \frac{\rho c}{S} \frac{1}{j \tan k\ell} = -j \frac{\rho c}{S} \cot k\ell$$

Z_1 is the impedance of a duct , cross-sectional area S, length l, and with a closed end. Internal tubes in expansion chambers can be represented by this expression of impedance.

APPENDIX 5

Impedance of an Open Pipe with Flow.

Quoting again equation III-7

$$Z_1 = \frac{\left[\cos \frac{k\ell}{1-M^2} - jM \sin \frac{k\ell}{1-M^2}\right] Z_2 + j\left[\frac{\rho c}{S} \sin \frac{k\ell}{1-M^2}\right]}{j\left[\frac{S}{\rho c}(1-M^2) \sin \frac{k\ell}{1-M^2}\right] Z_2 + \left[\cos \frac{k\ell}{1-M^2} + jM \sin \frac{k\ell}{1-M^2}\right]}$$

For an open pipe, $Z_2 = 0$, and

$$Z_1 = \frac{j \frac{\rho c}{S} \sin \frac{k\ell}{1-M^2}}{\cos \frac{k\ell}{1-M^2} + jM \sin \frac{k\ell}{1-M^2}}$$

$$\frac{1}{Z_1} = \frac{S}{\rho c}\left[M - j \cot \frac{k\ell}{1-M^2}\right]$$

For M = 0

$$\frac{1}{Z_1} = \frac{S}{\rho c}\left(-j \cot k\ell\right)$$

$$Z_1 = j \frac{\rho c}{S} \tan k\ell$$

APPENDIX 6.

Effect of Open-ended Outlet Pipe.

Consider the open-ended outlet pipe shown in figure IV-6. P_{out} , A_{out} and B_{out} are complex amplitudes of resultant, incident and reflected pressure waves respectively at the junction point of the output side branch and the outlet pipe. P_{open} , A_{open} and B_{open} are amplitudes at the open end of the outlet pipe. U is the mean flow velocity. Then,

$$A_{open} = A_{out}\, e^{-j \frac{k\ell_t}{1+M}}$$

$$B_{open} = B_{out}\, e^{+j \frac{k\ell_t}{1-M}}$$

$$P_{open} = A_{open} + B_{open} = 0$$

$$\therefore \quad A_{open} = -B_{open}$$

$$A_{out}\, e^{-j \frac{k\ell_t}{1+M}} = -B_{out}\, e^{+j \frac{k\ell_t}{1-M}}$$

$$P_{out} = A_{out} + B_{out}$$

$$= A_{out}\left(1 - e^{-j \frac{2k}{1-M^2}\ell_t}\right)$$

$$= A_{out}\left(1 - \cos \frac{2k}{1-M^2}\ell_t + j \sin \frac{2k}{1-M^2}\ell_t\right)$$

$$|P_{out}| = |A_{out}| \cdot \left|\left(1 - \cos \frac{2k\ell_t}{1-M^2}\right) + j \sin \frac{2k}{1-M^2}\ell_t\right|$$

$$= |A_{out}| \cdot 2 \sin \frac{k\ell_t}{1-M^2}$$

$$|A_{out}| = \frac{|P_{out}|}{2 \sin\left(k\ell_t/(1-M^2)\right)}$$

For M = 0 , $$|A_{out}| = \frac{|P_{out}|}{2 \sin k\ell_t}$$

APPENDIX 7.

To prove that the Transducer Position along an Open Outlet Pipe is Immaterial to Amplitude Measurement.

Consider the outlet pipe end of a system similar to that shown in figure IV-6 with a uniform internal flow U in the outlet pipe. The system reads :-

$$\begin{bmatrix} P_3 \\ V_3 \end{bmatrix} = \begin{bmatrix} \cos \frac{k\ell_3}{1-M^2} - j M \sin \frac{k\ell_3}{1-M^2} & j \frac{\rho c}{S} \sin \frac{k\ell_3}{1-M^2} \\ j \frac{S}{\rho c}(1-M^2) \sin \frac{k\ell_3}{1-M^2} & \cos \frac{k\ell_3}{1-M^2} + jM \sin \frac{k\ell_3}{1-M^2} \end{bmatrix}$$

$$\begin{bmatrix} 1 & 0 \\ \frac{S}{\rho c} M - j \frac{S}{\rho c} \cot \frac{k\ell_t}{1-M^2} & 1 \end{bmatrix} \begin{bmatrix} P_{out} \\ V_{out} \end{bmatrix}$$

(See Appendix 5)

$$= \begin{bmatrix} A & B \\ C & D \end{bmatrix} \begin{bmatrix} P_{out} \\ V_{out} \end{bmatrix}$$

Where $A = \cos \frac{k\ell_3}{1-M^2} + \sin \frac{k\ell_3}{1-M^2} \cot \frac{k\ell_t}{1-M^2}$

$$C = j \frac{S}{\rho c}(1-M^2) \sin \frac{k\ell_3}{1-M^2} + \frac{S}{\rho c} M \cos \frac{k\ell_3}{1-M^2} + \frac{S}{\rho c} M \cot \frac{k\ell_t}{1-M^2} \sin \frac{k\ell_3}{1-M^2} + j \left(\frac{S}{\rho c} M^2 \sin \frac{k\ell_3}{1-M^2} - \frac{S}{\rho c} \cot \frac{k\ell_t}{1-M^2} \cos \frac{k\ell_3}{1-M^2} \right)$$

$$P_3 = \left[\cos \frac{k\ell_3}{1-M^2} + \sin \frac{k\ell_3}{1-M^2} \cot \frac{k\ell_t}{1-M^2} \right] P_{out}$$

$$|P_3| = \left[\cos \frac{k\ell_3}{1-M^2} + \sin \frac{k\ell_3}{1-M^2} \cot \frac{k\ell_t}{1-M^2} \right] 2 \sin \frac{k\ell_t}{1-M^2} |A_{out}|$$

$$= 2 \sin \frac{k(\ell_3 + \ell_t)}{1-M^2} |A_{out}|$$

For $V_{out} = 0$,

$$V_3 = \left[\frac{S}{\rho c} M\left(\cos \frac{k\ell_3}{1-M^2} + \cot \frac{k\ell_t}{1-M^2} \sin \frac{k\ell_3}{1-M^2}\right) + j \frac{S}{\rho c}\left(\sin \frac{k\ell_3}{1-M^2} - \cot \frac{k\ell_t}{1-M^2} \cos \frac{k\ell_3}{1-M^2}\right)\right] P_{out}$$

$$|V_3| = \frac{S}{\rho c}\left\{M^2\left(\cos \frac{k\ell_3}{1-M^2} + \cot \frac{k\ell_t}{1-M^2} \sin \frac{k\ell_3}{1-M^2}\right)^2 + \left(\sin \frac{k\ell_3}{1-M^2} - \cot \frac{k\ell_t}{1-M^2} \cos \frac{k\ell_3}{1-M^2}\right)^2\right\}^{1/2} 2 \sin \frac{k\ell_t}{1-M^2} |A_{out}|$$

$$= 2\frac{S}{\rho c}\left\{M^2\left(\sin \frac{k\ell_t}{1-M^2} \cos \frac{k\ell_3}{1-M^2} + \cos \frac{k\ell_t}{1-M^2} \sin \frac{k\ell_3}{1-M^2}\right)^2 + \left(\sin \frac{k\ell_3}{1-M^2} \sin \frac{k\ell_t}{1-M^2} - \cos \frac{k\ell_3}{1-M^2} \cos \frac{k\ell_t}{1-M^2}\right)^2\right\}^{1/2} |A_{out}|$$

$$= 2\frac{S}{\rho c}\left\{M^2 \sin^2 \frac{(\ell_t + \ell_3)k}{1-M^2} + \cos^2 \frac{(\ell_t + \ell_3)k}{1-M^2}\right\}^{1/2} |A_{out}|$$

For $M = 0$ $\quad |V_3| = 2\frac{S}{\rho c} \cos k(\ell_t + \ell_3) \quad |A_{out}|$

The above shows that individual lengths of ℓ_1 and ℓ_t do not affect attenuation. The combined length $\ell_t + \ell_3$ of the outlet pipe is the important dimension. As long as this length remains constant, the position of the transducer is unimportant.

APPENDIX 8. COMPUTER PROGRAMS.

TRANSMISSION LOSS OF SIMPLE EXPANSION CHAMBER.

```
      MASTER ACOU
      REAL LEN,IMP,KON,LENN,MACH
      COMPLEX X(7,2,2),Y(7,2,2)
      DIMENSION KON(1000),AREA(7),IMP(7),LEN(7),AREAN(7),LENN(7),MACH(7)
     1,ATTEN(500)
C     ATTENUATION OF SILENCERS BY MATRIX METHODS
C     LEN=LENGTH OF MATRIX SECTION
C     AREA=AREA OF MATRIX SECTION
C     LENN=LENGTH OF RESONATOR NECK
C     AREAN=AREA OF RESONATOR NECK
C     L=NO. OF MATRICES
C     P=DENSITY OF MEDIUM
C     C=VELOCITY OF SOUND
C     NOL=NO. OF SETS OF INPUT DATA FOR LEN
C     NOA=NO. OF SETS OF INPUT DATA FOR AREA
C     MACH= LOCAL MACH NO. OF GAS FLOW
      READ (1,53) L
   53 FORMAT (1I1)
      READ (1,51) NOA,NOL,NOH,P,C
   51 FORMAT (3I1,2F10.5)
      NUMA=1
      X(1,1,1),X(1,2,2),X(L+2,1,1),X(L+2,2,2)=CMPLX(1.,0.)
      X(1,1,2),X(L+2,1,2)=CMPLX(0.,0.)
    1 WRITE (2,52)
   52 FORMAT (1H1,9HAREAS ARE)
      DO 10 N=2,L+1
      READ (1,54) AREA(N)
   54 FORMAT (F0.0)
      WRITE (2,55) AREA(N)
   55 FORMAT (1H ,1F10.8,4X)
   10 CONTINUE
      NUML=1
    2 WRITE (2,56)
   56 FORMAT (1H0,11HLENGTHS ARE)
      DO 11 N=2,L+1
      READ (1,57) LEN(N)
   57 FORMAT (F0.0)
      WRITE (2,58) LEN(N)
   58 FORMAT (1H ,1F10.8,4X)
   11 CONTINUE
      NUMM=1
    3 DO 17 N=2,L+1
      READ (1,63) MACH(N)
   63 FORMAT (F0.0)
   17 CONTINUE
      WRITE (2,65) MACH(2)
   65 FORMAT (1H0,24HMACH NO IN 1 INCH PIPE =,1F8.4)
      WRITE (2,59)
   59 FORMAT (1H0,4HFREQ,6X,5HATTEN,8X,4HFREQ,6X,
     15HATTEN,8X,4HFREQ,6X,5HATTEN,8X,4HFREQ,6X,5HATTEN,8X,
     14HFREQ,6X,5HATTEN)
      X(L+2,2,1)=CMPLX(AREA(L+1)/(P*C)*(1+MACH(L+1)),0.)
      X(1,2,1)=CMPLX(AREA(2)/(P*C)*(1-MACH(2)),0.)
      NOO=0
      DO 12 M=50,3000,10
      NOO=NOO+1
      FRE=M
      DO 15 I=1,2
      DO 15 J=1,2
      DO 15 N=1,L+1
   15 Y(N,I,J)=CMPLX(0.,0.)
      KON(NOO)=2.*3.14159*FRE/C
      DO 16 N=2,L+1
      IMP(N)=KON(NOO)*LEN(N)/(1.0-MACH(N)*MACH(N))
```

```
      X(N,1,1)=CMPLX(COS(IMP(N)),-MACH(N)*SIN(IMP(N)))
      X(N,1,2)=CMPLX(0.,P*C/AREA(N)*SIN(IMP(N)))
      X(N,2,1)=CMPLX(0.,AREA(N)/(P*C)*(1.0-MACH(N)*MACH(N))*SIN(IMP(N)))
      X(N,2,2)=CMPLX(COS(IMP(N)),MACH(N)*SIN(IMP(N)))
16    CONTINUE
      DO 21 N=1,L+1
      DO 20 I=1,2
      DO 20 J=1,2
      DO 20 K=1,2
20    Y(N,I,J)=Y(N,I,J)+X(N,I,K)*X(N+1,K,J)
      IF (N-(L+1))0,21,21
      DO 22 I=1,2
      DO 22 J=1,2
22    X(N+1,I,J)=Y(N,I,J)
21    CONTINUE
      ATT=CABS(Y(L+1,2,1))
      ATT=ATT/(2.*AREA(2))*P*C
      ATTEN(NOO)=20.*ALOG10(ATT)
12    CONTINUE
      DO 71 NOO=0,294,5
      NOO1=NOO+1
      NOO2=NOO+2
      NOO3=NOO+3
      NOO4=NOO+4
      NOO5=NOO+5
      NOO6=40+10*NOO1
      NOO7=40+10*NOO2
      NOO8=40+10*NOO3
      NOO9=40+10*NOO4
      NOO10=40+10*NOO5
      WRITE(2,61) NOO6,ATTEN(NOO1),NOO7,ATTEN(NOO2),NOO8,ATTEN(NOO3),
     1NOO9,ATTEN(NOO4),NOO10,ATTEN(NOO5)
61    FORMAT (1H ,1I4,4X,1F8.4,7X,1I4,4X,1F8.4,7X,1I4,4X,1F8.4
     1,7X,1I4,4X,1F8.4,7X,1I4,4X,1F8.4)
71    CONTINUE
      NUMM=NUMM+1
      IF(NUMM-NOM)3,3,0
      NUML=NUML+1
      IF(NUML-NOL)2,2,0
      NUMA=NUMA+1
      IF(NUMA-NOA)1,1,0
      STOP
      END
```

HELMHOLTZ RESONATOR WITH FLOW.

```
      MASTER RESO
      REAL LEN,IMP,KON,LENN,MACH
      COMPLEX X(20,2,2)
      COMPLEX Y(20,2,2)
      DIMENSION KON(1000),ATTEN(1000)
      DIMENSION AREA(20),AREAN(20),IMP(20),LEN(20),LENN(20),MACH(20)
C     ATTENUATION OF SILENCERS BY MATRIX METHODS
C     SIMPLE EXPANSION CHAMBER
C     LEN=LENGTH OF MATRIX SECTION
C     AREA=AREA OF MATRIX SECTION
C     LENN=LENGTH OF RESONATOR NECK
C     AREAN=AREA OF RESONATOR NECK
C     L=NO OF MATRICES
C     P=DENSITY OF MEDIUM
C     C=VELOCITY OF SOUND
C     NOL=NO OF SETS OF INPUT DATA FOR LEN
C     NOA=NO OF SETS OF INPUT DATA FOR AREA
C     MACH=LOCAL MACH NO. OF GAS FLOW
C     M1 IS HIGHEST FREQUENCY
C
      L=3
C
C     L3=0 FOR INFINITE INLET PIPE
C     L3=1 FOR FINITE INLET PIPE
C
      L3=0
      L1=L+2
C
      M1=1000
C
      NUMA=1
```

```
      NOA=0
      NOL=1
      NOM=1
      P=1.2053
      C=343.7
      NUMA=1
 61   FORMAT (1H ,I14,4X,1F8.4,7X,I14,4X,1F8.4,7X,I14,4X,1F8.4
     1,7X,I14,4X,1F8.4,7X,I14,4X,1F8.4)
 55   FORMAT(1H ,1F10.8,4X)
 54   FORMAT(F8.4)
 57   FORMAT(F8.4)
 52   FORMAT (1H1,9HAREAS ARE)
 56   FORMAT(1H0,11HLENGTHS ARE)
 72   FORMAT(1H0,18HAREAN AND LENN ARE)
 65   FORMAT (1H0,24HMACH NO IN 1 INCH PIPE =,1F18.4)
 59   FORMAT (1H0,4HFREQ,6X,5HATTEN,8X,4HFREQ,6X,
     15HATTEN,8X,4HFREQ,6X,5HATTEN,8X,4HFREQ,6X,5HATTEN,8X,
     14HFREQ,6X,5HATTEN)
 53   FORMAT (I12)
 51   FORMAT (3I2,2F10.5)
 60   FORMAT(F10.8)
      X(1,1,1),X(1,2,2),X(L+2,1,1),X(L+2,2,2)=CMPLX(1.,0.)
      X(1,1,2),X(L+2,1,2)=CMPLX(0.,0.)
 1    WRITE (2,52)
      DO 10 N=2,L+1
      READ(1,60) AREA(N)
      WRITE(2,60)AREA(N)
 10   CONTINUE
      NUML=1
 2    WRITE(2,56)
C
C     N=3 REFERS TO CYLINDRICAL CHAMBER OF RESONATOR
C
      DO 11 N=2,L+1
      READ(1,57) LEN(N)
      WRITE(2,57) LEN(N)
 11   CONTINUE
 4    WRITE(2,72)
C
      CALL DATA(L,AREAN,LENN , L1                    )
C
      NUMM=1
 3    DO 17 N=2,L+1
      READ(1,57)MACH(N)
 17   CONTINUE
      WRITE(2,65) MACH(2)
      WRITE (2,59)
      X(L+2,2,1)=CMPLX(AREA(L+1)/(P*C)*(1+MACH(L+1)),0.)
      X(1,2,1)=CMPLX(0.0,0.0)
      IF(L3) 0.0,117
      X(1,2,1)=CMPLX(AREA(2)/(P*C)*(1-MACH(2)),0.)
 117  CONTINUE
      NOO=0
      DO 12 M=50,M1,10
      NOO=NOO+1
      FRE=M
      DO 15 I=1,2
      DO 15 J=1,2
      DO 15 N=1,L+1
 15   Y(N,I,J)=CMPLX(0.,0.)
      KON(NOO)=2.*3.14159*FRE/C
C
      DO 16 N=2,L+1,2
C
      IMP(N)=KON(NOO)*LEN(N)/(1.0-MACH(N)*MACH(N))
      X(N,1,1)=CMPLX(COS(IMP(N)),-MACH(N)*SIN(IMP(N)))
```

```
      X(N,1,2)=CMPLX(0.,P*C/AREA(N)*SIN(IMP(N)))
      X(N,2,1)=CMPLX(0.,AREA(N)/(P*C)*(1.0-MACH(N)*MACH(N))*SIN(IMP(N)))
      X(N,2,2)=CMPLX(COS(IMP(N)),MACH(N)*SIN(IMP(N)))
 16   CONTINUE
C
      DO 171 N=3,L,2
      IMP(N)=KON(N00)*LEN(N)
      X(N,1,1),X(N,2,2)=CMPLX(1.,0.)
      X(N,1,2)=CMPLX(0.,0.)
      Z=-P*C/(AREA(N)*TAN(IMP(N))) + P*KON(N00)*C*LENN(N)/AREAN(N)
      Z=1/Z
      X(N,2,1)=CMPLX(0.,Z)
 171  CONTINUE
C
      DO 21 N=1,L+1
      DO 20 I=1,2
      DO 20 J=1,2
      DO 20 K=1,2
 20   Y(N,I,J)=Y(N,I,J)*X(N,I,K)*X(N+1,K,J)
      IF  (N-(L+1)) 0,21,21
      DO 22 I=1,2
      DO 22 J=1,2
 22   X(N+1,I,J)=Y(N,I,J)
 21   CONTINUE
      ATT=CABS(Y(L+1,2,1))
      IF(L3) 0,0,121
      ATT=ATT/(2.*AREA(2))*P*C
      IF(L3)123,123,0
 121  ATT=ATT/(AREA(2)*(1.0+MACH(2)))*P*C
 123  CONTINUE
      ATTEN(N00)=20.*ALOG10(ATT)
 12   CONTINUE
      M2=(M1-60)/10
      DO 71 N00=0,M2,5
      N001=N00+1
      N002=N00+2
      N003=N00+3
      N004=N00+4
      N005=N00+5
      N006=40+10*N001
      N007=40+10*N002
      N008=40+10*N003
      N009=40+10*N004
      N0010=40+10*N005
      WRITE(2,61) N006,ATTEN(N001),N007,ATTEN(N002),N008,ATTEN(N003),
     1N009,ATTEN(N004),N0010,ATTEN(N005)
 71   CONTINUE
      NUMH=NUMH+1
      IF(NUMH-NOM)3,3,0
      NUML =NUML+1
      IF(NUML-NOL)2,2,0
      NUMA=NUMA+1
      IF(NUMA-NOA)1,1,0
      STOP
      END

          SUBROUTINE DATA (L,AREAN,LENN ,L1
          REAL LENN
          DIMENSION AREAN(L1),LENN(L1)
          DO 18 N=3,L,2
          READ(1,62)AREAN(N),LENN(N)
          WRITE(2,73) AREAN(N),LENN(N)
     18   CONTINUE
     62   FORMAT(F10.8)
     73   FORMAT(1H ,1F8.6,4X,1F8.6)
          RETURN
          END
```

EXPANSION CHAMBER WITH INTERNAL TUBES.

```
      MASTER ACOU
      REAL LEN,IMP,KON,LENN,MACH
      COMPLEX X(7,2,2),Y(7,2,2)
      DIMENSION KON(1000),AREA(7),IMP(7),LEN(7),AREAN(7),LENN(7),MACH(7
     1,ATTEN(500)
C     ATTENUATION OF SILENCERS BY MATRIX METHODS
C     LEN=LENGTH OF MATRIX SECTION
C     AREA=AREA OF MATRIX SECTION
C     LENN=LENGTH OF RESONATOR NECK
C     AREAN=AREA OF RESONATOR NECK
C     L=NO. OF MATRICES
C     P=DENSITY OF MEDIUM
C     C=VELOCITY OF SOUND
C     NOL=NO. OF SETS OF INPUT DATA FOR LEN
C     NOA=NO. OF SETS OF INPUT DATA FOR AREA
C     MACH= LOCAL MACH NO. OF GAS FLOW
      READ (1,53) L
   53 FORMAT (1I1)
      READ (1,51) NOA,NOL,NOM,P,C
   51 FORMAT (3I1,2F10.5)
      NUMA=1
      X(1,1,1),X(1,2,2),X(L+2,1,1),X(L+2,2,2)=CMPLX(1.,0.)
      X(1,1,2),X(L+2,1,2)=CMPLX(0.,0.)
    1 WRITE (2,52)
   52 FORMAT (1H1,9HAREAS ARE)
      DO 10 N=2,L+1
      READ (1,54) AREA(N)
   54 FORMAT (F0.0)
      WRITE (2,55) AREA(N)
   55 FORMAT (1H ,1F10.8,4X)
   10 CONTINUE
      NUML=1
    2 WRITE (2,56)
   56 FORMAT (1H0,11HLENGTHS ARE)
      DO 11 N=2,L+1
      READ (1,57) LEN(N)
   57 FORMAT (F0.0)
      WRITE (2,58) LEN(N)
   58 FORMAT (1H ,1F10.8,4X)
   11 CONTINUE
      NUMM=1
    3 DO 17 N=2,L+1
      READ (1,63) MACH(N)
   63 FORMAT (F0.0)
   17 CONTINUE
      WRITE (2,65) MACH(2)
   65 FORMAT (1H0,24HMACH NO IN 1 INCH PIPE =,1F8.4)
      WRITE (2,59)
   59 FORMAT (1H0,4HFREQ,6X,5HATTEN,8X,4HFREQ,6X,
     15HATTEN,8X,4HFREQ,6X,5HATTEN,8X,4HFREQ,6X,5HATTEN,8X,
     14HFREQ,6X,5HATTEN)
      X(L+2,2,1)=CMPLX(AREA(L+1)/(P*C)*(1+MACH(L+1)),0.)
      X(1,2,1)=CMPLX(AREA(2)/(P*C)*(1-MACH(2)),0.)
      NOO=0
      DO 12 M=50,3000,10
      NOO=NOO+1
      FRE=M
      DO 15 I=1,2
      DO 15 J=1,2
      DO 15 N=1,L+1
   15 Y(N,I,J)=CMPLX(0.,0.)
      KON(NOO)=2.*3.14159*FRE/C
      DO 16 N=2,L+1,2
      IMP(N)=KON(NOO)*LEN(N)/(1.0-MACH(N)*MACH(N))
```

```
      X(N,1,1)=CMPLX(COS(IMP(N)),-MACH(N)*SIN(IMP(N)))
      X(N,1,2)=CMPLX(0.,P*C/AREA(N)*SIN(IMP(N)))
      X(N,2,1)=CMPLX(0.,AREA(N)/(P*C)*(1.0-MACH(N)*MACH(N))*SIN(IMP(N))
      X(N,2,2)=CMPLX(COS(IMP(N)),MACH(N)*SIN(IMP(N)))
16    CONTINUE
      DO 171N=3,L,2
      IMP(N)=KON(NOO)*LEN(N)
      X(N,1,1),X(N,2,2)=CMPLX(1.,0.)
      X(N,1,2)=CMPLX(0.,0.)
      X(N,2,1)=CMPLX(0.,AREA(N)/(P*C)*TAN(IMP(N)))
171   CONTINUE
      DO 21 N=1,L+1
      DO 20 I=1,2
      DO 20 J=1,2
      DO 20 K=1,2
20    Y(N,I,J)=Y(N,I,J)+X(N,I,K)*X(N+1,K,J)
      IF (N-(L+1))0,21,21
      DO 22 I=1,2
      DO 22 J=1,2
22    X(N+1,I,J)=Y(N,I,J)
21    CONTINUE
      ATT=CABS(Y(L+1,2,1))
      ATT=ATT/(2.*AREA(2))*P*C
      ATTEN(NOO)=20.*ALOG10(ATT)
12    CONTINUE
      DO 71 NOO=0,294,5
      NOO1=NOO+1
      NOO2=NOO+2
      NOO3=NOO+3
      NOO4=NOO+4
      NOO5=NOO+5
      NOO6=40+10*NOO1
      NOO7=40+10*NOO2
      NOO8=40+10*NOO3
      NOO9=40+10*NOO4
      NOO10=40+10*NOO5
      WRITE(2,61) NOO6,ATTEN(NOO1),NOO7,ATTEN(NOO2),NOO8,ATTEN(NOO3),
     1NOO9,ATTEN(NOO4),NOO10,ATTEN(NOO5)
61    FORMAT (1H ,1I4.4X,1F8.4,7X,1I4,4X,1F8.4,7X,1I4,4X,1F8.4
     1,7X,1I4,4X,1F8.4,7X,1I4,4X,1F8.4)
71    CONTINUE
      NUMM=NUMM+1
      IF(NUMM-NOM)3,3,0
      NUML=NUML+1
      IF(NUML-NOL)2,2,0
      NUMA=NUMA+1
      IF(NUMA-NOA)1,1,0
      STOP
      END
```

TRANSMISSION LOSS FOR SIMPLE EXPANSION CHAMBER IN SERIES WITH HELMHOLTZ RESONATOR.

```
      MASTER ACOU
      REAL LEN,IMP,KON,LENN,MACH
      COMPLEX X(7,2,2),Y(7,2,2)
      DIMENSION KON(1000),AREA(7),IMP(7),LEN(7),AREAN(7),LENN(7),MACH(7
     1,ATTEN(500)
C     ATTENUATION OF SILENCERS BY MATRIX METHODS
C     LEN=LENGTH OF MATRIX SECTION
C     AREA=AREA OF MATRIX SECTION
C     LENN=LENGTH OF RESONATOR NECK
C     AREAN=AREA OF RESONATOR NECK
C     L=NO. OF MATRICES
C     P=DENSITY OF MEDIUM
C     C=VELOCITY OF SOUND
C     NOL=NO. OF SETS OF INPUT DATA FOR LEN
C     NOA=NO. OF SETS OF INPUT DATA FOR AREA
C     MACH= LOCAL MACH NO. OF GAS FLOW
      READ (1,53) L
   53 FORMAT (1I1)
      READ (1,51) NOA,NOL,NOM,P,C
   51 FORMAT (3I1,2F10.5)
      NUMA=1
      X(1,1,1),X(1,2,2),X(L+2,1,1),X(L+2,2,2)=CMPLX(1.,0.)
      X(1,1,2),X(L+2,1,2)=CMPLX(0.,0.)
    1 WRITE (2,52)
   52 FORMAT (1H1,9HAREAS ARE)
      DO 10 N=2,L+1
      READ (1,54) AREA(N)
   54 FORMAT (F0.0)
      WRITE (2,55) AREA(N)
   55 FORMAT (1H ,1F10.8,4X)
   10 CONTINUE
      NUML=1
    2 WRITE (2,56)
   56 FORMAT (1H0,11HLENGTHS ARE)
      DO 11 N=2,L+1
      READ (1,57) LEN(N)
   57 FORMAT (F0.0)
      WRITE (2,58) LEN(N)
   58 FORMAT (1H ,1F10.8,4X)
   11 CONTINUE
    4 WRITE(2,72)
   72 FORMAT(1H0,18HAREAN AND LENN ARE)
      DO 18 N=5,L,4
      READ (1,62) AREAN(N),LENN(N)
   62 FORMAT (F0.0)
      WRITE(2,73)AREAN(N),LENN(N)
   73 FORMAT(1H ,1F10.8,4X,1F10.8)
   18 CONTINUE
      NUMM=1
    3 DO 17 N=2,L+1
      READ (1,63) MACH(N)
   63 FORMAT (F0.0)
   17 CONTINUE
      WRITE (2,65) MACH(2)
   65 FORMAT (1H0,24HMACH NO IN 1 INCH PIPE =,1F8.4)
      WRITE (2,59)
   59 FORMAT (1H0,4HFREQ,6X,5HATTEN,8X,4HFREQ,6X,
     15HATTEN,8X,4HFREQ,6X,5HATTEN,8X,4HFREQ,6X,5HATTEN,8X,
     14HFREQ,6X,5HATTEN)
      X(L+2,2,1)=CMPLX(AREA(L+1)/(P*C)*(1+MACH(L+1)),0.)
      X(1,2,1)=CMPLX(AREA(2)/(P*C)*(1-MACH(2)),0.)
      NOO=0
      DO 12 M=50,3000,10
      NOO=NOO+1
```

```
      FRE=M
      DO 15 I=1,2
      DO 15 J=1,2
      DO 15 N=1,L+1
   15 Y(N,I,J)=CMPLX(0.,0.)
      KON(NOO)=2.*3.14159*FRE/C
      DO 16 N=2,L+1,2
      IMP(N)=KON(NOO)*LEN(N)/(1.0-MACH(N)*MACH(N))
      X(N,1,1)=CMPLX(COS(IMP(N)),-MACH(N)*SIN(IMP(N)))
      X(N,1,2)=CMPLX(0.,P*C/AREA(N)*SIN(IMP(N)))
      X(N,2,1)=CMPLX(0.,AREA(N)/(P*C)*(1.0-MACH(N)*MACH(N))*SIN(IMP(N)))
      X(N,2,2)=CMPLX(COS(IMP(N)),MACH(N)*SIN(IMP(N)))
   16 CONTINUE
      DO 19 N=3,L,4
      IMP(N)=KON(NOO)*LEN(N)/(1.0-MACH(N)*MACH(N))
      X(N,1,1)=CMPLX(COS(IMP(N)),-MACH(N)*SIN(IMP(N)))
      X(N,1,2)=CMPLX(0.,P*C/AREA(N)*SIN(IMP(N)))
      X(N,2,1)=CMPLX(0.,AREA(N)/(P*C)*(1.0-MACH(N)*MACH(N))*SIN(IMP(N)))
      X(N,2,2)=CMPLX(COS(IMP(N)),MACH(N)*SIN(IMP(N)))
   19 CONTINUE
      DO 171 N=3,L,4
      IMP(N)=KON(NOO)*LEN(N)
      X(N,1,1),X(N,2,2)=CMPLX(1.,0.)
      X(N,1,2)=CMPLX(0.,0.)
      Z=-P*C/(AREA(N)*TAN(IMP(N)))+P*KON(NOO)*C*LENN(N)/AREAN(N)
      Z=1/Z
      X(N,2,1)=CMPLX(0.,Z)
  171 CONTINUE
      DO 21 N=1,L+1
      DO 20 I=1,2
      DO 20 J=1,2
      DO 20 K=1,2
   20 Y(N,I,J)=Y(N,I,J)+X(N,I,K)*X(N+1,K,J)
      IF (N-(L+1))0,21,21
      DO 22 I=1,2
      DO 22 J=1,2
   22 X(N+1,I,J)=Y(N,I,J)
   21 CONTINUE
      ATT=CABS(Y(L+1,2,1))
      ATT=ATT/(2.*AREA(2))*P*C
      ATTEN(NOO)=20.*ALOG10(ATT)
   12 CONTINUE
      DO 71 NOO=0,294,5
      NOO1=NOO+1
      NOO2=NOO+2
      NOO3=NOO+3
      NOO4=NOO+4
      NOO5=NOO+5
      NOO6=40+10*NOO1
      NOO7=40+10*NOO2
      NOO8=40+10*NOO3
      NOO9=40+10*NOO4
      NOO10=40+10*NOO5
      WRITE(2,61) NOO6,ATTEN(NOO1),NOO7,ATTEN(NOO2),NOO8,ATTEN(NOO3),
     1NOO9,ATTEN(NOO4),NOO10,ATTEN(NOO5)
   61 FORMAT (1H ,1I4,4X,1F8.4,7X,1I4,4X,1F8.4,7X,1I4,4X,1F8.4
     1,7X,1I4,4X,1F8.4,7X,1I4,4X,1F8.4)
   71 CONTINUE
      NUMM=NUMM+1
      IF(NUMM-NOM)3,3,0
      NUML=NUML+1
      IF(NUML-NOL)2,2,0
      NUMA=NUMA+1
      IF(NUMA-NOA)1,1,0
      STOP
      END
```

SIMPLE EXPANSION CHAMBER WITH FINITE OUTLET PIPE.

```
      MASTER ACOU
      REAL LEN,IMP,KON,LENN,MACH,IMPT,LENT
      COMPLEX X(7,2,2),Y(7,2,2)
      DIMENSION KON(1000),AREA(7),IMP(7),LEN(7),AREAN(7),LENN(7),MACH(7
     1,ATTEN(500)
     1,COT(7)
C     ATTENUATION OF SILENCERS BY MATRIX METHODS
C     LEN=LENGTH OF MATRIX SECTION
C     AREA=AREA OF MATRIX SECTION
C     LENN=LENGTH OF RESONATOR NECK
C     AREAN=AREA OF RESONATOR NECK
C     LENT=LENGTH OF TAIL PIPE
C     RT=RADIUS OF TAIL PIPE
C     L=NO. OF MATRICES
C     P=DENSITY OF MEDIUM
C     C=VELOCITY OF SOUND
C     NOL=NO. OF SETS OF INPUT DATA FOR LEN
C     NOA=NO. OF SETS OF INPUT DATA FOR AREA
C     MACH= LOCAL MACH NO. OF GAS FLOW
      READ (1,53) L
  53  FORMAT (1I1)
      READ (1,51) NOA,NOL,NOM,P,C
  51  FORMAT (3I1,2F10.5)
      NUMA=1
      X(1,1,1),X(1,2,2),X(L*2,1,1),X(L+2,2,2)=CMPLX(1.,0.)
      X(1,1,2),X(L*2,1,2)=CMPLX(0.,0.)
  1   WRITE (2,52)
  52  FORMAT (1H1,9HAREAS ARE)
      DO 10 N=2,L+1
      READ (1,54) AREA(N)
  54  FORMAT (F0.0)
      WRITE (2,55) AREA(N)
  55  FORMAT (1H ,1F10.8,4X)
  10  CONTINUE
      NUML=1
  2   WRITE (2,56)
  56  FORMAT (1H0,11HLENGTHS ARE)
      DO 11 N=2,L+1
      READ (1,57) LEN(N)
  57  FORMAT (F0.0)
      WRITE (2,58) LEN(N)
  58  FORMAT (1H ,1F10.8,4X)
  11  CONTINUE
      NUMM=1
  5   WRITE(2,74)
  74  FORMAT(1H0,15HLENT AND RT ARE)
      READ(1,66) LENT,RT
  66  FORMAT(F0.0)
      WRITE(2,75)LENT,RT
  75  FORMAT(1H ,1F10.8,4X,1F10.8)
  3   DO 17 N=2,L+1
      READ (1,63) MACH(N)
  63  FORMAT (F0.0)
  17  CONTINUE
      WRITE (2,65) MACH(2)
  65  FORMAT (1H0,24HMACH NO IN 1 INCH PIPE =,1F8.4)
      WRITE (2,59)
  59  FORMAT (1H0,4HFREQ,6X,5HATTEN,8X,4HFREQ,6X,
     15HATTEN,8X,4HFREQ,6X,5HATTEN,8X,4HFREQ,6X,5HATTEN,8X,
     14HFREQ,6X,5HATTEN)
      X(1,2,1)=CMPLX(AREA(2)/(P*C)*(1-MACH(2)),0.)
      NOO=0
      DO 12 M=50,3000,10
      NOO=NOO+1
```

```
      FRE=M
      DO 15 I=1,2
      DO 15 J=1,2
      DO 15 N=1,L+1
15    Y(N,I,J)=CMPLX(0.,0.)
      KON(NOO)=2.*3.14159*FRE/C
      IMPT=KON(NOO)*LENT/(1.0-MACH(L+1)*MACH(L+1))
      ZTR=MACH(L+1)*AREA(L+1)/(P*C)
      ZTC=-AREA(L+1)/(P*C)*COS(IMPT)/SIN(IMPT)
      X(L+2,2,1)=CMPLX(ZTR,ZTC)
      DO 16 N=2,L+1,1
      IMP(N)=KON(NOO)*LEN(N)/(1.0-MACH(N)*MACH(N))
      X(N,1,1)=CMPLX(COS(IMP(N)),-MACH(N)*SIN(IMP(N)))
      X(N,1,2)=CMPLX(0.,P*C/AREA(N)*SIN(IMP(N)))
      X(N,2,1)=CMPLX(0.,AREA(N)/(P*C)*(1.0-MACH(N)*MACH(N))*SIN(IMP(N)))
      X(N,2,2)=CMPLX(COS(IMP(N)),MACH(N)*SIN(IMP(N)))
16    CONTINUE
      DO 21 N=1,L+1
      DO 20 I=1,2
      DO 20 J=1,2
      DO 20 K=1,2
20    Y(N,I,J)=Y(N,I,J)+X(N,I,K)*X(N+1,K,J)
      IF (N-(L+1))0,21,21
      DO 22 I=1,2
      DO 22 J=1,2
22    X(N+1,I,J)=Y(N,I,J)
21    CONTINUE
      ATT=CABS(Y(L+1,2,1))
      ATT=ATT*ABS(2.*SIN(IMPT))
      ATT=ATT/(2.*AREA(2))*P*C
      ATTEN(NOO)=20.*ALOG10(ATT)
12    CONTINUE
      DO 71 NOO=0,294,5
      NOO1=NOO+1
      NOO2=NOO+2
      NOO3=NOO+3
      NOO4=NOO+4
      NOO5=NOO+5
      NOO6=40+10*NOO1
      NOO7=40+10*NOO2
      NOO8=40+10*NOO3
      NOO9=40+10*NOO4
      NOO10=40+10*NOO5
      WRITE(2,61) NOO6,ATTEN(NOO1),NOO7,ATTEN(NOO2),NOO8,ATTEN(NOO3),
     1NOO9,ATTEN(NOO4),NOO10,ATTEN(NOO5)
61    FORMAT (1H ,1I4,4X,1F8.4,7X,1I4,4X,1F8.4,7X,1I4,4X,1F8.4
     1,7X,1I4,4X,1F8.4,7X,1I4,4X,1F8.4)
71    CONTINUE
      NUMM=NUMM+1
      IF(NUMM-NOM)3,3,0
      NUML=NUML+1
      IF(NUML-NOL)2,2,0
      NUMA=NUMA+1
      IF(NUMA-NOA)1,1,0
      STOP
      END
```

RESONATOR WITH FINITE OUTLET PIPE.

```
      MASTER OUTLET
      REAL LEN,IMP,KON,LENN,MACH,IMPT,LENT
      COMPLEX X(15,2,2),Y(15,2,2)
      DIMENSION KON(1000),AREA(15),IMP(15),LEN(15),AREAN(15),LENN(15
     1MACH(15)
     1,ATTEN(500)
     1,COT(15)
C     ATTENUATION OF SILENCERS BY MATRIX METHODS
C     LEN=LENGTH OF MATRIX SECTION
C     AREA=AREA OF MATRIX SECTION
C     LENN=LENGTH OF RESONATOR NECK
C     AREAN=AREA OF RESONATOR NECK
C     LENT=LENGTH OF TAIL PIPE
C     RT=RADIUS OF TAIL PIPE
C     L=NO. OF MATRICES
C     P=DENSITY OF MEDIUM
C     C=VELOCITY OF SOUND
C     NOL=NO. OF SETS OF INPUT DATA FOR LEN
C     NOA=NO. OF SETS OF INPUT DATA FOR AREA
C     MACH= LOCAL MACH NO. OF GAS FLOW
      L=3
  53  FORMAT (1I0)
      NOA=3
      NOL=1
      NOM=1
      P=1.21
      C=610.0
  51  FORMAT (3I1,2F10.5)
      NOMA=1
      X(1,1,1),X(1,2,2),X(L+2,1,1),X(L+2,2,2)=CMPLX(1.,0.)
      X(1,1,2),X(L+2,1,2)=CMPLX(0.,0.)
   1  WRITE (2,52)
  52  FORMAT (1H1,9HAREAS ARE)
      DO 10 N=2,L+1
      READ (1,54) AREA(N)
  54  FORMAT(F10.8)
      WRITE (2,55) AREA(N)
  55  FORMAT (1H ,1F10.8,4X)
  10  CONTINUE
      NOML=1
   2  WRITE (2,56)
  56  FORMAT (1H0,11HLENGTHS ARE)
      DO 11 N=2,L+1
      READ (1,57) LEN(N)
  57  FORMAT(F8.4)
      WRITE (2,58) LEN(N)
  58  FORMAT (1H ,1F10.8,4X)
  11  CONTINUE
   4  WRITE(2,72)
  72  FORMAT(1H0,18HAREAN AND LENN ARE)
      DO 18 N=3,L,2
      READ (1,62) AREAN(N),LENN(N)
  62  FORMAT(F10.8)
      WRITE(2,73)AREAN(N),LENN(N)
  73  FORMAT (1H ,1F10.8,4X,1F10.8)
  18  CONTINUE
      NOMM=1
   5  WRITE(2,74)
  74  FORMAT(1H0,15HLENT AND RT ARE)
```

```
      READ(1,66) LENT,RT
66    FORMAT(F10.8)
      WRITE(2,75)LENT,RT
 75   FORMAT(1H ,1F10.8,4X,1F10.8)
 3    DO 17 N=2,L+1
      READ (1,63) MACH(N)
63    FORMAT(F8.4)
 17   CONTINUE
      WRITE (2,65) MACH(2)
 65   FORMAT (1H0,24HMACH NO IN 1 INCH PIPE =,1F8.4)
      WRITE (2,59)
 59   FORMAT (1H0,4HFREQ,6X,5HATTEN,8X,4HFREQ,6X,
     15HATTEN,8X,4HFREQ,6X,5HATTEN,8X,4HFREQ,6X,5HATTEN,8X,
     14HFREQ,6X,5HATTEN)
      X(1,2,1)=CMPLX(AREA(2)/(P*C)*(1-MACH(2)),0.)
      NOO=0
      DO 12 M=10,1000,10
      NOO=NOO+1
      FRE=M
      DO 15 I=1,2
      DO 15 J=1,2
      DO 15 N=1,L+1
 15   Y(N,I,J)=CMPLX(0.,0.)
      KON(NOO)=2.*3.14159*FRE/C
      IMPT=KON(NOO)*LENT/(1.0-MACH(L+1)*MACH(L+1))
      ZTR=MACH(L+1)*AREA(L+1)/(P*C)
      ZTC=-AREA(L+1)/(P*C)*COS(IMPT)/SIN(IMPT)
      X(L+2,2,1)=CMPLX(ZTR,ZTC)
      DO 16 N=2,L+1,2
      IMP(N)=KON(NOO)*LEN(N)/(1.0-MACH(N)*MACH(N))
      X(N,1,1)=CMPLX(COS(IMP(N)),-MACH(N)*SIN(IMP(N)))
      X(N,1,2)=CMPLX(0.,P*C/AREA(N)*SIN(IMP(N)))
      X(N,2,1)=CMPLX(0.,AREA(N)/(P*C)*(1.0-MACH(N)*MACH(N))*SIN(IMP(N)))
      X(N,2,2)=CMPLX(COS(IMP(N)),MACH(N)*SIN(IMP(N)))
 16   CONTINUE
      DO 171N=3,L,2
      IMP(N)=KON(NOO)*LEN(N)
      X(N,1,1),X(N,2,2)=CMPLX(1.,0.)
```

```
      X(N,1,2)=CMPLX(0.,0.)
      Z=-P*C/(AREA(N)*TAN(IMP(N)))+P*KON(NOO)*C*LENN(N)/AREAN(N)
      Z=1/Z
      X(N,2,1)=CMPLX(0.,Z)
  171 CONTINUE
      DO 21 N=1,L+1
      DO 20 I=1,2
      DO 20 J=1,2
      DO 20 K=1,2
   20 Y(N,I,J)=Y(N,I,J)+X(N,I,K)*X(N+1,K,J)
      IF (N-(L+1))0,21,21
      DO 22 I=1,2
      DO 22 J=1,2
   22 X(N+1,I,J)=Y(N,I,J)
   21 CONTINUE
      ATT=CABS(Y(L+1,2,1))
      ATT=ATT*ABS(2.*SIN(IMPT))
      ATT=ATT/(2.*AREA(2))*P*C
      ATTEN(NOO)=20.*ALOG10(ATT)
   12 CONTINUE
      DO 71 NOO=0,95,5
      NOO1=NOO+1
      NOO2=NOO+2
      NOO3=NOO+3
      NOO4=NOO+4
      NOO5=NOO+5
      NOO6=10*NOO1
      NOO7=10*NOO2
      NOO8=10*NOO3
      NOO9=10*NOO4
      NOO10=10*NOO5
      WRITE(2,61) NOO6,ATTEN(NOO1),NOO7,ATTEN(NOO2),NOO8,ATTEN(NOO3),
     1NOO9,ATTEN(NOO4),NOO10,ATTEN(NOO5)
   61 FORMAT (1H ,I14,4X,1F8.4,7X,I14,4X,1F8.4,7X,I14,4X,1F8.4
     1,7X,I14,4X,1F8.4,7X,I14,4X,1F8.4)
   71 CONTINUE
      NUMM=NUMM+1
      IF(NUMM-NOM)5,5,0
      NUML=NUML+1
      IF(NUML-NOL)2,2,0
      NUMA=NUMA+1
      IF(NUMA-NOA)1,1,0
      STOP
      END
```

SIMPLE EXPANSION CHAMBER WITH FINITE INLET PIPE.

```
      MASTER RESO
      REAL LEN,IMP,KON,LENN,MACH
      COMPLEX X(20,2,2)
      COMPLEX Y(20,2,2)
      DIMENSION KON(1000),ATTEN(1000)
      DIMENSION AREA(20),AREAN(20),IMP(20),LEN(20),LENN(20),MACH(20
C     ATTENUATION OF SILENCERS BY MATRIX METHODS
C     SIMPLE EXPANSION CHAMBER
C     LEN=LENGTH OF MATRIX SECTION
C     AREA=AREA OF MATRIX SECTION
C     LENN=LENGTH OF RESONATOR NECK
C     AREAN=AREA OF RESONATOR NECK
C     L=NO OF MATRICES
C     P=DENSITY OF MEDIUM
C     C=VELOCITY OF SOUND
C     NOL=NO OF SETS OF INPUT DATA FOR LEN
C     NOA=NO OF SETS OF INPUT DATA FOR AREA
C     MACH=LOCAL MACH NO. OF GAS FLOW
C     M1 IS HIGHEST FREQUENCY
C
      L=3
C
C     L3=0 FOR INFINITE INLET PIPE
C     L3=1 FOR FINITE INLET PIPE
C
      L3=1
      L1=L+2
C
      M1=1000
C
      NUMA=1
      NOA=1
      NOA=1
      NOL=2
      NOM=2
      P=1.2053
      C=343.0
      NUMA=1
 61   FORMAT (1H ,1I4,4X,1F8.4,7X,1I4,4X,1F8.4,7X,1I4,4X,1F8.4
     1,7X,1I4,4X,1F8.4,7X,1I4,4X,1F8.4)
 55   FORMAT(1H ,1F10.8,4X)
 54   FORMAT(F8.4)
 57   FORMAT(F8.4)
 52   FORMAT (1H1,9HAREAS ARE)
 56   FORMAT(1H0,11HLENGTHS ARE)
 72   FORMAT(1H0,18HAREAN AND LENN ARE)
 65   FORMAT (1H0,24HMACH NO IN 1 INCH PIPE =,1F18.4)
 59   FORMAT (1H0,4HFREQ,6X,5HATTEN,8X,4HFREQ,6X,
     15HATTEN,8X,4HFREQ,6X,5HATTEN,8X,4HFREQ,6X,5HATTEN,8X,
     14HFREQ,6X,5HATTEN)
 53   FORMAT (1I2)
 51   FORMAT (3I2,2F10.5)
 60   FORMAT(F10.8)
      X(1,1,1),X(1,2,2),X(L+2,1,1),X(L+2,2,2)=CMPLX(1.,0.)
      X(1,1,2),X(L+2,1,2)=CMPLX(0.,0.)
 1    WRITE (2,52)
      DO 10 N=2,L+1
      READ(1,60) AREA(N)
      WRITE(2,60)AREA(N)
 10   CONTINUE
      NUML=1
 2    WRITE(2,56)
C
C     N=3 REFERS TO CYLINDRICAL CHAMBER OF RESONATOR
```

```
C
      DO 11 N=2,L+1
      READ(1,57) LEN(N)
      WRITE(2,57) LEN(N)
 11   CONTINUE
 4    WRITE(2,72)
C
C
      NUMM=1
 3    DO 17 N=2,L+1
      READ(1,57)MACH(N)
 17   CONTINUE
      WRITE(2,65) MACH(2)
      WRITE (2,59)
      X(L+2,2,1)=CMPLX(AREA(L+1)/(P*C)*(1+MACH(L+1)),0.)
      X(1,2,1)=CMPLX(0.0,0.0)
      IF(L3) 0,0,117
      X(1,2,1)=CMPLX(AREA(2)/(P*C)*(1-MACH(2)),0.)
 117  CONTINUE
      NOO=0
      DO 12 M=50,M1,10
      NOO=NOO+1
      FRE=M
      DO 15 I=1,2
      DO 15 J=1,2
      DO 15 N=1,L+1
 15   Y(N,I,J)=CMPLX(0.,0.)
      KON(NOO)=2.*3.14159*FRE/C
C
      DO 16 N=2,L+1
C
      IMP(N)=KON(NOO)*LEN(N)/(1.0-MACH(N)*MACH(N))
      X(N,1,1)=CMPLX(COS(IMP(N)),-MACH(N)*SIN(IMP(N)))
      X(N,1,2)=CMPLX(0.,P*C/AREA(N)*SIN(IMP(N)))
      X(N,2,1)=CMPLX(0.,AREA(N)/(P*C)*(1.0-MACH(N)*MACH(N))*SIN(IMP(N)
      X(N,2,2)=CMPLX(COS(IMP(N)),MACH(N)*SIN(IMP(N)))
 16   CONTINUE
C
 171  CONTINUE
C
      DO 21 N=1,L+1
      DO 20 I=1,2
      DO 20 J=1,2
      DO 20 K=1,2
 20   Y(N,I,J)=Y(N,I,J)+X(N,I,K)*X(N+1,K,J)
      IF  (N-(L+1)) 0,21,21
      DO 22 I=1,2
      DO 22 J=1,2
 22   X(N+1,I,J)=Y(N,I,J)
 21   CONTINUE
      ATT=CABS(Y(L+1,2,1))
      IF(L3) 0,0,121
      ATT=ATT/(2.*AREA(2))*P*C
      IF(L3)123,123,0
 121  ATT=ATT/(AREA(2)*(1.0+MACH(2)))*P*C
 123  CONTINUE
      ATTEN(NOO)=20.*ALOG10(ATT)
 12   CONTINUE
      M2=(M1-60)/10
      DO 71 NOO=0,M2,5
      NOO1=NOO+1
      NOO2=NOO+2
      NOO3=NOO+3
      NOO4=NOO+4
      NOO5=NOO+5
      NOO6=40+10*NOO1
```

```
      N007=40+10*N002
      N008=40+10*N003
      N009=40+10*N004
      N0010=40+10*N005
      WRITE(2,61) N006,ATTEN(N001),N007,ATTEN(N002),N008,ATTEN(N003),
     1N009,ATTEN(N004),N0010,ATTEN(N005)
71    CONTINUE
      NUMM=NUMM+1
      IF(NUMM-NOM)3,3,0
      NUML =NUML+1
      IF(NUML-NOL)2,2,0
      NUMA=NUMA+1
      IF(NUMA-NOA)1,1,0
      STOP
      END
```

```
      SUBROUTINE DATA (L,AREAN,LENN ,L1                    )
      REAL LENN
      DIMENSION AREAN(L1),LENN(L1)
      DO 18 N=3,L,2
      READ(1,62)AREAN(N),LENN(N)
      WRITE(2,73) AREAN(N),LENN(N)
18    CONTINUE
62    FORMAT(F10.8)
73    FORMAT(1H ,1F8.6,4X,1F8.6)
      RETURN
      END
```

HELMHOLTZ RESONATOR WITH FINITE INLET PIPE.

```
      MASTER RESO
      REAL LEN,IMP,KON,LENN,MACH
      COMPLEX X(20,2,2)
      COMPLEX Y(20,2,2)
      DIMENSION KON(1000),ATTEN(1000)
      DIMENSION AREA(20),AREAN(20),IMP(20),LEN(20),LENN(20),MACH(20)
C     ATTENUATION OF SILENCERS BY MATRIX METHODS
C     SIMPLE EXPANSION CHAMBER
C     LEN=LENGTH OF MATRIX SECTION
C     AREA=AREA OF MATRIX SECTION
C     LENN=LENGTH OF RESONATOR NECK
C     AREAN=AREA OF RESONATOR NECK
C     L=NO OF MATRICES
C     P=DENSITY OF MEDIUM
C     C=VELOCITY OF SOUND
C     NOL=NO OF SETS OF INPUT DATA FOR LEN
C     NOA=NO OF SETS OF INPUT DATA FOR AREA
C     MACH=LOCAL MACH NO. OF GAS FLOW
C     M1 IS HIGHEST FREQUENCY
C
      L=3
C
C     L3=0 FOR INFINITE INLET PIPE
C     L3=1 FOR FINITE INLET PIPE
C
      L3=1
      L1=L+2
C
      M1=1000
C
      NUMA=1
```

```
      NOA=3
      NOL=1
      NOM=2
      P=1.2053
      C=610.0
      NUMA=1
 61   FORMAT (1H ,1I4,4X,1F8.4,7X,1I4,4X,1F8.4,7X,1I4,4X,1F8.4
     1,7X,1I4,4X,1F8.4,7X,1I4,4X,1F8.4)
 55   FORMAT(1H ,1F10.8,4X)
 54   FORMAT(F8.4)
 57   FORMAT(F8.4)
 52   FORMAT (1H1,9HAREAS ARE)
 56   FORMAT(1H0,11HLENGTHS ARE)
 72   FORMAT(1H0,18HAREAN AND LENN ARE)
 65   FORMAT (1H0,24HMACH NO IN 1 INCH PIPE =,1F18.4)
 59   FORMAT (1H0,4HFREQ,6X,5HATTEN,8X,4HFREQ,6X,
     15HATTEN,8X,4HFREQ,6X,5HATTEN,8X,4HFREQ,6X,5HATTEN,8X,
     14HFREQ,6X,5HATTEN)
 53   FORMAT (1I2)
 51   FORMAT (3I2,2F10.5)
 60   FORMAT(F10.8)
      X(1,1,1),X(1,2,2),X(L+2,1,1),X(L+2,2,2)=CMPLX(1.,0.)
      X(1,1,2),X(L+2,1,2)=CMPLX(0.,0.)
 1    WRITE (2,52)
      DO 10 N=2,L+1
      READ(1,60) AREA(N)
      WRITE(2,60)AREA(N)
 10   CONTINUE
      NUML=1
 2    WRITE(2,56)
C
C     N=3 REFERS TO CYLINDRICAL CHAMBER OF RESONATOR
C
      DO 11 N=2,L+1
      READ(1,57) LEN(N)
      WRITE(2,57) LEN(N)
 11   CONTINUE
 4    WRITE(2,72)
C
      CALL DATA(L,AREAN,LENN , L1                    )
C
      NUMM=1
 3    DO 17 N=2,L+1
      READ(1,57)MACH(N)
 17   CONTINUE
      WRITE(2,65) MACH(2)
      WRITE (2,59)
      X(L+2,2,1)=CMPLX(AREA(L+1)/(P*C)*(1+MACH(L+1)),0.)
      X(1,2,1)=CMPLX(0.0,0.0)
      IF(L3) 0,0,117
      X(1,2,1)=CMPLX(AREA(2)/(P*C)*(1-MACH(2)),0.)
 117  CONTINUE
      NOO=0
      DO 12 M=50,M1,10
      NOO=NOO+1
      FRE=M
      DO 15 I=1,2
      DO 15 J=1,2
      DO 15 N=1,L+1
 15   Y(N,I,J)=CMPLX(0.,0.)
      KON(NOO)=2.*3.14159*FRE/C
C
      DO 16 N=2,L+1,2
C
      IMP(N)=KON(NOO)*LEN(N)/(1.0-MACH(N)*MACH(N))
      X(N,1,1)=CMPLX(COS(IMP(N)),-MACH(N)*SIN(IMP(N)))
```

```
      X(N,1,2)=CMPLX(0.,P*C/AREA(N)*SIN(IMP(N)))
      X(N,2,1)=CMPLX(0.,AREA(N)/(P*C)*(1.0-MACH(N)*MACH(N))*SIN(IMP(N)))
      X(N,2,2)=CMPLX(COS(IMP(N)),MACH(N)*SIN(IMP(N)))
 16   CONTINUE
C
      DO 171 N=3,L,2
      IMP(N)=KON(NOO)*LEN(N)
      X(N,1,1),X(N,2,2)=CMPLX(1.,0.)
      X(N,1,2)=CMPLX(0.,0.)
      Z=-P*C/(AREA(N)*TAN(IMP(N))) + P*KON(NOO)*C*LENN(N)/AREAN(N)
      Z=1/Z
      X(N,2,1)=CMPLX(0.,Z)
 171  CONTINUE
C
      DO 21 N=1,L+1
      DO 20 I=1,2
      DO 20 J=1,2
      DO 20 K=1,2
 20   Y(N,I,J)=Y(N,I,J)+X(N,I,K)*X(N+1,K,J)
      IF  (N-(L+1)) 0,21,21
      DO 22 I=1,2
      DO 22 J=1,2
 22   X(N+1,I,J)=Y(N,I,J)
 21   CONTINUE
      ATT=CABS(Y(L+1,2,1))
      IF(L3) 0,0,121
      ATT=ATT/(2.*AREA(2))*P*C
      IF(L3)123,123,0
 121  ATT=ATT/(AREA(2)*(1.0+MACH(2)))*P*C
 123  CONTINUE
      ATTEN(NOO)=20.*ALOG10(ATT)
 12   CONTINUE
      M2=(M1-60)/10
      DO 71 NOO=0,M2,5
      NO01=NOO+1
      NO02=NOO+2
      NO03=NOO+3
      NO04=NOO+4
      NO05=NOO+5
      NO06=40+10*NO01
      NO07=40+10*NO02
      NO08=40+10*NO03
      NO09=40+10*NO04
      NO010=40+10*NO05
      WRITE(2,61) NO06,ATTEN(NO01),NO07,ATTEN(NO02),NO08,ATTEN(NO03),
     1NO09,ATTEN(NO04),NO010,ATTEN(NO05)
 71   CONTINUE
      NUMM=NUMM+1
      IF(NUMM-NOM)3,3,0
      NUML =NUML+1
      IF(NUML-NOL)2,2,0
      NUMA=NUMA+1
      IF(NUMA-NOA)1,1,0
      STOP
      END

      SUBROUTINE DATA (L,AREAN,LENN ,L1)
      REAL LENN
      DIMENSION AREAN(L1),LENN(L1)
      DO 18 N=3,L,2
      READ(1,62)AREAN(N),LENN(N)
      WRITE(2,73) AREAN(N),LENN(N)
 18   CONTINUE
 62   FORMAT(F10.8)
 73   FORMAT(1H ,1F8.6,4X,1F8.6)
      RETURN
      END
```

REFERENCES

(1) Lord RAYLEIGH. "The theory of sound, Vols. I & II", Dover Publications Inc., 1945.

(2) H. LAMB. "The dynamical theory of sound", Dover Publications Inc., 1960.

(3) G. W. STEWART and R. B. LINDSAY. "Acoustic", D. Van Nostrand Co. Inc., 1930.

(4) D. D. DAVIS, G. M. STOKES, D. MOORE and G. L. STEVENS. "Theoretical and experimental investigation of mufflers with comments on engine-exhaust muffler design", NACA Report 1192, 1952.

(5) C. D. HAYNES and R. L. KELL. "Engine exhaust silencing". Motor Industry Research Association Reports I, II & III, 1964.

(6) J. IGARASHI and M. TOYAMA. "Fundamentals of acoustical silencers. (I) Theory and experiments of acoustic low-pass filters", Aeronautical Research Institute, U. Of Tokyo, Report No. 339, Dec. 1958.

(7) J. IGARASHI and T. MIWA. "Fundamentals of acoustical silencers. (II) Determination of four terminal constants of acoustical elements", Aeronautical Research Institute, U. of Tokyo, Report No. 344, May 1959.

(8) G. W. STEWART. "Acoustic wave filters", Phys. Rev., 20,528, 1922.

(9) G. W. STEWART. "Acoustic wave filters: an extension of the theory", Phys. Rev., 23, 90, 1924.

(10) G. W. STEWART. "Acoustic wave filters: attenuation and phase factors", Phys. Rev., 23, 520, 1924.

(11) R. B. LINDSAY. "The filtration of sound, I", Jn. of Applied Physics, Vol. 9, Oct. 1938.

(12) R. B. LINDSAY. "Finite acoustic filters", JASA, Vol. 8, No.4, April 1937.

(13) R. F. LAMBERT. "Acoustic filtering in a moving medium", JASA, Vol. 28, No. 6, Nov. 1956.

(14) R. F. LAMBERT. "Side branch insertion loss in a moving medium", JASA, Vol. 28, No. 6, Nov. 1956.

(15) M. FUKUDA. "A study on the exhaust muffler of internal combustion engine", Bulletin of JSME, Vol.6, No.22, 1963.

(16) A. V. SREENATH and M. L. MUNJAL. "Evaluation of noise attenuation due to exhaust mufflers", JSV (1971)12(1).

(17) A. H. DAVIS and N. FLEMING. "Further model experiments concerning the acoustical features of exhaust silencers", ARC Report 1421, 1935.

(18) K. R. CZARNECKI and D. D. DAVIS. "Dynamometer-stand investigation of the muffler used in the demonstration of light-airplane noise reduction', NACA Technical Note No. 1688, 1948.

(19) F. MECHEL, P. MERTENS and W. SCHILZ. "Research on sound propagation in sound absorbent ducts with superimposed air streams", AMRL-TDR-62-140, Vol. III, Physik Inst., Göttingen, 1962.

(20) E. MEYER, F. MECHEL and G. KURTZE. "Experiments on the influence of flow on sound attenuation in absorbing ducts", JASA, Vol. 30, No. 3, March 1958.

(21) D. H. TACK and R. F. LAMBERT. "Influence of shear flow on sound attenuation in a lined duct", JASA, 38, 1965.

(22) P. E. DOAK and P. G. VAIDYA. "Attenuation of plane wave and higher order mode sound propagation in lined ducts", JSV (1970)12(2).

(23) S. H. KO. "Sound attenuation in acoustically lined circular ducts in the presence of uniform flow and shear flow", JSV (1972)22(2).

(24) P. MUNGUR and H. E. PLUMBLEE. "Propagation and attenuation of sound in a soft-walled annular duct containing a sheared flow", conference on basic aerodynamic noise research, NASA SP-207, 1969.

(25) E. J. RICE. "Propagation of waves in an acoustically lined duct with a mean flow", conference on basic aerodynamic noise research, NASA SP-207, 1969.

(26) R. J. ALFREDSON. "The design and optimisation of exhaust silencers" Ph.D thesis. University of Southampton. 1970.

(27) H. MARTIN. "Measurement of the noise of the motor vehicles", Proc. of the symposium on engine noise and noise suppression, I. Mech. E., 1958.

(28) V. MASON. "Some experiments on the propagation of sound along a cylindrical duct containing flowing air", JSV (1969)10(2).

(29) P. D. DEAN. "On the local measurement of wall impedance and its use in the prediction of sound attenuation in absorbing flow ducts", Symposium on acoustics of flow ducts, U. of Southampton, 1972.

(30) J. D. TRIMMER. "Sound waves in a moving medium", JASA, Vol. 9, Oct. 1937.

(31) D. S. WHITEHEAD. "The vibration of air in a duct with a subsonic mean flow", Aeronautical Quarterly 12, 1, 1961.

(32) D. C. PRIDMORE-BROWN. "Sound propagation in a fluid flowing through an attenuating duct", J. Fluid Mech. 1958, 4, 393.

(33) P. MUNGUR and G. M. L. GLADWELL. "Acoustic wave propagation in a sheared fluid contained in a duct", JSV (1969)9(1).

(34) S. D. SAVKAR. "Propagation of sound in ducts with shear flow", JSV (1971)19(3).

(35) L. E. KINSLER and A. R. FREY. "Fundamentals of acoustics", John Wiley & Sons Inc., 1962.

(36) W. EVERSMAN. "The effect of mach number on the tuning of an acoustic lining in a flow duct", JASA Vol. 48, No. 2, part 1, 1970.

(37) U. INGARD. "Influence of fluid motion past a plane boundary on sound reflection, absorption and transmission", JASA (31)2, 1959.

(38) R. KAMO. "Suppression of engine exhaust noise", ASME preprint 58-A-144, 1959.

(39) F. C. KARAL. "The analogous acoustical impedance for discontinuities and constrictions of circular cross section". JASA Vol. 25, No. 2, 1953.

(40) H. LEVINE and J. SCHWINGER. "On the radiation of sound from an unflanged circular pipe". Phys. Rev. 73, 383, 1948.

(41) B. PHILLIPS. "Effect of high-wave amplitude and mean flow on a Helmholtz resonator", NASA TMX-1582, 1968.

(42) B. PHILLIPS and C. J. MORGAN. "Mechanical absorption of acoustic oscillations in simulated rocket combustion chambers", NASA TN D-3792, 1967.

(43) C. M. HARRIS (Editor). "Handbook of noise control", McGraw-Hill Inc. 1957.

(44) P. M. MORSE and K. N. INGARD. "Theoretical acoustics", McGraw-Hill Inc., 1968.

(45) S. N. RSCHEVKIN. "The theory of sound", Pergamon Press Ltd., 1963.

(46) P. M. MORSE. "Vibration and sound", McGraw-Hill Inc., 1948.

(47) C. E. McAULIFFE. "The influence of high speed air flow on the behaviour of acoustical elements". M.I.T., MS thesis, 1950.

(48) J. S. ANDERSON. "The effect of an air flow on a Helmholtz resonator in a circular duct", Eighth International Congress on Acoustics, 1974.

(49) J.S.ANDERSON and T.NETTLETON. "Digital Spectral and Correlation Analysis." City University Research Memorandum No ML 31, 1971.

Additional Section.

NOISE PROPAGATION THROUGH RIGHT-ANGLED BENDS.

SUMMARY.

The transmission of noise through a sharp right-angled bend in a circular pipe has been investigated for the frequency range from 4 kHz to 6 kHz. Theory developed for right-angled bends in square pipes is modified to suit the circular pipe. Various hypotheses for this modification have been tried, and the method of matrix multiplication used to obtain theoretical results.

NOTATION.

A	amplitude of incident pressure wave in an acoustic element.
a	length of one side of square pipe.
B	amplitude of reflected pressure wave in an acoustic element.
c	velocity of sound.
d	diameter of circular pipe.
f	frequency of vibration.
j	$\sqrt{-1}$
k	wave number = $2\pi/\lambda$
P	resultant pressure amplitude.
S	cross-sectional area of an acoustic element.
V	Volume velocity amplitude.
λ	wave-length
ρ	density of fluid medium.

INTRODUCTION.

Various forms of discontinuities in ducts and their effect on noise propagation has been investigated in the past. One of the most important of these discontinuities is the right-angled bend. The method used for these investigations is usually the electrical analogy and the discontinuity is represented by an equivalent circuit. The theory for wave propagation through a right-angled bend with non-reflective termination in a square tube has been established by Miles (5). Assuming plane wave propagation through the pipes, except at the bend, and by means of variational methods, he derived a step-by-step approximation as the complete solution to the problem.

Lippert in a series of papers investigated noise transmission in rectangular tubes through bends of various forms (2) (3) (4). In his paper (3), he calculated for a right-angled bend in a square tube the reflected and transmitted wave amplitudes and phase angles by measuring the wave patterns in the input and output tubes, and compared the wave amplitudes with the theoretical prediction by Miles's theory. Good agreement between theoretical prediction and experimental results was obtained. Approximately 80% of the incident wave was transmitted at a wave length equal to three times the length of one side of the square tube. During the measuring process, it was found that the standing waves in the input tube were very regular and the progressive waves in the output tube had constant amplitudes, showing that disturbances by higher modes was confined to a short distance from the bend and that the non-reflecting terminal was effective. It was also found that the loss of sound energy within the bend was small and that the first order approximation of Miles's theory is sufficiently accurate. Second order approximation gives only slight improvement.

In another paper (2), Lippert again measured the wave patterns in the input and output tubes and then obtained the reflection and transmission factors and hence the impedance matrix for this discontinuity. Theoretical analysis for this case has not yet been attempted. By using the same method, Lippert went on to determine the amplitudes and phase angles of the reflected and transmitted waves for bends of smaller angle and larger angle than 90° (4). It was found that for bends with angles smaller than 90°, the wave amplitudes and phase angles underwent systematic changes with change of frequency. This systematic change disappeared for bends having greater angles than 90°.

A rounded right angle bend was also investigated and the results obtained were quite different from those of a sharp right-angled bend.

THEORY.

For a right-angled bend in a square pipe as shown in Figure 1 P_1 , V_1 and P_2 , V_2 can be related by the following relationship :

$$\begin{bmatrix} P_1 \\ V_1 \end{bmatrix} = \begin{bmatrix} \frac{AM1}{AM2}\left\{\frac{1}{AM1}\cos(PH2) + \cos(PH1+PH2)\right\} & j\frac{AM1}{AM2}\frac{S}{\rho c}\left\{\frac{1}{AM1}\sin(PH2) - \sin(PH1+PH2)\right\} \\ j\frac{AM1}{AM2}\frac{\rho c}{S}\left\{\frac{1}{AM1}\sin(PH2) + \sin(PH1+PH2)\right\} & \frac{AM1}{AM2}\left\{\frac{1}{AM1}\cos(PH2) - \cos(PH1+PH2)\right\} \end{bmatrix} \begin{bmatrix} P_2 \\ V_2 \end{bmatrix}$$

where,

$$AM1 = \frac{1 - \frac{1}{\theta^2} + \cot^2\theta}{\sqrt{(1 + 1/\theta^2 - \cot^2\theta)^2 + 4\cot^2\theta}}$$

$$AM2 = 2 \Big/ \left\{ \theta\sqrt{(1 + 1/\theta^2 - \cot^2\theta)^2 + 4\cot^2\theta} \right\}$$

$$PH1 = \pi + \tan^{-1}\left\{2\cot\theta / (1 + 1/\theta^2 - \cot^2\theta)\right\}$$

$$PH2 = \tan^{-1}\left\{(1 + 1/\theta^2 - \cot^2\theta) / 2\cot\theta\right\}$$

$$\theta = \frac{2\pi a}{\lambda} = ka$$

(For proof see Appendix 1)

Thus the effect of the right-angled bend can be accounted for by inserting the appropriate four element matrix in the series representing the whole set-up.

Value of the Equivalent 'a'.

Since Miles's theory was derived for a pipe with a square cross-section, therefore, 'a' , the length of one side of the square cross-section and 'd', the diameter of the pipe under investigation has to be related in such a way that Miles's theory can also be applied to circular pipes. Four hypotheses were investigated and listed as follows :

(a) Hydraulic radius $a = d = 0.0287$ m ,

(b) Equal cross-sectional area $a = \sqrt{\frac{\pi}{4}}\, d = 0.0254$ m ,

(c) Equal wetted perimeter $a = \frac{\pi}{4} d = 0.0225$ m ,

(d) Equal volume between input and output planes $a = \sqrt[3]{\frac{\pi}{4}} d = 0.0265$ m.

These four , together with three other values of a (a = 0.0235 m, 0.0240 m , 0.0245 m) were used in the computer program to calculate the theoretical attenuation of sound due to the bend.

APPARATUS AND EXPERIMENTAL METHODS.

Following the literature survey on sound propagation through bends, the test rig described in another report (1) was modified to investigate the behaviour of a sharp right-angled bend in circular pipes. The set-up was as shown in Figure 2.

Two pieces of 1 in diameter p.v.c. pipes were used as shown. One of the ends of each pipe has a 45° cut. They were then joined by means of a wooden block to form a sharp right-angled bend. The other end of the pipes are terminated by foam to form non-reflective terminations. The microphone was inserted into the pipe as shown and was covered by sand to avoid interference. Sine wave signals from 100 Hz to 6 kHz at 50 Hz intervals were fed to the loudspeaker. The sound measured by the microphone was recorded. The same procedure was repeated with a straight pipe, the distance travelled by the sound between the loudspeaker and the microphone beeing 2.45 m in both cases. Attenuation-frequency characteristics were plotted and are shown in Graphs 1 and 2.

DISCUSSION OF RESULTS.

Graph 1 shows theoretical attenuation-frequency characteristics for a = 0.0225 m, 0.0235 m , 0.0240 m, 0.0245 m and 0.0254 m . Experimental results are also shown in the graph. All results are shown between 4 kHz and 6 kHz because attenuation was significant only at frequencies above 4 kHz. Due to the scattered nature of the experimental results, they appear to agree fairly well with all the theoretical curves , but the best agreement is with a = 0.0225 m .

Graph 2 shows theoretical attenuation-frequency characteristics for a = 0.0287 m and a = 0.0265 m from 5 kHz to 7 kHz . The curves behave rationally up to the frequency corresponding to a wave length equal to twice the characteristic dimension of the pipe , i.e. $\lambda = 2a$. At this point the theoretical attenuation equals infinity and the theory breaks down beyond this point.

CONCLUSION.

The theory for noise transmission through square pipes can be modified to suit circular pipes by using a suitable relationship between the diameter of the circular pipe and one side of the square pipe. It has been found that the values of 'a' derived from the hypotheses of equal cross-sectional area and equal wetted perimeter form the limits of a region for values of theoretical attenuation. The experimental results substantially fell within this region. Attenuation of noise started to occur at around 4.5 kHz, the frequency corresponding to a wave-length equal approximately to three times the diameter of the circular pipe.

REFERENCES.

(1) LAI,T.C. 'Theoretical and Experimental Attenuation Characteristics of Acoustic Filters.'
The City University Research Memorandum No ML 30, 1971.

(2) LIPPERT,W.K.R. 'A Method of Measuring Discontinuity Effects in Ducts.'
Acustica, 4 , 307 , 1954.

(3) LIPPERT,W.K.R. ' The Measurement of Sound Reflection and Transmission at Right-angled Bends in Rectangular Tubes.'
Acustica, 4 , 313 , 1954.

(4) LIPPERT,W.K.R. 'Wave Transmission around Bends of Different Angles in Rectangular Ducts.'
Acustica, 5 , 274 , 1955.

(5) MILES,J.W. 'The Diffraction of Sound due to Right-angled Joints in Rectangular Tubes.'
Journal of the Acoustical Society of America, 19 , no 4 , July 1947.

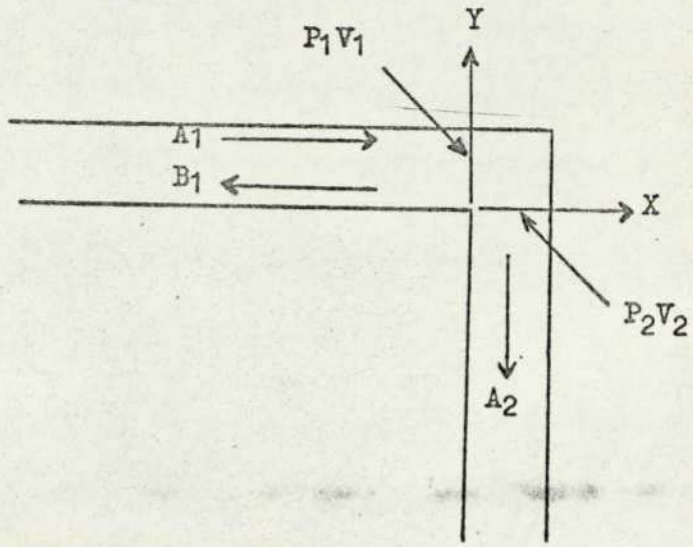
Y
P_1V_1
A_1
B_1
X
P_2V_2
A_2

Fig. 1

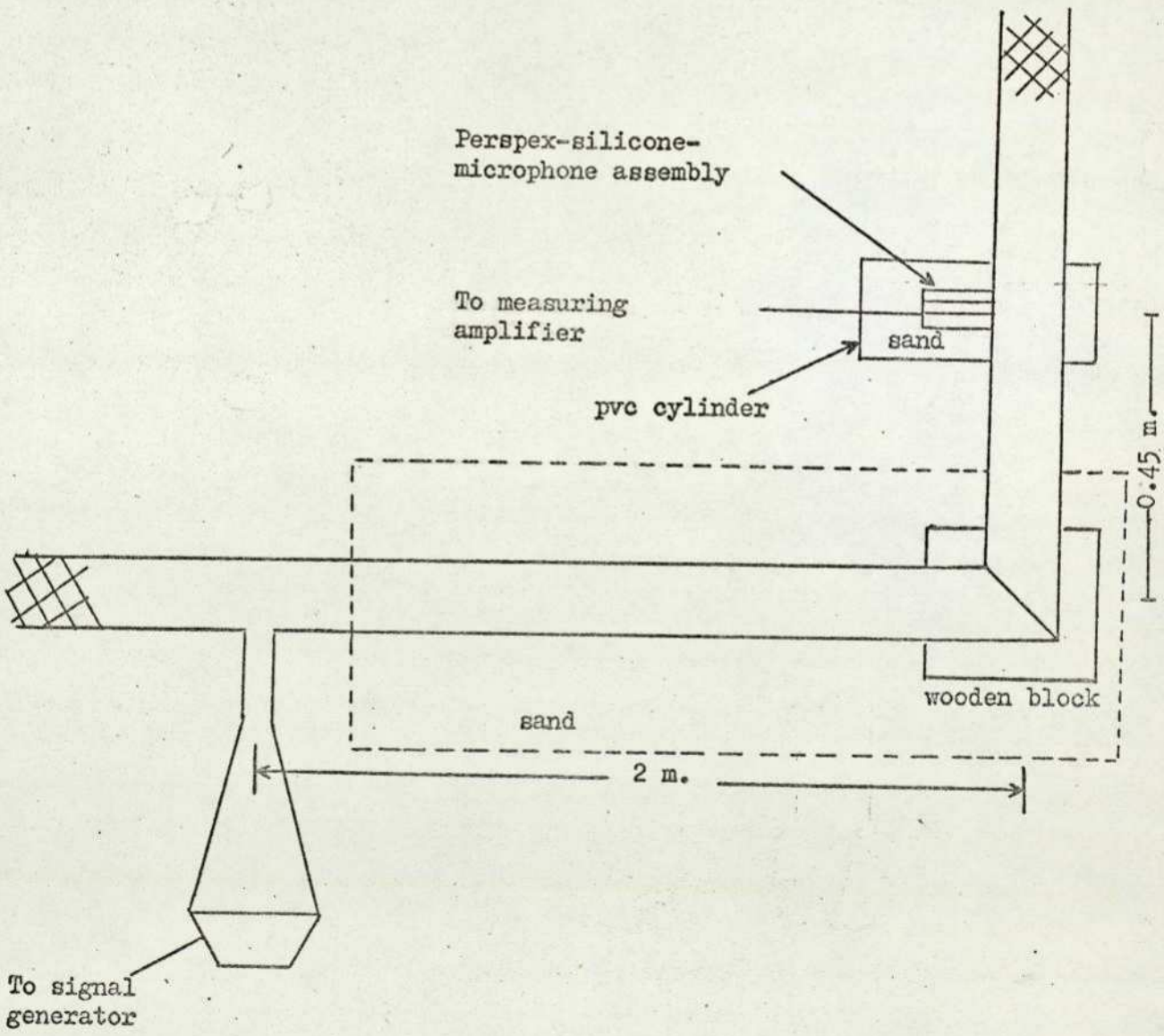
Perspex-silicone-
microphone assembly
To measuring
amplifier
sand
pvc cylinder
0.45 m.
wooden block
sand
2 m.
To signal
generator

Fig. 2

RESULTS

Attenuation due to a Sharp Right-Angled Bend in a Circular Pipe

Freq. Hz	Atten. dB	Hz	dB	Hz	dB	Hz	dB
100	0	1550	2	3050	2	4550	6
150	0	1600	2	3100	2	4600	5
200	1	1650	0	3150	1	4650	1
250	0	1700	-1	3200	0	4700	1
300	-1	1750	-1	3250	0	4750	4
350	-1	1800	-3	3300	2	4800	3
400	-2	1850	-3	3350	2	4850	2
450	-2	1900	-2	3400	1	4900	1
500	-2	1950	-1	3450	0	4950	3
550	-1	2000	-1	3500	0	5000	3
600	1	2050	-1	3550	-1	5050	7
650	1	2100	-1	3600	1	5100	8
700	1	2150	-1	3650	2	5150	5
750	2	2200	-1	3700	2	5200	3
800	2	2250	0	3750	1	5250	3
850	2	2300	0	3800	2	5300	5
900	2	2350	1	3850	2	5350	6
950	2	2400	0	3900	2	5400	6
1000	1	2450	0	3950	3	5450	6
1050	0	2500	2	4000	2	5500	4
1100	-1	2550	3	4050	-2	5550	5
1150	-1	2600	3	4100	-2	5600	9
1200	-1	2650	3	4150	-1	5650	10
1250	-1	2700	2	4200	2	5700	10
1300	0	2750	5	4250	2	5750	6
1350	1	2800	0	4300	1	5800	9
1400	2	2850	1	4350	1	5850	11
1450	2	2900	1	4400	2	5900	13
1500	2	2950	1	4450	4	5950	14
		3000	1	4500	6	6000	13

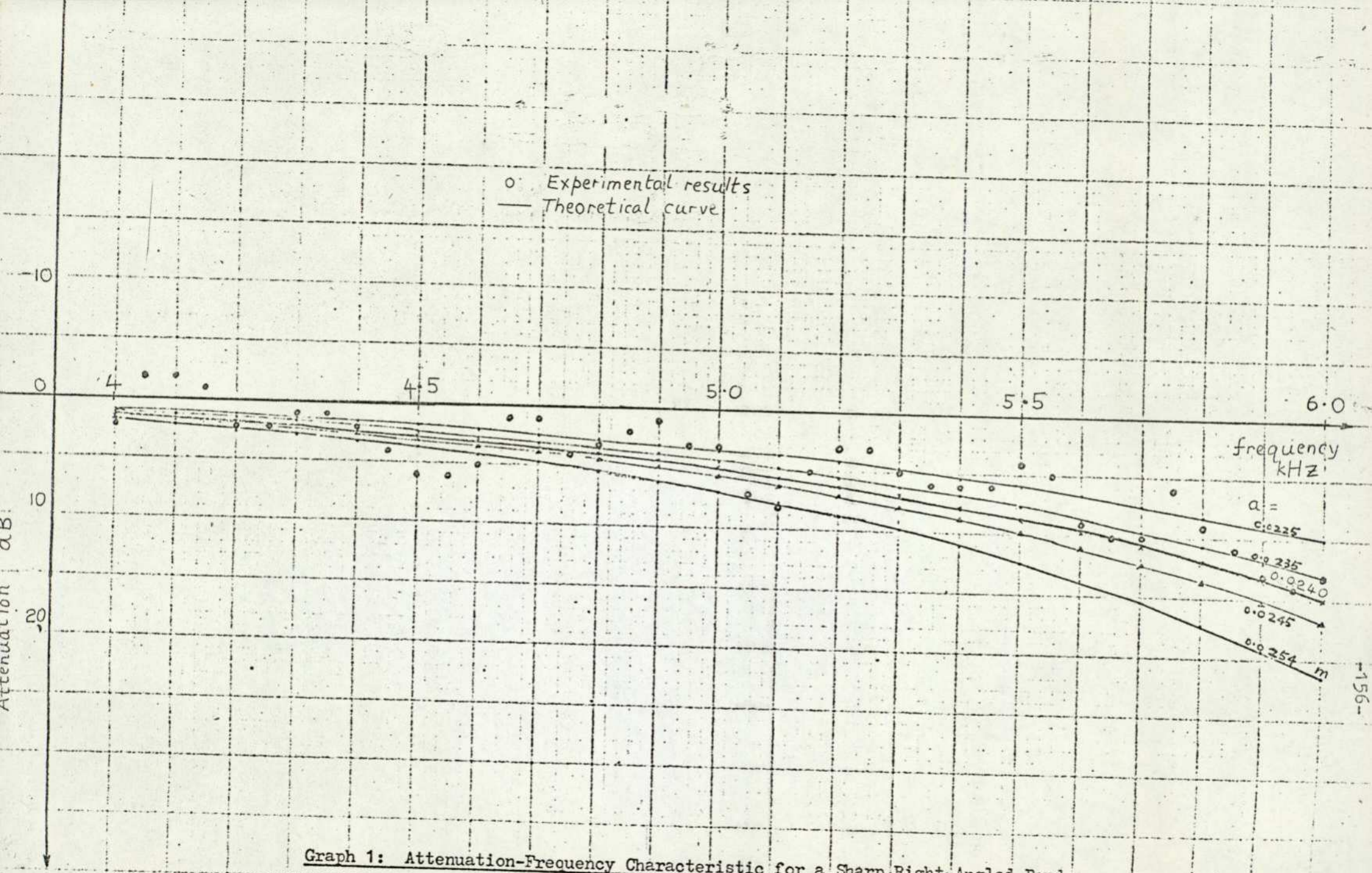

Graph 1: Attenuation-Frequency Characteristic for a Sharp Right-Angled Bend

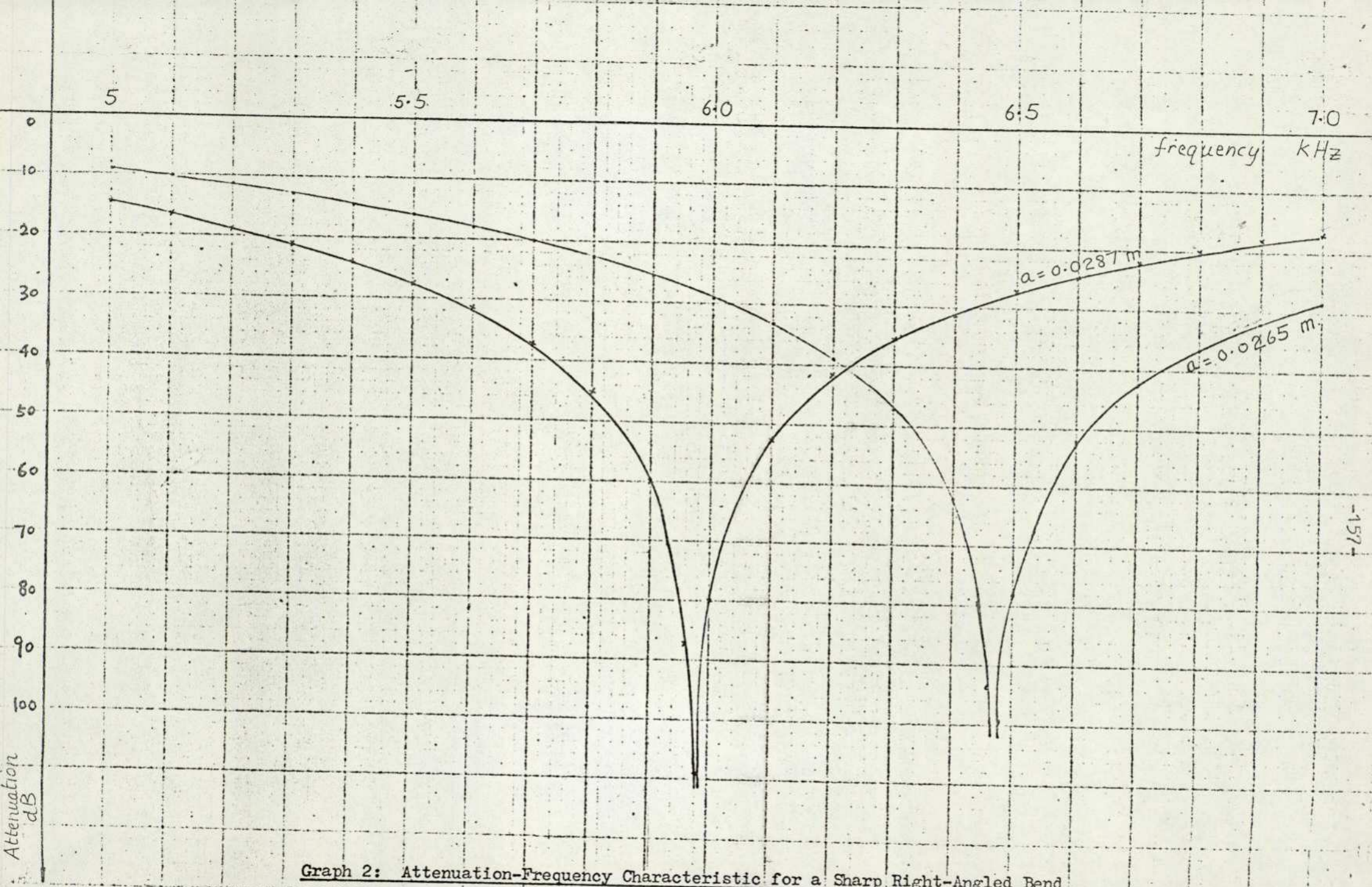

Graph 2: Attenuation-Frequency Characteristic for a Sharp Right-Angled Bend

Appendix 1.

Referring to Figure 1 , the reflection and transmission factors of the right-angled bend are (3) :

$$\frac{B_1}{A_1} = \frac{1 - \frac{1}{\theta^2} + \cot^2\theta}{\sqrt{\left(1 + \frac{1}{\theta^2} - \cot^2\theta\right)^2 + 4\cot^2\theta}} \; e^{j\left[\pi + \tan^{-1}\left(\frac{2\cot\theta}{1 + \frac{1}{\theta^2} - \cot^2\theta}\right)\right]}$$

$$= AM1 \; e^{j\,PH1}$$

$$\frac{A_2}{A_1} = \frac{2}{\theta\sqrt{\left(1 + \frac{1}{\theta^2} - \cot^2\theta\right)^2 + 4\cot^2\theta}} \; e^{-j\left[\tan^{-1}\left(\frac{1 + \frac{1}{\theta^2} - \cot^2\theta}{2\cot\theta}\right)\right]}$$

$$= AM2 \; e^{-j\,PH2}$$

$$P_1 = A_1 + B_1 = A_1\left[1 + AM1\, e^{j\,PH1}\right]$$

$$= A_1\left[1 + AM1\cos(PH1) + j\,AM1\sin(PH1)\right]$$

$$V_1 = \frac{S}{\rho c}(A_1 - B_1) = \frac{S}{\rho c} A_1\left[1 - AM1\, e^{j\,PH1}\right]$$

$$= \frac{S}{\rho c} A_1\left[1 - AM1\cos(PH1) - j\,AM1\sin(PH1)\right]$$

$$P_2 = A_2 = A_1\left[AM2\, e^{-j\,PH2}\right]$$

$$= A_1\, AM2\left[\cos(PH2) - j\sin(PH2)\right]$$

$$V_2 = \frac{S}{\rho c} A_2 = \frac{S}{\rho c} A_1\, AM2\left[\cos(PH2) - j\sin(PH2)\right]$$

Assume,

$$\begin{bmatrix} P_1 \\ V_1 \end{bmatrix} = \begin{bmatrix} a_1 + j\,a_2 & b_1 + j\,b_2 \\ c_1 + j\,c_2 & d_1 + j\,d_2 \end{bmatrix} \begin{bmatrix} P_2 \\ V_2 \end{bmatrix}$$

Further assume , $a_2 , b_1 , c_1 , d_2 = 0$

$$P_1 = a_1 P_2 + j\,b_2 V_2 \qquad \text{——— (1)}$$

Real part of (1) is $1 + AM1 \cos(PH1)$

$$= a_1 AM2 \cos(PH2) + b_2 \frac{S}{\rho c} AM2 \sin(PH2) \quad \text{—— (2)}$$

Imaginary part of (1) is $AM1 \sin(PH1)$.

$$= -a_1 AM2 \sin(PH2) + b_2 \frac{S}{\rho c} AM2 \cos(PH2) \quad \text{—— (3)}$$

$\sin(PH2) \times (2) + \cos(PH2) \times (3)$ gives

$$b_2 = \frac{AM1}{AM2} \frac{\rho c}{S} \left\{ \frac{1}{AM1} \sin(PH2) + \sin(PH1 + PH2) \right\}$$

$\cos(PH2) \times (2) - \sin(PH2) \times (3)$ gives

$$a_1 = \frac{AM1}{AM2} \left\{ \frac{1}{AM1} \cos(PH2) + \cos(PH1 + PH2) \right\}$$

$$V_1 = j c_2 P_2 + d_1 V_2 \quad (4)$$

Real part of (4) is $\frac{S}{\rho c} \left\{ 1 - AM1 \cos(PH1) \right\}$

$$= c_2 AM2 \sin(PH2) + d_1 \frac{S}{\rho c} AM2 \cos(PH2) \quad \text{—— (5)}$$

Imaginary part of (4) $- \frac{S}{\rho c} AM1 \sin(PH1)$

$$= c_2 AM2 \cos(PH2) - d_1 \frac{S}{\rho c} AM2 \sin(PH2) \quad \text{—— (6)}$$

$\cos(PH2) \times (5) - \sin(PH2) \times (6)$ gives

$$d_1 = \frac{AM1}{AM2} \left\{ \frac{1}{AM1} \cos(PH2) - \cos(PH1 + PH2) \right\}$$

$\sin(PH2) \times (5) + \cos(PH2) \times (6)$ gives

$$c_2 = \frac{S}{\rho c} \frac{AM1}{AM2} \left\{ \frac{1}{AM1} \sin(PH2) - \sin(PH1 + PH2) \right\}$$

$$\therefore \begin{bmatrix} P_1 \\ V_1 \end{bmatrix} = \begin{bmatrix} \frac{AM1}{AM2} \left\{ \frac{1}{AM1} \cos(PH2) + \cos(PH1 + PH2) \right\} & j \frac{AM1}{AM2} \frac{\rho c}{S} \left\{ \frac{1}{AM1} \sin(PH2) + \sin(PH1+PH2) \right\} \\ j \frac{AM1}{AM2} \frac{S}{\rho c} \left\{ \frac{1}{AM1} \sin(PH2) - \sin(PH1 + PH2) \right\} & \frac{AM1}{AM2} \left\{ \frac{1}{AM1} \cos(PH2) - \cos(PH1 + PH2) \right\} \end{bmatrix} \begin{bmatrix} P_2 \\ V_2 \end{bmatrix}$$

RIGHT ANGLE BEND.

```
      MASTER ACOU
      REAL LEN,IMP,KON,LENN,MACH,IMPT,LENT
      COMPLEX X(7,2,2),Y(7,2,2)
      DIMENSION KON(1000),AREA(7),IMP(7),LEN(7),AREAN(7),LENN(7),MACH(7
     1,ATTEN(500)
     1,COT(7)
C     ATTENUATION OF SILENCERS BY MATRIX METHODS
C     LEN=LENGTH OF MATRIX SECTION
C     AREA=AREA OF MATRIX SECTION
C     LENN=LENGTH OF RESONATOR NECK
C     AREAN=AREA OF RESONATOR NECK
C     LENT=LENGTH OF TAIL PIPE
C     RT=RADIUS OF TAIL PIPE
C     L=NO. OF MATRICES
C     P=DENSITY OF MEDIUM
C     C=VELOCITY OF SOUND
C     NOL=NO. OF SETS OF INPUT DATA FOR LEN
C     NOA=NO. OF SETS OF INPUT DATA FOR AREA
C     MACH= LOCAL MACH NO. OF GAS FLOW
      READ (1,53) L
   53 FORMAT (1I1)
      READ (1,51) NOA,NOL,NOM,P,C
   51 FORMAT (3I1,2F10.5)
      NUMA=1
      X(1,1,1),X(1,2,2),X(L+2,1,1),X(L+2,2,2)=CMPLX(1.,0.)
      X(1,1,2),X(L+2,1,2)=CMPLX(0.,0.)
    1 WRITE (2,52)
   52 FORMAT (1H1,9HAREAS ARE)
      DO 10 N=2,L+1
      READ (1,54) AREA(N)
   54 FORMAT (F0.0)
      WRITE (2,55) AREA(N)
   55 FORMAT (1H ,1F10.8,4X)
   10 CONTINUE
      NUML=1
    2 WRITE (2,56)
   56 FORMAT (1H0,11HLENGTHS ARE)
      DO 11 N=2,L+1
      READ (1,57) LEN(N)
   57 FORMAT (F0.0)
      WRITE (2,58) LEN(N)
   58 FORMAT (1H ,1F10.8,4X)
   11 CONTINUE
      NUMM=1
    3 DO 17 N=2,L+1
      READ (1,63) MACH(N)
   63 FORMAT (F0.0)
   17 CONTINUE
      WRITE (2,65) MACH(2)
   65 FORMAT (1H0,24HMACH NO IN 1 INCH PIPE =,1F8.4)
      WRITE (2,59)
   59 FORMAT (1H0,4HFREQ,6X,5HATTEN,8X,4HFREQ,6X,
     15HATTEN,8X,4HFREQ,6X,5HATTEN,8X,4HFREQ,6X,5HATTEN,8X,
     14HFREQ,6X,5HATTEN)
      X(1,2,1)=CMPLX(AREA(2)/(P*C)*(1-MACH(2)),0.)
      X(L+2,2,1)=CMPLX(AREA(L+1)/(P*C)*(1+MACH(L+1)),0.)
      NOO=0
      DO 12 M=4000,7000,10
      NOO=NOO+1
      FRE=1
      DO 15 I=1,2
      DO 15 J=1,2
      DO 15 N=1,L+1
   15 Y(N,I,J)=CMPLX(0.,0.)
```

```
      KON(NOO)=2.*3.14159*FRE/C
      DO 16 N=2,L+1,2
      IMP(N)=KON(NOO)*LEN(N)/(1.0-MACH(N)*MACH(N))
      X(N,1,1)=CMPLX(COS(IMP(N)),-MACH(N)*SIN(IMP(N)))
      X(N,1,2)=CMPLX(0.,P*C/AREA(N)*SIN(IMP(N)))
      X(N,2,1)=CMPLX(0.,AREA(N)/(P*C)*(1.0-MACH(N)*MACH(N))*SIN(IMP(N)))
      X(N,2,2)=CMPLX(COS(IMP(N)),MACH(N)*SIN(IMP(N)))
16    CONTINUE
      DO 171 N=3,L,2
      IMP(N)=KON(NOO)*LEN(N)
      COT(N)=1./TAN(IMP(N))
      AL=1.+1./IMP(N)**2-COT(N)**2
      AM1=(1.-1./IMP(N)**2-COT(N)**2)/SQRT(AL**2+4.*COT(N)**2)
      AM2=2./(IMP(N)*SQRT(AL**2+4.*COT(N)**2))
      PH1=3.14159+ATAN(2.*COT(N)/AL)
      PH2=ATAN(AL/(2.*COT(N)))
      AMT=AM1/AM2
      PHT=PH1+PH2
      X(N,1,1)=CMPLX(AMT*(COS(PH2)/AM1+COS(PHT)),0.)
      X(N,2,2)=CMPLX(AMT*(COS(PH2)/AM1-COS(PHT)),0.)
      X(N,1,2)=CMPLX(0.,AMT*P*C/AREA(N)*(SIN(PH2)/AM1+SIN(PHT)))
      X(N,2,1)=CMPLX(0.,AMT*AREA(N)/(P*C)*(SIN(PH2)/AM1-SIN(PHT)))
171   CONTINUE
      DO 21 N=1,L+1
      DO 20 I=1,2
      DO 20 J=1,2
      DO 20 K=1,2
20    Y(N,I,J)=Y(N,I,J)+X(N,I,K)*X(N+1,K,J)
      IF (N-(L+1))0,21,21
      DO 22 I=1,2
      DO 22 J=1,2
22    X(N+1,I,J)=Y(N,I,J)
21    CONTINUE
      ATT=CABS(Y(L+1,2,1))
      ATT=ATT/(2.*AREA(2))*P*C
      ATTEN(NOO)=20.*ALOG10(ATT)
12    CONTINUE
      DO 71 NOO=0,294,5
      NOO1=NOO+1
      NOO2=NOO+2
      NOO3=NOO+3
      NOO4=NOO+4
      NOO5=NOO+5
      NOO6=3990+10*NOO1
      NOO7=3990+10*NOO2
      NOO8=3990+10*NOO3
      NOO9=3990+10*NOO4
      NOO10=3990+10*NOO5
      WRITE(2,51) NOO6,ATTEN(NOO1),NOO7,ATTEN(NOO2),NOO8,ATTEN(NOO3),
     1NOO9,ATTEN(NOO4),NOO10,ATTEN(NOO5)
61    FORMAT (1H ,1I4,4X,1F8.4,7X,1I4,4X,1F8.4,7X,1I4,4X,1F8.4
     1,7X,1I4,4X,1F8.4,7X,1I4,4X,1F8.4)
71    CONTINUE
      NUMM=NUMM+1
      IF(NUMM-NOM)3,3,0
      NUML=NUML+1
      IF(NUML-NOL)2,2,0
      NUMA=NUMA+1
      IF(NUMA-NOA)1,1,0
      STOP
      END
```